Seasonal Variations in the Moduli of Unbound Pavement Layers

PUBLICATION NO. FHWA-HRT-04-079

JULY 2006

U.S. Department of Transportation
Federal Highway Administration

Research, Development, and Technology
Turner-Fairbank Highway Research Center
6300 Georgetown Pike
McLean, VA 22101-2296

FOREWORD

The in situ moduli of unbound pavement materials vary on a seasonal basis as a function of temperature and moisture conditions. Knowledge of these variations is required for accurate prediction of pavement life for pavement design and other pavement management activities. The primary objective of this study is to advance the rational estimation of seasonal variations in backcalculated pavement layer moduli using data collected via the Seasonal Monitoring Program of the Long-Term Pavement Performance (LTPP) Program. Principal components of this endeavor included: evaluation of the moisture predictive capabilities of the Enhanced Integrated Climatic Model (EICM); development of empirical models to predict backcalculated pavement layer moduli as a function of moisture content, stress state, and other explanatory variables; and trial application of the models developed to prediction backcalculated moduli for unbound pavement layers.

This investigation yielded two key findings. First, it provided the impetus for developing EICM Version 2.6 by demonstrating the practical inadequacies of EICM Versions 2.0 and 2.1 when applied to the prediction of in situ moisture content, and then demonstrated that improvement in the moisture predictive capability of the EICM had been achieved in Version 2.6. Second, the research identified fundamental discrepancies between layer moduli backcalculated using linear layered-elastic theory and the laboratory resilient modulus test conditions.

Gary L. Henderson
Director, Office of Infrastructure
Research and Development

Notice

Quality Assurance Statement

The Federal Highway Administration (FHWA) provides high-quality information to serve Government, industry, and the public in a manner that promotes public understanding. Standards and policies are used to ensure and maximize the quality, objectivity, utility, and integrity of its information. FHWA periodically reviews quality issues and adjusts its programs and processes to ensure continuous quality improvement.

Technical Report Documentation Page

1. Report No.	2. Government Accession No.	3. Recipient's Catalog No.
FHWA-HRT-04-079		

4. Title and Subtitle	5. Report Date
Seasonal Variations in the Moduli of Unbound Pavement Layers	July 2006
	6. Performing Organization Code

7. Author(s)	8. Performing Organization Report No.
Cheryl Allen Richter	

9. Performing Organization Name and Address	10. Work Unit No. (TRAIS)
Federal Highway Administration 6300 Georgetown Pike McLean, VA 22101	11. Contract or Grant No.

12. Sponsoring Agency Name and Address	13. Type of Report and Period Covered
Federal Highway Administration 6300 Georgetown Pike McLean, VA 22101-2296	14. Sponsoring Agency Code

15. Supplementary Notes

16. Abstract

The in situ moduli of unbound pavement materials vary on a seasonal basis as a function of temperature and moisture conditions. Knowledge of these variations is required for accurate prediction of pavement life for pavement design and other pavement management activities. The primary objective of this study is to advance the rational estimation of seasonal variations in backcalculated pavement layer moduli using data collected via the Seasonal Monitoring Program of the Long-Term Pavement Performance Program. Principal components of this endeavor included: evaluation of the moisture predictive capabilities of the Enhanced Integrated Climatic Model (EICM); development of empirical models to predict backcalculated pavement layer moduli as a function of moisture content, stress state, and other explanatory variables; and trial application of the models developed to prediction backcalculated moduli for unbound pavement layers.

This investigation yielded two key findings. First, it provided the impetus for developing EICM Version 2.6 by demonstrating the practical inadequacies of EICM Versions 2.0 and 2.1 when applied to the prediction of in situ moisture content, and then demonstrated that substantial improvement in the moisture predictive capability of the EICM had been achieved in Version 2.6. Second, the research identified fundamental discrepancies between layer moduli backcalculated using linear-layered elastic theory and the laboratory resilient modulus test conditions.

Other important findings included (1) variation in moisture content is not always the most important factor associated with seasonal variations in pavement layer moduli, and (2) a model form that fits linear elastic backcalculated moduli reasonably well. The overall accuracy of the modulus predictions achieved in the trial application of the predictive models was not fully acceptable. Several avenues for further research to improve upon these results are identified.

17. Key Words	18. Distribution Statement
LTPP, Seasonal Monitoring Program, modulus, pavement, Enhanced Integrated Climatic Model, linear layered elastic theory	No restrictions. This document is available to the public through the National Technical Information Service, Springfield, VA 22161.

19. Security Classification (of this report)	20. Security Classification (of this page)	21. No. of Pages	22. Price
Unclassified	Unclassified	283	

SI* (MODERN METRIC) CONVERSION FACTORS

APPROXIMATE CONVERSIONS TO SI UNITS

Symbol	When You Know	Multiply By	To Find	Symbol
		LENGTH		
in	inches	25.4	millimeters	mm
ft	feet	0.305	meters	m
yd	yards	0.914	meters	m
mi	miles	1.61	kilometers	km
		AREA		
in^2	square inches	645.2	square millimeters	mm^2
ft^2	square feet	0.093	square meters	m^2
yd^2	square yard	0.836	square meters	m^2
ac	acres	0.405	hectares	ha
mi^2	square miles	2.59	square kilometers	km^2
		VOLUME		
fl oz	fluid ounces	29.57	milliliters	mL
gal	gallons	3.785	liters	L
ft^3	cubic feet	0.028	cubic meters	m^3
yd^3	cubic yards	0.765	cubic meters	m^3
	NOTE: volumes greater than 1000 L shall be shown in m^3			
		MASS		
oz	ounces	28.35	grams	g
lb	pounds	0.454	kilograms	kg
T	short tons (2000 lb)	0.907	megagrams (or "metric ton")	Mg (or "t")
		TEMPERATURE (exact degrees)		
^oF	Fahrenheit	5 (F-32)/9 or (F-32)/1.8	Celsius	^oC
		ILLUMINATION		
fc	foot-candles	10.76	lux	lx
fl	foot-Lamberts	3.426	$candela/m^2$	cd/m^2
		FORCE and PRESSURE or STRESS		
lbf	poundforce	4.45	newtons	N
lbf/in^2	poundforce per square inch	6.89	kilopascals	kPa

APPROXIMATE CONVERSIONS FROM SI UNITS

Symbol	When You Know	Multiply By	To Find	Symbol
		LENGTH		
mm	millimeters	0.039	inches	in
m	meters	3.28	feet	ft
m	meters	1.09	yards	yd
km	kilometers	0.621	miles	mi
		AREA		
mm^2	square millimeters	0.0016	square inches	in^2
m^2	square meters	10.764	square feet	ft^2
m^2	square meters	1.195	square yards	yd^2
ha	hectares	2.47	acres	ac
km^2	square kilometers	0.386	square miles	mi^2
		VOLUME		
mL	milliliters	0.034	fluid ounces	fl oz
L	liters	0.264	gallons	gal
m^3	cubic meters	35.314	cubic feet	ft^3
m^3	cubic meters	1.307	cubic yards	yd^3
		MASS		
g	grams	0.035	ounces	oz
kg	kilograms	2.202	pounds	lb
Mg (or "t")	megagrams (or "metric ton")	1.103	short tons (2000 lb)	T
		TEMPERATURE (exact degrees)		
^oC	Celsius	1.8C+32	Fahrenheit	^oF
		ILLUMINATION		
lx	lux	0.0929	foot-candles	fc
cd/m^2	$candela/m^2$	0.2919	foot-Lamberts	fl
		FORCE and PRESSURE or STRESS		
N	newtons	0.225	poundforce	lbf
kPa	kilopascals	0.145	poundforce per square inch	lbf/in^2

*SI is the symbol for the International System of Units. Appropriate rounding should be made to comply with Section 4 of ASTM E380.
(Revised March 2003)

TABLE OF CONTENTS

Chapter 1: Introduction and Research Objectives 1
Introduction 1
Research Objectives 1
Research Approach 2
Chapter 2: Literature Review 3
Introduction 3
Soil Modulus: M_r versus E 3
Addressing Seasonal Variations in Pavement Design and Evaluation 5
Factors Influencing the Moduli of Unbound Pavement Materials 10
Stress Conditions 10
Moisture Conditions 16
Density and Soil Structure 18
Material Characteristics 18
Soil State with Respect to Freezing and Thawing 22
Additional Factors Influencing Backcalculated Moduli 23
Relating Resilient Moduli to Material Parameters 24
Seasonal Variations as Observed in Field Investigations 34
Environmental Effects Models Applicable to Pavement Design 35
Related Work With the Integrated Climatic Model 37
Chapter 3: Data Acquisition and Assessment 39
Introduction 39
Data Sources 39
Backcalculated Moduli 40
Backcalculation of Pavement Layer Moduli 40
Evaluation of Backcalculated Layer Moduli 41
Variation in Moduli Under Nonfrozen Conditions 43
Moisture Parameters 58
Input to the Integrated Climatic Model 63
Climatic Boundary Conditions 64
Infiltration and Drainage 65
Asphalt Material Properties 65
Material Properties 65
Initial Temperature and Pore Pressure Profile 66
Summary 66
Chapter 4: Evaluation of Volumetric Moisture Predictions From the Integrated Climatic Model 67
Introduction 67
Evaluation of EICM Version 2.0 67
Evaluation of EICM Version 2.1 71
Sections Considered 71
Layer Structure 71
Layer Porosity 71

Soil-Water Characteristic Curve Parameters (Gardner Coefficients) 71
Results 71
Application of EICM Version 2.6 74
Layer Structure 75
Layer Porosity 75
Specific Gravity 75
Saturated Permeability 75
Initial Volumetric Water Content 75
Soil-Water Characteristic Curve Model and Parameters (Gardner Coefficients) 75
Results 76
Evaluation of eICM Version 2.6 User Sensitivity 83
Between-User Differences in Model Application 83
Discussion And Conclusions Regarding EICM Moisture Predictions 91
Chapter 5: Prediction of Backcalculation Pavement Layer Moduli 93
Introduction 93
Exploration of Relationships Between Backcalculated Moduli and Explanatory Variables 93
Models of the Form $E/P_a = k_1\theta/_{Pa}^{k2}(\tau/P_a+1)^{k3}$ 100
Factors Contributing to Differences Between Laboratory and Field-Based Constitutive Model Coefficients 105
Alternative Model Forms 113
Individual Pavement Layer Models 113
Soil Class Models 117
Summary 120
Chapter 6: Application of Research Results To Estimate Seasonal Variations in Moduli of Unbound Pavement Layers 123
Introduction 123
Procedure for Prediction of Seasonal Variations in Backcalculated Pavement Layer Moduli 124
Required Input Data 124
Part 1: Derivation of Section- and Layer-Specific Regression Models 125
Part 2: Estimation of Pavement Layer Moduli for Future Date 129
Trial application 130
Results Obtained with Section/Layer-Specific Models Derived From the Full Data Set 134
Results Obtained With Section/Layer-Specific Models Derived From Limited Data Sets 138
Results Obtained with Soil Class Models 142
Summary Observations 145
Chapter 7: Conclusions and Recommendations 147
Conclusions 147
The Enhanced Integrated Climatic Model 147
Models for Prediction of Backcalculated Pavement Layer Moduli 148
Variations in Backcalculated Moduli for Unbound Pavement Layers 150

Application of Research Results To Predict Moduli Backcalculated for Unbound Pavement Layers Using Linear Layered-Elastic Theory 150
Recommendations 151
The Enhanced Integrated Climatic Model 151
The State of the Art of Backcalculation of Pavement Layer Moduli 151
Consideration of Stress Dependency in Pavement Modeling 152
LTPP Data Used in This Investigation 152
Appendix A: Variation in TDR Moisture Data 153
Appendix B: Input Data for the Enhanced Integrated Climatic Model 159
Appendix C: Between-user Differences in Application of EICM Version 2.6 213
Appendix D: Materials Data Used In Development of E Predictive Models 219
Appendix E: Multiple Regression Results for Individual Pavement Layers 227
Appendix F: Trial Application Results Based on Section/Layer-Specific Models Derived From All Available Data 247
Appendix G: Trial Application Results Obtained With One-date Section/Layer-Specific Models 253
Appendix H: Trial Application Results Obtained With Two-Date Section/Layer-Specific Models 257
Appendix I: Trial Application Results Obtained With Soil Class Models 259
References 263

LIST OF FIGURES

Figure 1. Chart for estimating effective roadbed soil resilient modulus for flexible pavements designed using the serviceability criteria 6
Figure 2. Locations of LTPP seasonal monitoring sections considered in this study. 41
Figure 3. Seasonal variation in daily average moduli, section 040113 (Arizona) 52
Figure 4. Seasonal variations in daily average moduli, section 091803 (Connecticut) 53
Figure 5. Seasonal variations in daily average moduli, section 131005 (Georgia) 54
Figure 6. Seasonal variations in daily average moduli, section 271018 (Minnesota) 55
Figure 7. Seasonal variations in daily average layer moduli, section 481077 (Texas) 56
Figure 8. Seasonal variation in moduli, section 501002 (Vermont) 56
Figure 9. Frequency histogram for ratio of within-day standard deviation/ maximum TDR Model 1 error. 62
Figure 10. Predicted and monitored moisture contents for section 091803 (Connecticut), 6/30/94 69
Figure 11. Predicted and monitored moisture contents for section 271018 (Minnesota), 8/8/94 70
Figure 12. Comparison of monitored and predicted base-layer moisture for EICM Version 2.1 72
Figure 13. Comparison of monitored and predicted subgrade moisture for EICM Version 2.1 73
Figure 14. Sample EICM Version 2.1 moisture-profile plot, section 091803 (Connecticut) ... 74
Figure 15. Comparison of monitored and predicted base moisture for EICMVersion 2.6 76
Figure 16. Comparison of monitored and predicted subgrade moisture for EICM Version 2.6 77
Figure 17. Variation in monitored and predicted base moisture, section 041024 78
Figure 18. Monitored and predicted subgrade moisture content, section 091803 (Connecticut) 79
Figure 19. Monitored and predicted subgrade moisture, section 231026 (Maine) 79
Figure 20. Monitored and predicted subgrade moisture, section 501002 (Vermont) 81
Figure 21. Monitored and predicted subgrade moisture (shallow depths), section 831801 (Manitoba) 82
Figure 22. Monitored and predicted subgrade moisture (greater depths), section 831801 (Manitoba) 82
Figure 23. Comparison of EICM Version 2.6 moisture predictions for all sections 85
Figure 24. Monitored and predicted moisture contents for all sections 86
Figure 25. Comparison of moisture predictions, section 081053 86
Figure 26. Monitored and predicted base moisture content, section 481077 (Texas) 87
Figure 27. Monitored and predicted subgrade moisture content, section 481077 (Texas) 88
Figure 28. Comparison of predicted volumetric moisture contents for section 091803 (Connecticut). 88
Figure 29. Monitored and predicted moisture content, section 091803 (Connecticut). 89
Figure 30. Monitored and predicted base moisture, section 131005 (Georgia) 90
Figure 31. Monitored and predicted subgrade moisture, section 131005 (Georgia) 90

Figure 32. Vertical load stress versus modulus, section 040113 A-1-a base layer 107
Figure 33. Radial load stress versus modulus, section 040113 A-1-a base layer..... 107
Figure 34. Bulk load stress versus modulus, section 040113 A-1-a base layer 108
Figure 35. Load-induced octahedral shear stress versus modulus, section 040113 A-1-a base layer..... 108
Figure 36. Comparison of radial and vertical stress components for granular base and subbase layers..... 109
Figure 37. Comparison of radial and vertical stress components for coarse-grained subgrade layers 110
Figure 38. Comparison of radial and vertical stress components for fine-grained subgrade layers 111
Figure 39. Comparison of bulk and octahedral shear stresses for granular base and subbase layers..... 112
Figure 40. Comparison of bulk and octahedral shear stresses for coarse-grained subgrade layers 112
Figure 41. Comparison of bulk and octahedral shear stresses for fine-grained subgrade layers..... 113
Figure 42. Calculation of overburden stress..... 128
Figure 43. Backcalculated modulus versus estimated temperature compatible modulus for all sections considered in trial applications 132
Figure 44. Backcalculated versus section/layer-specific predicted modulus for models derived using all data..... 135
Figure 45. Backcalculated modulus versus estimated temperature compatible modulus for section 271018 (Minnesota) 138
Figure 46. Backcalculated modulus versus section/layer-specific one-date predicted modulus 139
Figure 47. Backcalculated versus site/layer-specific two-date predicted modulus..... 140
Figure 48. Backcalculated versus soil class predicted moduli—all sections 144
Figure 49. Section 040113 (Arizona) E versus E predicted for section-specific models based on data for all available test dates 247
Figure 50. Section 040114 (Arizona) E versus $E_{predicted}$ for section-specific models based on data for all available test dates 247
Figure 51. Section 091803 (Connecticut) E versus $E_{predicted}$ for section-specific models based on data for all available test dates 248
Figure 52. Section 131031 (Georgia) E versus $E_{predicted}$ for section-specific models based on data for all available test dates..... 248
Figure 53. Section 161010 (Idaho) E versus $E_{predicted}$ for section-specific models based on data for all available test dates..... 249
Figure 54. Section 231026 (Maine) E versus $E_{predicted}$ for section-specific models based on data for all available test dates..... 249
Figure 55. Section 271018 (Minnesota) E versus $E_{predicted}$ for section-specific models based on data for all available test dates 250
Figure 56. Section 331001 (New Hampshire) E versus $E_{predicted}$ for section-specific models based on data for all available test dates 250

Figure 57. Section 351112 (New Mexico) E versus $E_{predicted}$ for section-specific models based on data for all available test dates 251
Figure 58. Section 481077 (Texas) E versus $E_{predicted}$ for section-specific models based on data for all available test dates..... 251
Figure 59. Section 561007 (Wyoming) E versus $E_{predicted}$ for site-specific models based on data for all available test dates..... 252
Figure 60. Section 871622 (Ontario) E versus $E_{predicted}$ for section-specific models based on data for all available test dates..... 252
Figure 61. Section 040113 (Arizona) E versus $E_{predicted}$ for section-specific models based on data for a single test date 253
Figure 62. Section 091803 (Connecticut) E versus $E_{predicted}$ for section-specific models based on data for a single test date 253
Figure 63. Section 271018 (Minnesota) E versus E predicted for section-specific models based on data for a single test date (A (top) and B (bottom)) 254
Figure 64. Section 481077 (Texas) E versus $E_{predicted}$ for section-specific models based on data for a single test date 255
Figure 65. Section 040113 (Arizona) E versus $E_{predicted}$ for section-specific models based on data for two test dates 257
Figure 66. Section 091803 (Connecticut) E versus $E_{predicted}$ for section-specific models based on data for two test dates..... 257
Figure 67. Section 271018 (Minnesota) E versus $E_{predicted}$ for section-specific models based on data for two test dates..... 258
Figure 68. Section 481077 (Texas) E versus $E_{predicted}$ for section-specific models based on data for two test dates 258
Figure 69. Section 040113 (Arizona) E versus E predicted for soil class models 259
Figure 70. Section 040114 (Arizona) E versus E predicted for soil class models 259
Figure 71. Section 091803 (Connecticut) E versus $E_{predicted}$ for soil class models 260
Figure 72. Section 131031 (Georgia) E versus $E_{predicted}$ for soil class models 260
Figure 73. Section 231026 (Maine) E versus $E_{predicted}$ for soil class models..... 261
Figure 74. Section 481077 (Texas) E versus E predicted for soil class models..... 261
Figure 75. Section 871622 (Ontario) E versus $E_{predicted}$ for soil class models..... 262

LIST OF TABLES

Table 1. Difference between laboratory and backcalculated moduli at equivalent stress states, Mr/E 4
Table 2. Subgrade moduli used in the Asphalt Institute DAMA program 7
Table 3. Monthly granular base k1 values used in the Asphalt Institute DAMA program 8
Table 4. Seasonal variations of unbound material moduli for Washington State 8
Table 5. Parameters found to affect laboratory resilient moduli of unbound materials 11
Table 6. Dimensionless constitutive model coefficients for Equations 8 (in kPa (psi)) and 10 (dimensionless) 15
Table 7. Summary of K1 and K2 statistics by aggregate class 19
Table 8. Summary of dimensionless K_1-K_3 parameters for selected materials modeled using Equation 5 20
Table 9. Summary of average elastic coefficients and exponents for LTPP materials modeled using Equation 5 (dimensionless) 20
Table 10. Representative (best fit) regression constants for Equation 17 Mr in MPa 27
Table 11. Representative regression constants for Equation 18 28
Table 12. Regression constants for Equation 21 29
Table 13. Resilient modulus prediction equations developed by Santha 30
Table 14. Titus Glover and Fernando predictive models for constitutive model coefficients 31
Table 15. Predictive equations for Equation 5 constitutive model coefficients as derived by Von Quintus and Killingsworth 32
Table 16. Representative modular ratios 35
Table 17. Seasonal multipliers for base and subgrade soils in Nevada 35
Table 18. Layer thickness ranges for LTPP Seasonal Monitoring Program test sections considered in this investigation 39
Table 19. Distribution of soil classification by pavement layer 39
Table 20. Modulus ranges used in screening of layer moduli (MPa) 42
Table 21. Variation in moduli with applied FWD load by soil class 44
Table 22. Variation in moduli with load for individual A-3 layers 44
Table 23. Pooled single-point within-day variation in moduli by soil class and layer type 46
Table 24. Within-day variation in moduli of A-1-b pavement layers 47
Table 25. Extent of variation in backcalculated moduli by soil class 49
Table 26. Extent of variation in backcalculated moduli by pavement layer 50
Table 27. Volumetric moisture models used in determining moisture content from LTPP TDR data (as reported by Jiang and Tayabji) 59
Table 28. Minimum and maximum estimated errors (95 percent confidence interval) for TDR moisture content prediction models (adapted from Jiang and Tayabji) 60
Table 29. Assumed crack lengths for distresses quantified in terms of area 65
Table 30. LTPP Seasonal Monitoring Program sections used in evaluation of the EICM 68
Table 31. Between-user differences in predicted moisture content for EICM Version 2.6 84
Table 32. Summary statistics for correlation between E and mean layer moisture 94

Table 33. Summary statistics with regard to observed correlation between E and applied FWD load 95
Table 34. Relative strength of correlation between log E and bulk and octahedral shear stress parameters (number of layers and soil classes represented) 96
Table 35. Sign of observed modulus-stress correlation 97
Table 36. Distribution of strongest modulus-stress correlations with respect to stress computation depth 98
Table 37. Change in modulus versus change in moisture content by layer type 99
Table 38. Combinations of K_0 and stress components considered in regression modeling 102
Table 39. Regression coefficients for alternative stress computations 103
Table 40. Log-transformed models used in regression modeling 114
Table 41. Summary of regression coefficients for models 2A and 2B 115
Table 42. Summary of goodness-of-fit statistics for Models 1, 2A and 2B 116
Table 43. Selected soil class models for prediction of pavement layer moduli using linear layered-elastic theory 119
Table 44. Model forms considered for k_1, k_2, and k_3 in Model 2 120
Table 45. Data required for derivation of section/layer-specific models 125
Table 46. Data required to predict backcalculated pavement layer moduli 126
Table 47. Soil parameters required for application of soil class models to predict backcalculated pavement layer moduli 127
Table 48. Modulus ranges 130
Table 49. Data sets considered in trial application of modulus prediction 131
Table 50. Site-specific, limited data set Model 3 and 3B coefficients and goodness-of-fit statistics 133
Table 51. Summary statistics and t-test results for section/layer-specific complete data set model predictions 137
Table 52. Summary statistics and t-test results for section/layer-specific one-date model predictions 141
Table 53. Summary statistics and t-test results for section/layer-specific two-date model predictions 142
Table 54. Summary statistics and t-test results for soil class model predictions 143
Table 55. Pooled within-day standard deviation of volumetric moisture from individual TDR probes (percent) 153
Table 56. Number of test dates considered in computation of pooled standard deviation for individual TDR moisture probes 154
Table 57. Mean number of moisture observations per day considered in computation of within-day standard deviation 155
Table 58. Pooled within-day standard deviation divided by maximum Model 1 error 156
Table 59. Data sets for which individual within-day standard deviations exceed three times the overall pooled value 157
Table 60. Input data and sources for the EICM Versions 2.0 and 2.1 for the Connecticut (091803) and Minnesota (271018) sections 159

Table 61. Input data and sources for EICM Version 2.1 for the Maine (231026), New Hampshire (331001), Vermont (501002), and Manitoba (831801) sections. . 164
Table 62. Input data and sources for EICM Version 2.6 for the Arizona (041024), Colorado (081053), Connecticut (091803), and Georgia (131005) sections. 169
Table 63. Input data and sources for EICM Version 2.6 for the Maine (231026), Minnesota (271018), and New Hampshire (331001) sections 175
Table 64. Input data and sources for EICM Version 2.6 for the Texas (481077), Vermont (501002), and Manitoba (831801) sections..... 181
Table 65. Daily rainfall, temperature, and water table depth input for sections 091803 and 131005 (Connecticut and Georgia)..... 186
Table 66. Daily rainfall, temperature, and water table depth input for sections 231026 and 271018 (Maine and Minnesota)..... 198
Table 67. Initial temperature profile data by section used as input to the EICM..... 210
Table 68. Initial moisture profile data by section used in running EICM Version 2.1 212
Table 69. Between-user differences in the application of EICM Version 2.6 213
Table 70. Material density, relative density, and PI used in soil class models 219
Table 71. Material gradation used in soil class models..... 222
Table 72. Source tables for materials data used in predictive models for backcalculated pavement layer moduli 225
Table 73. Multiple regression results for Model 1 227
Table 74. Multiple regression results for set 1 (both load and overburden with K_0 values of 0.7 and 0.5 for base and subbase/subgrade layers, respectively) 229
Table 75. Multiple regression results for set 2 (overburden only in computation of octahedral shear stress, K_0 values of 0.7 and 0.5 for base and subbase/subgrade layers, respectively) 230
Table 76. Multiple regression results for set 3 (both load and overburden with K_0 values of 1.0 for all layers) 231
Table 77. Multiple regression results for set 4 (both load and overburden with K_0 values of 2.0 and 1.0 for base and subbase/subgrade layers, respectively) 233
Table 78. Multiple regression results for set 5 (octahedral shear stress based on computed for load stresses only, K_0 values of 2.0 and 1.0 for base and subbase/subgrade layers, respectively)..... 235
Table 79. Multiple regression results for set 6 (bulk and octahedral shear stress computed based on load only)..... 236
Table 80. Multiple regression results for set 7 (bulk stress computed based on load stresses only, octahedral shear stress computed based on both load and overburden with K_0 values of 0.7 and 0.5 for base and subbase/subgrade layers, respectively)..... 238
Table 81. Regression results for individual layers using Model 2A 240
Table 82. Regression results for individual layers using Model 2B..... 242
Table 83. Goodness-of-fit statistics for Models 1 and 2 244

CHAPTER 1: INTRODUCTION AND RESEARCH OBJECTIVES

INTRODUCTION

Among the more important considerations in pavement design is the fact that the in situ moduli of the pavement layers vary on a seasonal basis, due to variations in the environmental conditions within the pavement structure. For the sections under study in the Seasonal Monitoring Program[1] of the Long-Term Pavement Performance (LTPP) program, the observed amplitude of seasonal variations in backcalculated moduli for unbound pavement layers, exclusive of frost effects and expressed as a percentage of the minimum observed modulus, ranges from 1 percent to more than 300 percent.

Seasonal variations in pavement layer moduli are important because the deflections, stresses, and strains induced in the pavement by traffic loads, and the resultant incremental damage imparted to the pavement, vary with the moduli of the pavement layers. Unlike most structures, pavements are designed with a finite life expectancy, with design lives greater than 25 to 35 years being the exception, not the rule. The key to cost-effective management of a network of pavements lies in the ability to predict the condition of each pavement at any selected time, and when each will fail (i.e., performance) with a reasonable degree of accuracy and precision. This cannot be achieved without considering the seasonal variations in the pavement layer moduli, and resultant variations in incremental damage.

The work discussed here applied data collected through the Seasonal Monitoring Program of the LTPP program to study the issue of seasonal variations in unbound pavement layers, exclusive of frost effects. Within the Seasonal Monitoring Program, data characterizing both the structural changes in the pavement and the key factors believed to cause those changes are collected monthly. Selected site-specific weather data are collected continuously. The test sections at which these data are collected are geographically dispersed and thus represent a broad array of temperature and moisture conditions prevalent in the United States. Details of test sections and the data used in this investigation are provided in Chapter 3.

RESEARCH OBJECTIVES

The overall goal of this research was to advance the state of the art relative to the estimation of seasonal variations in backcalculated pavement layer moduli for unbound pavement materials under nonfrozen conditions. Four specific objectives, elaborated in the next section, support that goal:

1. Characterizing the extent of variation in backcalculated pavement layer moduli obtained for the LTPP Seasonal Monitoring test sections.

2. Evaluating the moisture prediction capabilities of the Enhanced Integrated Climatic Model (EICM).

3. Developing models to predict backcalculated pavement layer moduli as a function of moisture, stress state, and other pertinent variables.

4. Demonstrating how the results associated with objectives 1–3 may be applied to estimate backcalculated pavement layer moduli for unbound pavement materials.

RESEARCH APPROACH

This study applied data collected via the Seasonal Monitoring Program of the LTPP program to build upon the foundation embodied in the EICM for the prediction of backcalculated pavement layer moduli for unbound pavement layers under nonfrozen conditions. The overall research approach was comprised of four major tasks:

1. Assembly, manipulation and assessment of data from the LTPP Seasonal Monitoring Program. This task is the foundation for all subsequent work. In addition to yielding the data sets used in the subsequent analysis, the data assessment element of this task provided more broadly based information on the extent of seasonal variations in pavement layer moduli than has heretofore been available. This information is of value in its own right, and provides a basis for evaluating the outcome of work toward objectives 3 and 4. Task 1 and its outcomes are discussed in detail in Chapter 3.

2. Evaluation of the moisture-predictive capabilities of the EICM. In this task, LTPP Seasonal Monitoring Program data were applied to evaluate the accuracy of pavement moisture predictions obtained using the EICM. This work was originally undertaken to establish the accuracy of moisture predictions obtained using Version 2.0 of the EICM, and subsequently evolved to include evaluation of Versions 2.1 and 2.6 of the EICM, as well. A detailed discussion of task 2 is in Chapter 4.

3. Development of models to predict backcalculated layer moduli for unbound materials. This task sought to provide the "missing link" between the moisture predictions obtained with the EICM and the desired end result—estimates of layer moduli on a seasonal basis. A detailed discussion of task 3 is in Chapter 5.

4. Trial application of the regression models developed in task 3 to demonstrate their use in estimating seasonal variations in unbound pavement layers. In this task, a procedure for applying the outcome of task 3 was proposed and applied to predict pavement layer moduli for several test sections representing varying climatic conditions. The procedures and results obtained in task 4 trial applications are in Chapter 6.

Overall conclusion and recommendations drawn from this study are presented in Chapter 7.

CHAPTER 2: LITERATURE REVIEW

INTRODUCTION

As noted previously, this investigation is concerned with the seasonal variations exclusive of frost effects that occur in the moduli of the unbound base, subbase, and subgrade materials within pavement structures. To provide the context for this investigation, a brief discussion of the different methods of determining moduli for unbound pavement materials is followed by an overview of the means by which seasonal variations are addressed in the pavement design and evaluation process. Subsequent sections address the factors that influence the moduli of unbound pavement materials, efforts to develop relationships between those factors and moduli, the findings of field investigations of seasonal variations, related investigations, and existing environmental-effects models applicable to pavements.

SOIL MODULUS: M_r VERSUS E

The modulus of a material is a measure of stiffness, by definition, the ratio of stress to strain. The term modulus, by itself, is used here in the generic sense, and carries with it no implication as to how it was determined. In pavement engineering practice, several primary methods are used to determine the moduli of unbound pavement materials. The first is the laboratory resilient modulus, or M_r test. Another approach is to interpret nondestructive pavement deflection data through a process known as backcalculation to estimate the in situ moduli of the layer materials. The notation E (for Elastic modulus) is commonly used to refer to backcalculated moduli, and that convention will be used here, whereas the notation M_r will be used exclusively for the laboratory test result.

While M_r and E are used to characterize pavement stiffness for the same general purposes, it is important to understand that quantitative differences in magnitude may exist between these parameters. Numerical differences between E and M_r (for nominally the same materials) are well documented in the literature, as will be discussed in the next several paragraphs.

Lee, Mahoney, and Jackson compared layer moduli backcalculated using the EVERCALC program with those obtained via laboratory resilient modulus testing for 5 base layers and 16 subgrade soils at "similar stress states."[2] They reported differences in the range of 0 to 36 percent for the five base layers, with the lab moduli being consistently greater than the backcalculated moduli. Moisture content differences in the range of –0.3 to 1.0 percent (lab - backcalculated) may have contributed to the observed differences. For the subgrade layers, differences in the range of –2 to +84 percent were observed. For 11 of the 16 soils, the backcalculated moduli were greater than the lab values. As with the base layer moduli, differences in moisture content in the range of –2.2 to 4.2 percent probably contributed to the observed differences.

Daleiden et al. report a mean ratio of laboratory resilient moduli to backcalculated subgrade modulus of 0.57.[3] The corresponding standard deviation and ranges were 0.67 and 0.01 to 10.34, respectively. The data used in their analysis were from LTPP test sections in the southern and north Atlantic regions.

The authors of the 1993 *AASHTO Guide for Design of Pavement Structures* (1993 guide) suggest that moduli backcalculated for fine-grained subgrade soils should be multiplied by an adjustment factor, C, not greater than 0.33 to approximate values obtained in laboratory testing.[4] They further state that the relationships between laboratory and backcalculated moduli may differ for granular materials, and that this subject requires further research.

Von Quintus and Killingsworth sought to improve upon the guidance provided in the 1993 Guide through analysis of LTPP data.[5] They reported the results presented in Table 1. The MODULUS program was used in the backcalculation for this analysis.

Table 1. Difference between laboratory and backcalculated moduli at equivalent stress states, Mr/E[5]

Layer Description	Mean	Standard Deviation	Coefficient of Variation, %
Granular base/subbase under a PCC surface	1.32	0.978	74.1
Granular base/subbase above a stabilized material	1.43	1.14	79.9
Granular base/subbase under an asphalt concrete surface/base	0.62	0.271	43.8
Subgrade soil under a stabilized subgrade	0.75	0.095	12.7
Subgrade soil under a pavement without a granular base/subbase	0.52	0.180	34.6
Subgrade soil under a pavement with a granular base/subbase	0.35	0.183	52.2

Overall, the literature suggests that backcalculated base and subbase layer moduli tend to be less than the corresponding laboratory values, while moduli for subgrade layers tend to be greater than the lab values, though exceptions do occur. M_r/E ratios in the range of 0.35 to 1.42 are typical, with the higher values corresponding to base layers, and the smaller end of the range representing subgrade layers.

A number of factors contribute to the observed differences between M_r and E. Whereas the laboratory resilient modulus, M_r, is appropriately termed a material property (a readily measured characteristic of a well-defined material sample), the backcalculated modulus, E, is not. The

value of E depends not only on the "true" in situ characteristics of the material comprising the layer (including, but not limited to, stress state and moisture content), but also on the theoretical model used to derive (backcalculate) the value, the limitations of that model, and the details of the application of that model. Further discussion of issues related to the backcalculation process is provided in later sections of this chapter, and in Chapter 3. Other factors that may contribute to the reported differences include differences between the moisture, compaction, and confining conditions of the materials at the time of testing.

ADDRESSING SEASONAL VARIATIONS IN PAVEMENT DESIGN AND EVALUATION

The degree to which seasonal variations in unbound pavement materials have been addressed in pavement design and evaluation, and the approaches taken to addressing them, are widely varied. Historically, the more widely known pavement design and evaluation procedures have provided for consideration of seasonal variations only indirectly. For example, early versions of the AASHTO pavement design procedure used a "regional factor" to adjust the design structural capacity of the pavement for climatic conditions more or less severe than those present at the AASHO Road Test, but did not directly address seasonal variations in the pavement structure.[6]

The 1986 *AASHTO Guide for Design of Pavement Structures* (1986 guide) was a watershed in relation to the treatment of environmental effects in pavement design: It was the first widely used pavement design methodology to incorporate explicit consideration of site-specific seasonal variations in the stiffness of the subgrade soil, through the effective subgrade soil resilient modulus.[7] Conceptually, the effective subgrade soil resilient modulus is a damage-weighted average. A nomographic solution is provided for the determination of the relative damage, u_f. This approach was retained in the 1993 guide.

One limitation of the 1986 guide (and the 1993 guide as well) is that it makes no explicit provision for consideration of seasonal variations in the overlying pavement layers. Furthermore, incomplete knowledge of the magnitude and duration of the subgrade modulus fluctuations that occur, and the manner in which they vary as a function of location, materials, and other factors, made it difficult for highway agencies to take full advantage of this advance.

Recognition of the need for explicit consideration of seasonal variations in the structural characteristics of pavement materials has paralleled, if not arisen from, the development of mechanistically-based approaches to pavement design and evaluation. Within this context, the ultimate approach to considering seasonal variations is to divide the design period into "n" discrete periods, such that the pavement structure and loading conditions within a given period may be treated as constant. Cumulative damage concepts are applied to sum the damage caused to the pavement in each period (i.e., each combination of pavement structure and loading conditions) to obtain an estimate of the total damage induced over the design life.

Month	Roadbed Soil Modulus, M_r	Relative Damage, u_f
January	137,895 kPA (20,000 psi)	0.01
February	137,895 kPa (20,000 psi)	0.01
March	17,237 kPa (2,500 psi)	1.51
April	27,579 kPa (4,000 psi)	0.51
May	27,579 kPa (4,000 psi)	0.51
June	48,263 kPa (7,000 psi)	0.13
July	48,263 kPa (7,000 psi)	0.13
August	48,263 kPa (7,000 psi)	0.13
September	48,263 kPa (7,000 psi)	0.13
October	48,263 kPa (7,000 psi)	0.13
November	27,579 kPa (4,000 psi)	0.51
December	137,895 kPa (20,000 psi)	0.01
Summation: $\sum u_f$ =		3.72

Average u_f: = $\sum u_f/n$ =0.31

Effective roadbed soil resilient modulus, M_r kPa (psi) = 34,474 (5,000) (corresponds to average u_f)

$u_f = 1.18 \times 10^{83.72} M_r^{-2.32}$

Figure 1. Chart for estimating effective roadbed soil resilient modulus for flexible pavements designed using the serviceability criteria [4]

With modern computing capabilities, the approach is straightforward and provides an easy mechanism to account for and explain differences in pavement performance that occur as a result of environmentally induced variations in the structural characteristics of pavement materials. This general methodology has been implemented by several researchers. (See references 8, 9, 10, 11.) The number of discrete periods considered ranges from 4 (i.e., the 4 seasons) to 12 (1 per month).

Within the ninth edition of the Asphalt Institute's procedure for design of flexible pavements (known as MS-1), seasonal variations are considered by way of three representative temperature regimes defined by the mean annual air temperatures (MAAT) of 7 °C, 15.5 °C, and 24 °C.[12] Separate design charts are provided for each temperature regime. In developing the design charts for the 7 °C and 15.5 °C temperature regimes, the subgrade modulus and the k_1 coefficient in the constitutive model $M_r = k_1\theta^{k2}$ for the granular base layer were varied on a monthly basis (within a cumulative damage framework) to reflect the effects of freezing, thawing, and recovery, while

the moduli for the asphalt bound layers were varied as a function of the mean monthly temperature. The monthly values used for the granular base and subgrade layers are presented in Table 2 and Table 3, respectively. Values for December are equal to the "normal" values used to define the quality of the material under consideration.

Treatment of seasonal variations in the U.S. Air Force design procedure is similar to that in MS-1, in that design temperatures are used to determine monthly values for the asphalt concrete (AC) modulus.[13] However, only two subgrade soil conditions are considered: normal and thawed. As in the development of MS-1, the variations in modulus are considered within a cumulative damage framework.

Table 2. Subgrade moduli used in the Asphalt Institute DAMA program [12]

MAAT °C/ Normal M_r	Subgrade Modulus (by month), 10^3											
	Dec	**Jan**	**Feb**	**Mar**	**Apr**	**May**	**June**	**July**	**Aug**	**Sept**	**Oct**	**Nov**
7 4.5	4.5	15.9	27.3	38.7	50.0	0.9	1.62	2.34	3.06	3.78	4.5	4.5
7 12.0	12.0	21.5	31.0	40.5	50.0	6.0	7.2	8.40	9.6	10.8	12.0	12.0
7 22.5	22.5	29.4	36.3	43.1	50.0	15.8	17.1	18.5	19.8	21.2	22.5	22.5
15.5 4.5	4.5	4.5	27.3	5.0	1.35	2.14	2.93	3.71	4.5	4.5	4.5	4.5
15.5 12.0	12.0	12.0	31.0	50.0	7.2	8.4	9.6	10.8	12.0	12.0	12.0	12.0
15.5 22.5	22.5	22.5	38.3	50.0	18.0	19.1	20.3	21.4	22.5	22.5	22.5	2.5

Table 3. Monthly granular base k1 values used in the Asphalt Institute DAMA program[12]

MAAT °C Normal M_r	Monthly Value for $k_1 10^3$, $M_r = k_1\theta^{k2}$, $k_2 = 0.5$, M_r in kPa (psi)											
	Dec	**Jan**	**Feb**	**Mar**	**Apr**	**May**	**June**	**July**	**Aug**	**Sept**	**Oct**	**Nov**
7 8.0	8.0	12.0	16.0	20.0	24.0	2.0	3.2	4.4	5.6	6.8	8.0	8.0
7 12.0	12.0	18.0	24.0	30.0	36.0	3.0	4.8	6.6	8.4	10.2	12.0	12.0
15.5 8.0	8.0	16.0	24.0	2.0	3.5	5.0	6.5	8.0	8.0	8.0	8.0	8.0
15.5 12.0	12.0	24.0	36.0	3.0	5.25	7.5	9.75	12.0	12.0	12.0	12.0	12.0

A common limitation in much of the work done to date, including the 1993 AASHTO guide, is the absence of significant, broadly applicable, and well supported quantitative guidance as to appropriate design values—seasonal or otherwise—to use for base, subbase, and subgrade layers. Definitive guidance in this regard has been developed, but is generally limited with respect to the geographic range over which it is valid. For example, the developers of the mechanistic-empirical overlay design procedure used in the State of Washington have established a set of seasonal factors describing the relative seasonal moduli for typical Washington State base and subgrade materials for each of the two major environmental zones present in the State.[14,15] These factors, summarized in Table 4, may be used to estimate the moduli for different seasonal conditions using the modulus for any one condition as a starting point. For example, if one knows the modulus of the material in question under dry conditions, one can estimate the modulus of that material under wet conditions by multiplying the dry value by the wet/thaw factor for the material type and environmental zone in question.

Table 4. Seasonal variations of unbound material moduli for Washington State[15]

	Base		Subgrade	
Region	**Wet/Thaw**	**Dry/Other**	**Wet/Thaw**	**Dry/Other**
Eastern	0.65	1.00	0.95	1.00
Western	0.80	1.00	0.90	1.00

The seasonal factor approach to considering seasonal variations presumes substantial uniformity in the materials used and the environmental conditions present within each region for which seasonal factors are identified. It does not obviate the need for basic knowledge. Rather, it represents an approach to using that knowledge, once it becomes available. Further, while the *approach* is "transportable," the *results* (seasonal adjustment factors) are not. Hence, these and other "local" solutions are insufficient to address fully the general need to characterize, quantitatively, the magnitude and timing of seasonal fluctuations in the moduli of unbound

pavement materials. More broadly applicable information is key to both effective use of the most widely accepted existing pavement design procedure (the 1993 AASHTO guide) and the development and use of improved pavement design and performance prediction procedures.

The state of the art with respect to consideration of seasonal variations in pavement performance modeling is reflected in the development of the *2002 Guide for Design of New and Rehabilitated Pavement Structures*, currently ongoing through National Cooperative Highway Research Program (NCHRP) project 1-37A. (See references 16, 17, 18, 19). In this work, the EICM simulation model is used to provide predictions of climatic conditions (temperature, moisture, and frost) within the pavement structure as they vary with time. For unbound materials, the moisture prediction output of the EICM is used in models relating M_r change to changes in moisture to estimate the change in M_r from the initial as-constructed condition to the equilibrium condition. The specific relationship used is seen in Equation 1:

$$\log \frac{M_r}{M_{ropt}} = a + \frac{b-a}{1 + EXP(\beta + k_s * (S - S_{opt}))}$$
$$a = \min(\log(M_r / M_{ropt}))$$
$$b = \max(\log(M_r / M_{ropt}))$$
$$\beta = \ln(-b/a) \qquad (1)$$

In this relationship, M_{ropt} and S_{opt}, are the resilient modulus and degree of saturation for the laboratory optimum moisture and density condition, while S is the degree of saturation for the moisture condition associated with M_r. This relationship is discussed further in the next section, under the subheading "Moisture Conditions." The EICM predictions of freezing and thawing are used to determine when freezing and thawing occur, so that appropriate modulus values may be assigned; predictions of the soil moisture suction are used to determine the extent of recovery, and in turn, the modulus at a given time after thaw has occurred, but before full recovery.

In summary, over the past 40 years, approaches to considering seasonal variations in the pavement design process have advanced from the use of purely empirical regional adjustment factors that do not explicitly address the issue of seasonal variations to explicit methods which relate changes in modulus to the factors that cause those changes. The latter approach is embodied in the development of the *2002 Guide for Design of New and Rehabilitated Pavement Structures*.

FACTORS INFLUENCING THE MODULI OF UNBOUND PAVEMENT MATERIALS

Many factors affect the moduli of unbound pavement materials. Some are inherent to the materials themselves; others are associated with the environment in which the materials exist or the loading or stress conditions to which they are subjected. The factors found to be important in a number of laboratory investigations are summarized in Table 5. At first glance, there is considerable variation in the specific parameters considered. However, when one takes into consideration differences in the scope of the various investigations (i.e., whether the investigator was looking at a single crushed aggregate, or an assortment of fine-grained and granular materials), and the relationships between the different variables identified, there is more consensus than disagreement. Specifically, there is broad agreement that the most important factors include stress conditions, moisture conditions (most often characterized by the degree of saturation), density, and material characteristics (gradation or fines content, angularity, plasticity). Although rarely addressed in the laboratory setting, frost and thaw effects are critical when in situ conditions are considered for areas subject to freezing.

Stress Conditions

Stress conditions are generally regarded as the most important influence on resilient behavior of granular and fine-grained materials. Most often, the behavior of granular soils has been found to vary primarily as a function of the bulk stress (first stress invariant), while the applied deviator stress has been found to be more important for fine-grained soils. The stress-sensitive nature of the resilient modulus of granular materials has traditionally been characterized by Equation 2.

$$M_r = K_1 \theta^{K_2} \tag{2}$$

where θ is the bulk stress (i.e., the sum of the principal stresses), and K_1 and K_2 are regression constants, or a variant of Equation 2, in which the confining pressure is used in place of the bulk stress.

For the bulk stress model (Equation 2), reported values for K_1 range from about 4,826 to well over 689,476 kPa (700 to well over 100,000 psi), depending on material type.[20] Most unbound pavement materials have K_1 values in the range of 10,342 to 82,737 kPa (1500 to 12,000 psi). Corresponding values for K_2 range from about 0.3 to 0.7, with 0.5 being a reasonable representative value.

The resilient modulus of fine-grained materials has more often been characterized by Equation 3.

$$M_r = k_1 \sigma_d^{-k_2} \tag{3}$$

where σ_d is the applied deviator stress and k_1 and k_2 are regression constants. Note that the negative sign on the k_2 coefficient in Equation 3 implies stress softening behavior (which is typical of fine-grained soils), whereas stress-hardening behavior is more often observed in granular materials.

Table 5. Parameters found to affect laboratory resilient moduli of unbound materials

Material Type	Material Parameters	Stress Parameter(s)	Authors
Fine-grained	Age, compaction method, density, water content	Repeated stress	Monismith et al.[21]
Granular	Type and gradation, void ratio, % saturation	Confining pressure	
Granular	Density, % passing 200, aggregate type, % saturation	Confining pressure or bulk stress	Hicks and Monismith [22]
Granular	Density, gradation, aggregate type, % saturation, degree of crushing	Confining pressure, bulk stress	Monismith et al.[23]
Subgrade	% saturation, volume moisture content, plasticity index (PI), group index, % silt, % clay, California Bearing Ratio (CBR), % swell, specific gravity, % organic carbon	Deviator stress	Thompson and Robnett[24]
Clays	Initial and final suction, saturation, volume moisture content, volume soil content[25]	Deviator stress, mean stress, no. of load cycles	Edris and Lytton[25]
Granular	Degree of saturation, degree of compaction, gradation	Bulk stress	Rada and Witczak[26]
Granular	Moisture tension, dry density, temperature	Bulk stress or second stress invariant and octahedral shear stress	Cole, Irwin, and Johnson[27]
Base and subgrade	Dry density, moisture content, % passing 200, consolidation ratio	2nd stress invariant and oct. shear stress (base); cyclic dev. stress and maximum shear stress (subgrade)	Ishibashi, Irwin, and Lee [28]

Table 5. Parameters found to affect laboratory resilient moduli of unbound materials, continued

Material Type	Material Parameters	Stress Parameter(s)	Authors
Granular	Soil type, moisture tension, frozen, and total water content, temperature, dry unit weight, state with respect to freeze/thaw	bulk stress or second stress invariant/octahedral shear stress	Cole, Johnson, et al [29,30,31,32]
Subgrade	Not investigated as such	Saturated soil: efficiency. Confining stress and deviation. Stress; unsaturated soil: net confining stress, matric suction, and deviation Stress	Fredlund and Rahardjo[33]
Base and subgrade	Soil type, % saturation, grain-size distribution, density	Bulk stress due to overburden, bulk stress due to load and overburden, octahedral shear stress, anisotropic consolidation ratio	Yang[34]
Granular base	Gradation, material type	Bulk stress	Thompson and Smith [35]
Fine-grained	Moisture Content, plasticity index, relative density, sample age	Confining pressure	Pezo et al.[36]
Granular and cohesive	Moisture Content, optimum Moisture Content, % saturation, compaction, gradation, % swell, % shrinkage, density, CBR	Granular: bulk stress and cyclic deviation. Stress Cohesive: cyclic deviation. Stress	Santha [37]
Coarse-grained	Density, gradation, moisture cont., type	Bulk stress	Kolisoja[38]
Granular	Moisture content, temperature, dry density	Bulk stress	Jin et al.[39]
Fine-grained	Dry density, moisture content, soil type	Deviator stress	Li and Selig[40]
Granular and fine-grained	Suction, Dielectric constant, gradation, Atterberg limits	Bulk stress and octahedral shear stress	Titus-Glover and Fernando [41]

Equation 4 has also been used to characterize the resilient behavior of fine-grained materials.

$$M_r = K_2 + K_3[K_1 - (\sigma_1 - \sigma_3)] \quad for\ K_1 > (\sigma_1 - \sigma_3)$$
$$M_r = K_2 + K_4[(\sigma_1 - \sigma_3) - K_1] \quad for\ K_1 < (\sigma_1 - \sigma_3) \tag{4}$$

In Equation 4, σ_1 and σ_3 are the major and minor principal stresses, respectively, and the K_n values are regression constants, as before.[42]

Brown and Pappin note that use of Equation 2 in pavement analysis is likely to lead to inaccurate results due to the limited range of stress paths considered in its development.[20] They further point out the need to consider effective stresses (as opposed to total stresses) in modeling the behavior of saturated or partially saturated soils, particularly those that are fine grained.

Uzan evaluated Equation 2, finding that it does not adequately describe the behavior of granular materials.[43] He further found that the relationship described by Equation (5).

$$M_r = K_1 p_a \left[\frac{\theta}{p_a}\right]^{K_2} \left[\frac{\sigma_d}{p_a}\right]^{K_3} \tag{5}$$

in which θ is the bulk stress and σ_d is the dynamic deviatoric stress, results in better agreement with observed behavior. (p_a is atmospheric pressure, introduced to make the relationship independent of the system of measurements.)

Ishibashi et al. explored a number of constitutive models with regard to their ability to explain the resilient behavior of several fine-grained and granular materials.[28] An unusual aspect of their work was the consideration of anisotropic as well as isotropic consolidation. This is important because the anisotropic consolidation state, although rarely addressed in laboratory testing, may be a more accurate representation of the in situ condition of the pavement materials. Further, the effect of the consolidation ratio was found to be quite significant. For the four soils considered, they found that Equations 6 and 7 were well suited to explain the behavior of granular and fine-grained materials, respectively.

$$\frac{M_r}{k_c^n} = K_1 \left[\frac{J_2}{\tau_{oct}}\right]^{K_2} \tag{6}$$

$$\frac{M_r}{k_c^n} = K_3 \left[\frac{\sigma_d}{\tau_f}\right]^{K_4} \tag{7}$$

In these equations, J_2 is the second stress invariant ($\sigma_1\sigma_2 + \sigma_2\sigma_3 + \sigma_3\sigma_1$), σ_d is the repeated deviatoric stress, τ_{oct} is the octahedral shear stress ($1/3[(\sigma_1-\sigma_2)^2 + (\sigma_2-\sigma_3)^2 + (\sigma_3-\sigma_1)^2]^{1/2}$), τ_f is the maximum shear stress, k_c is the consolidation ratio (vertical consolidation stress divided by horizontal consolidation stress, or $1/k_0$), and K_1, K_2, K_3, K_4, and n are regression constants. Reported values for K_1 and K_2 were in the range of 11,032 to 64,121 kPa (1,600 to 9,300 psi) and 0.14 to .61, respectively, while K_3 and K_4 values of 68,948 to 147,548 kPa (10,000 to 21,400

psi) and -0.25 to -0.60, respectively, were obtained. The value of n was found to be approximately 1.5 for the granular materials modeled with Equation 6, and 0.5 for Equation 7 (fine-grained soils), indicating that the consolidation ratio has a greater effect on the behavior of the granular materials than on the fine-grained materials. However, this analysis neglected the influence of several key factors.

Subsequently, Yang[34] conducted a more complete analysis of the same data set considered by Ishibashi et al.[28] In this analysis, Yang used Equation 8, which is applicable to both fine-grained and granular materials.

$$E_r = k_1(\theta_{l_0}^2 + \theta_{l_P}^2)^{k_2}(1+\tau_{oct})^{k_3}k_c^{k_4} \tag{8}$$

In this model, θ_{l_0} is the bulk stress due to overburden only; and θ_{l_p} is the bulk stress due to overburden and load. Other variables are as previously defined. In contrast to the n values reported by Ishibashi et al., Yang obtained k_4 values of 0.83 and 0.91 for the granular materials; 0.52 and 0.51 for the fine-grained materials; and 0.69 for the combined data set. These values for k_4 are believed to more accurately reflect the true influence of the consolidation ratio than the n values obtained by Ishibashi et al., by virtue of the fact that more of the other influential factors were accounted for in the analysis. This work will be discussed in greater detail later in this chapter.

Santha conducted an investigation of the resilient moduli of 45 granular soils, in which he compared Equation 2 with Equation 5.[37] His results support Uzan's conclusion that Equation 5 is superior to Equation 2 in describing the behavior of granular soils. For Equation 5, he reported K_1 values ranging from 130 to 918, with a mean of 421; K_2 values of 0.145 to 0.479 (mean 0.33) and K_3 values of −0.152 to −0.574 (mean −0.37). (All coefficients are dimensionless.) Thus, the moduli decrease with increasing repeated vertical (deviator) stress (negative K_3), and increase with increasing bulk stress (positive K_2).

In his study of the resilient behavior of 42 cohesive soils, Santha used Equation 9.

$$M_r = K_1 P_a \left[\frac{\sigma_d}{P_a}\right]^{K_3} \tag{9}$$

Note that Equation 9 is a special case of Equation 5, in which K_2, the coefficient of the bulk stress term, is taken to be zero (i.e., modulus is independent of the bulk stress). For the cohesive soils, Santha reports K_1 values ranging from 188 to 1,263, with a mean of 645; and K_3 values of -0.07 to -0.60, with a mean of -0.026. (All coefficients are dimensionless.)

Witczak and Uzan[44] evaluated several constitutive relationships, including equations (8) and (10), by applying each to the laboratory test data previously developed by Rada and Witczak[26].

$$M_r = (k_1 p_a)\left(\frac{\theta}{p_a}\right)^{k_2}\left(\frac{\tau_{oct}}{p_a}\right)^{k_3} \tag{10}$$

They found that equations (8) and (10) fit the observed material behavior far more closely than any other constitutive model form evaluated. The coefficients obtained for these models for the materials investigated are summarized in Table 6. As with Equations 5 and 8 (and unlike Equations 2, 3, 4, 6, 7, and 9), Equation 10 has the advantage of being applicable to both granular and fine-grained materials. The data set used in this investigation did not address the issue of anisotropic consolidation, so no evaluation of that aspect of Equation 8 was possible.

Table 6. Dimensionless constitutive model coefficients for Equations 8 (in kPa (psi)) and 10 (dimensionless)[44]

Model	Ln K_1	K_2	K_3
7	8.2 to 9.5	0.15 to 0.5	-0.4 to 0.3
9	5.5 to 6.4	0.5 to 0.95	-0.5 to 0.1

Von Quintus and Killingsworth also concluded that Equation 10 is well suited to the characterization of the stress sensitivity of laboratory resilient moduli.[5] More details regarding their work in this regard are presented under "Material Characteristics."

More recently, Andrei evaluated fourteen different constitutive model forms.[45] The models considered ranged from single-variable (θ or τ), two-parameter models to the general two-variable, five-parameter model given in Equation 11, and several special cases of the latter.

$$M_r = K_1 P_a \left(\frac{\theta - 3k_6}{P_a} \right)^{k_2} \left(\frac{\tau_{oct}}{P_a} + k_7 \right)^{k_3} \quad (11)$$

$k_1, k_2 \geq 0$
$k_3, k_6 \leq 0$
$k_7 \geq 1$

Both log-log and semi-log model forms were considered in Andrei's work. He concluded that Equation 11 yielded the best overall fit of the evaluation data set, with the proviso that the regression constants must be constrained, as noted, to ensure rationality.

Other stress- or load-related parameters that have been investigated with regard to their influence on the resilient behavior of granular and/or fine-grained materials in the laboratory include the number of stress applications and the loading sequence (duration of stress application and rest periods). (See references 21, 23, 26, 28.) The effect of variations in the loading sequence has generally been found to be small in comparison to other factors.[26,28] Similarly, as long as the number of load applications is great enough that the material being tested has reached an equilibrium state (as would be the case for moderate to high volume pavements), the effect of number of load applications is not especially significant.[23,26,28]

Moisture Conditions

Moisture is generally regarded as being second only to stress conditions in its influence on the moduli of unbound pavement materials, with increases in moisture content typically resulting in significant reductions in the resilient modulus of the soil. (See references 21-26, 34, 36-40) Monismith et al. note that the modulus of a fully saturated material may be as much as 50 percent lower than that of the same soil in a partially saturated condition.[21] However, Chou suggests that the general trend of decreasing modulus with increasing moisture content is much less significant when effective stress conditions rather than total confining pressures are used as the basis of comparison.[42]

For "typical" Illinois fine-grained soils, Thompson and Robnett studied the effect of degree of saturation on resilient modulus.[24] For saturation (S_r) ranging from 50 to 100 percent, and densities corresponding to 95 and 100 percent of AASHTO T-99 compaction, they obtained the relationships given in Equations 12 and 13, respectively (M_r in units of kPa (ksi)).

$$M_r = 45.2 - 0.428\, S_r \tag{12}$$

$$M_r = 32.9 - 0.334\, S_r \tag{13}$$

Thus, as the degree of saturation varies from 50 to 100 percent, the predicted resilient modulus decreases by roughly an order of magnitude. This work considered total (as opposed to effective) stress conditions.

Rada and Witczak note that the reduction in stiffness of granular materials with increasing moisture content is especially significant at degrees of saturation in excess of 80–85 percent, where a rapid loss of stiffness occurs with increasing saturation.[26] However, the magnitude of this effect varies from one material to another. Kolisoja's results appear to differ somewhat, in that the resilient modulus increases with increasing saturation up to 35–45 percent, and falls off gradually thereafter.[38] However, the maximum degree of saturation investigated by Kolisoja was 77 percent. Hence, the behavior of the soils in question as they approach the fully saturated condition is not known.

Noureldin conducted an investigation of (among other things) the effect of changes in moisture content on the (backcalculated) moduli of granular base and subgrade materials for one test site in Saudi Arabia, with all other factors (for all practical purposes) held constant.[46] For this site, he found that an increase in the base course moisture content from 5 to 9 percent (4 percent increase) corresponded to a 22.4 percent reduction in the modulus. The corresponding increase in moisture content for the subgrade was from 6.8 to 13 percent (6.2 percent increase) accompanied by a 35 percent reduction in the modulus.

Ksaibati et al. looked at the effect of moisture on backcalculated moduli for highway pavement base and subgrade materials in Florida.[47] They observed modulus changes of up to 96 percent as the moisture content varied, with the magnitude of the change depending on the deflection

testing device (falling weight deflectometer (FWD) or Dynaflect) used to obtain the data. However, based on the discussion provided, it appears that the potential for changes in modulus due to stress state variations arising from temperature-induced variations in the stiffness of the overlying AC layers was not considered. Thus, the author believes that some portion of the observed variation may in fact be attributable to stress sensitivity, as opposed to pure moisture effects.

Whereas most researchers have characterized moisture conditions on the basis of moisture content or degree of saturation, Edris and Lytton used soil suction, which is related to moisture content and saturation, along with the internal stress state of the soil.[25] Although there is a tremendous amount of scatter in the data presented, the general trend is for the modulus to increase with increasing suction up to a point, and then level off. Although the authors assert that suction is a more appropriate parameter than moisture content or degree of saturation for use in characterizing the effect of moisture conditions on resilient behavior, the data presented do not appear to support that assertion. While no goodness of fit statistics are presented, the graphical presentations of the data show much less scatter, and much clearer trends when either moisture content or degree of saturation, rather than suction, is used as the explanatory variable. Titus-Glover and Fernando also used suction (as well as moisture content and saturation) as an explanatory variable in their development of regression models to predict the coefficients for Equation 5.[41] The set of models selected as being best included the suction term as an explanatory variable for K_1, but not for K_2 or K_3. This work is discussed in more detail under "Relating Resilient Moduli To Material Parameters."

Recent work by Witczak, Andrei, and Houston examined the laboratory modulus-moisture data assembled and used in a number of earlier research efforts, and found relationships of the general form presented in Equation 14,

$$\log \frac{M_r}{M_{rref}} = k_w * (m - m_{ref}) \tag{14}$$

with M_{rref} being the resilient modulus at a reference moisture state represented by m_{ref}, and m being the moisture state associated with M_r. [16] They considered both gravimetric moisture content and degree of saturation as the variables used to characterize moisture state (m), and recommend the use of degree of saturation, because data errors are more readily identified when degree of saturation is considered. They also recommend use of the laboratory optimum condition for the reference values. Witczak et al. developed the modified model presented as Equation 15 because the laboratory data set on which Equation 14 is based was composed entirely of test results within ±30 percent of optimum, whereas field data indicate that lesser degrees of saturation often occur in practice.

$$\begin{aligned} \log \frac{M_r}{M_{rref}} &= a + \frac{b - a}{1 + EXP(\beta + k_s * (S - S_{opt}))} \\ a &= \min(\log(M_r / M_{ropt})) \\ b &= \max(\log(M_r / M_{ropt})) \\ \beta &= \ln(-b / a) \end{aligned} \tag{15}$$

This relationship is being used in the 2002 AASHTO Guide.

Density and Soil Structure

Some measure of density has been considered in most investigations of the factors affecting the resilient behavior of granular and fine-grained materials. (See references 21-23, 26-28, 34, 36-40.) Among the parameters considered are density, degree of compaction (relative to Standard Proctor density, for example) or compaction energy, and void content. Although density affects the moduli of both granular and fine-grained materials, it has been found that the magnitude of this effect is small in comparison to those of stress and moisture conditions. This is especially true when density variations are small.

For granular soils, resilient modulus tends to increase with increasing density. Further, this general trend is relatively independent of moisture content or degree of saturation.[22,23,29] Hicks and Monismith found that for granular materials, the influence of changes in density decreased as the percent fines increased.[22] It has also been found that the effect of variations in density is greater for partially crushed aggregate than for crushed aggregate.[23]
For fine-grained soils, the resilient modulus may increase or decrease with increasing density, depending on the moisture conditions.[40] Wetter than optimum, the modulus tends to decrease with increasing density; whereas, dryer than optimum, the trend is for modulus to increase with increasing density. In addition, soils having a flocculated structure (typically resulting from static compaction methods) tend to have higher moduli than those having a dispersed structure (from, for example, kneading compaction).[28]

Material Characteristics

When one considers the many factors (such as gradation, mineralogy, angularity, surface roughness, and plasticity) that make one soil different from another, it is intuitive that material characteristics will have an effect on the moduli of the materials. Evidence that this is indeed the case may be found in work by Rada and Witczak [26] and Titus-Glover and Fernando,[41] among others. Key results from Rada and Witczak's investigation of the resilient behavior of a broad array of granular materials are presented in Table 7. The coefficients given in the table are for the bulk stress model (Equation 2). Note that the mean values for the different classes vary considerably, and that even within a given aggregate class, K_1 values may vary by more than an order of magnitude. While some of this variation is more than likely attributable to differences in moisture conditions and density, it is reasonable to assume that much of it is attributable to differences in other material characteristics.

The results obtained by Titus-Glover and Fernando when they applied Equation 5 to test results for a somewhat broader array of material types are summarized in Table 8.[41] The testing from which these results were derived was conducted at the optimum moisture content for each material, which ranged from 3.97 percent for the sand to 19.76 percent for the fat clay. As with the results of Rada and Witczak, there is considerable variation in the model coefficients between the material types.

More recently, Von Quintus and Killingsworth obtained the results presented in Table 9 for laboratory test results from 125 LTPP test sections, evaluated using Equation 5.[5] They report that average R^2 values of 0.85 or greater were obtained in all cases. Substantial, differences are observed between many of the mean values presented in Table 9 and those presented in Table 8. However, most of the Table 8 values fall within the ranges reported in Table 9 for comparable materials. The between-material variability reflected in the ranges and standard deviations (SD) reported in Table 9 is very high.

Table 7. Summary of K1 and K2 statistics by aggregate class [26]

Aggregate Class	No. of Data Points	K_1 Parameter (kPa (psi))			K_2 Parameter		
		Mean	SD	Range	Mean	SD	Range
Silty sands	8	11,170 (1620)	5,378 (780)	4,895 to 26,407 (710 to 3830)	0.62	13	0.36 to 0.80
Sand gravel	37	33,646 (4480)	29,647 (4300)	5,929 to 88,529 (860 to 12840)	0.53	17	0.24 to 0.80
Sand-aggregate blends	78	29,992 (4350)	18,133 (2630)	12,962 to 76,325 (1880 to 11070)	0.59	13	0.23 to 0.82
Crushed stone	115	49,711 (7210)	51,642 (7490)	11,756 to 390,726 (1705 to 56670)	0.45	23	−0.16 to 0.86
Limerock	13	27,786 (4030)	70,602 (10240)	39,300 to 578,194 (5700 to 83860)	0.40	11	0.00 to 0.54
Slag	20	167,198 (24250)	137,275 (19910)	64,121 to 636,800 (9300 to 92360)	0.37	13	0.00 to 0.52
All data	271	63,708 (9240)	77,394 (11225)	4,895 to 636,800 (710 to 92360)	0.52	17	−0.16 to 0.86

Table 8. Summary of dimensionless K_1-K_3 parameters for selected materials modeled using Equation 5[41]

Material	K_1	K_2	K_3
Limestone	243	0.95	$-6.5*10^{-5}$
Iron ore	75	1.01	$-2.2*10^{-5}$
Sandy gravel	152	0.88	$-2.9*10^{-4}$
Caliche	322	0.88	$-9.8*10^{-5}$
Shellbase	318	0.80	$-9.8*10^{-5}$
Sand	498	0.77	−0.01
Silt	195	0.071	$-6.5*10^{-5}$
Lean clay	195	0.068	−0.19
Fat clay	122	0.19	−0.36

Table 9. Summary of average elastic coefficients and exponents for LTPP materials modeled using Equation 5 (dimensionless)[5]

Material	Mean K_1 (Range) SD	Mean K_2 (Range) SD	Mean K_3 (Range) SD
Clay	594 (87 to 2039) 472	0.44 (−0.20 to 0.53) 0.16	−0.19 (−0.55 to 0.30) 0.22
Silts	426 (136 to 838) 187	0.42 (−0.05 to 0.66) 0.17	−0.23 (−0.57 to 0.05) 0.15
Sands	598 (103 to 3494) 351	0.44 (−0.33 to 0.99) 0.21	−0.12 (−0.43 to 0.89) 0.16
Gravels	836 (229 to 3172) 710	0.23 (−0.27 to 0.59) 0.22	−0.08 (−0.33 to 0.67) 0.23
Base	869 (250 to 2323) 292	0.65 (−01.8 to 1.07) 0.15	−0.04 (−0.33 to 0.61) 0.13

Parameters describing gradation are perhaps the most widely investigated material characteristics. Several investigators have approached this issue by varying the fines content for several different aggregates. (See references 22–23, 26, 28.) The results reported typically show inconsistent trends, with the effect of increased fines content varying from one material to another[23,26]. Although one would intuitively expect that extreme increases in the fines content will have a very marked affect on behavior, regression equations developed by Rada and Witczak indicate that the influence of fines content in the range of 3 to 17 percent is negligible in comparison to stress, moisture, and density parameters.[26]

The results of Monismith, Hicks, and Salam show an increase in modulus as the fines content increased from a coarse (2–3 percent fines) to a medium (5–6 percent fines) gradation for both crushed and partially crushed materials.[23] However a decrease in modulus occurred as the fines content was further increased from a medium gradation to a fine gradation (8–10 percent fines).

Ishibashi et al. looked at four soils. Two were gravelly silty sand base materials differing only in fines content. Two were subgrade materials, which were identical but for the substitution of a sandy silty clay material for the minus number 7 fraction of the original gravelly sandy silt in one soil.[28] For both the base and subgrade materials, the material having the higher fines content exhibited the lower modulus.

Thompson and Smith looked at the resilient modulus of seven Illinois granular materials, including two crushed stones, two crushed gravels, two gravels, and a partially (30–35 percent) crushed gravel.[48] The partially crushed gravel, and one material from each of the other types conformed to one gradation specification, while the remaining three materials conformed to another. The two gradation specifications differed only in the percentage passing the no. 200 sieve. The one with the lower fines content required 2 ±2 percent passing 200, whereas the higher fines content required 8 ±4 percent passing 200. The materials were tested at or near the maximum dry density, which varied from 1962 kg/m^3 (122.5 pcf) (low fines content crushed stone) to 2300 kg/m^3 (143.6 pcf) (high fines content crushed stone) and the optimum moisture content, which varied from a low of 4.0 percent (low fines content crushed stone) to a high of 9.0 percent (partially crushed stone, high fines content). At a bulk stress of 138 kPa (20 psi), their resilient modulus results ranged from a high value of 244 MPa (35.4 ksi) for the crushed stone having the higher fines content to a low of 134 MPa (19.4 ksi) for the partially crushed gravel, which also had the higher fines content. Looking at the pairs of similar material, in all cases, the material with the higher fines content had a slightly higher modulus. How much of the difference is attributable to the different fines content, and how much is attributable to different moisture and density conditions cannot be discerned from the data.

Chen et al. considered six base/subbase materials used in Oklahoma, three limestones, one sandstone, one granite, and one rhyolite, with all six materials prepared to have the same gradation.[49] Their results showed a 20- to 50-percent variation in resilient modulus with aggregate type, with the magnitude of the difference depending on the bulk stress. The samples used were compacted to 95 percent maximum dry density (relative to AASHTO T180-90D), at optimum moisture content. The ranges for the densities and optimum moisture contents were 2355 to 2403 kg/m^3 (147 to 150 pcf) and 5.2 to 6.0 percent, respectively—quite narrow relative to those for the materials studied by Thompson and Smith. Hence, it is reasonable to believe that much (but not all) of the observed between material variation in modulus can be attributed to other characteristics of the materials.

One factor that contributes to between material differences in resilient behavior is the particle shape or angularity, in the sense that crushed aggregates typically exhibit higher moduli than partially crushed aggregates, due to the increasing angularity and surface roughness present in

the crushed material.[23] The magnitude of this effect has been found to increase with increasing fines content.

In their investigation of Illinois subgrade soils, Thompson and Robnett found that percent clay, plasticity index, liquid limit, percent organic carbon, percent silt, and group index were all significant factors (at the 0.01 level) in explaining observed material variations in resilient behavior.[24] Interestingly, their analysis of variance results indicated that soil classification (AASHTO, Unified, or U.S. Department of Agriculture) is not a significant factor in determining the resilient behavior of the soils studied. Thus, they concluded that soil classification is not sufficient to characterize the resilient behavior of fine-grained soils. This is not surprising when one considers that, at the extremes, two soils having the same classification may be quite different, or conversely, that two soils having similar characteristics may be just different enough to fall into different classifications.

Soil State with Respect to Freezing and Thawing

Although seldom considered in laboratory investigations (due to the complexity of the required testing), the state of granular and fine-grained soils with respect to freezing and thawing can have a very great effect on their resilient behavior, and thus be an important consideration in the design and evaluation of pavements in regions subject to frost penetration. Whereas most efforts to characterize the resilient behavior of soils have addressed only nonfrozen materials, investigations at the U.S. Army Corps of Engineers' Cold Regions Research and Engineering Laboratory (CRREL) have considered a range of soil states encompassing frozen, thawed, recovering (from thaw weakening), and fully recovered conditions. (See references 27, 29-32, 50, 51, 52). Details of the CRREL investigations are presented in the section "Relating Resilient Moduli to Material Parameters." Key findings relating to the impact of freezing and thawing on resilient modulus are as follows.

Cole, Irwin, and Johnson obtained core samples of a frozen sand base material, and conducted laboratory resilient modulus testing on the samples in frozen, thawed, and recovered states.[27] Constitutive models considered in this work included the bulk stress model (Equation 2), and Equation 16.

$$K_1(J_2/\tau_{oct})^{K_2} \tag{16}$$

In the frozen state, the resilient modulus of the sand base material remained around 10,000 MPa (1450 ksi) (depending on the applied deviator stress) at temperatures in the range of −10 °C to about −4 °C, at which point it began to decrease rapidly with increasing temperature, reaching 1,000 MPa (145 ksi) at a temperature near 0 ºC. In the thawed state, the observed resilient moduli varied (with stress and moisture tension levels) in the range of 40 to 200 MPa (5.8 to 29 ksi).

Subsequent work by Cole et al.[29] and Johnson, Bentley, and Cole[30] expanded this effort to look at additional granular materials and additional test sites in a similar fashion. They found that for frozen soils, the modulus is primarily a function of unfrozen water content, with

applied stress becoming significant as the temperature approached the melting point. A significant reduction in modulus upon thawing was followed by a gradual increase as the materials drained during the recovery period.

Further extension of this work is reported by Cole et al.[31] and by Johnson et al.[32] They note that the modulus of frozen soil may be two to three orders of magnitude greater than the thawed state modulus for the same soil. The relatively fine-grained soils exhibited lower moduli in the frozen state than did the more coarse-grained soils. The difference was attributed to the greater unfrozen moisture content of the fine-grained material. In general, stress dependency in the frozen soils was found to be negligible in comparison to the temperature effects. The lone exception to this was a silty fine sand subgrade for which stress level was a significant factor in the frozen state. The M_r versus temperature relationship was found to be a strong function of the relationship between temperature and unfrozen moisture content for each soil. For the thawed soils, as in previous investigations, K_1 was found to be primarily a function of moisture tension, with some soils being more sensitive to variations in moisture tension than others. During the recovery period, the observed increase in modulus with increasing moisture tension ranged from a factor of 1.5 for a silty fine sand to a factor of 3.5 for a silty sandy gravel.

Collectively, the CRREL investigations show that the phenomena associated with freezing, thawing, and subsequent recovery result in substantial changes in the moduli of an array of granular materials, including a crushed stone, a broad array of sands, a silty sandy gravel, and a dense graded stone. They further show that temperature and moisture conditions (the later characterized in their work by moisture tension) must be considered in any attempt to predict seasonal variations in the modulus of unbound materials. Additional details on the CRREL work are presented under "Relating Resilient Moduli to Material Parameters."

Additional Factors Influencing Backcalculated Moduli

The influential factors discussed thus far affect the moduli of unbound pavement materials irrespective of the method by which the moduli are determined (i.e., through laboratory testing or through backcalculation from pavement deflection data). Several additional factors influence the backcalculation of pavement layer moduli, and thus the moduli derived through that process. In broad terms, the most important of those factors (assuming the input data are accurate, and the backcalculation has been done "correctly") are the extent to which the model used accurately characterizes the pavement structure and its response to load, and the extent to which measured surface deflections are sensitive to the modulus of the individual pavement layers, or between-layer differences in modulus. These factors will be discussed in the next several paragraphs.

The basic problem addressed in the backcalculation process is to identify a set of layer moduli that are theoretically consistent with input data consisting of a set pavement layer thicknesses and Poisson's ratios, a given applied load, and a measured pavement deflection basin resulting from that load. There is no closed-form solution to this problem. In fact, for any given set of input data, more than one solution may exist. Thus, the analyst must exercise considerable judgment in evaluating the results of the backcalculation process. A number of criteria have

been established to aid in this evaluation.[53,54] Applying these criteria has proven helpful, but not infallible.

There are some situations where it is virtually impossible to derive a meaningful set of backcalculated layer moduli from pavement-deflection data. Those situations arise when the measured deflection basin is insensitive to either the modulus of one layer or to differences in modulus between two adjacent layers.[55] The first situation quite often exists for pavements having thin AC surface layers (where the definition of "thin" is typically on the order of 5–8 cm). The second situation occurs quite often when stabilized base layers are present, or where the moduli of two adjacent layers are very similar. Often, the outcome of these situations is a compensating error effect, wherein the backcalculated modulus of one layer is erroneously high, while the modulus for the adjacent layer is erroneously low.

Measurement errors and errors in layer thickness arising from spacial variability in the pavement may also result in moduli that are higher or lower than the "true" (unknown) value. As a rule, the backcalculated moduli for the upper layers of the pavement are more sensitive to errors in layer thickness than are deeper layers.[56]

Most often, the backcalculation of pavement layer moduli from deflection data utilizes a static linear layered elastic model of the pavement structure.[57,58,59] Key assumptions are that the pavement layers are linear (i.e., not stress dependent), elastic, homogeneous, and continuous in the horizontal plane. Real pavements violate all of these assumptions to one degree or another, and there is little doubt that the discrepancies between model and reality have an impact on the backcalculated layer moduli. For the purposes of backcalculation, the most problematic discrepancies are the particulate nature and stress dependency of the unbound materials. Some backcalculation procedures use approximate methods to address stress dependency, with mixed success.[60] Use of a finite-element model (rather than the more simplistic layered-elastic model) as the basis for backcalculation is seen as a mechanism to more correctly model the particulate nature of unbound materials. However, much more research is required to develop accurate finite-element-based backcalculation programs suitable for use in pavement engineering practice.

Despite the challenges of the backcalculation process, and the noted discrepancies between model and reality, backcalculation based on linear layered-elastic theory enjoys widespread use as the best available nondestructive technology for estimating the in situ stiffness of pavement layers. While theoretically imperfect, when used with engineering judgment, the technology yields reasonable and useful results and fills a very real need.

RELATING RESILIENT MODULI TO MATERIAL PARAMETERS

The CRREL work cited in preceding discussions, as well as that of Yang,[34] Santha, [37] and Titus-Glover and Fernando,[41] is of particular interest because these investigators were quite successful in their efforts to relate the coefficients in the resilient modulus constitutive models they studied to selected material characteristics. Their work and findings with regard to relationships between resilient modulus constitutive model coefficients and material parameters are discussed in this section.

In addition to the sand core samples discussed previously, Cole, Irwin, and Johnson conducted laboratory resilient modulus testing of a sandy gravel subgrade material.[27] The subgrade samples were compacted in the laboratory to a level approximating the in situ conditions, and tested only in the unfrozen state. Two stress models were considered in analysis of the test results: the bulk stress model (Equation 2) and Equation 16. Note that Equation 16 is a special case of Equation 6, in which the exponent n on the consolidation ratio is taken to be zero. It is also identical in form to the bulk stress model, with the ratio J_2/τ_{oct} replacing the bulk stress as the stress parameter. In many cases, Equation 16 was found to yield a better fit of the data.

For the materials investigated, the CRREL investigators found that the coefficient K_1 was a function of the soil moisture tension and density, whereas K_2 was more or less constant for a particular soil (but varied between soils). For the thawed and nonfrozen materials, models of the general form given in Equation 17 were found to fit the data well.

$$M_r = c_1 [f(\psi)]^{c_2} f(\sigma)^{c_3} f(\gamma_d)^{c_4}$$

$$M_r = \text{resilient modulus (Mpa)} \quad (17)$$
$$c_1, c_2, c_3, c_4 = \text{regression constants}$$
$$\psi = \text{moisture tension (kPa)}$$
$$f(\psi) = [101.38 - \psi)/1\text{kPa}$$
$$f(\sigma) = \text{stress function}/1\text{kPa}$$
$$f(\gamma_d) = \text{dry unit weight (Mg/ m}^3\text{)}/1\text{Mg/ m}^3$$

Typical values for the constants are given in Table 10. By rearranging Equation 17 to correspond to the form of Equations 2 and 16, one can see that $K_1 = c_1 f(\psi)^{c_2} f(\gamma_d)^{c_4}$ and $K_2 = c_3$.

For the frozen soils, CRREL investigators found that a model of the general form given in Equation 18 fit the data very well in most cases.

$$M_r = c_1 (w_u / w_t)^{c_2}$$

$$w_u = \text{unfrozen moisture content}$$
$$w_t = \text{total moisture content}$$
$$c_1, c_2 = \text{regression constants} \quad (18)$$

Representative regression constants for Equation 18 are presented in Table 11. In one case, a silty fine sand subgrade, stress state was a significant factor for the frozen material. Models

obtained for this case are given in Equations 19 and 20 (all variables as previously defined; M_r in MPa; T in ºC).

$$M_r = 2.59(w_u / w_t)^{-0.85}(\theta/1kPa)^{0.93}$$
$$w_u = 3.14 * 10^{-2}(-T)^{0.29} \quad (19)$$
$$w_t = 0.29$$

$$M_r = 2.66(w_u / w_t)^{-1.02}[(J_2 / \tau_{oct})/1kPa]^{0.78}$$
$$w_u = 3.14 * 10^{-2}(-T)^{-0.29} \quad (20)$$
$$w_t = 0.29$$

Table 10. Representative (best fit) regression constants for Equation 17 Mr in MPa[27,29,31]

Material State and Type/ Load Pulse	Stress Term	c_1	c_2	c_3	c_4	n	R^2/SE	Ref.	Eq. No.
Thawed graves sand/RPB	J_2/τ_{oct}	$6.68*10^4$	−2.2948	0.414	NA	186	0.89/ 0.144	29	13
Recovered graves sand/RPB	J_2/τ_{oct}	4.80	NA	0.4046	NA	36	0.87/ 0.185	29	16
Thawed dense graded stone/RPB	J_2/τ_{oct}	$1.56*10^5$	−1.76	0.136	NA	64	0.65/ 0.202	29	36
Thawed crushed stone base/both	J_2/τ_{oct}	$3.68*10^4$	−2.15	0.30	3.44	222	0.84/ 0.16	31	7
Thawed gravelly sand/both	θ	$8.00*10^8$	−2.99	0.37	−5.55	149	0.82/ 0.19	31	13
Nonfrozen Silty Fine Sand/Both	θ	$7.73*10^3$	−1.34	0.35	NA	262	0.78/ 0.17	31	16
Thawed silty sandy gravel/both	θ	$1.56*10^6$	−3.69	0.36	7.72	173	0.74/ 0.23	31	20
Thawed silty fine sand/both	J_2/τ_{oct}	$3.80*10^6$	−2.36	−3.25	−3.06	293	0.74/ 0.19	31	24
Nonfrozen silty fine sand	J_2/τ_{oct}	$2.49*10^6$	2.73	0.26	2.07	278	0.82/ 0.14	31	31

NOTES:
Standard Error referenced to ln(M_r) γ_d = dry unit weight (Mg/m^2)
γ_0 = 1 Mg/m^2), f(γ_d) = γ_d/γ_0

Table 11. Representative regression constants for Equation 18[27,29,31]

Material Type/ Load Pulse	c_1	c_2	n	R^2	Std. Error[1]	Ref.	Eq. No.
Graves sand/FWD	32.14	−1.96	73	0.95	0.446	23	10
Ikalanian sand/RPB	86.4	−1.32	87	0.92	0.749	23	18
Hart Bros. sand/RPB	40.85	−1.59	99	0.92	0.623	23	23
Hyannis sand/RPB	33.45	−2.03	69	0.95	0.617	23	32
Dense graded stone/RPB	82.27	−2.03	32	0.97	0.413	23	35
Sibley till/ RPB	101	−3.446	108	0.87	0.71	23	38
Crushed stone base/both[2]	18.9	−4.82	78	0.78	0.66	25	9
Gravelly sand/both[3]	81.8	−4.02	149	0.82	0.19	25	14
Silty sandy gravel/both[4]	$1.00*10^3$	−2.63	173	0.74	0.23	25	21

NOTES:
1. Standard Error referenced to $\ln(M_r)$
2. $w_u = -3*10^{-2}(-T)^{-0.25}$, $w_t = 0.075$, T = temperature (ºC)/1ºC
3. $w_u = -3*10^{-2}(-T)^{-0.25}$, $w_t = 0.055$
4. $w_u = -3*10^{-2}(-T)^{-0.22}$, $w_t = 0.05$

Equation 21 gives the general form of a series of regression equations developed by Yang using Equation 8 as the basic constitutive model.[34]

$$M_r = 10^{c_1}(1+S)^{c_2}(RC)^{c_3}M^{c_4}(\theta_{l_0}^{\ 2}+\theta_{l_p}^{\ 2})^{c_5(1-F)}(1-\tau_{oct})^{c_6F}k_c^{k_4} \quad (21)$$

In this equation, S is the degree of saturation, in percent; RC is the relative degree of compaction, expressed as a decimal fraction of the standard Proctor density; F is the fines content (i.e., percent passing the No. 200 sieve); and M is a material constant, as defined in Equation 22.

$$M = \frac{(1/2(10^{F-S/100}+10^{S/100-F}))*(1+PI)}{Density\ Factor} \quad (22)$$

$$Density\ Factor = \frac{D_{80}}{(7.14(D_{80}/D_{40}+D_{40}/D_{20}+D_{20}/D_{10}))^{1/2}}$$

By comparing Equation 8 and Equation 21, it can be seen that k_1 is predicted on the basis of the relative density, gradation (specifically, the percent passing 200, D_{80}, D_{40}, D_{20}, and D_{10}), plasticity index (PI), and degree of saturation, while k_2 and k_3 were related to the percent passing 200. The values obtained for the regression constants are presented in Table 12. Note that the constant k_4 varied within the range of 0.51 to 0.91, depending on the data set under consideration (implying that it, too, is a function of material characteristics). Higher k_4 values corresponded to base materials, while the values near 0.5 were associated with subgrade soils, but no predictive relationship was developed. Moisture content and density are not statistically significant in the equation, as these parameters were held constant in the development of the data set.

Table 12. Regression constants for Equation 21[34]

Material	c_1	c_2	c_3	c_4	c_5	c_6	k_c	R	SE[1]
Base I (N=98)	8.7	−2.2	9	1.2	0.37	−2.8	0.83	0.933	0.084
Base II (N=53)	3.84	0	0	0	0.22	−1.8	0.91	0.924	0.075
Base I & II (N=151)	9.2	−2.3	6	1.4	0.30	−1.6	0.89	0.922	0.085
Subgrade I (N=96)	10.4	−3.2	17	0	0.50	−1.5	0.52	0.914	0.075
Subgrade II (N=64)	4.33	0	0	0	0.18	−0.9	0.51	0.865	0.060
Subgrade I & II (N=160)	10.2	−3.0	16	0	0.41	−1.3	0.53	0.901	0.075
All materials (N=311)	6.8	−1.46	7.8	0.42	0.22	−0.34	0.69	0.863	0.105

[1]Standard Error referenced to $\log_{10}$

Likewise, Santha developed regression equations to predict the coefficients (K_1–K_3) for Equations 5 and 9, for granular and cohesive soils, respectively, based on moisture content (MC), optimum moisture content (MOIST), percent saturation (SATU), percent compaction (COMP), percent passing numbers 40 and 60 sieves (S40 and S60), percent clay (CLY), percent silt (SLT), percent swell (SW), percent shrinkage (SH), density (DEN), and California Bearing Ratio (CBR).[37] Santha's approach differed from that of Yang in several respects, including: (1) the constitutive model considered; (2) the use of separate regression analyses for each of the model coefficients; and (3) the use of a much more extensive data set. The results are presented in Table 13. The R^2 values reported are quite good, and the predicted moduli quite reasonable. However, one wonders whether all of the variables used are necessary, in light of the probable intercorrelation among several of them (e.g., moisture content and moisture content ratio). Santha does not address this possibility.

Table 13. Resilient modulus prediction equations developed by Santha[37]

	Equation	R^2
Granular materials	$Log K_1 = 3.479 - 0.07 MC + 0.24 \frac{MC}{MOIST} + 3.681 COMP + 0.011 SLT + 0.006 CLY - 0.025 SW - 0.039 DEN + 0.004 \left(\frac{SW^2}{CLY} \right) + 0.003 \left(\frac{DEN^2}{S} 40 \right)$	**0.94**
	$K_2 = 6.044 - 0.053 MOIST - 2.076 COMP + 0.0053 SATU - 0.0056 CLY + 0.0088 SW - 0.0069 SH - 0.027 DEN + 0.012 CBR + 0.003^{SW^2/CLY} - 0.31 (SW+SH)/CLY$	**0.96**
	$K_3 = 3.752 - 0.068 MC + 0.309 MCR - 0.006 SLT + 0.0053 CLY + 0.026 SH - 0.33 DEN - 0.0009 (SW^2/CLY) + 0.00004 (SATU^2/SH) - 0.0026 (CBR*SH)$	**0.87**
Fine-grained materials	$Log K_1 = 19.813 - 0.045 MOIST - 0.131 MC - 9.171 COMP + 0.037 SLT + 0.015 LL - 0.016 PI - 0.021 SW - 0.052 DEN + 0.00001 (S40*SATU)$	**.95**
	$K_3 = 10.274 - 0.097 MOIST - 1.06 MCR - 3.471 COMP + 0.0088 S40 - 0.0087 PI + 0.014 SH - 0.046 DEN$	**0.88**

Titus-Glover and Fernando developed predictive models for the coefficients in Equation 10, finding that k_1 could be predicted quite well with the plastic limit (PL), specific gravity of soil binder (G_{sb}), volumetric moisture content (θ_w), tangent of friction angle (tanφ), percent passing number 40 (N40), suction (U, in pF (water-holding energy)), and dielectric constant (ε_r) as variables.[41] Similarly, the predictive equation developed for k_2 used the specific gravity of the soil binder, the gravimetric moisture content, and the liquid limit (LL), while that for k_3 is based on the dielectric constant, liquid limit, and gravimetric moisture content. The specific equations developed are presented in Table 14. The goodness-of-fit statistics indicate that the resulting equation for k_2 is not as strong as that for k_1, but still acceptable. The goodness-of-fit statistics for k_3 are very good. However, they are applicable primarily to fine-grained soils, as granular materials were not used in the development on the presumption that k_3 is approximately zero for granular materials.

Table 14. Titus Glover and Fernando predictive models for constitutive model coefficients[41]

Equation	R^2	N
$k_1 = 28659 - 417.297PL - 5706.38\,G_{sb} + 12780\,\theta_w - 75.443N40 - 5462.069 \tan\phi + 58.975N\,40_N * U_N + 256.002N\,40_N * \tan\phi_N - 309.3217\,U_N * \varepsilon_{rN}$ *where* $N\,40_N$ = *normalized* $N40 = n40 - 57.215$ $\tan\phi_n$ = *normalized* $\tan\phi = \tan\phi - 0.92877$ U_N = *normalized suction* $= U - 2.12231$ ε_{rN} = *normalized dielectric constant* $= \varepsilon_r - 12.5981$	0.93	26
$k_2 = -0.127927 + 0.515759\,g_{SB} - 0.084802w + 0.00027N\,40_n^2 - 0.009607L\,L_{NW_N} - 0.192586L\,L_N \text{TAN}\,\Phi_N + 0.003981L\,L_N^2$ *where* W_N = *normalized gravimetric moisture content* $= W - 8.94172$ $L\,L_N$ = *normalized liquid limit* $= LL - 24.41888$	0.75	26
$k_3 = 1.807384 - 0.181851\,\varepsilon_r - 2.808291L\,L_N * W_N - 0.016342L\,L_N * \varepsilon_r$ *where* $L\,L_N$ = *normalized liquid limit* $= LL - 28.6667$ W_N = *normalized gravimetric moisture content* $= W - 13.451.$	0.92	9

Von Quintus and Killingsworth also attempted to develop regression models to predict the coefficients for Equation 5 using data from the LTPP database.[5] The equations they developed are presented in Table 15. Although the goodness-of-fit statistics reported for the transformed regressions are quite good in some cases, comparisons of the measured and predicted moduli yielded poor results. Thus, they do not recommend use of these models, by virtue of high potential for error in the predicted values.

In summary, several researchers have had reasonable success in developing models to predict M_r as a function of soil parameters. Although the specific parameters used varied among researchers, all considered some indicator of moisture conditions and soil density. Most also considered one or more parameters representing the gradation of the soil, and some measure or indicator of plasticity.

Table 15. Predictive equations for Equation 5 constitutive model coefficients as derived by Von Quintus and Killingsworth[5]

Soil Type	Equation	R^2/ Standard Error
Clay	$LogK_1 = 17.622 - 0.2647W_{opt} - 0.4430W_s + 2.6732\left(\frac{\gamma_{ds}}{\gamma_{d\max}}\right) + 0.1320\%silt + 0.6422LL - 0.3742PI - 0.1963\gamma_{d\max} - 0.00087P_{40}S$	1.0/ $8.5X10^{-4}$
	$K_2 = 0$	
	$K_3 = 3.3673 - 0.01464W_{opt} - 1.7371\left(\frac{W_s}{W_{opt}}\right) - 0.1264\left(\frac{\gamma_{ds}}{\gamma_{d\max}}\right) - 0.02400P_{40} - 0.03483PI + 0.001779\gamma_{d\max}$	0.81/ 0.115

Table 15. Predictive equations for Equation 5 constitutive model coefficients as derived by Von Quintus and Killingsworth[5], continued

Soil Type	Equation	R^2/ Standard Error
Silt	$LogK_1 = 1.9823 + 0.01394W_s - 0.5934\left(\frac{W_s}{W_{opt}}\right) + 0.1500\left(\frac{\gamma_{ds}}{\gamma_{dmac}}\right) + 0.00831\gamma_{d\max} + 0.000334\left(\frac{\gamma_{d\max}^2}{P_{40}}\right)$	0.810/ 0.112
	$K_2 = 6.4676 - 0.0861W_{opt} - 0.5458\left(\frac{\gamma_{ds}}{\gamma_{d\max}}\right) + 0.0080S - 0.04226\gamma_{d\max}$	0.688/ 0.117
	$K_3 = 5.7391 + 0.07929W_s - 1.1778\left(\frac{W_s}{W_{opt}}\right) + 0.008037\%silt + 0.04549\gamma_{d\max}$	0.568/ 0.137
Sand	$LogK_1 = 2.7602 - 0.00702W_s - 0.08076\left(\frac{W_s}{W_{opt}}\right) + 0.05750\left(\frac{\gamma_{ds}}{\gamma_{dmac}}\right) + 0.000279\gamma_{d\max}$	0.160/ 0.164
	$K_2 = 0.7386 - 0.01497W_{opt} + 0.3916\left(\frac{\gamma_{ds}}{\gamma_{d\max}}\right) - 0.00604S - 0.00157\gamma_{d\max}$	0.226/ 0.167
	$K_3 = -0.04978 - 0.0092W_s + 0.008377\left(\frac{W_s}{W_{opt}}\right) - 0.0052\%silt + 0.00487\gamma_{d\max}$	0.304/ 0.112

W_{opt} = Optimum water content
W_s = Water content of test specimen
γ_{ds} = Dry density of test specimen
γ_{dmax} = Maximum dry unit weight of soil
%silt = Percentage of silt
LL = Liquid limit
PI = Plasticity inex
P_{40} = Percentage passing the No. 40 sieve
S = Degree of saturation

SEASONAL VARIATIONS AS OBSERVED IN FIELD INVESTIGATIONS

It is well established that the in situ structural properties of pavement layers vary on a seasonal basis. The laboratory investigations discussed in the preceding section begin to explain why these variations occur, but do not, by themselves provide a complete basis for estimating the magnitude of the changes, and the duration of the different states, as is needed for design and evaluation. To address this issue fully, one must turn to field investigations. Early work in this regard, like that of Scrivner et al., was most often directed at characterizing the degree and duration of the weakened state occurring as a result of spring thaw in Northern regions to provide a basis for the application of spring load restrictions.[61] More recent investigations have addressed the need to characterize the full annual cycle of changes for purposes of pavement design and performance evaluation.

Yang investigated the seasonal variations in deflections and in situ moduli of six flexible pavements in and around Ithaca, NY, over a three-and-one-half-year period.[34] He found that significant seasonal variation occurs in all of the pavement layers. Even within this small geographic region, between-site differences in seasonal behavior (e.g., the duration of the thaw-weakened state) were observed, due to differences in the materials and drainage characteristics of the different pavements.

Newcomb et al. investigated seasonal variations at a number of sites in Washington State and Nevada.[62] They found that, for the Washington sites, seasonal variations in the moduli of the subgrade materials were much less significant than those observed in granular base materials. The data for the Nevada sites were less extensive, typically encompassing less than one year. Interestingly, they noted a tendency toward more variation from point-to-point than from season-to-season.

More recently, Uhlmeyer, Mahoney, et al. investigated seasonal variations in a broad array of highway and Forest Service pavements in the State of Washington.[63] Their findings in this study supported the earlier conclusion that seasonal variations in the base layer are greater than those in the subgrade for the conditions encountered in Washington State. They selected the set of moduli ratios presented in Table 16 as being "representative of flexible pavements located in areas with modest annual freezing and thawing." They also found that the apparent magnitude of the "seasonal effect" was reduced significantly if the stress sensitivity of the pavement materials was considered, rather than treating the soils as being linearly elastic. This finding is especially noteworthy because the stress-sensitive nature of pavement materials is frequently neglected in field investigations.

Table 16. Representative modular ratios[63]

Month	Modular Ratios	
	Aggregate Base	Subgrade
January	0.6	0.9
February	0.6	0.8
March	0.6	0.8
April	0.6	0.8
May	0.7	0.9
June	0.8	0.9
July	0.9	0.9
August	1.0	1.0
September	1.0	1.0
October	0.8	0.8
November	0.7	0.8
December	0.6	0.9

Sebaaly et al. explored the seasonal variations in the moduli of pavements in each of three districts in Nevada over a five-year period.[64] Taking the summer moduli as the baseline condition, they developed a series of seasonal factors (multipliers) to estimate the moduli in each of four seasons for each district, as summarized in Table 17. The general approach is identical to that previously described for the State of Washington.[15] The factors applicable to the base and subgrade moduli for a given season are quite similar in magnitude, but the ranges are broader for the subgrade soils.

Table 17. Seasonal multipliers for base and subgrade soils in Nevada[64]

Layer	Spring	Summer	Fall	Winter
Base	0.68–0.70	1.00	0.93–0.98	0.87–0.95
Subgrade	0.70–0.79	1.00	0.85–1.02	0.77–0.81

Similarly, Lindly and White explored the differences between subgrade moduli backcalculated from pavement deflection data obtained in the spring and summer of a single year for 15 pavement sites in Indiana.[65] For the sites investigated, they found that the mean spring modulus was 79 to 87 percent of that obtained for the summer.

ENVIRONMENTAL EFFECTS MODELS APPLICABLE TO PAVEMENT DESIGN

At present, the most comprehensive model addressing the effects of climate on pavements is the EICM.[66] As noted previously, this model provides the basis for consideration of seasonal variations in the *2002 Guide for Design of New and Rehabilitated Pavement Structures* currently under development through NCHRP 1-37A. The EICM is an enhanced version of the Integrated Climatic Model (ICM) developed by Lytton et al. in the mid-1980s.[67]

As its name implies, the ICM integrated three separate models addressing different aspects of climatic effects on the pavement into a single comprehensive package. Those models are the Climatic-Materials-Structures (CMS) model, developed at the University of Illinois;[68] the Infiltration and Drainage (ID) model, developed at the Texas Transportation Institute;[69] and the CRREL Frost Heave and Thaw Settlement Model, developed by the U.S. Army Corps of Engineers' CRREL.[70] Collectively, the elements of the ICM provide the capability to simulate climatic conditions at the pavement site; temperature, moisture, and freeze-thaw conditions internal to the pavement; asphalt stiffness; and base, subbase, and subgrade moduli, all as a function of time.

Solaimanian and Bolzan conducted an independent evaluation of the temperature prediction capabilities of the ICM.[71] Two types of analysis were conducted as a part of their investigation: (1) sensitivity analysis to evaluate the effects of various input parameters on the predicted pavement temperature profile; and (2) comparison of the model predictions to monitored temperature profiles. Their work did not encompass the moisture prediction capabilities of the ICM.

Factors considered in the Solaimanian and Bolzan sensitivity analysis included air temperature, percent sunshine, solar radiation, emissivity, absorptivity, and thermal conductivity. Comparisons of predicted and measured temperature profiles were conducted for five geographically dispersed sites in the United States and Canada. They reported good agreement between measured and predicted pavement surface temperatures, with the proviso that proper selection of boundary conditions, climatic parameters, and material properties is necessary to obtain reasonable results. Further evaluation of the model and enhancements to both the user interface and the manner in which the model considers the effect of windspeed were recommended.

Larson and Dempsey report that the following enhancements to the original ICM are embodied in Version 2.0 of the EICM: [66]

- Enhancements to the user interface to simplify the creation of input files.
- Improvements to the computational engine to provide for the use of metric units, variable length analysis periods, and use of actual daily climatic data (instead of average values).
- Enhancements to facilitate manipulation of program output files.

In addition, they recommend further improvements to the model to (1) more accurately determine the quantity of water entering the subgrade; (2) allow use of hourly climatic data; and (3) facilitate manipulation and use of EICM output.

The following remarks summarize the state of the EICM as it existed when this study, and related work undertaken as a part of the NCHRP 1-37A, were initiated.

- The EICM uses very sophisticated algorithms to simulate climatic conditions, both external and internal to the pavement.

- A limited independent evaluation of the temperature-prediction capabilities found the model output to be reasonable. Similar findings relative to the moisture prediction capabilities were not reported in the literature, although the original developers of the ICM state that it provides reasonable predictions.
- The EICM moisture and temperature prediction results are not effectively used in the simulation of seasonal variations in the moduli of unbound pavement materials because the very simple relationships used to estimate moduli neglect key factors.

The work discussed in Chapter 4 begins to address the need for independent evaluation of the EICM moisture-prediction capabilities, and the work discussed in Chapter 5 addresses the need for predictive models to use with EICM moisture output to predict backcalculated pavement layer moduli. Work undertaken to develop the approach for considering seasonal variations in the 2002 guide (discussed previously under "Addressing Seasonal Variations in Pavement Design and Evaluation," and in the next section) has brought about substantial progress toward effective application of the EICM capabilities.

RELATED WORK WITH THE INTEGRATED CLIMATIC MODEL

One element of the work discussed herein is an evaluation of the moisture predictive capabilities of the ICM. This work was conducted in cooperation with work by the NCHRP 1-37A research team to develop the 2002 guide methodology for considering seasonal variations in unbound pavement layers that was summarized previously. (See references 16,17,18,19.) The author's initial findings relative to the adequacy of moisture predictions obtained using Version 2.0 and 2.1 of the EICM resulted in the initiation of refinements to the EICM as a part of the NCHRP 1-37A research. The model improvements are summarized in Chapter 4, and documented in detail in reference 19. The author's subsequent evaluation of the revised model is documented in Chapter 4.

CHAPTER 3: DATA ACQUISITION AND ASSESSMENT

INTRODUCTION

As indicated previously, this investigation used data obtained via the LTPP Seasonal Monitoring Program. This chapter provides information regarding the LTPP data that were used, as well as the data manipulation and assessment that were conducted prior to application of the data in model evaluation and development. In addition, information on the variability observed in the data is presented to provide context for evaluating the outcome of the work presented in Chapters 4 through 6.

DATA SOURCES

The locations of the LTPP seasonal monitoring test sections considered here are shown in Figure 2. In the figure, square symbols designate test sections used in the evaluation of the EICM, discussed in Chapter 4. All sections shown in the figure were used in the development of predictive models for backcalculated pavement layer moduli, discussed in Chapter 5.

The layer thickness ranges for these test sections are summarized in Table 18, while the distribution of soil classifications for the test sections is summarized in Table 19. While the more fine-grained subgrade soil classifications are relatively scarce, the test sections represent a reasonably broad array of conditions.

Table 18. Layer thickness ranges for LTPP Seasonal Monitoring Program test sections considered in this investigation

Layer Type	Minimum Thickness (m)	Maximum Thickness (m)
Asphalt concrete	0.071	0.282
Granular base	0.102	0.655
Treated base	0	0.122
Granular subbase	0	0.668
Total thickness above subgrade	0.206	1.069

Table 19. Distribution of soil classification by pavement layer

Layer Type	Number of Test Sections with Layer Classification of:						
	A-1-a	A-1-b	A-2-4	A-2-6	A-3	A-4	A-6
Granular Base	16	5	1	–	–	–	–
GS Granular Subbase	1	3	–	1	–	–	–
Subgrade Soil	2	3	6	1	3	5	2

The data used in the analyses presented herein are drawn from DataPave 2.0, except as follows: [72]

- Data tables SMP_TDR_AUTO_MOISTURE and SMP_FROST_PENETRATION, SMP_FREEZE_STATE are from release 10.0 of the LTPP Information Management System.
- Tables TST_... are from release 10.2 of the LTPP Information Management System.
- Backcalculated moduli and supporting data used in the analysis are prerelease versions of the data subsequently uploaded to LTPP database tables MON_DEFL_BACKCALCULATION... for the initial release from those tables.
- In a few instances, input data required for application of the ICM were obtained from the seasonal monitoring installation reports for the test sections. Data from this source are annotated as such in the tables where the data are presented.

The review, manipulation, and processing of these data prior their application are discussed in the remainder of this chapter.

BACKCALCULATED MODULI

Backcalculated layer modulus is the key dependent variable considered in this investigation. The first subsection of this chapter provides an overview of the process used in the backcalculation of those layer moduli. Subsequent subsections discuss the evaluation of those moduli and findings with regard to the variability in the backcalculated moduli.

Backcalculation of Pavement Layer Moduli

The backcalculated pavement layer moduli used in this investigation were derived through a separate study by Von Quintus and Simpson.[73] The backcalculated layer moduli considered in this investigation were provided to the author prior to detailed review or the application of the quality control checks ordinarily applied prior to the release of data from the LTPP database. The author's evaluation of the backcalculation results to assess their adequacy for use in this study are discussed below.

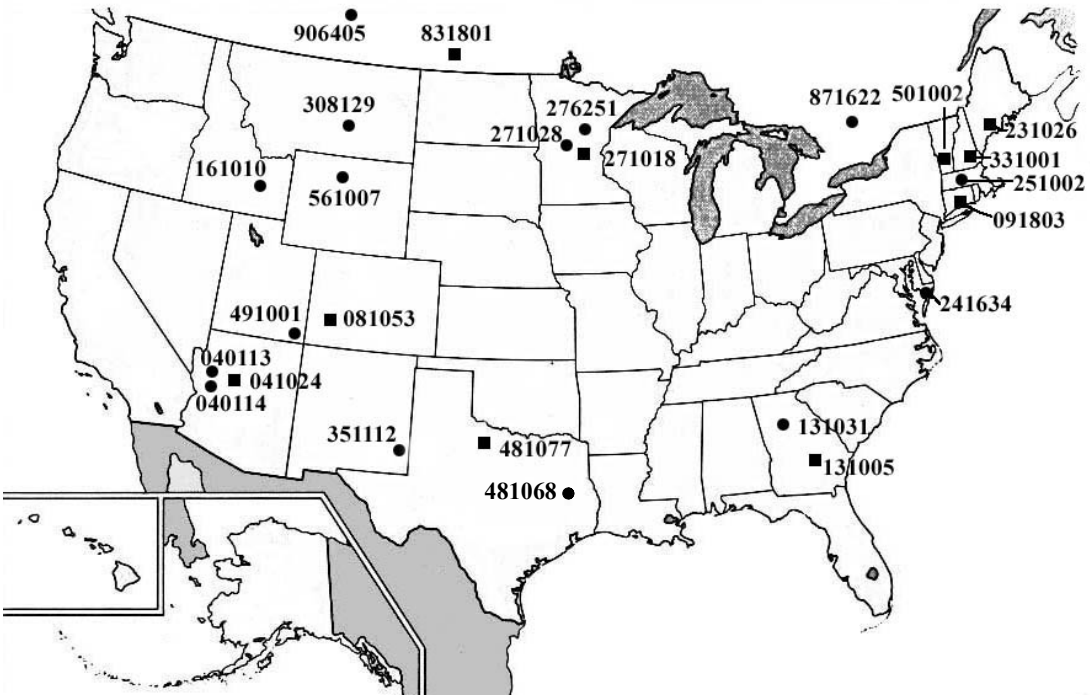

■ - test sections used in the evaluation of the EICM.

● - test sections not used in the evaluation of the EICM.

Figure 2. Locations of LTPP seasonal monitoring sections considered in this study

Evaluation of Backcalculated Layer Moduli

As noted in Chapter 2, one complicating factor in the backcalculation of pavement layer moduli from deflection data is that there is no closed-form solution to the problem. For any given set of measured load and deflections, layer thicknesses, and Poisson's ratios (the input to the backcalculation process), there may be several, sets of "matching" layer moduli. It is therefore incumbent upon the engineer to carefully evaluate the output of the backcalculation process to determine whether the moduli determined through that process are in fact plausible for the set of circumstances surrounding the collection of the deflection data. Absolute judgments as to the accuracy of any given set of backcalculated moduli are impossible to make, as the true values are never known. Furthermore, the acceptability of a given set of backcalculated moduli depends to some degree on the intended application.

Prior to being used in subsequent analysis, the backcalculated moduli were evaluated against several criteria. First, the moduli were subjected the following series of objective checks.

- Error Limits: Backcalculation results with root mean square errors (differences between measured and calculated deflections) greater than 2.0 percent were removed

from the working data set. Though somewhat arbitrary, the 2.0 percent error limit is a widely used rule of thumb for assessing the adequacy of backcalculation results. Backcalculation results having higher levels of error may be acceptable for use in some applications, but lack the precision needed for this application.

- Frost Affected Data: Backcalculation results for test dates on which one or more frozen layers were identified in the pavement cross section were removed from the working data set, in keeping with the scope of this investigation.
- Range Checks: Sets of backcalculation results (i.e., the values associated with a single input data set) for which one or more of the layer moduli fell outside the applicable range defined in Table 20 were removed from the working data set. The upper and lower bounds used in this screening were based on the values reported by Rada et al.[74] The purpose of this step in the process was to remove values that are clearly not plausible for the materials in question. For a given set of backcalculation results, an out-of-range value for any one layer resulted in deletion (from the working data set) of the moduli for all layers. This is deemed necessary due to compensating error effects that occur in the backcalculation process.

Table 20. Modulus ranges used in screening of layer moduli (MPa)[74]

Layer Type	Minimum	Maximum
Asphalt concrete	500	21,000
Granular base	35	1,100
Treated base	35	28,000
Granular subbase	35	700
Treated subgrade	35	28,000
Subgrade soil	No limit	1,100

- Proximity: Backcalculated moduli for test points more than 3 meters from the instrumentation used to monitor in situ temperature and moisture conditions were excluded. The application of this limit is based on the assumption that the moisture and temperature data are most representative of the materials closest to the monitoring location.

The final step in the evaluation process was a graphical evaluation, in which the backcalculated moduli remaining in the working data set were plotted as a function of time and (for the AC layers) temperature to facilitate identification of observations warranting further scrutiny. Tabular presentations of the data were reviewed to draw final conclusions as to whether individual sets of backcalculated moduli were or were not plausible. The factors considered in this evaluation were:

- Temperature trends in the AC layers.
- Time trends (both within day and month-to-month).
- The plausibility of the backcalculated moduli in relation to those for adjacent layers (taking into consideration the materials in question).
- Trends with respect to load level.

As with the range checks, all layer moduli associated with a given set of deflection data were treated as a set. Sets of moduli judged to be implausible were flagged as such, so that they could be excluded from analysis sets, but were not deleted from the database. Data reflecting consistent behavior that differed from expectations (e.g., consistent load-softening in a material classified as granular) were not flagged unless there was some other reason to consider them suspect.

Variation in Moduli Under Nonfrozen Conditions

Following the evaluation discussed in the previous section, an exploratory analysis of the backcalculated moduli and their inherent variation was undertaken. The purpose of this analysis was twofold:

1. To provide information on the amplitude of seasonal and load-associated variations in the backcalculated moduli.
2. To provide context (in terms of information on the expected within-day variation) for evaluating the outcome of subsequent parts of this study.

The findings of that work are discussed in the next few sections.

Variation with FWD Load

The extent to which the backcalculated moduli vary with FWD load level is characterized in Table 21. This table presents the mean layer moduli for the nominal 40-kN and 71-kN FWD loads, and the mean difference between them, for each AASHTO soil class represented in the data set. The statistics in this table indicate that the A-1-a, A-1-b, and A-2-4 soils tend to be load hardening, whereas the A-2-6, A-3, A-4, and A-6 soils tend to be load softening. The observed trends for the A-1-a, A-1-b, A-4, and A-6 soils are consistent with expectations, and the load softening of the A-2-6 is not unexpected, in light of the clay component in these materials. However, the load softening of the A-3 soils is not consistent with expectations. Rather, one would expect these granular materials to be load hardening. Statistics for the individual pavement layers considered in the computation of the A-3 soil class statistics in Table 21 are presented in Table 22. Possible explanations for the unexpected trends are offered in the next paragraphs.

The variation in the A-3 subgrade soils at sections 251002 and 271018 is very small, and is therefore attributed to errors in the backcalculated moduli, rather than true load-softening behavior. At sections 271018 and 276251, the moduli for the upper portion of the A-3 subgrade exhibit the expected load hardening behavior, whereas those for the lower portion exhibit a lesser degree of load softening. It is likely that this is attributable, at least in part, to compensating error effects.

Table 21. Variation in moduli with applied FWD load by soil class

Soil Class	Mean Layer Modulus		Difference (E_{71}-E_{40})				
	40-kN FWD Load (MPa)	71-kN FWD Load (MPa)	Mean (MPa)	Range (MPa)	Standard Deviation (MPa)	As Percent of E_{40}	Number of Obs.
A-1-a	222	247	25	−249 to 225	58	12%	718
A-1-b	228	261	33	−112 to 310	71	12%	315
A-2-4	254	300	47	−115 to 406	94	19%	171
A-2-6	159	147	−12	−25 to −1	8	−7%	19
A-3	287	267	−21	−106 to 40	25	−6%	145
A-4	204	193	−11	−60 to47	15	−5%	366
A-6	108	106	−2	−25 to 38	10	−1%	114

The load-softening behavior of the subgrade (layer 3 and 4) soil at section 351112 is attributed to the presence of fine-grained soils in the deeper subgrade strata. The soils, characterized in the boring log for the section as sandy clay, silty clay, and clayey silt, are below the depth at which samples were obtained for the laboratory characterization.

Table 22. Variation in moduli with load for individual A-3 layers

Section	Layer	Soil Class	Percent Passing 200	Mean Layer Modulus		Mean Difference (E_{70}-E_{40})		
				40-kN FWD Load (MPa)	71-kN FWD Load (MPa)	MPa	As percent of E_4)	Number of Obs.
251002	4	A-3	7.1	235	231	−4	−2%	1
271018	3	A-3	5.2	173	190	17	10%	8
271018	4	A-3	5.2	46	44	−3	−5%	8
276251	3	A-3	7.7	199	224	25	13%	1
276251	4	A-3	7.7	71	70	−1	−1%	1
351112	3	A-3	3.6	292	260	−32	−10%	63
351112	4	A-3	3.6	334	316	−18	−5%	63

Within-Day Variations

For a given nominal test location and FWD load level, within-day variations in backcalculated moduli for unbound pavement layers may occur as a result of both true within-day changes in the in situ moduli (arising from stress-state changes induced by temperature-related changes in the stiffness of an overlying AC layer, for example), or as a result of variations (errors) in the deflection testing and backcalculation process. The latter would include variations due to

deflection and load-measurement errors, variations in placement of the FWD relative to the nominal test point, variations in FWD load from the nominal values, and backcalculation errors.

The magnitude of the observed within-day variations in the backcalculated moduli is characterized in Table 23. The statistics presented in this table are pooled values, computed in accordance with American Society for Testing and Materials (ASTM) standard E122. The pertinent equations are Equations 23 and 24:

$$s_p = [\sum_{j=1}^{k}(n_j - 1)s_j^{\,2} / \sum_{j=1}^{k}(n_j - 1)]^{1/2} \quad (23)$$

and

$$COV_p = [\sum_{j=1}^{k}(n_j - 1)COV_j^{\,2} / \sum_{j=1}^{k}(n_j - 1)]^{1/2} \quad (24)$$

In computing these statistics, the individual s_j values represent the within-day standard deviation for a particular section, test point, nominal FWD load level, and layer, and n_j is the number of individual observations associated with that value. The values presented in Table 23 are pooled over all test points, sections, layers, and nominal FWD load levels for the soil class or layer type indicated. Thus, in this table k is the number of combinations of date, test section, test point, layer, and FWD load level for a given soil class or layer type.

In most cases, the variation in variability statistics with nominal FWD load level is small in comparison to the variation between the different layers. For example, the COV for section 091803), layer 2 varies in the range of 18 to 20 percent, whereas that for layer 3 varies in the range of 5 to 7 percent. Also, for the many of the pavement sections (e.g., 040113, 041024, 091803, 131005, 251002, 271018, 351112, 481077, 491001, 561007, and 871622), the base layer (layer 2) is more variable than either the subbase/upper subgrade (layer 3) or the subgrade/lower subgrade (layer 4), independent of the measure (standard deviation or coefficient of variation) considered. This may occur as an artifact of the testing and backcalculation process, or it may come about as a result of within-day variations in the stress state within the pavement structure arising from variations in the temperature (and therefore stiffness) of the AC surface layer. The author believes that both factors contribute to the observed variation.

Table 23. Pooled single-point within-day variation in moduli by soil class and layer type

Soil Class or Layer Type	Standard Deviation (MPa)	Coefficient of Variation (%)	k
A-1-a	44	18	1031
A-1-b	34	13	537
A-2-4	63	20	320
A-2-6	4	3	17
A-3	18	7	268
A-4	13	7	481
A-6	12	7	154
Base	55	19	951
Subbase	13	14	176
Subgrade	25	11	1685

Section 501002 is one pavement for which the variability of the upper subgrade is greater than that of the base whether one considers the standard deviation or the COV. Both the base and subgrade at this section are classified as A-1-a soils, such that the true in situ moduli may be very similar. If this is, in fact, the case, the similarity will be reflected in the measured deflections, and it will be difficult to distinguish between the two in the backcalculation process. Thus, the fact that the upper subgrade at this section appears to be more variable than the base may be attributable to the similarity of the materials—i.e., a spurious result.

The magnitude of variation for the more coarse-grained soils (A-1-a, A-1-b, and A-2-4) is consistently greater than that for the more fine-grained soils. However, the author believes that this occurrence is primarily attributable to the predominant use of the coarse-grained soils as base material, whereas the more fine-grained materials are generally seen only in the subgrade. That is, the extent of variability in the backcalculated moduli is driven more by the location of the soil in the pavement structure than by the grain-size distribution of the soil. This interpretation is supported by the data presented in Table 24, which presents within-day statistices pertaining to individual A-1-b pavement layers. The variation in the A-1-b base soils is generally (but not always) greater than that for the A-1-b subbase/subgrade soils.

Table 24. Within-day variation in moduli of A-1-b pavement layers

Section	Layer Number	Pooled Standard Deviation (MPa)				Pooled Coefficient of Variation			
		27-kN	40-kN	53-kN	71-kN	27-kN	40-kN	53-kN	71-kN
131031	2	61	53	87	83	11	12	18	17
271018	2	42	39	38	44	21	18	19	22
276251	2	–	–	–	30	–	–	–	9
491001	2	45	52	61	62	25	27	30	27
871622	2	35	56	59	63	13	18	14	15
040113	3	5	4	4	5	6	4	5	5
231026	3	21	17	15	16	11	11	10	11
251002	3	–	4	4	1	–	5	5	2
271028	3	14	10	13	10	7	5	5	4
331001	3	19	16	18	14	23	19	22	18
871622	3	7	8	8	8	5	5	5	5
906405	3	–	–	13	10	–	–	7	6
040113	4	4	6	5	4	3	4	4	2
231026	4	51	39	33	41	11	8	7	9
271028	4	6	5	3	3	3	2	2	2
906405	4	–	–	2	2	–	–	1	1

Seasonal Variations

The extent of seasonal variation in the moduli backcalculated for nonfrozen conditions is characterized in Table 25 and Table 26. Pavement layers for which the backcalculated moduli in the data set spanned less than 6 months were excluded in the computation of the statistics presented. For this reason, the means, minima, and maxima presented in Table 25 differ somewhat from those presented in Table 21, which considers all available pairs of data for the 40- and 71-kN load levels. The maxima and minima presented herein do not reflect the true maxima and minima occurring in all pavements because the data set has been restricted to frost-free conditions.

The amplitude of the observed variation varies with the nominal FWD load level. For 67 percent of the individual layers considered, the amplitude of the observed variation decreases between the minimum and maximum FWD loads. However, the variation from one load level to the next is not always monotonic. Some differences may be attributable to differences in the time span considered. The interaction of stress and moisture may also be a factor in the observed differences. The lower subgrade for section 131031 is somewhat exceptional in that the amplitude of variation varies by only 1 MPa between load levels.

The amplitude of the observed variation tends to be higher for the granular materials than it is for the more fine-grained materials. For example, in Table 25 it may be observed that the amplitude of variation for the A-1-a soil class varies in the range of 72 to 96 percent (depending on load level), whereas that for the A-4 soil class varies in the range of 53 to 63 percent. Similarly, in Table 26 it may be observed that the amplitude of variation decreases with increasing depth in the pavement, with the base layers being most variable on an absolute basis (152–168 MPa, compared with 57 to 76 MPa for subbase layers, and 8 to 88 MPa for subgrade layers). This observation is consistent with the findings of Newcomb et al. and Uhlmeyer et al.[62, 63] However, the subbase layers are more variable on a percentage basis (95 to 123 percent, compared with 90 to 101 percent for the base layers and 6 to 67 percent for the subgrade layers). It is hypothesized that the amplitude of variation (in absolute terms) tends to decrease with increasing depth because the observed seasonal variations are caused, in part, by changes in stress state arising from temperature-induced changes in the modulus of the overlying AC layer, and this effect is more pronounced for the layers closer to the pavement surface.

Table 25. Extent of variation in backcalculated moduli by soil class

AASHTO Soil Class	Statistic	Nominal FWD Load			
		27-kN	40-kN	53-kN	71-kN
A-1-a	Mean	223	221	234	247
	Min	157	164	181	183
	Max	294	288	295	320
	Amplitude of variation	138	124	114	136
	Variation (% of min)	96	75	72	75
	Number of layers	14	15	15	15
A-1-b	Mean	250	225	232	250
	Min	197	171	188	206
	Max	318	290	286	298
	Amplitude of variation	121	119	98	93
	Variation (% of min)	87	80	62	51
	Number of layers	11	12	12	13
A-2-4	Mean	180	183	182	186
	Min	133	134	127	124
	Max	233	242	241	228
	Amplitude of variation	100	109	114	104
	Variation (% of min)	66	81	101	88
	Number of layers	8	8	8	8
A-3	Mean	182	209	208	190
	Min	149	172	174	168
	Max	230	268	276	232
	Amplitude of variation	81	96	103	64
	Variation (% of min)	54	57	59	38
	Number of layers	6	4	4	6
A-4	Mean	204	201	191	186
	Min	168	167	160	155
	Max	245	248	228	217
	Amplitude of variation	77	81	68	62
	Variation (% of min)	57	63	58	53
	Number of layers	9	9	9	9
A-6	Mean	140	139	138	138
	Min	128	118	128	125
	Max	154	158	149	149
	Amplitude of variation	27	40	21	25
	Variation (% of min)	18	31	17	20
	Number of layers	4	4	4	4

Table 26. Extent of variation in backcalculated moduli by pavement layer

AASHTO Soil Class	Statistic	Nominal FWD Load			
		27-kN	40-kN	53-kN	71-kN
Base	Mean	258	258	276	302
	Min	187	181	202	214
	Max	339	354	355	383
	Amplitude of variation	152	173	153	168
	Variation (% of min)	95	101	101	90
	Number of layers	16	16	16	17
Subbase	Mean	117	117	122	127
	Min	84	85	94	100
	Max	160	159	160	157
	Amplitude of variation	76	74	66	57
	Variation (% of min)	121	123	114	95
	Number of layers	4	4	4	4
Subgrade (Layer 3)	Mean	158	151	148	155
	Min	118	116	118	128
	Max	197	189	190	196
	Amplitude of variation	80	74	72	67
	Variation (% of min)	67	62	58	55
	Number of layers	14	14	14	15
Subgrade (Layer 4)	Mean	226	226	219	205
	Min	189	192	191	178
	Max	277	269	259	234
	Amplitude of variation	88	77	69	56
	Variation (% of min)	46	38	33	29
	Number of layers	17	17	17	18
Subgrade (Layer 5)	Mean	140	141	144	143
	Min	133	134	141	139
	Max	147	155	149	150
	Amplitude of variation	14	21	8	11
	Variation (% of min)	10	15	6	8
	Number of layers	1	1	1	1

In the time variation in the backcalculated layer moduli at selected sections is illustrated in Figure 3 through figure 7. The moduli shown in these plots are daily average values for the nominal 53-kN FWD load, and the error limits shown in the plots are within-day standard deviations. In Figure 3, the observed variation with time for section 040113 (sited in Arizona) is negligible for the lower portion of the subgrade, and very modest for the upper portion of the subgrade and the base layer. Also, it may be noted that the magnitude of the seasonal variation is not much greater than the within-day variation illustrated by the error limits on the individual data points. Greater variability in all pavement layers is seen in Figure 4 through Figure 8. The subgrade data for sections 131005 (Georgia, Figure 5) and 481077 (Texas, Figure 7) follow a more-or-less sinusoidal trend. The variations for sections 091803 (Connecticut, Figure 4), 271018 (Minnesota, Figure 6) and 501002 (Vermont, Figure 8) are more difficult to characterize. The relationship between these variations and potential explanatory variables will be explored in Chapter 5.

In summary, the single-point within-day variation in backcalculated moduli for unbound pavement layers, expressed in terms of the coefficient of variation, was found to vary in the range of 1 to 38 percent. Pooled values of 19, 14, and 11 percent were computed for the base, subbase, and subgrade layers, respectively. The amplitude of the observed seasonal variation (exclusive of frost effects) was found to vary in the range of 6 to 123 percent of the observed minimum value, corresponding to amplitudes of 8 to 173 MPa. In absolute terms, the largest variations were observed for the base layers, and the smallest variations were observed for the deeper subgrade layers. On a percentage basis, the subbase layers were more variable than the base layers, and both base and subbase layers were more variable than the deep subgrade layers.

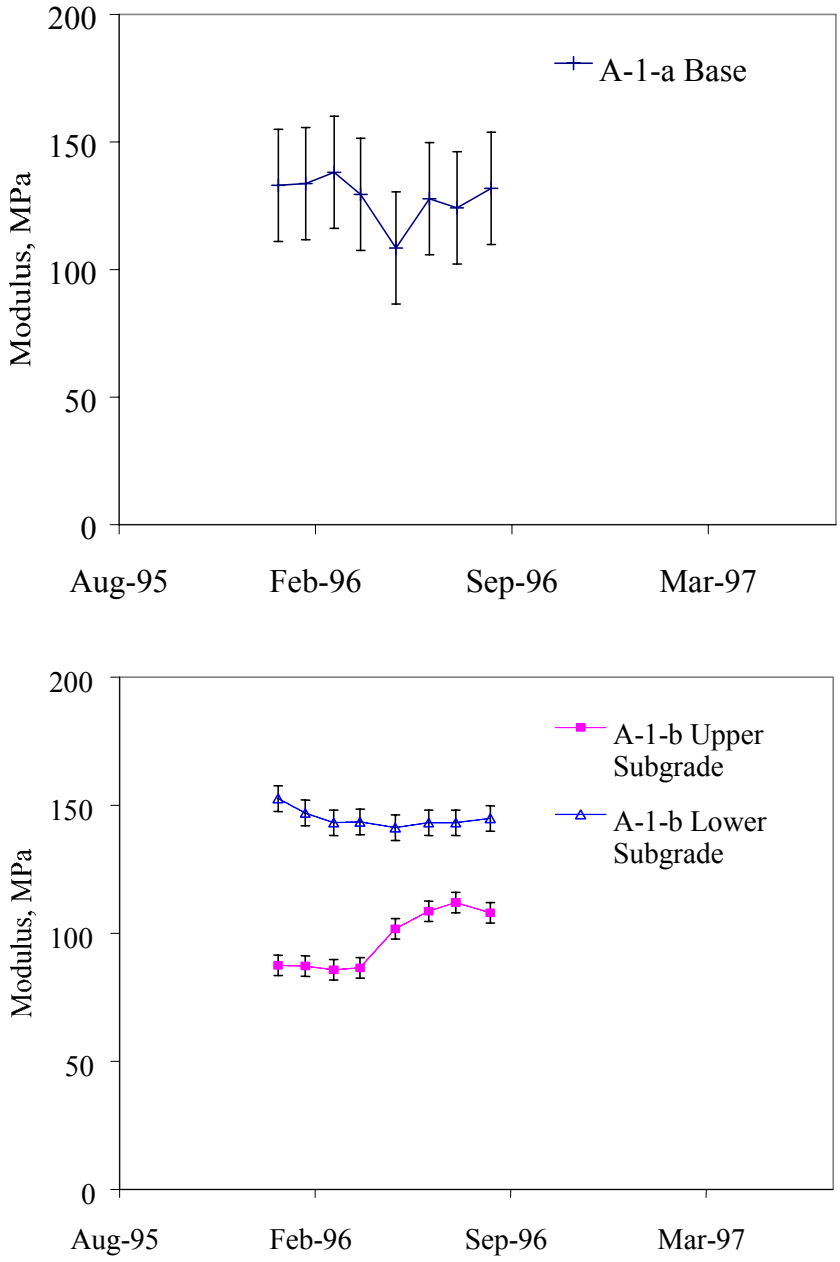

Figure 3. Seasonal variation in daily average moduli, section 040113 (Arizona)

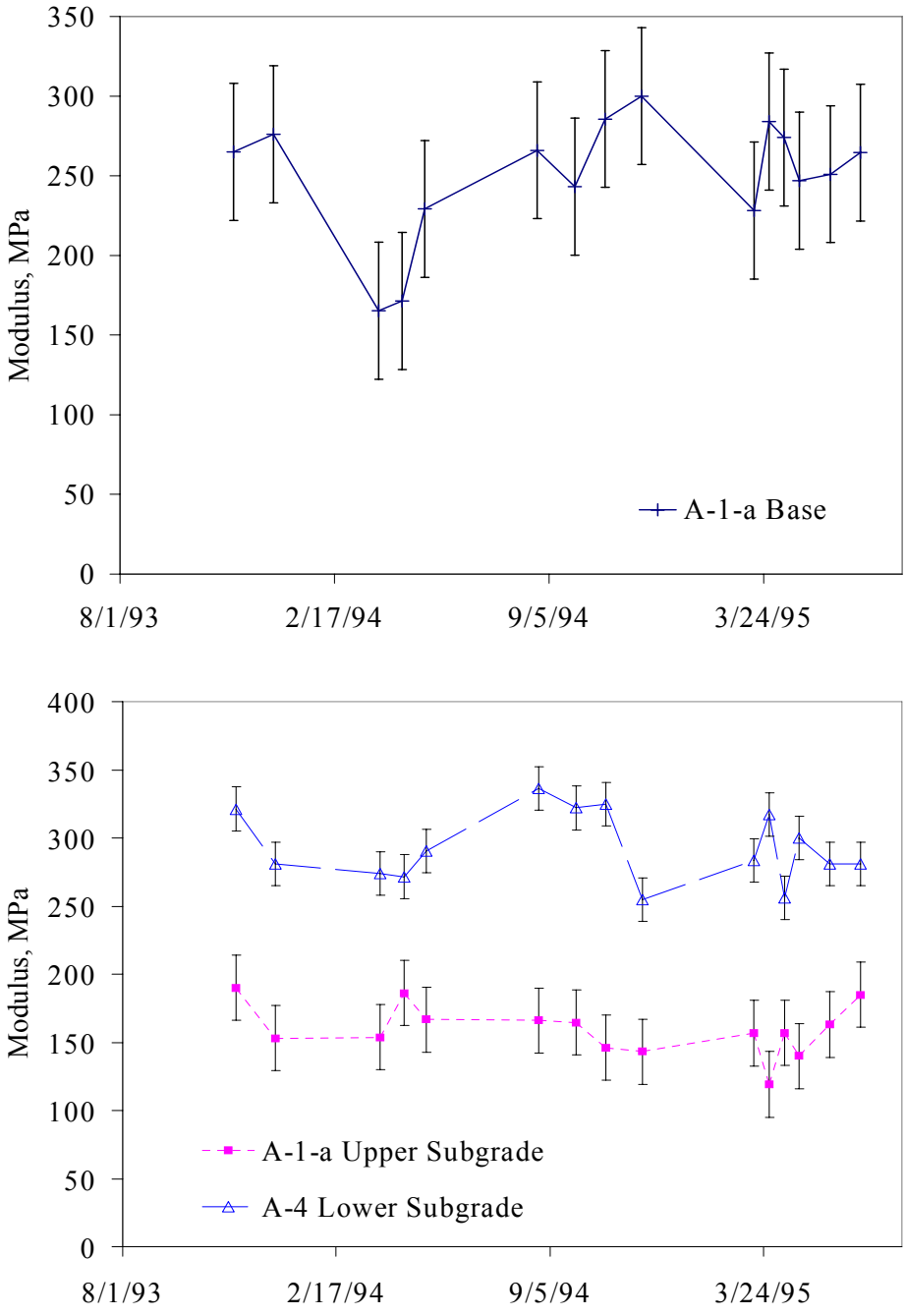

Figure 4. Seasonal variations in daily average moduli, section 091803 (Connecticut)

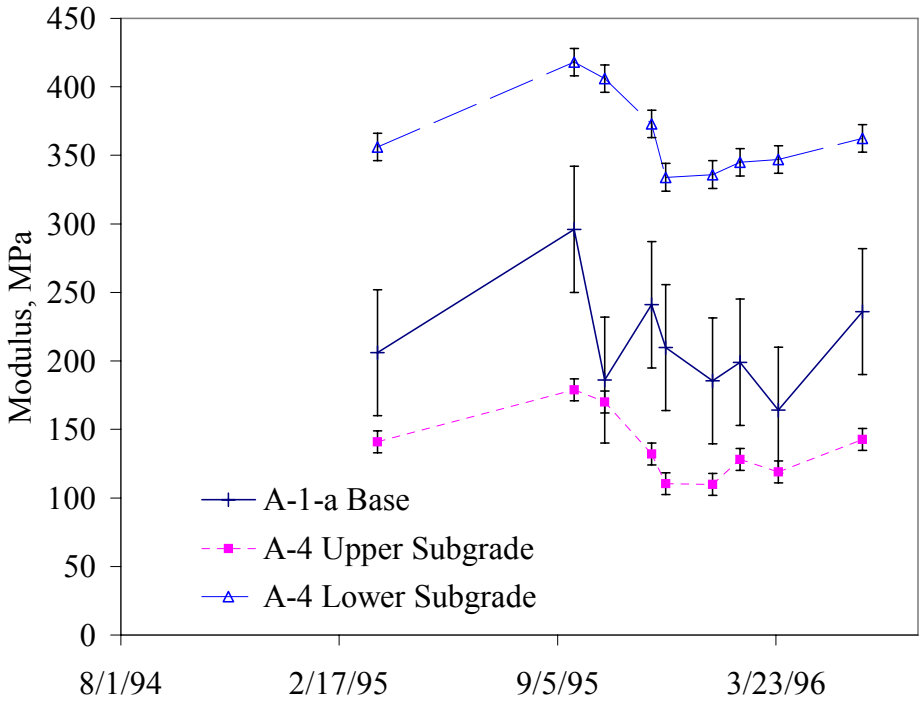

Figure 5. Seasonal variations in daily average moduli, section 131005 (Georgia)

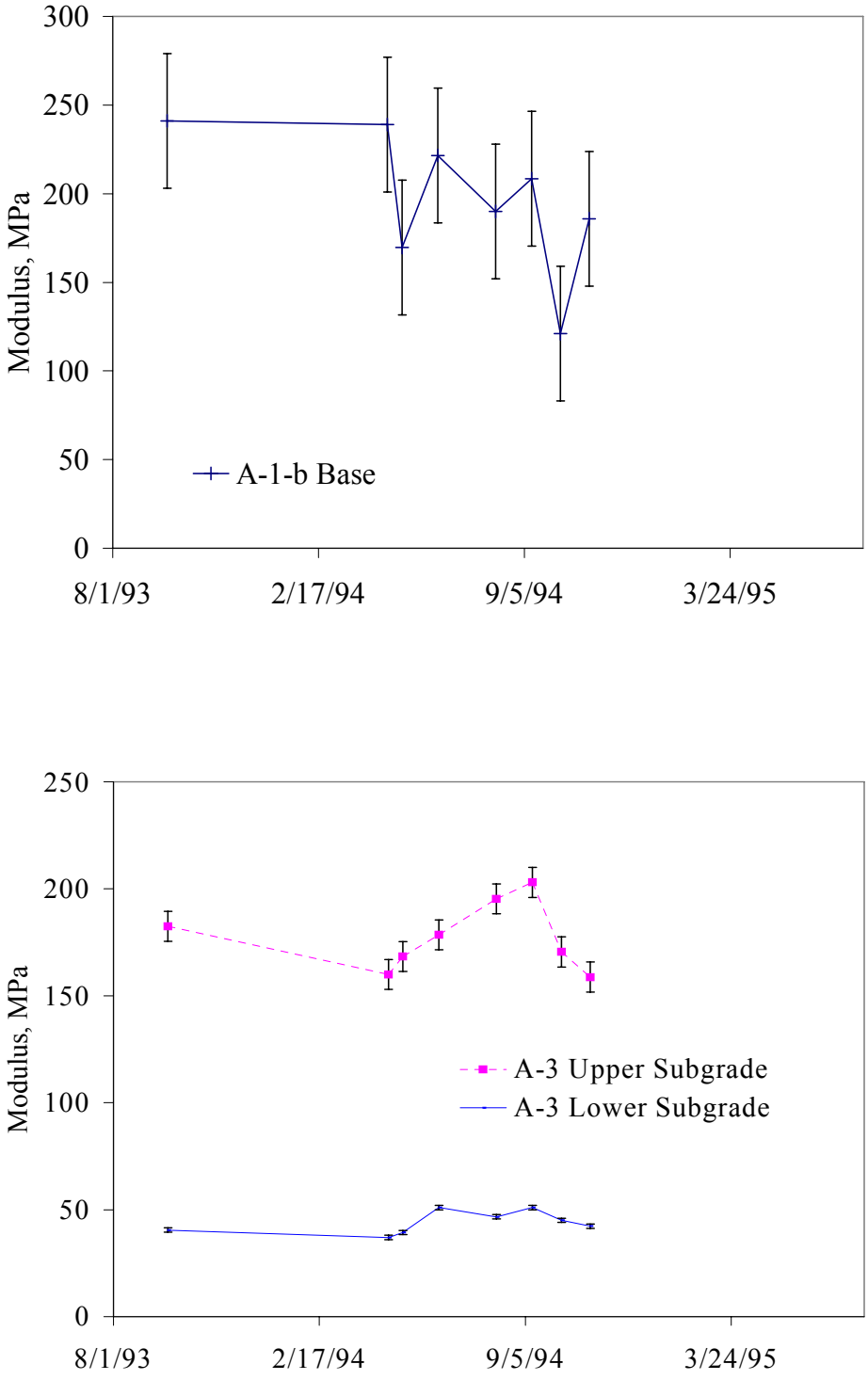

Figure 6. Seasonal variations in daily average moduli, section 271018 (Minnesota)

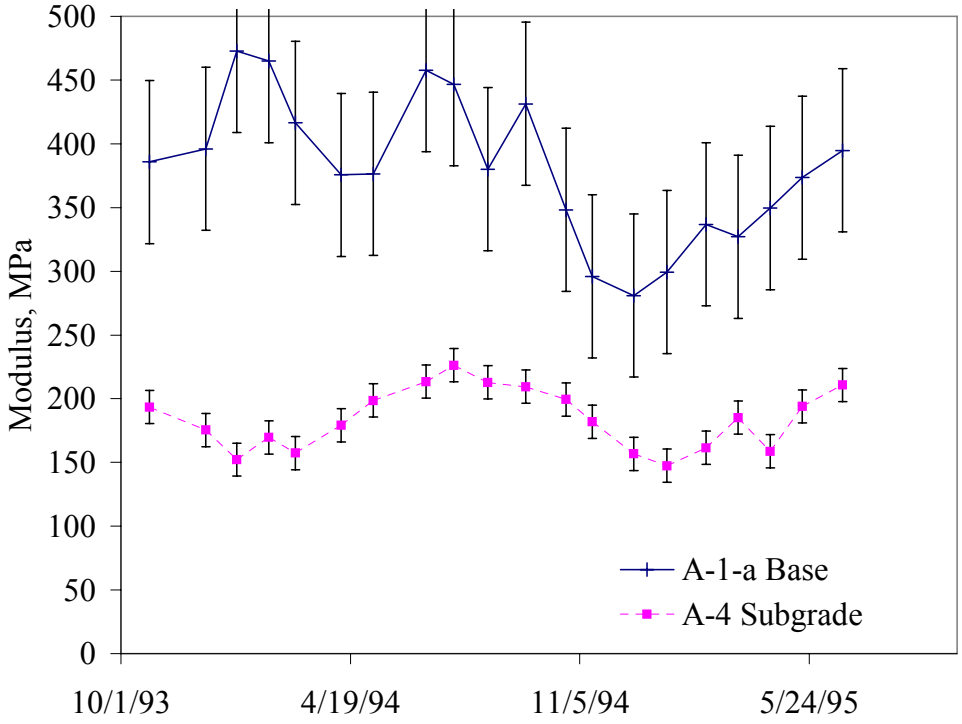

Figure 7. Seasonal variations in daily average layer moduli, section 481077 (Texas)

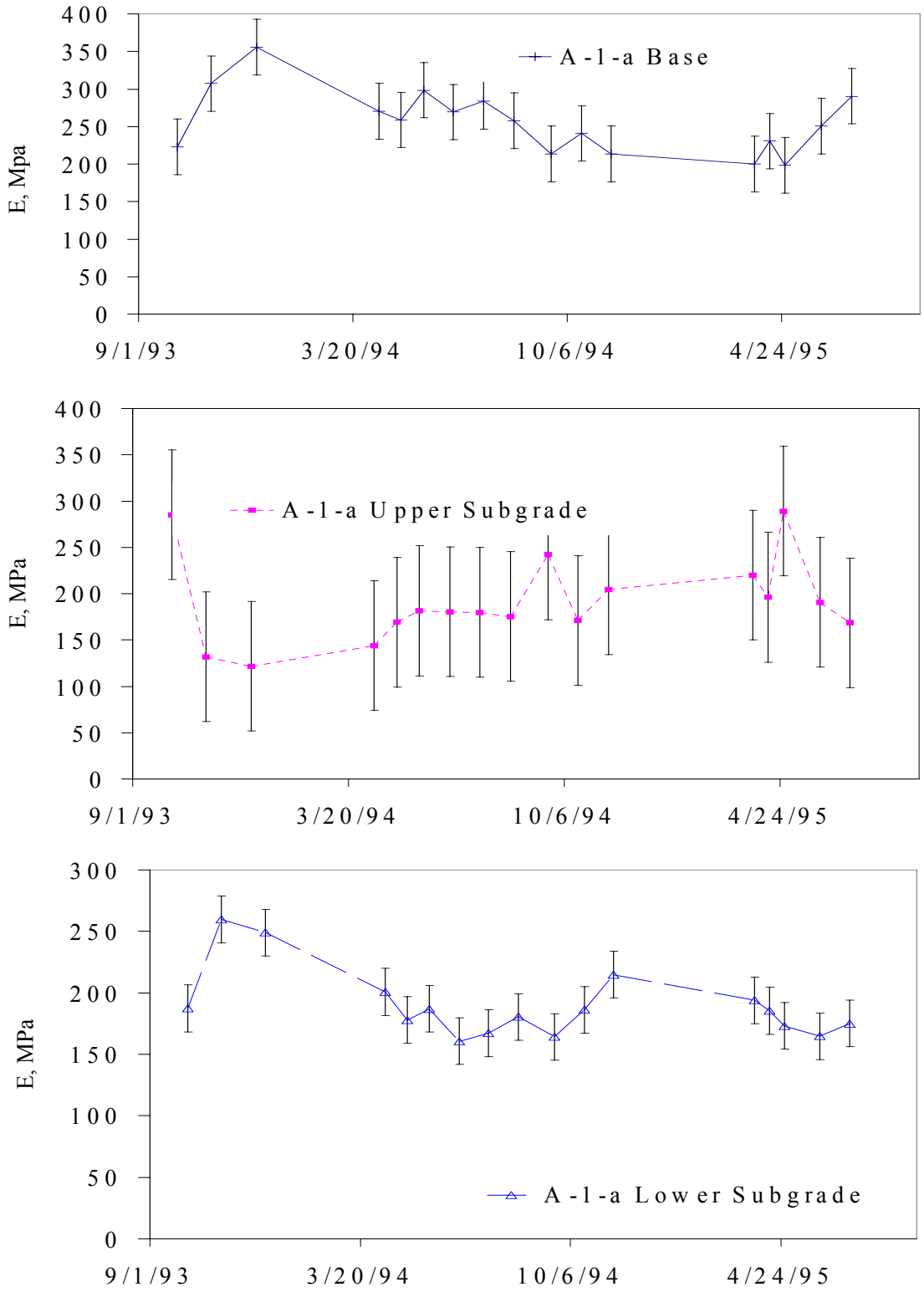

Figure 8. Seasonal variation in moduli, section 501002 (Vermont)

STRESS PARAMETERS

Stress parameters considered in the development of predictive models for backcalculated moduli discussed in Chapter 5 were the bulk stress ($\theta = \sigma_1 + \sigma_2 + \sigma_3$), and the octahedral shear stress ($\tau_{oct} = 1/3[(\sigma_1-\sigma_2)^2 + [(\sigma_2-\sigma_3)^2 (\sigma_3-\sigma_1)^2]^{1/2}$). Selection of the bulk and octahedral shear stresses was based on their prior use in the constitutive models discussed in Chapter 2.

Stress parameters were computed for each individual set of backcalculated layer moduli considered in the analysis (where a "set" is defined by test section, date, time, test point, and FWD load). Stresses were computed for a single radial location, that being the center of the loaded area. The depths at which the stresses were computed corresponded to the quarter-points for each finite layer, and 0.1, 0.2, and 0.3 m below the layer interface for semi-infinite subgrade layers.

In calculating the stress parameters, both load-induced and overburden stresses were considered. The load-induced stresses were computed through application of the CHEVLAY 2 layered-elastic analysis program to the backcalculated layer moduli.[26] To ensure consistency, the layer thicknesses and Poisson's ratios used in the stress calculations were those reported with the backcalculated moduli.

The calculation of overburden stresses took into consideration variations in total (wet) soil density with time due to fluctuations in moisture content, as well as variations in the depth of the water table. Effective stresses were used for soils below the water table, while total stresses were used for soils above the water table. Several different values of K_0 were considered in the overburden computations, as will be discussed in Chapter 5.

MOISTURE PARAMETERS

At each LTPP Seasonal Monitoring Program test section, moisture content is monitored through the use of Time Domain Reflectometry (TDR) probes placed at approximately 10 depths in the unbound base, subbase (if present), and subgrade layers. The number of monitoring depths within a given layer at a particular section varies from one to five, depending on the layer thicknesses at that particular section. The number of observations for a given probe on a given test date varies from one to three.

TDR is an indirect method of monitoring moisture. The raw data collected with the TDR instrumentation are interpreted to determine the dielectric constants (K_a) for the soil. The volumetric moisture content is then computed using regression equations relating the dielectric constant (and possibly other soil parameters) to moisture content. Knowledge of the soil dry density allows computation of the gravimetric moisture content. The specifics of the methodology as applied to the LTPP Seasonal Monitoring Program sections are presented elsewhere.[75,76,77] Both volumetric and gravimetric moisture contents are provided in the LTPP database. The work reported herein utilized the volumetric moisture contents.

Four different regression models were used in determining the moisture contents for the LTPP seasonal monitoring sections. The models are presented in Table 27. The conditions of application for each of the four models, as well as the minimum and maximum estimated errors (for 95 percent confidence limits) in the TDR moisture contents are summarized in Table 28. Note that the magnitude of the estimated error varies with the dielectric constant, and, thus, with the moisture content.

The vast majority of the data considered in this investigation were derived using the Coarse Ka Model (TDR Model 1). TDR Model 2 was used only for the deeper (subgrade soil) probes at sections 308129, 481068 and 871622. TDR Model 3 was used for many observations in the subgrade soil at section 501002, and for some data sets at other sections. TDR Model 4 was used only at sections 481077, 481068, 241634, and 081053.

The volumetric moisture data were reviewed through plots of the mean moisture content as a function of time, analysis of the within-day variation reflected in the data, and comparison of day-of-installation TDR moisture contents with laboratory values for samples collected from the backfill material as the probes were installed.

Table 27. Volumetric moisture models used in determining moisture content from LTPP TDR data (as reported by Jiang and Tayabji[76])

Model Name	Equation
1 Coarse Ka	$V_w = -5.7875 - 3.41763Ka - 0.13117Ka^2 + 0.00231Ka^3$
2 Fine Ka	$V_w = 0.4756 + 2.75634Ka - 0.061667Ka^2 + 0.000476Ka^3$
3 All soil Ka	$V_w = -0.8120 + 2.38682Ka - 0.04427Ka^2 + 0.000292Ka^3$
4 Fine gradation	$V_w = 1761.78 + 2.9145Ka - 0.07674Ka^2 + 0.000722Ka^3$ $- 19.6649P1.5 + 4.3667P0.5 + 5.1516P\#4 + 2.7737P\#10$ $+ 0.06057P\#200 - 0.2057PL + 0.10231LL$

V_w = volumetric moisture content	P#4 = % passing No. 4 sieve
Ka = bulk dielectric constant	P#10 = % passing No. 10 sieve
P1.5 = % passing 38 mm (1.5") sieve	P#200 = % passing No. 200 sieve
P0.5 = % passing 13 mm (½") sieve	PL = plastic limit; LL = liquid limit

Table 28. Minimum and maximum estimated errors (95 percent confidence interval) for TDR moisture content prediction models (adapted from Jiang and Tayabji[76])

Moisture Prediction Model	Minimum Error		Maximum Error		Applicable to:
	Limit %	Vol. Moisture Content %	Limit %	Vol. Moisture Content %	
1 Coarse Ka	5.1	0.0	5.4	33.8	Coarse-grained soils with 1.5<Ka<24.8
2 Fine Ka	8.2	12.2	13.5	46.2	Fine-grained soils with 3<Ka<58.4 and gradation and/or Atterberg limits either not available, or outside inference space for Model 4
3 All soil Ka	2.7	9.8	9.9	43.4	Coarse-grained soils with Ka>24.8 or fine-grained soils where neither model 2 nor model 4 can be applied
4 Fine gradation	7.1	8.7	8.3	50.8	Fine-grained soils with 3<Ka<58.8 and required gradation and Atterberg limits available and within inference space of model

The within-day variation for the TDR moisture data is characterized in Table 55 of Appendix A. The values shown are pooled values, computed in accordance with ASTM standard E122. The pertinent equation is:

$$s_p = [\sum_{j=1}^{k}(n_j - 1)s_j{}^2 / \sum_{j=1}^{k}(n_j - 1)]^{1/2} \quad (25)$$

For each combination of test section and TDR probe, n is the number of moisture observations in a given day, and k is the number of days for which moisture data are available for that probe. The number of test dates considered in the computation of the within day variation statistics is presented in Table 56 (Appendix A), while the average number of observations per day is presented in Table 57 (Appendix A). The pooled standard deviation and coefficient of variation computed over all moisture observations (i.e., k = number of combinations of monitoring date test, section, and TDR probe) are 1.18 and 8.8 percent, respectively.

The prediction error limits presented in Table 28 provide a frame of reference for evaluating the magnitude of the within-day variations in TDR monitored moisture, as characterized by the pooled standard deviation. In Table 58 (Appendix A), the pooled standard deviation for each probe is expressed as a decimal fraction of the maximum estimated error for TDR Model 1 from Table 28 —that is, 5.4. A single value was used for all TDR probes for simplicity. The value for TDR Model 1 was selected because it was used in the computation of the vast majority of the moisture data, and because it is conservative in comparison to the maximum values for the other TDR moisture models.

The TDR moisture error estimates presented in Table 28 are computed as twice the standard error of the prediction. Thus, Table 58 (Appendix A) values greater than 0.5 indicate that the within-day standard deviation is greater than the estimated standard error of the prediction. Ratios greater than 0.5 are denoted in the table by gray shading. They occur for most of the probes for section 481068 and one probe each for sections 040113, 161010, and 308129. The data in Table 58 (Appendix A) are summarized in the form of a frequency histogram in Figure 9. Values in the range of 0.1 to 0.3 occur with the greatest frequency, indicating that in most cases, the within-day standard deviation is small in comparison to the estimated model error.

Individual observations for the within-day standard were evaluated by comparing them to the overall pooled within-day standard deviation of 1.18. In cases where the within-day standard deviation for a given date and probe depth exceeded three times the pooled within-day standard deviation computed over all sections, the individual observations for that probe and test date were reviewed in an attempt to ascertain whether the high variance could be attributed to anything other than random error in the measurement process. The data sets identified for examination are listed in Table 59. They include observations associated with the high pooled within-day standard deviation values denoted by shading in Table 58. The findings of the review of these data were as follows.

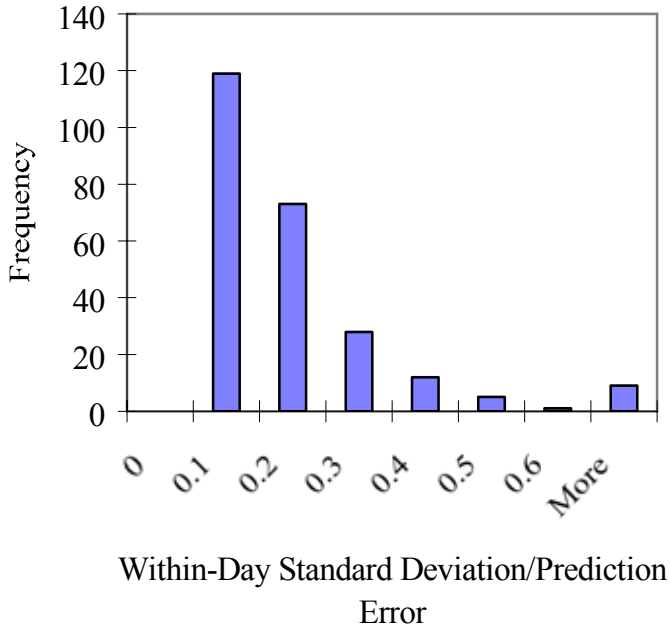

Figure 9. Frequency histogram for ratio of within-day standard deviation/ maximum TDR Model 1 error

- Section 091803, February 17, 1994, TDR Probe Numbers 3 and 4: At these monitoring depths, the observed moisture contents increased substantially (from approximately 9 percent to approximately 19 percent) over a 4-hour period in the morning. This increase, coupled with the time of year, suggested that the change might be attributable to thawing in the pavement. The temperature-depth data for this date are consistent with this hypothesis—i.e., the temperatures near the probes in question are close to 0° C. Therefore, the large increase in moisture content observed for section 091803 on February 17, 1994, was attributed to thawing of the materials surrounding the TDR probes, and the data were therefore excluded from the data set used in subsequent analysis, as this investigation is concerned with nonfrozen materials.

- For section 161010, TDR Probe Number 10, TDR Model 1 was used to derive some of the moisture contents for the test dates in question, and TDR model 3 was used to derive other values. The greater variability observed may be related to this fact. Removal of any or all of the data points does not appear to be justified.

- Section 481068 August 21, 1997, TDR Probe Numbers 2, 3, 5, 6, 7, and 10: The monitored moisture contents for these probes decreased by more than a factor of 10 over a 4-hour period from mid-morning to early afternoon. It is implausible that a change of this magnitude could occur within 4 hours. A review of the available data yielded no plausible explanation for a change in moisture of this magnitude. It is,

however, noted in the comments table that the piezometer pipe at the section was dry on this date, a fact that seems inconsistent with the higher moisture contents that were observed. Overall, it was noted that moisture data for this section were extremely scarce. For 8 of the 10 monitoring depths at this section, the only available moisture content data (as of Information Management System Release 10.0) were for the August 1997 monitoring date. This paucity of data, combined with the inconsistency of the data for the one date for which data are (relatively) plentiful led to the exclusion of this section from subsequent analysis.

In the remaining instances where the within-day standard deviation for a given section and test date exceeded three times the overall pooled within-day standard deviation, no plausible explanation for the observed variation was identified. That is, there was neither a clear indication that the data were erroneous, nor any indication of conditions likely to cause a within-day moisture content change of the magnitude reflected in the data. It was therefore assumed that the observed variance was attributable to random variation in the measurement processes, and that exclusion of these data from the analysis was not justified.

The observed within-day variation in moisture content reflects both true within-day changes in moisture content and variability arising from measurement errors. Because the observed values are, in most cases, small in comparison to the estimated error associated with the measurement technology used, as characterized in Table 28, it is reasonable to assume that within-day variation in the true moisture content of the soil surrounding a given TDR probe is small in comparison to the measurement error associated with the moisture content data. Therefore, the best available estimate of the in situ moisture content at a given time is the daily mean value for the test date in question. For this reason, and because a one-to-one correspondence between the time of TDR moisture observations and the time of FWD deflection tests does not exist, the analyses reported herein use the mean daily moisture content for a given test date, rather than the individual observations.

INPUT TO THE INTEGRATED CLIMATIC MODEL

Application of the EICM requires assembly of a data set characterizing the pavement cross-section, materials, and external environment. The broad categories of input data required by the EICM are as follows.

- Initialization data define the analysis period, the geographic location of the section under consideration, and the time increments to be used in the simulation and reporting of the results.

- Climatic boundary conditions, including temperature, precipitation, windspeed, percent sunshine, and water table depth data. Climatic data provided with the program may be used where section-specific weather data are not available.

- Thermal properties, which characterize the tendency of the pavement surface to absorb and emit heat, as well as the temperature range over which freezing and thawing occur.

- Infiltration and drainage inputs, which characterize both the extent of cracking in the surface, and the drainage characteristics of the base material and geometry.

- Asphalt material inputs, including layer thickness, mix design information, data defining the modulus-temperature relationship, and thermal characteristics.

- Material properties, including layer thickness, density, saturated permeability, and other data characterizing the base, subbase, and subgrade layers.

- Initial profiles, which characterize the temperature and (for Version 2.0 and 2.1 of the EICM only) moisture conditions of the pavement on the first day of the simulation period.

In applying the EICM, the author used section-specific data where they were available and pertinent to moisture prediction. However, some required data elements are not among the data assembled for the LTPP test sections. Default or assumed values were used for these parameters. Default or assumed values were also used for a few parameters (e.g., AC mix design information) not pertinent to moisture prediction as a matter of convenience. The following paragraphs provide an overview of the data that were used in applying the EICM. The data themselves (including assumed or default values) are presented in Appendix B. Details that varied from one version of the EICM to another are discussed in the pertinent sections of Chapter 4.

Climatic Boundary Conditions

Daily temperature and rainfall data (including the times at which the daily maximum and minimum temperature occurred), and (nominally) monthly depth to ground water data collected at each section for the time period of the simulation were used in the models. Windspeed and percent sunshine data used were those provided with the EICM for the weather stations identified in Table 60 to Table 64 of Appendix B, as these data are not collected at the seasonal monitoring sections. The recommended default values were used for the remaining variables. Missing observations were filled in through use of the "generate" function of the EICM, except as discussed in the next two paragraphs.

In a few instances, missing water table depth observations were accompanied by comments to the effect that the monitoring well was dry. Where this occurred, a depth to water table slightly greater than the depth of the bottom of the monitoring well was entered. This estimate is deemed more accurate than allowing the program to generate a value by interpolating between known values, which would yield an estimate inconsistent with the observed (dry) state of the monitoring well.

In one case, section 041024, the monitoring well was reported to be dry on all monitoring dates. For this section, a constant water table depth of 152 m (500 ft) was assumed.

Infiltration and Drainage

The EICM requires entry of the linear length of cracks and joints for use in computation of the amount of water infiltrating the pavement. The values used in the simulation were estimated from the yearly mean distress quantities for the year considered in the simulation, distress surveys having been conducted on a quarterly basis. Because several distresses observed at the test sections considered are recorded in terms of the affected pavement area, as opposed to the crack length, it was necessary to convert the distress areas recorded in the LTPP database to equivalent crack lengths. Assumptions made to estimate the equivalent crack length for distresses measured in units of area are summarized in Table 29.

Table 29. Assumed crack lengths for distresses quantified in terms of area

Distress	Crack Length (m) per Square Meter of Distress
Low severity alligator cracking	2
Moderate severity alligator cracking	5
High severity alligator cracking	12
Low severity block cracking	1.3
Moderate severity block cracking	4
High severity block cracking	5

Asphalt Material Properties

Program default values were used for the asphalt materials, as it was assumed that these variables would have no impact on the predicted moisture contents for the unbound layers.

Material Properties

For sections where multiple observations for a particular parameter were available, the ones used were those for sample locations closest to the location of the subsurface instrumentation. Default values were used for the saturated permeability, dry thermal conductivity, dry heat capacity, volume compressibility, and Gardner model parameters (Version 2.0 of the EICM only), as these parameters are not among the data available for the LTPP test sections. Assumed values were used for the frozen and unfrozen resilient modulus, Poisson's ratio, and the length of the recovery period, as these parameters have no bearing on moisture predictions.

Initial Temperature and Pore Pressure Profile

The initial temperature profiles used in the EICM models were derived from section-specific data obtained with thermistor probes installed in the pavement. Linear interpolation was used to estimate the soil temperature at each node from the temperatures at the two closest monitoring depths. The pavement surface temperatures were extrapolated from the available data (measurements having been taken at mid-layer, and approximately 0.025 m below the surface, and 0.025 m above the lower boundary of the layer). Temperatures for the deepest model nodes were estimated. Daily average values were used in all cases.

The initial pore pressure profiles used in applying Version 2.0 of the EICM were computed from the water table depth per the guidance provided in the EICM documentation.[66] Version 2.1 and subsequent versions of the EICM do not utilize an initial pore pressure profile.

SUMMARY

The data required for this investigation include backcalculated pavement layer moduli (the key dependent variable), in situ moisture data, pavement cross-section and materials data, and climatic data. These data were acquired from the LTPP database, and (in some cases) off-line files, reviewed and manipulated to create the database and EICM input files necessary for the pursuit of the project objectives. The application of these data to evaluate the moisture-predictive capabilities of the EICM and develop predictive models for backcalculated pavement layer moduli will be discussed in the next two chapters.

CHAPTER 4: EVALUATION OF VOLUMETRIC MOISTURE PREDICTIONS FROM THE INTEGRATED CLIMATIC MODEL

INTRODUCTION

As discussed in Chapter 2, the ICM was developed in the late 1980s to simulate temporal variations in the temperature, moisture, and freeze-thaw conditions internal to the pavement, and their impact on key pavement material properties.[78] It is based on a one-dimensional model of the pavement, but does consider both vertical and lateral drainage of the base. More recently, the ICM was updated and enhanced to improve the user interface, predictive capabilities, and operational aspects of the program.[79] The updated model is the EICM. Further details of the theory on which the program is based may be found in the referenced reports. As discussed in Chapter 2, the EICM will be used in the *2002 Guide for Design of New and Rehabilitated Pavement Structures*.

This chapter discusses the application of data collected at the 10 LTPP Seasonal Monitoring Program test sections, identified in Table 30, to evaluate the volumetric moisture prediction capabilities of the EICM. This work was performed in collaboration with efforts to enhance the moisture-predictive capabilities of the model, in preparation for its use in the 2002 guide. Several versions of the EICM were considered in this work: Version 2.0, Version 2.1, and Version 2.6. The evaluation of Version 2.0 was limited in scope, but is important because it provided the initial impetus for the modifications reflected in Version 2.1. Similarly, the evaluation of Version 2.1 provided the impetus for the more extensive model revisions reflected in Version 2.6 of the model.

The moisture prediction capabilities of the EICM were evaluated by applying the model to predict subsurface moisture contents for the selected LTPP test sections, and then comparing the results obtained to the data collected at those test sections. An overview of the data used in this evaluation is provided in Chapter 3. The actual data are presented in Appendix B.

EVALUATION OF EICM VERSION 2.0

Two test sections were considered in the evaluation of EICM Version 2.0: section 271018, which is located in Minnesota; and section 091803, located in Connecticut. The input data used in modeling these sections are summarized in Table 60, found in Appendix B. Two simulation periods were considered in the trial runs for these sections: a 1-day simulation period and a 365-day simulation period. This was done to test whether the model was prone to initialization effects—i.e., whether the model output varied with the length of the simulation period.

Table 30. LTPP Seasonal Monitoring Program sections used in evaluation of the EICM

Section	Surface	Base	Subbase	Subgrade	Water Table Depth	Remarks
041024 AZ	0.27 m HMAC*	0.22 m A-1-a	None	A-2-6	Very deep	Well dry on all dates
081053 CO	0.11 m HMAC	0.14 m A-1-a	0.60 m A-1-a	A-6	1.63 to 4.6 m	
091803 CT	0.18 m HMAC	0.37 m A-1-a	None	A-2-4	1.33 to 3.23 m	Minimal frost penetration
131005 GA	0.19 m HMAC	0.22 m A-1-a	None	0.66 m A-4, A-6 below	1.16 to >5.2 m	Lower subgrade classification inferred from boring log
231026 ME	0.16 m HMAC	0.49 m A-1-a	None	A-2-4	1.67 to 3.92 m	
271018 MN	0.11 m HMAC	0.10 m A-1-b	None	A-3	1.28 to 2.27 m	
331001 NH	0.22 m HMAC	0.49 m A-1-a	0.37 m A-1-b	A-2-4	3.80 to 4.11 m	
481077 TX	0.13 m HMAC	0.27m A-1-a	None	A-4	>4.6 m	Well dry on all dates
501002 VT	0.22 m HMAC	0.70 m A-1-a	None	A-1-a	0.78 to 1.44 m	
831801 MB*	0.11 m HMAC	0.15 m A-1-a	0.31 m A-1-a	A-2-4	1.64 to 3.30 m	

*HMAC – hot-mix asphalt concrete
**Manitoba province, Canada

The trial moisture predictions obtained for the two sections yielded poor agreement between the predicted moisture contents and the monitored data, as illustrated in Figure 10 and Figure 11. The data points for the two different simulation periods are essentially coincident, showing that varying the time period used in the simulation from one day to one year did not significantly alter the predicted moisture content for these sections. Other findings from initial trials with EICM Version 2.0 are as follows.

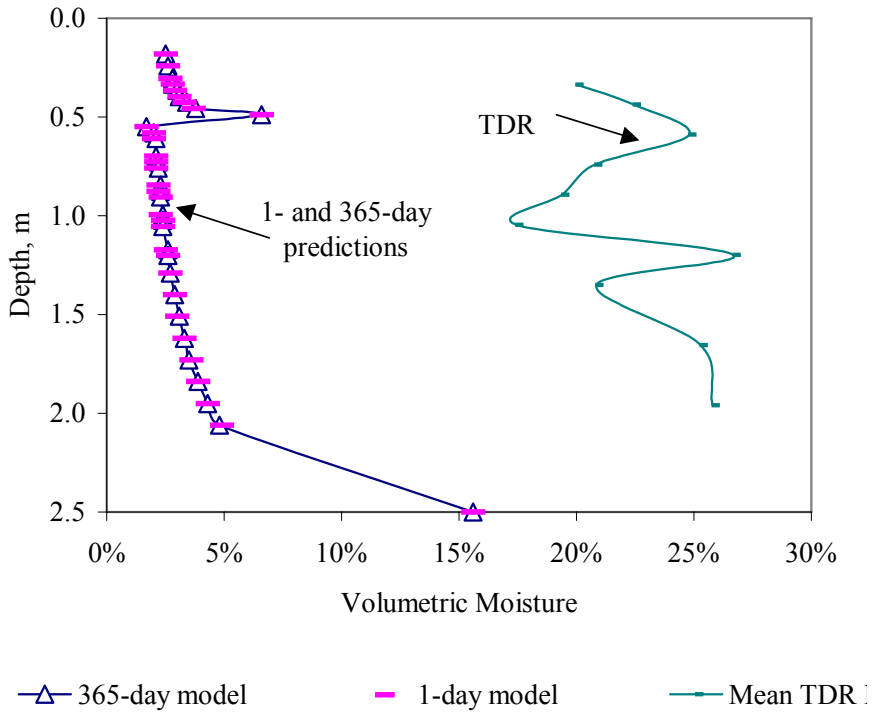

Figure 10. Predicted and monitored moisture contents for section 091803 (Connecticut), 6/30/94

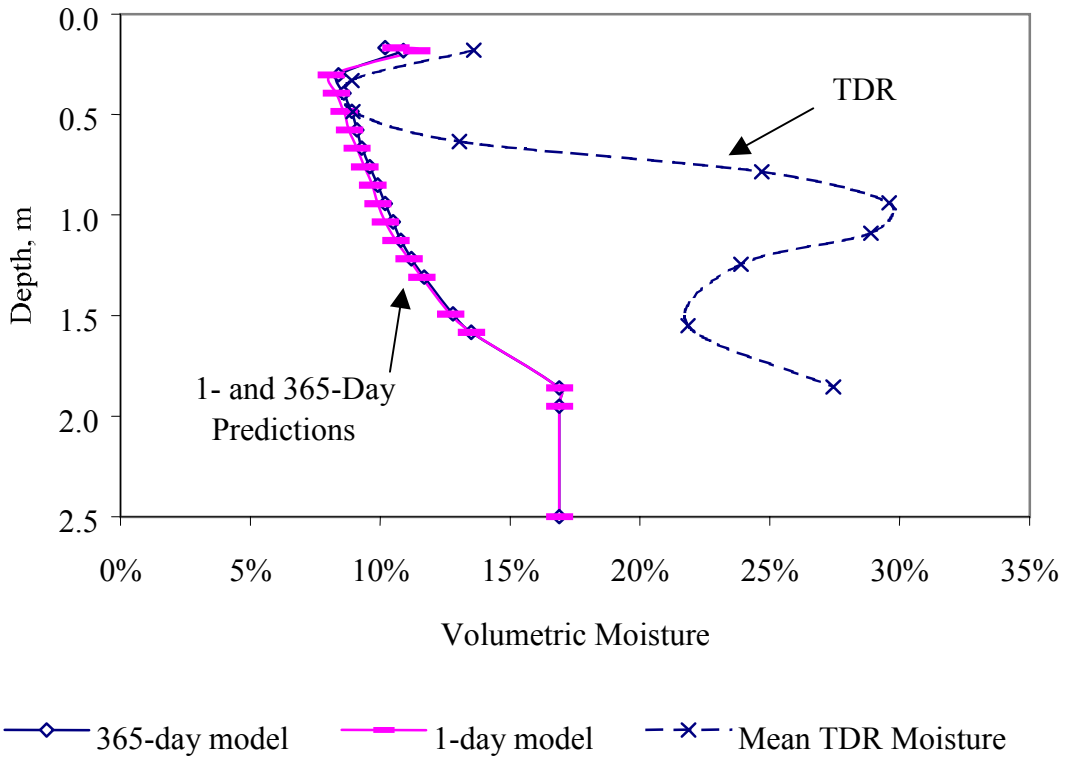

Figure 11. Predicted and monitored moisture contents for section 271018 (Minnesota), 8/8/94

- Varying the time increment used in the calculations from 1.0 to 0.01 hours had no effect on computed moisture contents.

- The EICM "generate" function, which is used to "fill in" (via interpolation) missing data for climatic data elements did not function properly when used with input data in metric units.

- Varying the time period used in the simulation from 1 day to 1 year may significantly alter the predicted moisture content when EICM-generated pore-pressure profile data are used in the simulation. (The results shown in Figure 10 and Figure 11 used pore-pressure profiles estimated from section-specific water table depth data.)

As a result of the poor agreement observed in these initial trials, the EICM was modified (by the model developer) to provide the capability to use section-specific moisture profile data to initialize the computations and correct the program "bugs" identified through the evaluation, with the result being EICM Version 2.1. The author's evaluation of EICM Version 2.1 is discussed in the next section of this chapter.

EVALUATION OF EICM VERSION 2.1

Sections Considered

Six of the test sections identified in Table 30 were used in the evaluation of Version 2.1 of the EICM—sections 091803 (Connecticut), 231026 (Maine), 271018 (Minnesota), 331001(New Hampshire), 501002 (Vermont), and 831801 (Manitoba). The input data used in modeling these sections with EICM Version 2.1 are summarized in Table 60 and Table 61 of Appendix B. Pertinent details unique to the application of Version 2.1 are as follows.

Layer Structure

In applying EICM Version 2.1, a single model layer was used for each of the nominal pavement layers, with the number of elements in each layer selected to yield nodes close to the depths at which the moisture monitoring instrumentation was installed in each test section.

Layer Porosity

In most cases, the maximum observed volumetric moisture content for each pavement layer was used as the basis for estimating the porosity of that layer, as only some of the data required to determine material-specific porosity values were available to the author at the time of this analysis. For section 271018, the porosity values used were derived from in situ density and moisture data, using an assumed soil specific gravity of 2.65 g/cm^3 (0.1 pound/inch^3).

Soil-Water Characteristic Curve Parameters (Gardner Coefficients)

EICM Version 2.1 and earlier versions use the Gardner model for the soil-water characteristic curve to model moisture movement through the soil. With Version 2.1, entry of the Gardner coefficients was made optional, and the capability to provide an initial moisture content profile to "calibrate" the model was added. Gardner coefficients are not among the data available for the LTPP test sections. Thus, user-supplied Gardner coefficients were not used.

Results

The moisture contents predicted by EICM Version 2.1 are compared with the moisture content data collected at the LTPP test sections in Figure 12 and Figure 13. In comparing the EICM Version 2.1 output to the field data, linear interpolation was used to estimate the EICM output for the specific depths at which the TDR probes are placed. Inspection of moisture-depth profile plots for the EICM output, such as that shown in Figure 14, suggests that this is a reasonable approximation for the small differences in depth under consideration. In addition, data for monitoring dates associated with actual or predicted frozen conditions (as reflected in one or more of the following indicators) have been omitted.

- Data in LTPP database table SMP_FROST_PENETRATION indicating the presence of one or more frozen layers in the pavement structure.

- Temperature data in table SMP_MRCTEMP_AUTO_DAY_STATS indicating that the minimum observed temperature at one or more depths in the pavement was less than 0 °C.

- Predicted moisture content of less than 1 percent occurring in winter months.

These data points were excluded to provide a "fair" comparison in light of the uncertain meaning of monitored moisture contents obtained in frozen or partially frozen soils. The EICM assumes that the unfrozen moisture content of frozen soil is zero. In contrast, the LTPP data show a reduced, but nonzero, moisture contents in frozen soils.

The error bands shown on the lines of equality are the maximum and minimum 95 percent confidence intervals applicable to the TDR moisture contents (see Table 28). (Only one error band is evident for the base materials, as the minimum and maximum applicable error limits are the same.) These error bands are plotted in the figure to provide a means of judging the extent to which the poor agreement between the monitored and predicted moisture contents may be attributable to error in the TDR-based moisture contents.

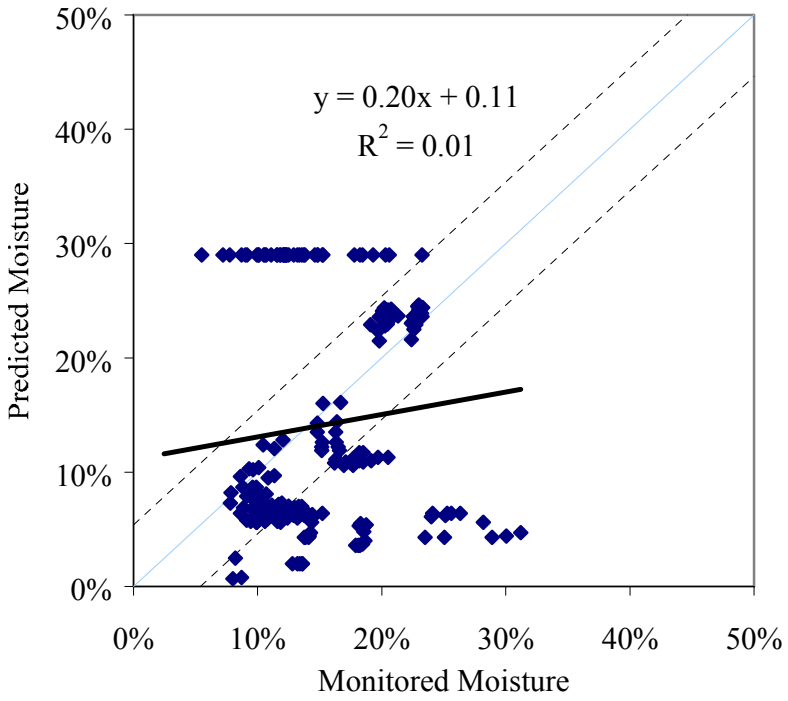

Figure 12. Comparison of monitored and predicted base-layer moisture for EICM Version 2.1

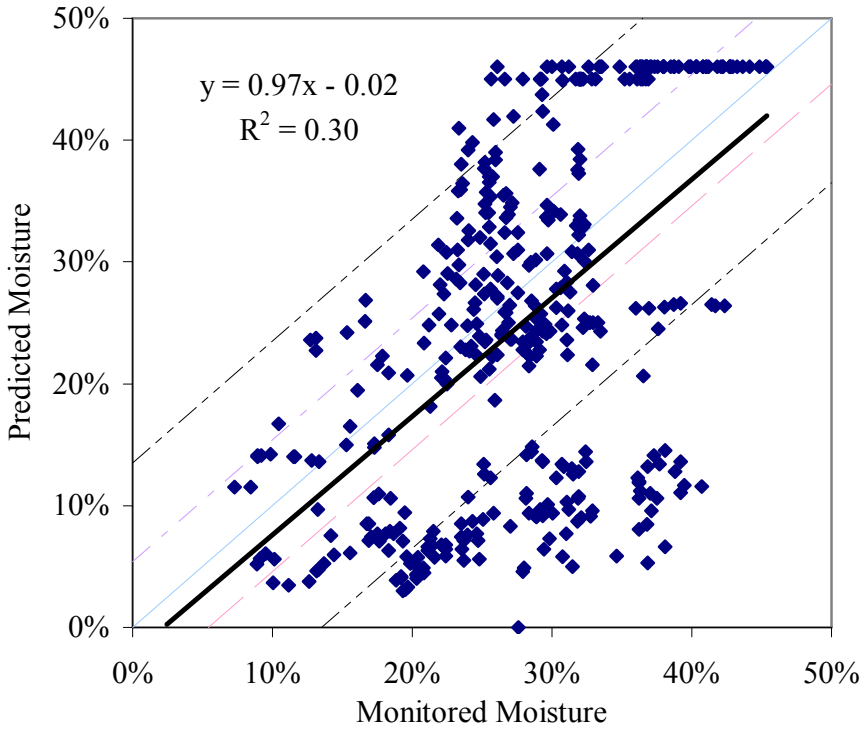

Figure 13. Comparison of monitored and predicted subgrade moisture for EICM Version 2.1

While good or excellent agreement is observed for some data points, overall agreement between the model and the field data is poor, as evidenced by both the low fraction of variation explained by the trend lines ($R^2 = 0.01$ and $R^2 = 0.30$) and the many data points that fall outside the estimated 95 percent confidence intervals for the monitored moisture data. Based on discussions with the model developer and others, it is believed that the discrepancies are attributable to several deficiencies, some in the EICM itself, and others in its application. These deficiencies point to the need for improvements in both the EICM and user documentation to support its use. Recommended changes arising from these discussions included the following.

EICM Changes

- Improvements to the soil-water characteristic curve model used in the simulation.

- Expanded capabilities for generating parameters for the soil-water characteristic curve, which reduce the need to input parameters not commonly available for pavement materials.

These changes were eventually implemented by others as a result of this study. This work was conducted as a part of the development of the *2002 Guide for Design of New and Rehabilitated Pavement Structures* under NCHRP project 1-37A.[19]

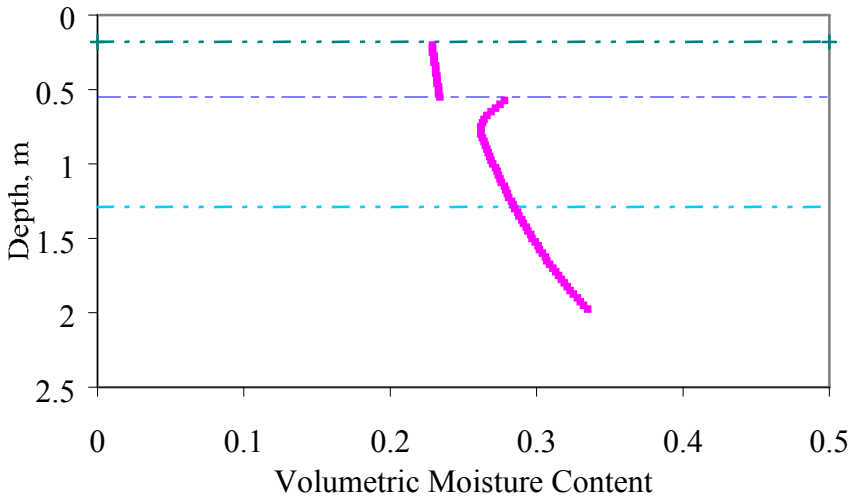

Figure 14. Sample EICM Version 2.1 moisture-profile plot, section 091803 (Connecticut)

Application Changes

- The user of the EICM is required to choose between two internal boundary conditions, one known as the "flux" condition, and the other referred to as "suction." The flux boundary condition assumes that water may enter the subgrade through a saturated subbase, whereas the suction condition assumes that subgrade moisture is controlled primarily by suction induced by the water table. EICM trials with Versions 2.0 and 2.1 used the suction boundary condition. The model developers recommended use of the flux condition in most cases.

- Subdivision of pavement subbase and subgrade layers to allow better characterization of the initial moisture profile. (Subdivision of the base layer is not recommended.)

These changes were implemented in the author's evaluation of subsequent versions of the EICM.

APPLICATION OF EICM VERSION 2.6

All sections identified in Table 30 were used in the evaluation of EICM Version 2.6. Four sections not used in the evaluation of Version 2.1 were considered, to provide more complete coverage of the range of climatic conditions found in the United States and Canada. The data used as input to this version of the model are presented in Table 62 to Table 64 of Appendix B. As noted previously, these data differ from those used with Version 2.1 due to: (1) differences between the two versions of the model; (2) implementation of the application

changes noted previously; and (3) additional data that became available in the intervening time period. Pertinent details unique to the application of Version 2.6 are as follows.

Layer Structure

In applying EICM Version 2.6, the pavement layers were subdivided, such that each TDR probe depth corresponded to a mid-depth node for a layer in the model. In cases where a single pavement layer corresponds to multiple model layers (e.g., pavement layer 3 for the Arizona section (041024) corresponds to model layers 3–13), a single entry in Tables 62–64 for any material property indicates that the same value was used for all model layers. Multiple entries indicate that different values were used for each model layer. The values used are listed in order from top to bottom. For example, model layer 5 at the Arizona section was 1.2 cm thick modeled with 2 elements, and had an initial volumetric water content of 19.95.

Layer Porosity

In the time frame between the application of EICM Version 2.1 and the release of EICM Version 2.6, the author obtained specific gravity data for some of the materials considered in this work, which enabled the computation of porosity for those materials. Where available, these values were used; otherwise, this field was left blank.

Specific Gravity

Specific gravity was not among the input parameters required for Version 2.1, and is an optional (but highly recommended) input parameter for Version 2.6. Specific gravities were entered where material-specific data were available. Otherwise, this field was left blank.

Saturated Permeability

Saturated permeability data are not available for the LTPP test sections. This field was left blank in all cases.

Initial Volumetric Water Content

Whereas EICM Version 2.1 required entry of an initial moisture profile (i.e., moisture on a node-by-node basis), Version 2.6 requires input of an initial moisture content for each model (as opposed to pavement) layer. The data used as input are identical. The manner in which they are used in the model differs. Details of the difference are discussed elsewhere.[19]

Soil-Water Characteristic Curve Model and Parameters (Gardner Coefficients)

Among the changes reflected in EICM Version 2.6 is the addition of the capability to use the soil-water characteristic curve model developed by Fredlund and Xing (discussed in reference 19) as an alternative to the Gardner model. The soil parameters required as input for this model are automatically selected, based on the soil classification and other routine soils data entered by the user. The Fredlund and Xing model was used in all applications of Version 2.6.

Results

The EICM V2.6 predicted moisture contents are compared with the LTPP moisture data in Figure 15 and Figure 16. As before, data points associated with actual or predicted frozen conditions were omitted, and the error bands on the lines of equality are the maximum and minimum 95 percent confidence intervals applicable to the TDR moisture contents. (Only one error band is evident for the base material because the minimum and maximum applicable error limits are coincident.)

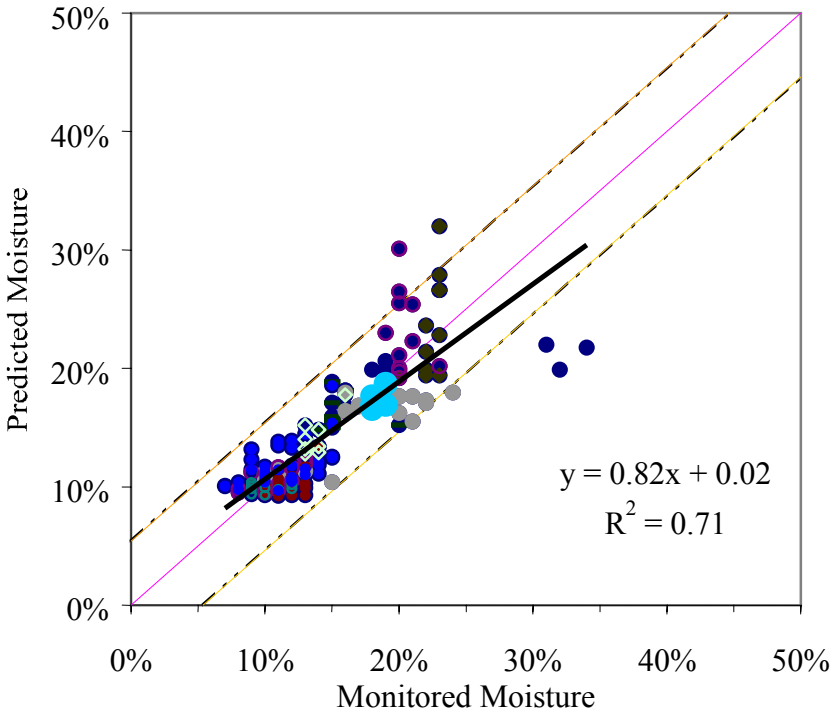

Figure 15. Comparison of monitored and predicted base moisture for EICM Version 2.6

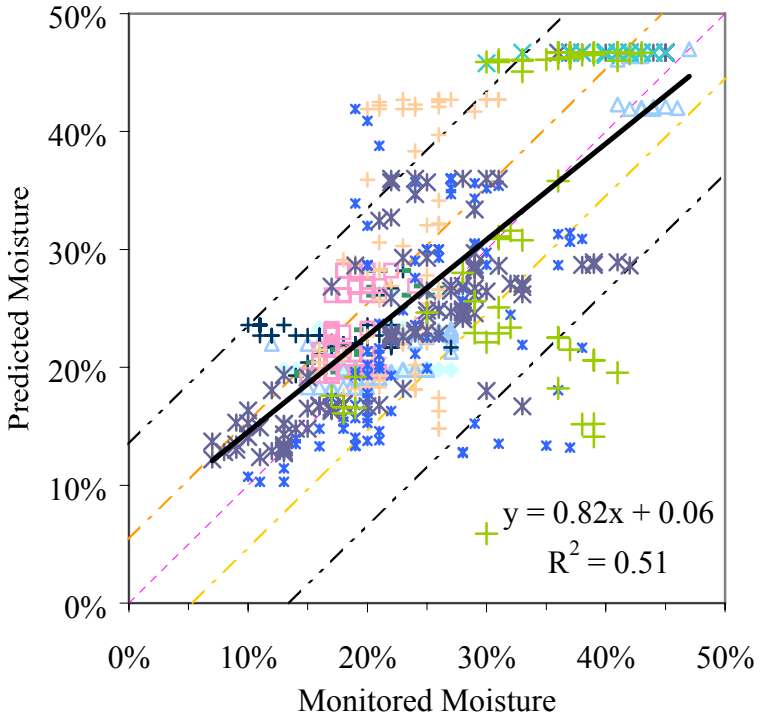

Figure 16. Comparison of monitored and predicted subgrade moisture for EICM Version 2.6

While not perfect, the agreement between the measured and predicted base moisture contents is reasonable, with the majority of the data points clustered about the line of equality within the 95 percent confidence limits for the monitored moisture data. These results are substantially better than those obtained with Version 2.1 of the model (see Figure 12). The results for the subgrade soils are not as good as those for the base, but are better than those obtained with Version 2.1 (Figure 13).

The data were examined to identify what conditions are associated with the data falling outside the maximum applicable confidence limits. Sections for which more than one data point fell outside the applicable confidence limits are discussed below.

As illustrated in Figure 17, the predicted base moisture content for section 041024 is relatively constant with time, whereas the monitoring data show a marked (approximately 10 percent on a volumetric basis) increase in moisture content between winter and summer months. The magnitude of this increase in monitored moisture content decreases with depth, and the data for the deeper monitoring depths show a decrease in moisture in this time frame, suggesting an upward migration of soil moisture in the hotter months of the year. It is likely that the discrepancy between the monitored and predicted moisture contents is attributable to

incompatibility between the theory on which the EICM is based and the true mechanisms of soil moisture movement in the arid climate in which this section is located.

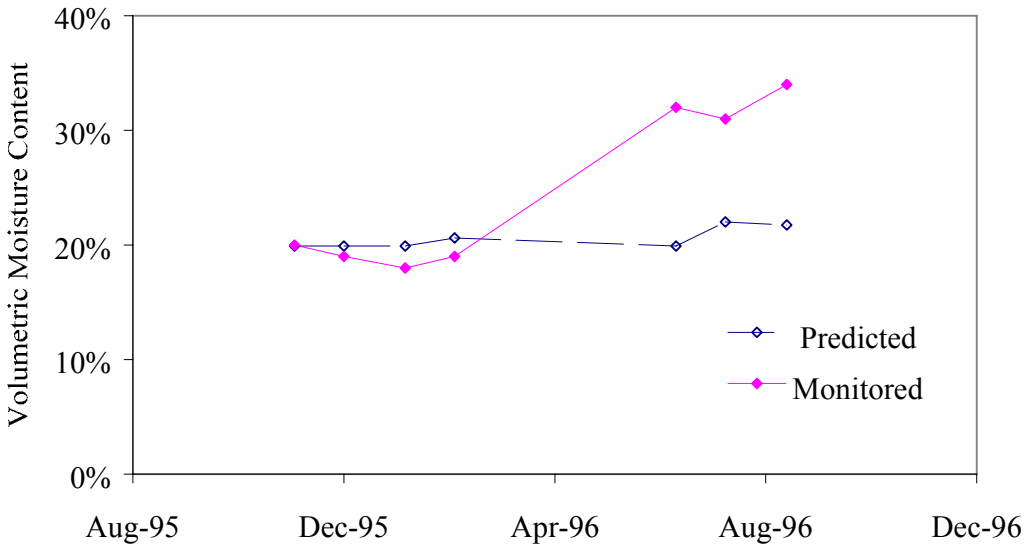

Figure 17. Variation in monitored and predicted base moisture, section 041024

Figure 18 shows the variation in monitored and predicted subgrade moisture content with time for section 091803 (Connecticut). The monitored data indicate that the base moisture content at this section is relatively constant with time, with the moisture content at the shallower depth being slightly lower than that at the greater depth. The predicted base moisture content for both depths is quite similar to the monitored moisture for the shallower depth through the summer and fall, but increases markedly in the spring. For the subgrade, the model tends to underpredict the actual moisture content for the first half of the simulation period (summer - early fall), and overpredict the moisture content for the later portion of the simulation period (late fall - spring). It is believed that the observed discrepancies can be attributed, at least in part, to use of model-generated (rather than material-specific) material parameters that (apparently) do not accurately reflect the drainage characteristics of the soils at this section.

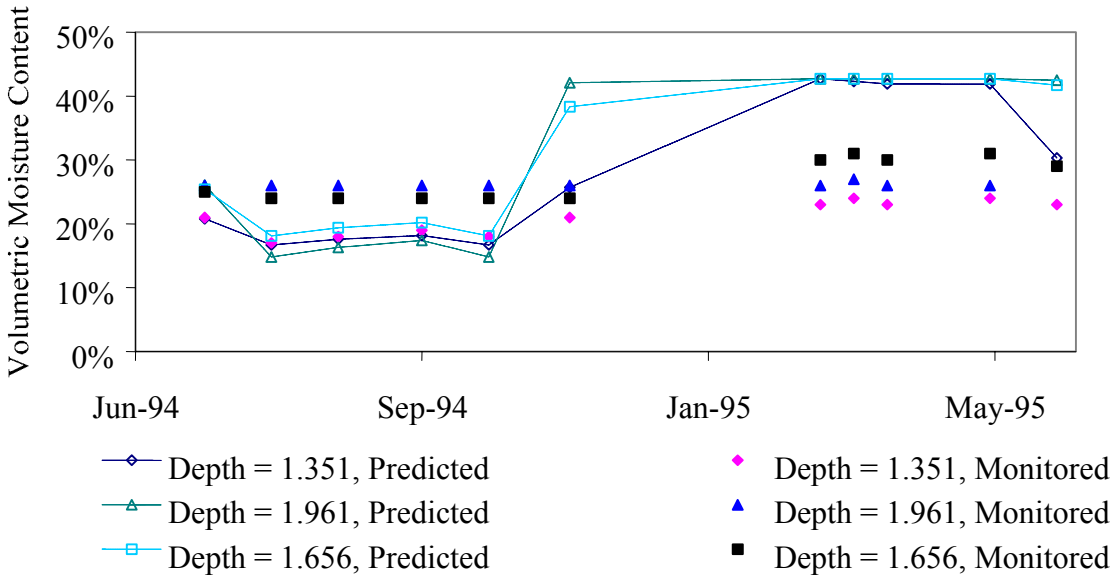

Figure 18. Monitored and predicted subgrade moisture content, section 091803 (Connecticut)

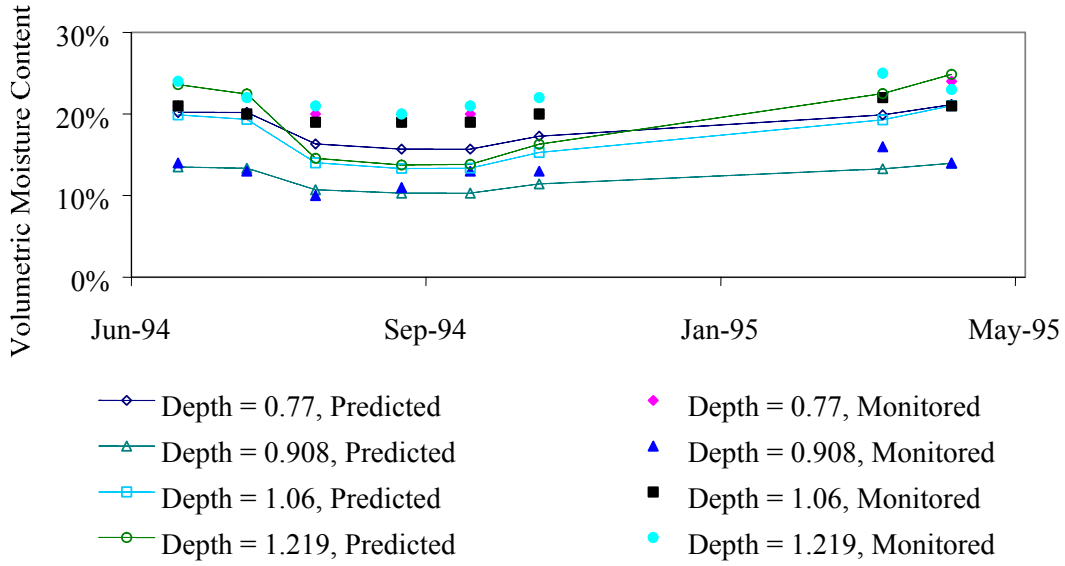

Figure 19. Monitored and predicted subgrade moisture, section 231026 (Maine)

The upper subgrade data for section 231026 (Maine) are plotted in Figure 19. For this section, the model consistently underpredicts the actual moisture content for all but the deepest (1.969 m) monitoring depth (not shown). The seasonal trends in moisture predicted by the model are reasonably consistent with those observed in the data, though the model tends to overpredict the magnitude of the changes. This discrepancy may be attributable, at least in part, to inconsistencies in the data for this section. The porosity for the subgrade material, computed from available materials data, and used as input to the EICM was 0.30, while the maximum observed volumetric moisture content for the layer was 0.37—greater than the computed porosity. This discrepancy may be due to spacial variations in porosity, disturbance of the soil that occurred when the TDR probes were installed, or errors in the TDR moisture data. The result is that the model will always underpredict (relative to the monitored moisture data) moisture for monitoring dates where the observed moisture content was greater than 0.30.

The predicted subgrade moisture content for section 501002 (Vermont), illustrated in Figure 20, remains at or near the saturation value throughout the year. The monitored moisture contents are both lower and more variable. As with section 091803, this discrepancy is attributed to the use of model-generated values for many of the key material parameters.

The time trends for the monitored and predicted subgrade moisture contents for section 831801 are illustrated in Figure 21 and Figure 22. For this section, the model consistently underpredicts subgrade moisture, though the monitored and predicted moisture contents for depths of 0.65 and 0.96 m are very similar. For the other depths, the model predicts increases in moisture where the data show decreasing moisture content, and vice versa. In contrast, there is good agreement between the monitored and predicted base moisture contents for this section. As with the sections discussed previously, it is probable that some of the observed discrepancy is attributable to the use of model-generated material parameters. However, the author is at a loss to fully explain the very poor agreement for the deeper monitoring depths in the subgrade soil.

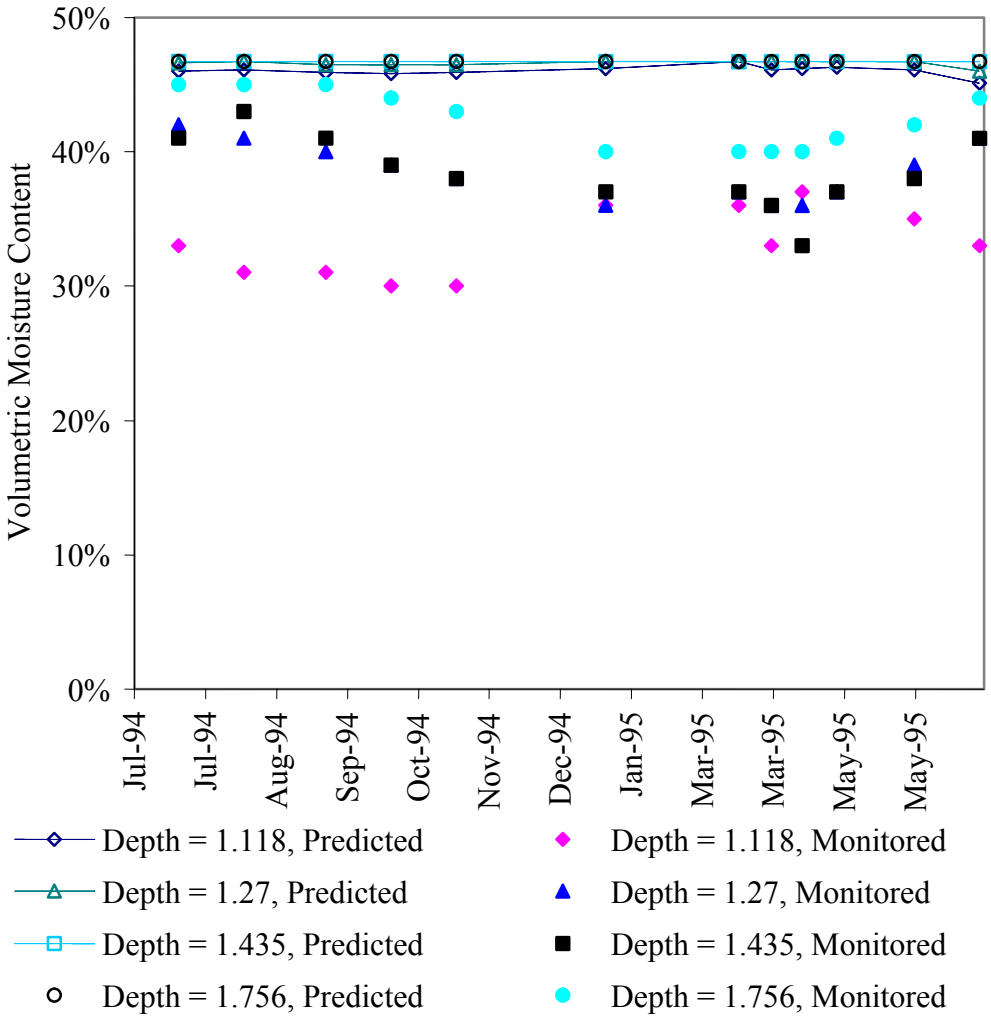

Figure 20. Monitored and predicted subgrade moisture, section 501002 (Vermont)

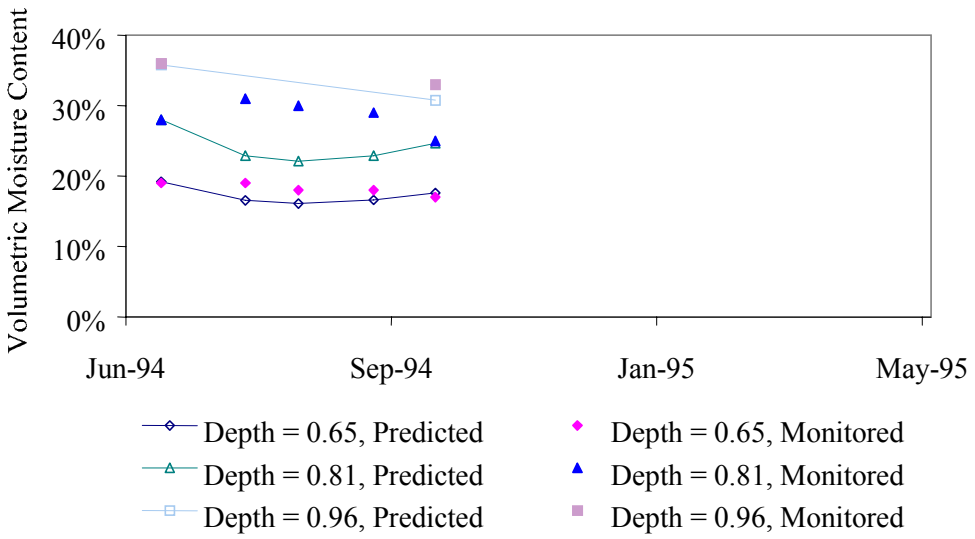

Figure 21. Monitored and predicted subgrade moisture (shallow depths), section 831801 (Manitoba)

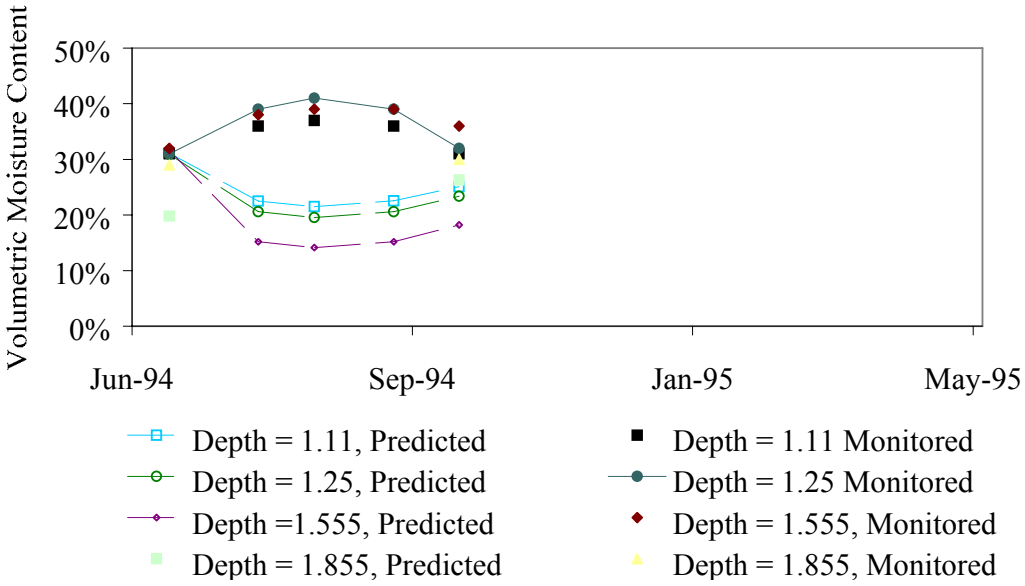

Figure 22. Monitored and predicted subgrade moisture (greater depths), section 831801 (Manitoba)

EVALUATION OF EICM VERSION 2.6 USER SENSITIVITY

Data assembled by the author to evaluate EICM Version 2.6 were also applied by members of the NCHRP 1-37A research team in their efforts to assess the outcome of the model changes. Although the basic data used in the 1-37A evaluation of the model were identical to those used by the author, there were subtle differences in the application of those data by virtue of the judgments that must be made in applying the model. Thus, two parallel and independent sets of applications of the EICM for the same nominal input data set were developed, creating an opportunity for a limited evaluation of the user-sensitivity of the model.

Between-User Differences in Model Application

The differences between the author's application of the EICM Version 2.6 and that of the NCHRP 1-37A research team are summarized in Appendix C, Table 69. The most prevalent differences were related to the entry of specific gravity, percent passing 200, and plasticity indices for base and subgrade materials. Whereas the author entered specific gravity values only when material-specific data were available, the NCHRP 1-37A research team entered estimated values when soil-specific data were not available. It is likely that this difference in the application of the model had some impact on the results obtained.

In several instances, the number of sublayers used differed between the two applications. These differences are, by definition, associated with differences in the number of elements in the sublayers and in equilibrium moisture content. Small differences in the number of sublayers and equilibrium moisture associated with differences in the number of sublayers are not noted.

The NCHRP 1-37A team reported entry of values for percent passing 200 and plasticity index (PI) in all cases, whereas the author entered values only when soil-specific values were both available, and required, based on the following understanding of their use: (1) for granular soils or nonplastic fine-grained soils, only the D60 is used; and (2) for fine-grained soils with PI greater than 0, only the percent passing 200 and the PI are used. Entry or failure to enter the parameters that are not used in the computations should have no impact on the predicted moisture contents.

Impact of Between-User Differences in Model Application

The overall impact of the application differences on the predicted moisture contents is explored in Table 31, Figure 23, and Figure 24. The information presented in Table 31 includes the two mean predicted moisture contents for each pavement layer at each section, the mean, standard deviation, minimum, and maximum values for the difference between the two predicted moisture contents, the number of paired moisture observation for each layer (n), and the Student's t statistic for the difference, for a paired t-test on the null hypothesis that the difference is equal to zero. The null hypothesis is accepted for only four layers—all of them base layers—at a 5 percent level of significance: Those layers, denoted by bold type in table 31, are the base layers for section 041024, 081053, 091803, and 501002.

Table 31. Between-user differences in predicted moisture content for EICM Version 2.6

Section	Layer	Mean EICM Predicted Moisture		Difference in EICM Predicted Moisture (1-37A-Author)				n	t
		Author	1-37A	Mean	Std. Dev.	Min.	Max.		
041024	**2**	**20.6%**	**20.3%**	**−0.3%**	**0.3%**	**−0.9%**	**−0.1%**	**7**	**−2.3**
041024	3	20.9%	21.1%	0.1%	0.3%	0.0%	1.8%	63	4.4
081053	**2**	**16.4%**	**16.0%**	**−0.4%**	**1.3%**	**−4.4%**	**0.4%**	**12**	**−1.1**
081053	3	20.1%	19.6%	−0.5%	1.3%	−4.0%	1.3%	28	−2.1
081053	4	43.8%	41.0%	−2.8%	2.3%	−6.0%	−0.9%	18	−5.2
091803	**2**	**23.3%**	**23.0%**	**−0.3%**	**3.4%**	**−8.3%**	**3.2%**	**20**	**−0.4**
091803	3	27.6%	25.0%	−2.7%	7.5%	−14.7%	8.3%	80	−3.2
131005	2	17.0%	16.7%	−0.3%	0.4%	−0.8%	0.5%	11	−2.5
131005	3	19.9%	18.5%	−1.4%	1.9%	−4.8%	0.5%	54	−5.4
131005	4	22.5%	11.4%	−11.1%	3.5%	−14.3%	−5.3%	44	−20.9
231026	2	13.2%	10.7%	−2.5%	0.9%	−4.5%	−1.6%	21	−12.7
231026	3	21.9%	18.1%	−3.8%	6.0%	−22.2%	10.1%	44	−4.2
271018	2	14.3%	14.7%	0.5%	0.4%	−0.1%	0.9%	8	3.1
271018	3	25.2%	23.8%	−1.4%	3.1%	−8.6%	7.9%	75	−3.9
331001	2	10.0%	10.1%	0.1%	0.4%	−0.5%	0.8%	30	2.1
331001	3	16.1%	15.8%	−0.2%	0.2%	−0.6%	0.3%	20	−4.6
331001	4	23.6%	23.9%	0.3%	0.8%	−0.6%	2.1%	47	2.8
481077	2	11.0%	15.6%	4.5%	0.1%	4.3%	4.8%	8	100.
481077	3	22.9%	26.7%	3.8%	2.2%	−2.9%	6.7%	79	15.1
501002	**2**	**12.1%**	**12.5%**	**0.4%**	**1.7%**	**−3.3%**	**4.9%**	**33**	**1.3**
501002	3	23.7%	17.9%	−5.8%	4.4%	−13.3%	1.1%	10	−4.2
501002	4	46.5%	39.5%	−7.0%	3.3%	−17.8%	−2.8%	55	−15.8
831801	2	17.3%	19.8%	2.4%	1.5%	−0.2%	3.5%	5	3.6
831801	3	15.0%	16.6%	1.6%	0.9%	0.1%	2.8%	10	5.6
831801	4	22.0%	30.9%	8.9%	6.1%	0.2%	28.4%	29	7.9

The overall results for the two sets of EICM applications are compared to each other in Figure 23, and to the monitored moisture data in Figure 24. As in previous figures in this chapter, the dashed lines in the figures denote the maximum applicable 95 percent confidence intervals for the related field moisture data. Overall, the results presented in Table 31, Figure 23, and Figure 24 show that between-user differences in the application of the EICM can affect the simulation results. The observed variation in the magnitude and significance of the between-user differences in the predicted moisture contents is to be expected, as the nature and extent of the between-user differences in the model application varied from one section (and layer) to another. A more detailed examination of the results obtained follows.

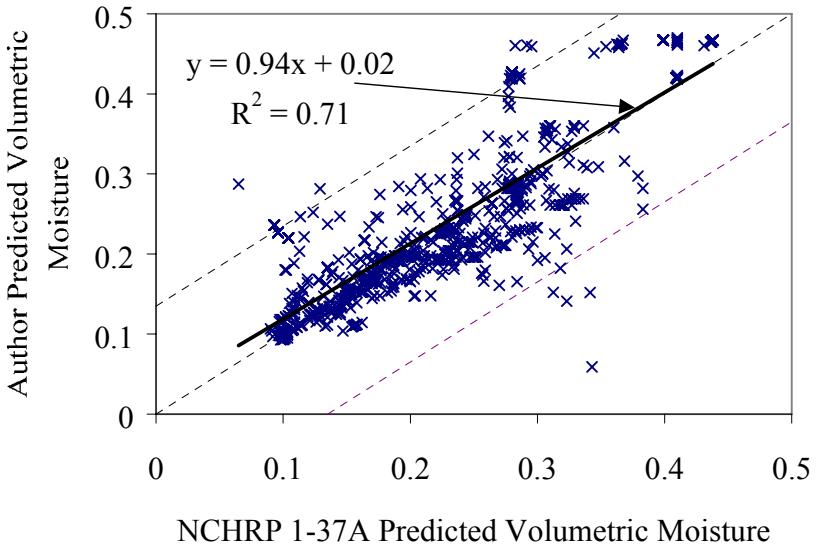

Figure 23. Comparison of EICM Version 2.6 moisture predictions for all sections

A graphic comparison of the two sets of predicted moisture contents for section 081053 is provided in Figure 25. This figure and the numerical information presented in Table 31 indicate that the differences in the application of the model for this section do not result in any meaningful difference in the predicted moisture contents. Similarly good agreement is observed for sections 041024 and 331001.

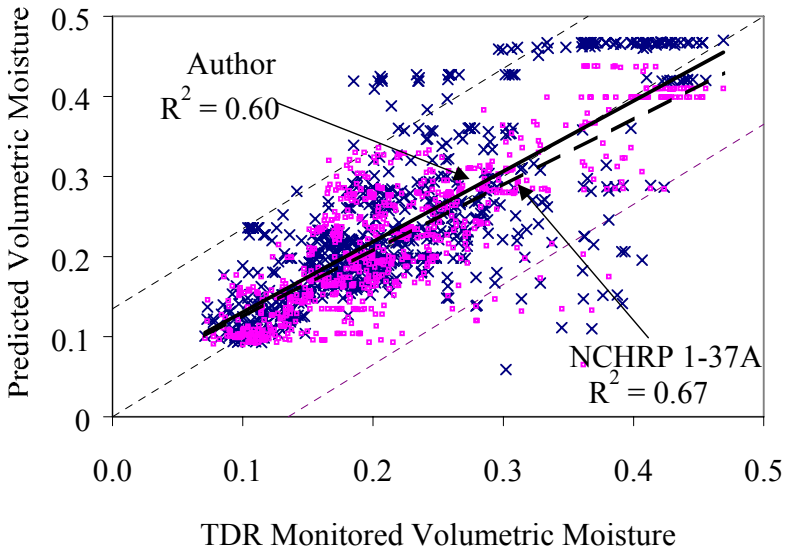

Figure 24. Monitored and predicted moisture contents for all sections

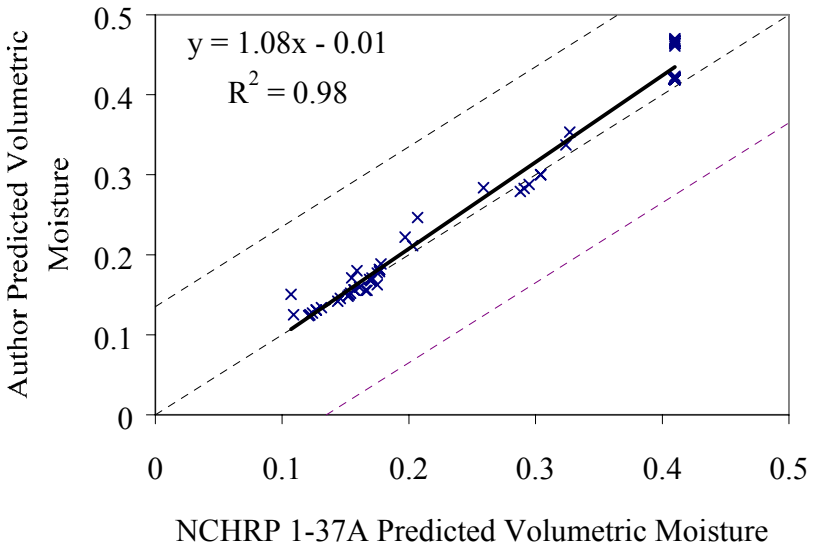

Figure 25. Comparison of moisture predictions, section 081053

Larger differences in the predicted moisture contents are observed for the remaining sections: 091803, 131005, 231026, 271018, 481077, 501002, and 831801. The results for section 481077 are illustrated in Figure 26 and Figure 27. Differences between the two applications for this section included differences in both the starting date (and thus, equilibrium moisture conditions) for the simulation, and data characterizing the base material, so the fact that significant differences are observed is not surprising. In Figure 26, one can see that both sets of predicted base moisture content fall within the 95 percent confidence limits for the monitored moisture data. The NCHRP 1-37 application tends to overpredict moisture, while most of the data points for the author's application fall closer to the line of equality. In Figure 27, one may observe that both applications tend to overpredict subgrade moisture, though the NCHRP 1-37A application does so to a greater degree than the author's application.

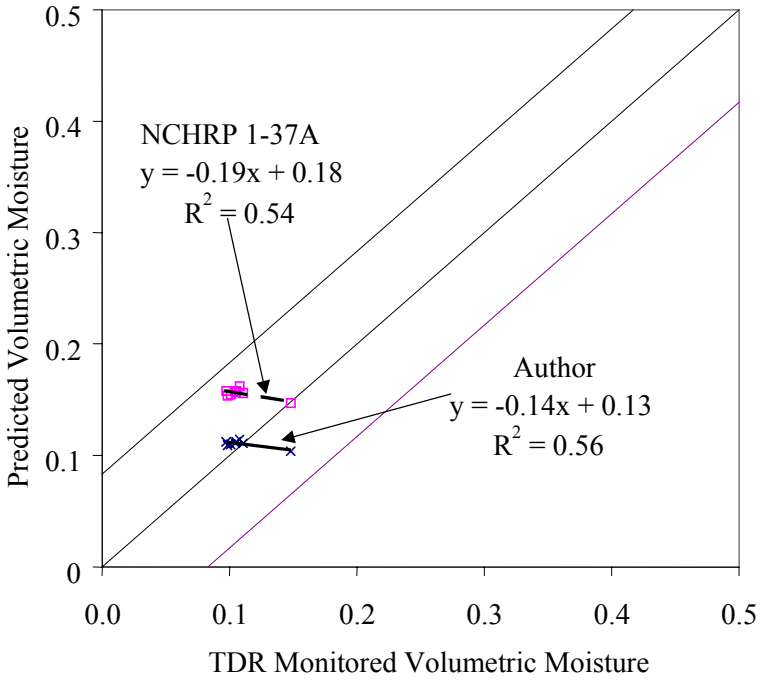

Figure 26. Monitored and predicted base moisture content, section 481077 (Texas)

The two sets of predicted moisture contents for section 091803 are compared to each other in Figure 28 and to the monitored moisture data in Figure 29. Agreement between the two sets of predictions is relatively poor. Thus, the observed relationships between the monitored and predicted values illustrated in Figure 29 are quite different, though the correlations are similar. The fact that the majority of the data points for the NCHRP 1-37A predictions fall within the 95 percent confidence limits for the monitored data, while those for the author's predictions do not, suggests (but does not by itself definitively prove) that use of one or more of the parameters estimated and entered by the NCHRP 1-37A research team, but not entered by the author (absent soil-specific data) improves the quality of the EICM results.

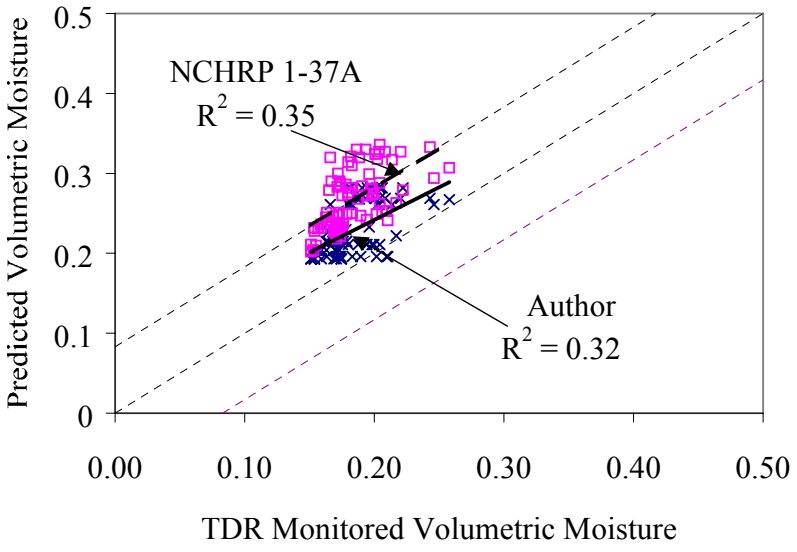

Figure 27. Monitored and predicted subgrade moisture content, section 481077 (Texas)

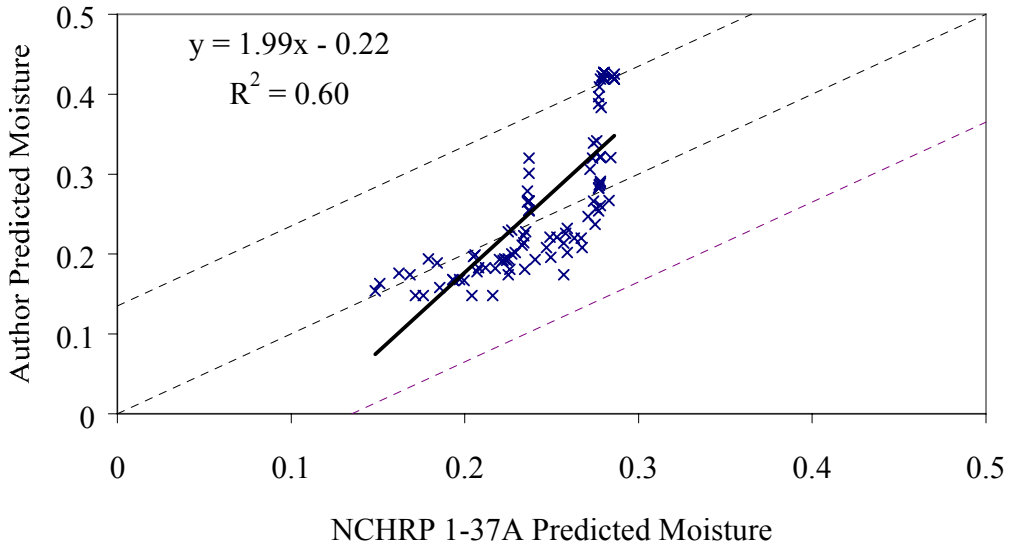

Figure 28. Comparison of predicted volumetric moisture contents for section 091803 (Connecticut)

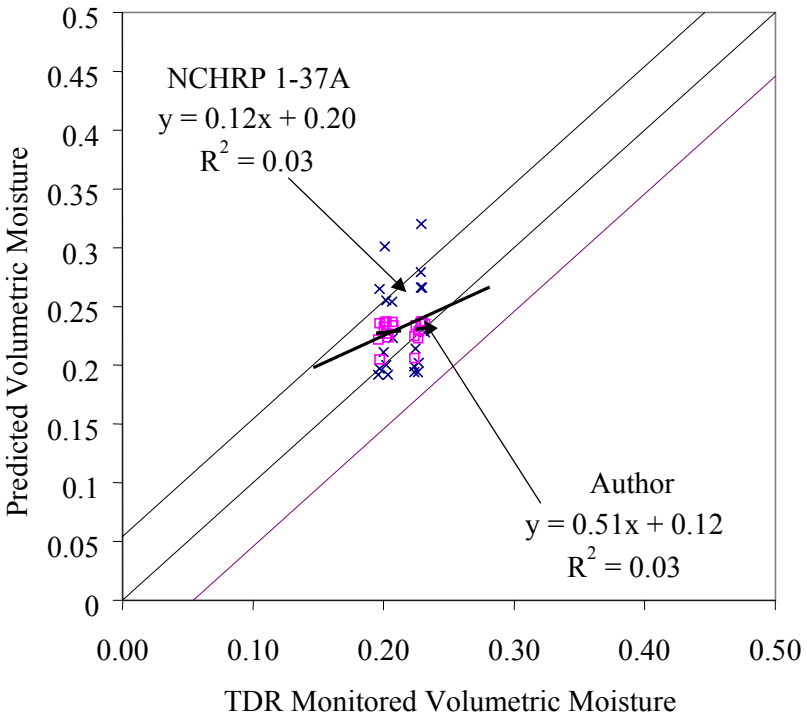

Figure 29. Monitored and predicted moisture content, section 091803 (Connecticut)

Predictions for section 131005 are compared with the monitored data in Figure 30 and Figure 31. The predicted values for the base and upper subgrade layers are very similar, but the differences for the subgrade are quite substantial. For this layer, the author did not enter the specific gravity, because soil-specific data were not available, while the 1-37A research team used estimated values. Soil-specific values for percent passing 200 and PI were entered by the 1-37A team, but not by the author (who understood them to be unnecessary). Differences in the start dates (and thus, the equilibrium water contents) used in the predictions may have also contributed to the observed differences. The NCHRP 1-37A model yields better overall agreement with the monitored moisture data.

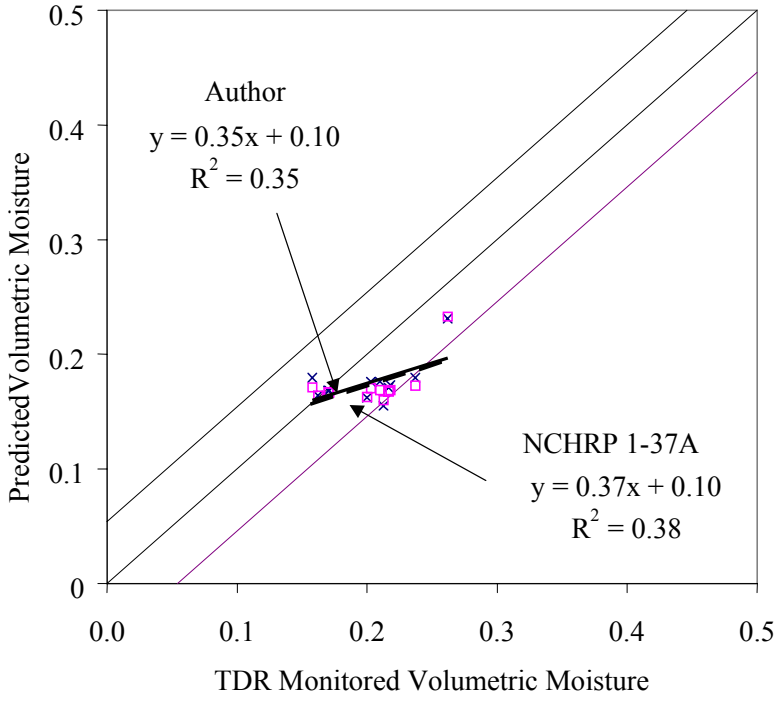

Figure 30. Monitored and predicted base moisture, section 131005 (Georgia)

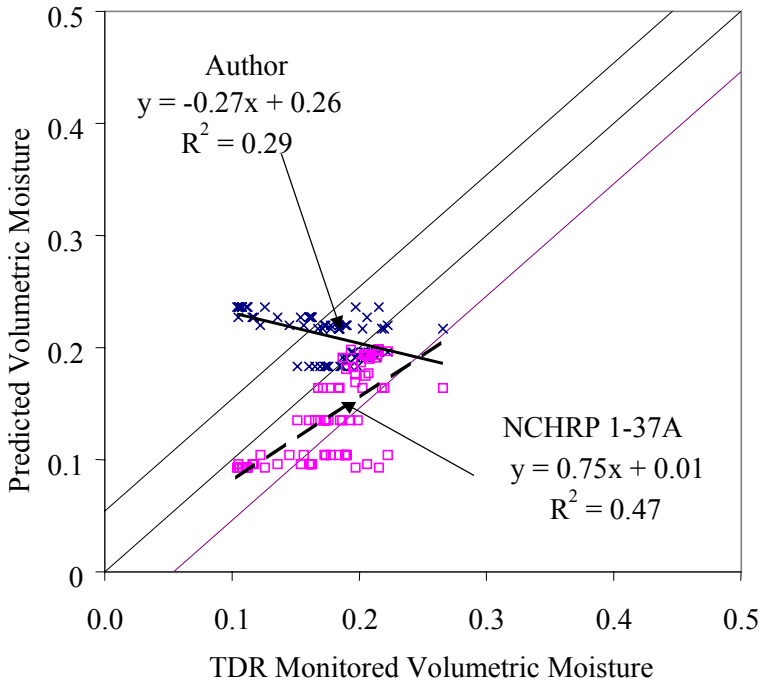

Figure 31. Monitored and predicted subgrade moisture, section 131005 (Georgia)

DISCUSSION AND CONCLUSIONS REGARDING EICM MOISTURE PREDICTIONS

The evaluation of the moisture-prediction capabilities of EICM Versions 2.0 and 2.1 presented here is in many respects imperfect because several key material parameters required by the model are not among the data collected for the test sections used in the evaluation. Thus, no judgments can be made as to whether the model itself does or does not yield accurate moisture predictions when applied with complete, material- and section-specific data for the pavements being modeled. However, the results of this evaluation do point out the practical limitations of EICM Versions 2.0 and 2.1, as the data used here are more complete than is often the case in a typical pavement design application. It can be concluded (and should come as no surprise) that the model may not yield accurate moisture predictions when assumed values are used for several key input parameters.

Furthermore, the program documentation guidance on the selection of appropriate values for key material parameters in the absence of complete section-specific data is insufficient to support use of the model in routine practice, where incomplete input data may be expected to be the norm, rather than the exception.

In contrast to Version 2.1, it can be concluded, based on the findings here, that EICM Version 2.6 can provide reasonable estimates of the variation in the in situ moisture content of unbound pavement materials. This is sometimes, but not always, true even when model-generated values are used for several key material parameters. The findings for section 041024 (Arizona) suggest that the model may not work well for sections in arid climates; however, more extensive evaluation will be needed to draw definitive conclusions in this regard.

It is apparent that the revisions made in the transition from EICM Version 2.1 to Version 2.6 have greatly enhanced the practical applicability of the model. While it may be very appropriate for use in a research setting, EICM Version 2.1 is difficult to use in practice because it requires input parameters, most notably the Gardner coefficients, that are not commonly obtained in the laboratory characterization of pavement materials. While soil-specific values of these parameters can be used with Version 2.6 if they are available, they are no longer essential to obtain reasonable results. Thus, in the author's judgment, Version 2.1 is most appropriately thought of as a research tool, while Version 2.6 can be considered a practical engineering tool. There remains room for improvement, however, in the user interface for the EICM, as a great deal of manual data manipulation is required to generate input data sets compatible with the EICM.

Lastly, both t-test results and the detailed results illustrated in Figure 23 through Figure 31 indicate that between-user differences in EICM-predicted moisture contents can be significant in both statistical and practical terms. These differences point to the need for: (1) very specific guidance on the use of data that are recommended, but not required; (2) care in entering correct information relative to material gradation; and (3) careful consideration of the selection of appropriate initial conditions for the moisture prediction. It would be appropriate to conduct further sensitivity analyses to evaluate the relative importance of these factors in causing the observed differences in predicted moisture.

CHAPTER 5: PREDICTION OF BACKCALCULATION PAVEMENT LAYER MODULI

INTRODUCTION

This chapter discusses the development of relationships to predict backcalculated moduli for unbound pavement layers. The models discussed address the effects of both moisture condition and stress state on the moduli of these layers in the nonfrozen condition.

The backcalculated pavement layer moduli used in this work are those from the LTPP database that remained in the working data set after the review process discussed under Evaluation of Backcalculated Layer Moduli" in Chapter 3. The stress parameters considered were computed by the author, as discussed under "STRESS PARAMETERS" in Chapter 3. Input to these computations included the backcalculated pavement layer moduli, the layer thickness, and Poisson's ratios used in the backcalculation process, and (in the case of overburden stresses) the layer densities, daily mean layer moisture contents, and water table depth data from the LTPP database. The moisture contents considered in this work were daily mean values computed from the TDR-based moisture content data for each pavement layer (see "Moisture Parameters," Chapter 3). The sources of variation reflected in the data set included variations with FWD load (by virtue of the use of multiple FWD load levels at each test date and time), point-to point variations, within-day variations (by virtue of repeated test cycles within a day), and longer-term variations (through use of data for multiple test dates).

EXPLORATION OF RELATIONSHIPS BETWEEN BACKCALCULATED MODULI AND EXPLANATORY VARIABLES

Attempts to develop predictive models for backcalculated pavement layer moduli were preceded by examination of a series of correlation matrices exploring the relationship between the backcalculated layer moduli, stress state variables, and the TDR-monitored moisture content.

The variables considered in these matrices are: Log(E); the mean volumetric moisture content (V_m) for the layer; the applied FWD load (P); the radial load stress (σ_r); the bulk and octahedral shear stresses due to load and overburden (θ, and τ); $\log(\theta/P_a)$; and $\log(\tau/P_a+1)$. Radial overburden was computed assuming $k_0 = 1.0$ in all cases. The stress parameters were computed for points directly beneath the center of the loaded area, and at depths of one-quarter-depth, mid-layer, and three-quarters-depth within the finite layers, and at 0.1, 0.2, and 0.3 m (3.9, 7.9, and 11.8 inches) beneath the layer interface for semi-infinite subgrade layers. Pertinent observations drawn from these correlation matrices are as follows.

The observed correlation between modulus and moisture content is summarized in Table 32. For 53 percent of the pavement layers, the correlation between modulus and moisture content is negative, indicating that increases in moisture are associated with decreases in modulus. The opposite is true for the remaining 47 percent of the pavement layers. The strength of the observed correlation, whether positive or negative, varies tremendously—from essentially zero, to 0.73 on the positive side, and 0.99 on the negative side. Both positive and negative correlations are observed for all of the soil classes represented in the data set, and all layers in the pavement structure. The prevalence of positive correlations is contrary to expectations.

Table 33 summarizes the observed correlation between modulus and applied FWD load. As was the case for the moisture-modulus correlations, the strength of the correlations between modulus and applied FWD load varies considerably, with values spanning the range from –0.80 to 0.92. For the majority of the base layers, the expected positive correlation, implying increasing modulus with increasing FWD load, is observed. The direction of the observed correlations is less consistent for the deeper layers. The prevalence of negative correlations (implying decreasing modulus with increasing FWD load) for granular layers is contrary to expectations, and inconsistent with the findings presented in Chapter 3 that were based on paired comparisons of moduli for different load levels with all other factors constant. For this reason, it is reasonable to attribute the unexpected frequency of negative correlations to the confounding influence of variations in moisture and other factors with time.

Table 32. Summary statistics for correlation between E and mean layer moisture

	Negative Correlation		**Positive Correlation**	
	Number of Layers	**Range**	**Number of Layers**	**Range**
Overall	**31**	**−0.01 to −0.99**	**28**	**0.01 to 0.73**
Layer 2 (base)	10 (A-1-a, A-1-b)	−0.03 to −0.70	12 (A-1-a, A-1-b, A-2-4)	0.03 to 0.58
Layer 3 (subbase or subgrade)	15 (A-1-b, A-2-4, A-2-6, A-3, A-4)	−0.00 to −0.99	7 (A-1-a, A-2-4, A-2-6, A-3, A-4, A-6)	0.04 to 0.52
Layer 4 (subgrade)	6 (A-2-4, A-3, A-4)	−0.21 to −0.99	9 (A-1-b, A-2-4, A-2-6, A-3, A-4)	0.01 to 0.73

In reviewing the correlation matrices, it was found that the backcalculated modulus is often less strongly correlated with moisture than with one or more of the stress parameters considered. This is true for all of the base layers, 82 percent of the subbase/upper subgrade (layer 3) layers, and 80 percent of the subgrade/lower subgrade (layer 4) layers. The exceptions occurred for the upper subgrade layer at section 131005 (A-4), the subgrade at section 251002 (an A-3 soil), both the subbase and subgrade layers at section 831801 (A-2-6 and A-2-4, respectively) and both the subbase and subgrade at section 241634 (both A-4). For 63 percent of the layers, the backcalculated modulus is more strongly correlated with the radial load stress computed at one or more depths than it is with either moisture, or the bulk or octahedral shear stresses.

Table 33. Summary statistics with regard to observed correlation between E and applied FWD load

Layer	Negative Correlation		Positive Correlation	
	Number of Layers	**Range**	**Number of Layers**	**Range**
All	**25**	**−0.01 to −0.80**	**34**	**0.00 to 0.92**
2 (base)	3 A-1-b	−0.06 to −0.15	19 A-1-a, A-1-b, A-2-4	0.00 to 0.92
3 (subbase or subgrade)	9 (A-1-b, A-2-4, A-2-6, A-3, A-4, A-6)	−0.01 to −0.66	13 (A-1-a, A-1-b, A-2-4, A-3, A-4)	0.00 to 0.80
4 (subgrade)	13 (A-1-b, A-2-4, A-2-6, A-3, A-4)	−0.03 to −0.88	2 (A-2-4, A-3)	0.10 to 0.35

The relative strength of the observed correlations between log E_n and the bulk and octahedral shear stress parameters is summarized in Table 34. This information is inconsistent with expectations based on laboratory M_r test results. Lab data typically indicate that bulk stress is the more important predictor of modulus for granular materials, whereas the correlations for the backcalculated moduli indicate that the octahedral shear stress is often the more important predictor for both granular and fine-grained materials. Conversely, based on laboratory data, one would expect the octahedral shear stress to be the more important predictor for the fine-grained soils, but the data in Table 34 indicate that this is not always the case, as A-4 soils are among those for which the backcalculated modulus is more strongly correlated with the bulk stress than with the octahedral shear stress.

Table 34. Relative strength of correlation between log E_n and bulk and octahedral shear stress parameters (number of layers and soil classes represented)

Layer	Bulk Stress Correlation Is Stronger	Octahedral Shear Stress Correlation Is Stronger	Relative Strength of Correlation Varies with Computation Depth
2	5 (A-1-a and A-1-b)	11 (A-1-a and A-1-b)	6 (mostly θ) (A-1-a)
3	2 (A-2-6)	12 (A-1-b, A-2-4, A-3, A-4)	8 (mostly τ) (A-1-a, A-1-b, A-2-4, A-3, A-6)
4	4 (A-1-b, A-2-4, A-4)	11 (A-1-b, A-2-4, A-2-6, A-3, A-4)	0

The sign (positive or negative) of the observed correlations between backcalculated modulus and the bulk and octahedral shear stress parameters is summarized in Table 35. Based on laboratory test experience, positive correlation (corresponding to increasing modulus with increasing stress) between modulus and the bulk stress is expected for all granular layers. For the backcalculated moduli, both positive and negative correlations with bulk stress occur. The relative frequency of occurrence of positive and negative correlations varies with the layer and the stress computation depth considered. Negative correlations (indicative of stress-softening behavior) are expected for the fine-grained soils. Again, some observed correlations for the backcalculated layer moduli are consistent with this expectation, while others are not.

The correlation matrices were reviewed to identify the depth at which the computed stress parameters were most strongly correlated with the backcalculated moduli. The findings of this review are summarized in Table 36. More often than not, the correlations for the one-quarter-depth and three-quarters-depth stress computation points are stronger than those for the mid-layer stresses. The frequencies with which the strongest correlations between E and bulk stress are observed at one-quarter-depth and three-quarters-depth in the layer are similar. The strongest correlations with octahedral shear stress occur most often at three-quarters-depth within the layer for the finite layers, and at 0.1-m below the layer interface for the semi-infinite subgrade layers. Between-depth differences in the strength of the observed correlation range from zero (for τ and log τ at section 351112, layer 4) to more than 0.60 (for log θ at section 040113, layer 2).

Table 35. Sign of observed modulus-stress correlation

Layer (Depth)	Number and Classification of Layers with…			
	Positive Correlation for Both θ and τ	Negative Correlation for Both θ and τ	Positive Correlation for θ and Negative Correlation for τ	Negative Correlation for θ and Positive Correlation for τ
2 (1/4-depth)	13 A-1-a and A-1-b	0	0	9 A-1-a and A-1-b
2 (mid-layer)	5 A-1-a	0	0	17 A-1-a and A-1-b
2 (3/4-depth)	2 A-1-a	0	0	20 A-1-a and A-1-b
3 (1/4-depth)	17 A-1-a, A-1-b, A-2-4, A-3, A-4	5 A-2-4, A-2-6, A-4, A-6	0	0
3 (mid-layer)	14 A-1-a, A-1-b, A-2-4, A-3, A-4	5 A-2-4,A-2-6, A-4, A-6	0	3 A-1-b, A-3
3 (3/4-depth)	10 A-1-a, A-1-b, A-2-4, A-4	5 A-2-4, A-2-6, A-4, A-6	0	7 A-1-b, A-3, A-4
4 (1/4-depth)	3 A-2-4, A-3, A-4	10 A-1-b, A-2-4, A-2-6, A-3, A-4	2 A-1-b and A-4	0
4 (mid-layer)	3 A-2-4, A-3, A-4	9 A-1-b, A-2-4, A-2-6, A-3, A-4	3 A-1-b, A-2-4, A-4	0
4 (3/4-depth)	3 A-2-4, A-3, A-4	9 A-1-b, A-2-4, A-2-6, A-3, A-4	3 A-1-b, A-2-4, A-4	0

Table 36. Distribution of strongest modulus-stress correlations with respect to stress computation depth

Stress Parameter	Number of Layers for Which Strongest Correlation with E Occurs at Given Depth					
	Finite Layers			Semi-Infinite Layers (Depth Below Interface)		
	1/4-Depth	Mid-Layer	3/4-Depth	0.1 m	0.2 m	0.3 m
θ	23	3	20	5	1 + 1tie*	7 + 1 tie
τ	17	0	27	9	2 ties	3 + 1 tie
Both	15	0	15	6	1 tie	3 + 1 tie

*A "tie" occurs where the correlations for both θ and τ were identical to two decimal places for two or more computation depths. If equal values occurred for only one of the two parameters, the observation was tallied with the depth for which the other stress parameter had the stronger correlation.

The relationship between variations in backcalculated modulus and moisture was also examined by looking at the ratio $\Delta E/\Delta V_w$, where ΔE and ΔV_w are the change in modulus and moisture relative to a reference condition. The reference condition that was used was the earliest available modulus/moisture observation for each nominal FWD load level for a particular test section and layer. Summary values by layer type are presented in Table 37. Pertinent observations follow the table.

Table 37. Change in modulus versus change in moisture content by layer type

Layer Type	Load Level	Change in Modulus, ΔE (kPa)		Change in Moisture Content, ΔV_w (%)		$\Delta E/\Delta V_w$ (kPa/%)				n
		Min.	Max.	Min.	Max.	Min.	Mean	Max.	Std. Dev.	
Base	1	−290	294	−5.9	11.4	−4590	27	5820	698	430
	2	−362	428	−6.8	11.4	−1992	11	3240	295	597
	3	−334	516	−4.9	11.4	−3000	6	3600	347	695
	4	−359	500	−5.9	11.4	−4860	−1	7860	565	763
Subbase	1	−117	107	−13.3	5.9	−212	−11	165	41	96
	2	−101	152	−12.7	5.9	−160	−7	184	49	131
	3	−126	161	−8.3	5.9	−117	−7	148	39	157
	4	−113	139	−6.5	9.9	−104	−7	176	37	152
Finite Subgrade	1	−268	113	−19.4	17.4	−1055	7	2728	254	428
	2	−209	157	−19.4	10.0	−2154	−16	1310	202	585
	3	−230	191	−19.4	10.0	−2051	−18	1343	187	700
	4	−225	121	−19.4	10.0	−1553	−7	1527	144	801
Semi-infinite Subgrade	1	−235	359	−6.5	20.8	−420	5	960	111	287
	2	−218	347	−16.6	20.8	−3520	−23	1920	219	378
	3	−106	283	−9.4	20.8	−4240	−29	800	255	448
	4	−241	275	−14.7	20.8	−884	8	3520	247	492

The ratio $\Delta E/\Delta V_w$ is highly variable, with a range of –4,590 to 7,860 kPa (-666 to 1140 psi) per 1-percent change in moisture content. Both positive and negative values of the ratio are observed for 92 percent of the individual layer and load level combinations. Thus, in most cases, both increases and decreases in backcalculated modulus are associated with increases in mean layer moisture content. Exceptions to this general rule occur on a consistent basis (across all FWD load levels) for the subgrade layer at section 041024 (Arizona), the subgrade layer at section 081053 (Colorado), and the base layer at section 906405 (Saskatchewan). However, in all of these cases, the number of observations considered is small, so it is not clear that these layers are truly exceptional in this regard.

The mean values of the ratio $\Delta E/\Delta V_w$ for individual layers and load levels vary in the range of –403 to 1,089 kPa (–58 to 158 psi) per one percent change in moisture content, with the overall mean value being –4. The coefficient of variation (COV) observed for individual combinations of layer and load level varies from a low of 13 percent for the base (layer 2) at section 041024 (Arizona), to a high of more than 20,000 percent for the upper subgrade (layer 3) at section 231026 (Maine), with the overall average COV being 761 percent. In many cases, both the mean ratio and the extent of variation therein vary between load levels, but universally applicable trends are not evident.

In looking at the statistics on a layer-type basis, it may be observed that the mean ratio for the base layers decreases with increasing load on a consistent basis. However, the standard deviations associated with the mean values are so large in comparison to the means that this trend in not particularly meaningful. The COV for the base layer group increases with increasing load, from a low of 2,605 percent for the nominal 27-kN (6,070 lbf) load to a high of 111,707 percent for the 71-kN (15,961 lbf) load level. In contrast, the subbase layer values for the 40-, 53-, and 71-kN (8,992-, 11,915-, and 15,961-lbf) load levels are remarkably similar. Overall, the high degree of variability in the ratio $\Delta E/\Delta V_w$ suggests that factors other than moisture (e.g., stress conditions) may be important to explaining the observed variations.

In summary, plots of modulus versus moisture, correlation matrices, and the ratio $\Delta E/\Delta V_w$ were examined with the following findings.

- Negative correlations between the bulk stress and E are a frequent occurrence.
- E is often more strongly correlated with σ_r than with other variables.
- The correlation between E and V_w is often relatively weak.
- The ratio $\Delta E/\Delta V_w$ is highly variable.

Together, these observations suggest that moisture is not always the primary driver of seasonal variations in backcalculated pavement layer moduli.

MODELS OF THE FORM $E/P_a = k_1\theta/_{Pa}{}^{k2}(\tau/P_a+1)^{k3}$

Initial efforts to develop predictive models for backcalculated pavement layer moduli focused on the model form presented as Equation 26,

$$\text{Model 1: } E/P_a = k_1\theta/P_a{}^{k2}(\tau/P_a+1)^{k3} \tag{26}$$

with k_1 taken to be k_0*10^{c1Vw}. (V_w is the volumetric moisture content, expressed as a percent; c_i and k_i are regression constants; and all other variables are as previously defined.) This model form was selected to be consistent with the constitutive model to be used for unbound materials in the *2002 Guide for Design of New and Rehabilitated Pavement Structures* that is currently under development. Note that it is a variant of Equation 11, in which k_6 is taken to be zero, and k_7 is assumed to be 1. This model will henceforth be referred to as Model 1.

Both load-induced and overburden stresses were included in the computation of the stress parameters. The horizontal overburden stresses were computed using k_0 values of 0.7 and 0.5 for the base and subbase/subgrade layers, respectively. Temporal variations in overburden due to variations in mean layer moisture content were considered in the calculation (although it is likely that the impact of this is very small). The stresses considered were those computed at a point directly beneath the center of the loaded area at 0.75-depth within each finite layer, and at 0.3 m below the layer interface for each semi-infinite layer.

For the purposes of the regression modeling, Model 1 was transformed by taking the log of both sides of Equation 26, so that standard multiple regression could be used to derive the regression coefficients. The transformed model (with the moisture term explicitly included) is given in Equation 27.

$$\log E / P_a = \log k_0 + c_1 V_w + k_2 \log(\theta / P_a) + k_3 \log(\tau / P_a + 1) \quad (27)$$

The multiple regression results obtained for individual pavement layers are presented in Table 73 in Appendix E: **Multiple Regression Results for Individual Pavement Layers**. From a standpoint of goodness of fit, as judged by the fraction of variance explained by the model (R^2) and the standard error ratio (S_e/S_y) computed for log E, as well as the bias and standard error ratio for E, many (but not all) models are quite good. However, although most of the materials in question are granular, the majority of the k_2 values are negative, indicating that the modulus decreases with increasing bulk stress (i.e., "stress softening"). This is inconsistent with the stress-hardening behavior typically exhibited by such materials in the laboratory and the load-hardening behavior of the pavement layers discussed previously. Most positive values for k_3 are similarly inconsistent with laboratory test findings. The signs of both k_2 and k_3, however, are consistent with correlations discussed previously.

Several alternative approaches to computation of the stress parameters were explored in an attempt to produce models with regression coefficients that are more consistent with laboratory test results. Those alternatives are summarized in Table 38. The factors that were varied were the assumed values for K_0 used in computing the horizontal overburden stresses, and whether overburden stresses were or were not included in the computation of the stress parameters. The K_0 values were varied to explore the possibility that the poor agreement between the regression results obtained with backcalculated layer moduli and laboratory test results came about as a result of incorrect assumed values for K_0 (the true values being unknown). The use of only the load-induced stresses for one or both of the stress parameters was pursued to explore the possibility that overburden stresses are not important to the observed variations in backcalculated pavement layer moduli. Stresses computed at three-quarters-depth in the pavement layer were used in this analysis, and, k_1 was taken to be constant (i.e., not a function of the volumetric moisture content). Thus, the transformed model form used in the multiple regression to obtain the model coefficients is:

$$\log(E / P_a) = \log k_1 + k_2 \log(\theta / P) + k_3 \log(\tau / P_a + 1) \quad (28)$$

The results obtained for the alternative stress computation assumptions are presented in Table 74 through Table 80 in Appendix E: **Multiple Regression Results for Individual Pavement Layers**. The regression coefficients for these models are summarized by soil class in Table 39. Only those regression results meeting a minimum goodness of fit standard of $R^2 \geq 0.60$ (in log space) were included in the preparation of this summary. A complete evaluation of the adequacy of these regression models was not undertaken, as the goal of achieving coefficients consistent with laboratory test results was not achieved.

Table 38. Combinations of K_0 and stress components considered in regression modeling

Set	k_0		Bulk Stress	Octahedral Shear Stress
	Base	Subbase/Subgrade		
1	0.7	0.5	Load + Overburden	Load + Overburden
2	0.7	0.5	Load + Overburden	Load Only
3	1.0	1.0	Load + Overburden	Load + Overburden
4	2.0	1.0	Load + Overburden	Load + Overburden
5	2.0	1.0	Load + Overburden	Load Only
6	Not Pertinent	Not Pertinent	Load Only	Load Only
7	0.7	0.5	Load Only	Load + Overburden

The results obtained with all stress data sets identified in Table 38 are qualitatively similar to those obtained in the initial effort. The majority of the k_2 values are negative for both the granular and fine-grained materials, and the k_3 values are typically positive. While the k_1 values are similar in magnitude to the laboratory resilient modulus coefficients reported by Von Quintus and Killingsworth (see Table 9), the k_2 and k_3 values differ in both magnitude and sign.[5] For example, Von Quintus and Killingsworth report k_1 values in the range of 250 to 2,323; k_2 values in the range of -0.18 to 1.07; and k_3 values in the range of −0.33 to 0.61 for base materials, while the corresponding Table 39 values for A-1-a soils vary in the ranges of 59 to 2078; −9.21 to −0.07; and -0.41 to 12.8, respectively. None of the options considered resolves the inconsistency with laboratory test results. Subsequent efforts to identify an alternative radial location for stress computation that would yield acceptable results from a standpoint of both goodness of fit and consistency with laboratory test results were similarly unsuccessful.

Table 39. Regression coefficients for alternative stress computations

	Set 1			Set 2			Set 3			Set 4		
	k_1	k_2	k_3	k_1	k_2	k_3	k_1	k_2	k_3	k_1	k_2	k_3
A-1-a												
Mean	1019	-0.84	2.58	1055	-0.85	2.44	1139	-1.14	2.91	1330	-0.67	1.87
Std. Dev.	449	1.60	2.95	418	1.46	2.91	409	2.34	3.00	414	0.36	1.06
Max	1907	-0.09	12.6	1935	-0.09	12.5	1962	-0.10	12.8	2078	-0.10	3.99
Min	59	-6.81	-0.26	170	-6.26	-0.39	668	-9.21	0.83	734	-1.47	-0.27
No. Layers	16			16			14			14		
A-1-b												
Mean	730	-0.69	3.53	913	-0.57	3.00	947	-0.91	3.56	1027	-0.72	2.93
Std. Dev.	536	0.70	2.64	554	0.58	2.19	500	1.01	2.64	572	0.73	2.20
Max	1592	-0.13	6.37	1647	-0.13	6.21	1685	-0.06	7.79	1810	-0.12	6.52
Min	232	-1.81	0.66	295	-1.69	0.63	298	-2.69	0.68	298	-2.23	0.64
No. Layers	6			7			8			7		
A-2-4												
Mean	895	-1.31	6.80	817	-1.67	8.17	842	-2.43	8.44	912	-2.42	8.42
Std. Dev.	770	1.74	6.07	1045	2.15	8.74	961	3.11	9.09	1059	3.11	9.12
Max	1534	-0.15	13.6	1556	-0.15	14.4	1521	-0.23	14.9	1661	-0.23	14.9
Min	40	-3.31	2.00	78	-3.19	1.99	163	-4.62	2.01	163	-4.62	1.97
No. Layers	3			2			2			2		
A-3												
Mean	73	-3.40	13.5	127	-3.39	12.9	236	-4.49	12.7	236	-4.49	12.7
No. Layers	1			1			1			1		
A-4												
Mean	152	-1.21	9.70	192	-1.12	9.23	201	-1.30	9.43	201	-1.30	9.43
No. Layers	1			1			1			1		

Table 39. Regression coefficients for alternative stress computations, continued

	Set 5			Set 6			Set 7		
	k_1	k_2	k_3	k_1	k_2	k_3	k_1	k_2	k_3
A-1-a									
Mean	1160	-0.67	1.75	1047	-0.26	2.72	972	-0.26	2.60
Std. Dev.	495	0.37	1.04	416	0.13	2.77	419	0.12	2.12
Max	2002	-0.09	3.99	1887	-0.08	12.2	1791	-0.07	9.03
Min	94	-1.54	-0.41	431	-0.47	0.67	247	-0.43	0.56
No. Layers	14			16			15		
A-1-b									
Mean	989	-0.72	2.96	1376	-0.25	3.28	890	-0.21	2.83
Std. Dev.	524	0.73	2.19	1481	0.19	3.16	482	0.14	1.87
Max	1694	-0.12	6.52	4580	0.01	8.16	1561	-0.09	5.52
Min	298	-2.23	0.64	307	-0.50	-1.35	280	-0.47	1.16
No. Layers	7			7			6		
A-2-4									
Mean	699	-1.97	7.82	1436	-0.19	2.03	1423	-0.18	2.06
Std. Dev.	769	2.33	6.52	–	–	–	–	–	–
Max	1580	-0.22	14.87	–	–	–	–	–	–
Min	163	-4.62	2.01	–	–	–	–	–	–
No. Layers	3			1			1		
A-3									
Mean	236	-4.49	12.74	165	-1.04	13.58	110	-0.99	13.22
No. Layers	1			1			1		
A-4									
Mean	201	-1.30	9.43	290	-0.57	5.97	262	-0.59	6.06
Std. Dev.	–	–	–	163	0.34	4.47	168	0.39	4.80
Max	–	–	–	406	-0.32	9.13	381	-0.31	9.46
Min	–	–	–	175	-0.81	2.81	143	-0.86	2.67
No. Layers	1			2			2		

FACTORS CONTRIBUTING TO DIFFERENCES BETWEEN LABORATORY AND FIELD-BASED CONSTITUTIVE MODEL COEFFICIENTS

In comparing backcalculated pavement layer moduli with laboratory resilient moduli, it is important to keep in mind what is being compared. As discussed previously, the laboratory test result is appropriately termed a material property—a measurable characteristic of the material. In contrast, the backcalculated layer modulus is more correctly thought of as a parameter—an estimate of the "average" material characteristic for the pavement layer, which does not fully account for spatial variations in stress state (and thus, stiffness). Furthermore, the interpretation process used to obtain the estimate is based on theory that approximates, but does not match, reality. Key theoretical assumptions that are violated to one degree or another are the assumptions of homogeneity, isotropy, and linearity.

In the interpretation of laboratory resilient modulus test data we have measurements of the confining pressure and the cyclic axial load from which the major and minor principal stresses applied to the test sample are computed. For the most common laboratory situation, the radial and vertical stresses are: (1) always compressive; (2) independent of each other; (3) independent of the modulus of the material; and (4) applicable to the sample as a whole. In contrast, when looking at backcalculated layer moduli, one must compute the applicable overburden and load-induced stresses. By virtue of the theory used (linear layered-elastic theory), the computed stresses are: (1) sometimes tensile; (2) not independent of each other; (3) not independent of the modulus of the material, and (4) applicable to a particular point in the pavement layer, rather than a well-defined volume of soil. Furthermore, it is probable that the location of the point at which the computed stress parameters are most representative of the layer as a whole varies not only from one pavement to another, but from point to point and day to day (if not hour to hour) by virtue of spatial and temporal variations in the pavement layer properties.

The stress parameters used in modeling the stress sensitivity of the backcalculated moduli are themselves a function of the backcalculated layer moduli. This has some important implications, chief among them the potential for the radial load stress to decrease as the modulus increases, with all other factors held constant. In Figure 32 and Figure 33, data for two different FWD load levels from a single FWD drop sequence are used to illustrate the impact of this possible occurrence on the relationship between backcalculated moduli and computed stress parameters.

For each set of backcalculated layer moduli, stresses were computed for the original set of backcalculated layer moduli, and for two modified data sets. In one version, the modulus for one (and only one) layer was multiplied by 1.3. In the other, the modulus for the same layer was divided by 1.3. The simulated variations (outer points in each curve) illustrate how the computed stresses vary with the modulus of one layer, when all other factors are held constant, while the actual data points (which appear as the center point in each curve) show the overall impact of FWD load level on the stresses and moduli for the layer under consideration (including load-related variations in the moduli of other layers. The stresses were computed for a point directly beneath the center of the applied load. Three different

computation depths were considered for each layer, corresponding to one-quarter-depth, mid-layer, and three-quarters-depth.

In Figure 32, the observed variation in computed vertical load stress is reasonably consistent with the laboratory test situation for granular materials—a direct relationship between modulus and vertical stress. However, the same cannot be said for the radial load stress, illustrated in Figure 33. For two of the three stress computation depths, there is an inverse relationship between the radial load stress computed for the original data (center point on curves) and the backcalculated modulus and FWD load. An inverse relationship between modulus and radial load stress also occurs for all three stress computation depths considered for the simulated variations in modulus. Also, note that some computed radial stresses are negative (tensile). The impact of these variations on the relationship between backcalculated modulus and the computed load-induced bulk and octahedral shear stresses is illustrated in Figures 34 and 35. In this case, the original data points all show an increase in both modulus and bulk load stress with increasing FWD load, while both direct and inverse relationships between modulus and bulk stress occur for the simulated variations. The computed octahedral shear stresses consistently increase with increasing modulus.

The trends shown in these figures do not represent universal truth. Rather, they illustrate that use of linear layered-elastic theory to backcalculate moduli and compute the associated load-induced stresses can result in inverse relationships between backcalculated layer moduli and bulk stress, even though the expected load-hardening behavior is observed in the backcalculated moduli. This situation is compounded by the fact that the computed radial load stress may also be negative. The varying trends in the computed radial load stress, and the occurrence of negative values, manifest themselves in varying trends in the computed bulk stress. The impact of the varying radial load stress trends and tensile radial load stresses on the computed octahedral shear stress is less obvious (but no less important), by virtue of the mathematical definition of that parameter.

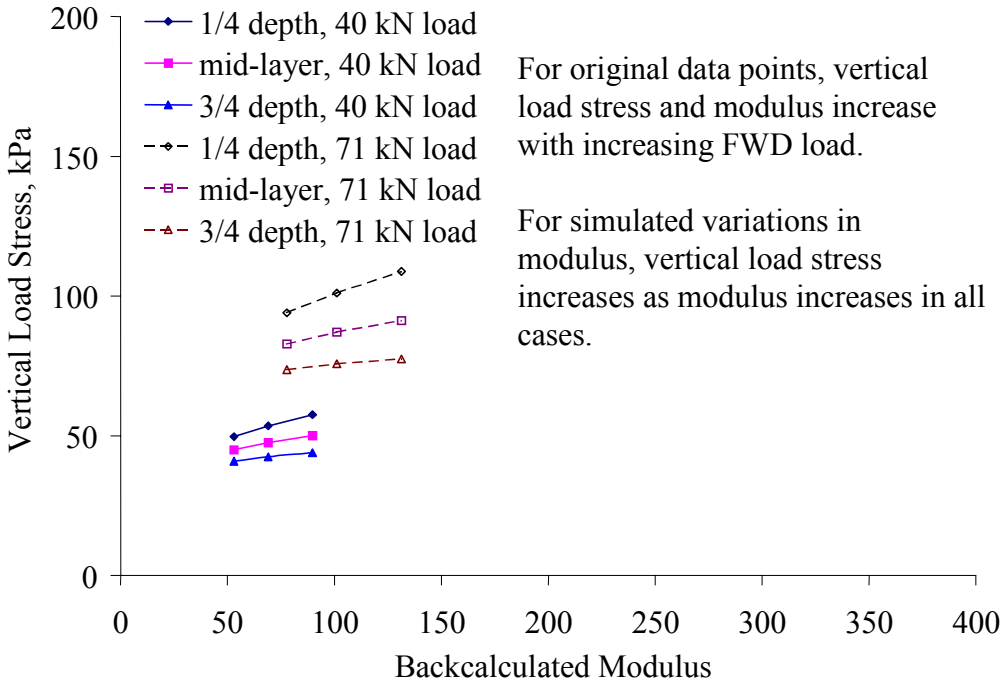

Figure 32. Vertical load stress versus modulus, section 040113 A-1-a base layer

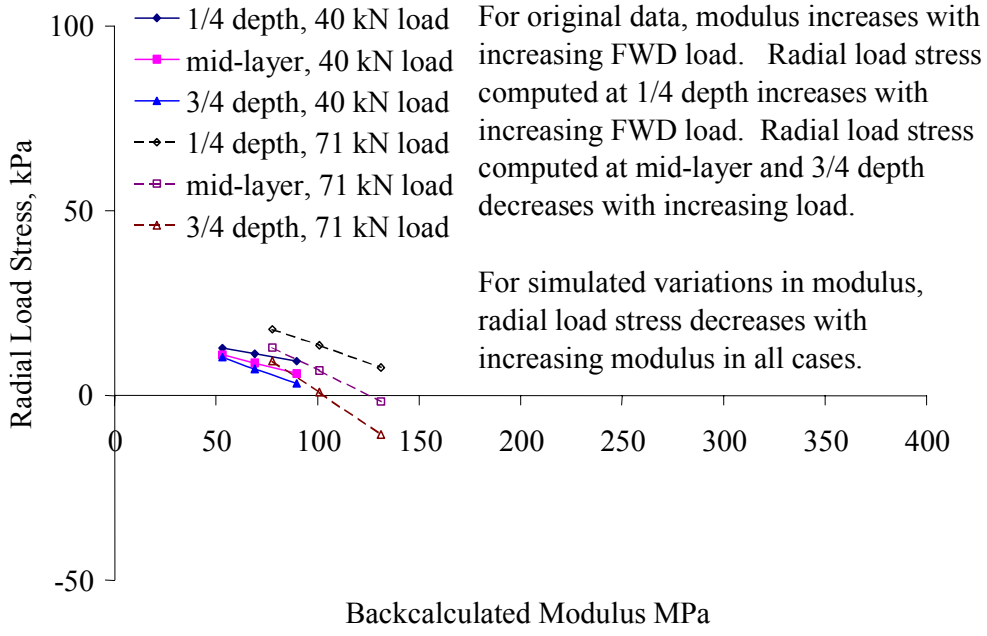

Figure 33. Radial load stress versus modulus, section 040113 A-1-a base layer

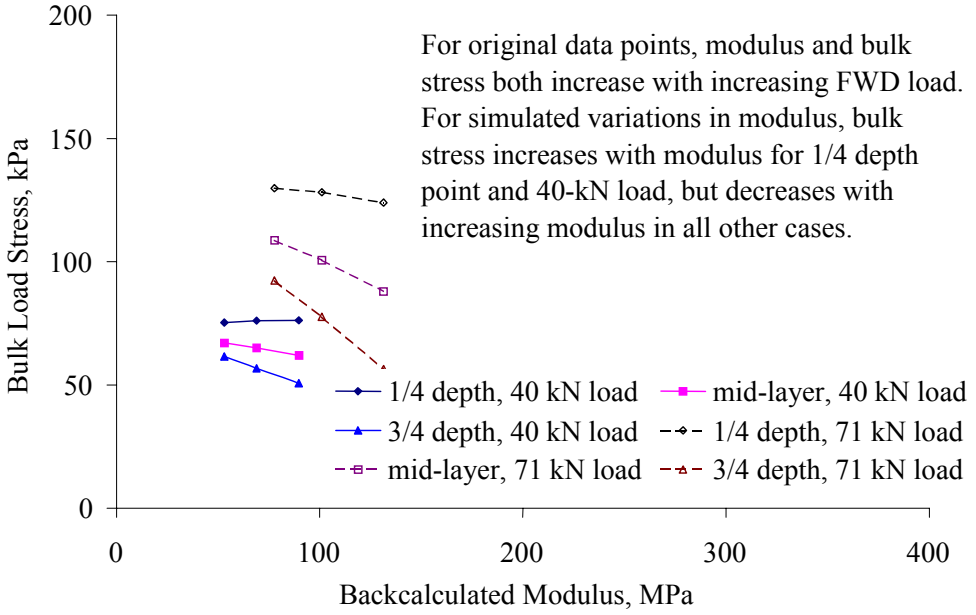

Figure 34. Bulk load stress versus modulus, section 040113 A-1-a base layer

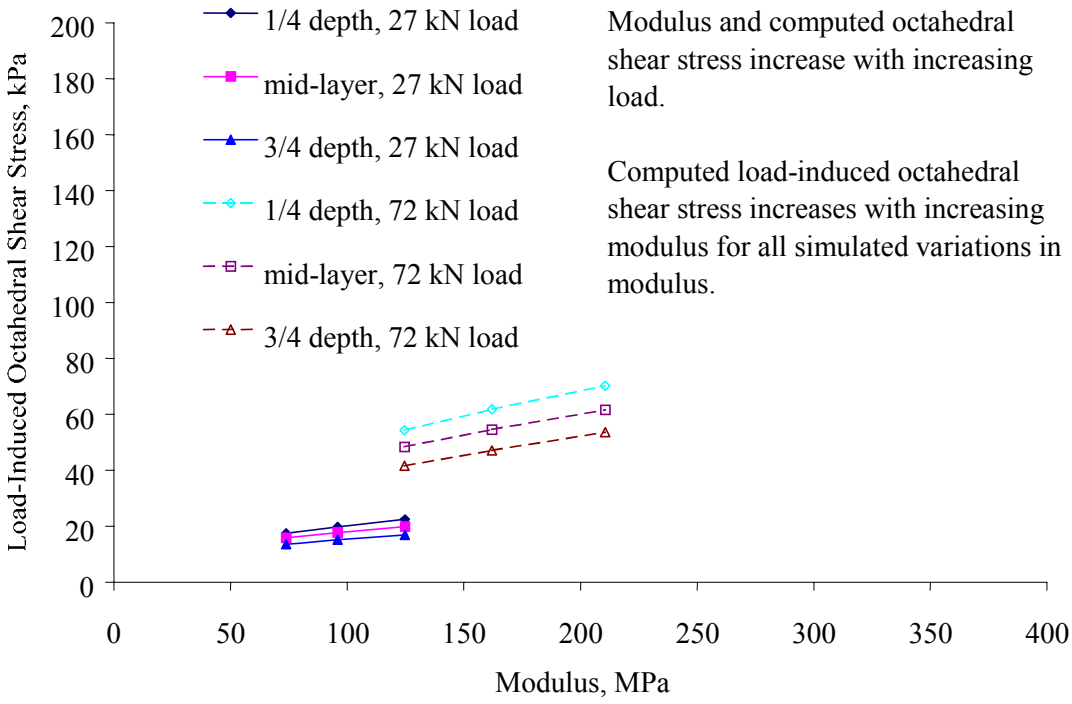

Figure 35. Load-induced octahedral shear stress versus modulus, section 040113 A-1-a base layer

The vertical and radial stresses (σ_v and σ_r) computed for the backcalculated moduli are compared with those for two laboratory resilient modulus test protocols in Figure 36 to Figure 38. The test protocols considered are the LTPP P-46 protocol,[80] and the proposed "harmonized" protocol developed under NCHRP project 1-28A.[45] The stresses plotted in these figures were computed for points directly below the center of the loaded area, at three-fourths-depth within the pavement layer, with $k_0 = 1.0$, for the first set of backcalculated moduli for each test date and FWD load level. Plots prepared with stresses computed at one-quarter-depth or mid-layer are qualitatively similar. While the stresses plotted in these figures do not represent universal truth, they are representative of the data set used in this investigation (see Table 18 and Table 19), and serve to illustrate the conditions that can exist when linear layered-elastic theory is used to backcalculate pavement layer moduli and compute the load-induced stresses in the pavement structure.

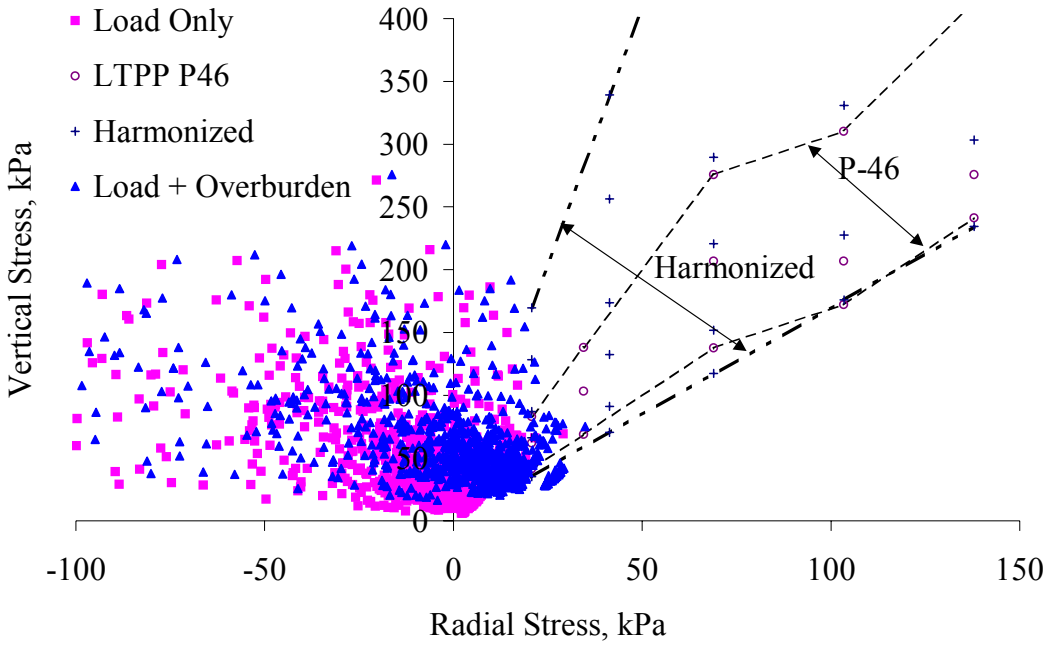

Figure 36. Comparison of radial and vertical stress components for granular base and subbase layers

The principal stresses defined in the two laboratory test protocols are similar, though those for the harmonized protocol are more extensive. While some computed stress data points for the base and subbase materials (Figure 36) fall within the bounds defined by the laboratory test protocols, many do not. Of particular significance is that a large fraction of the computed radial load stresses are negative, particularly for the base layers.

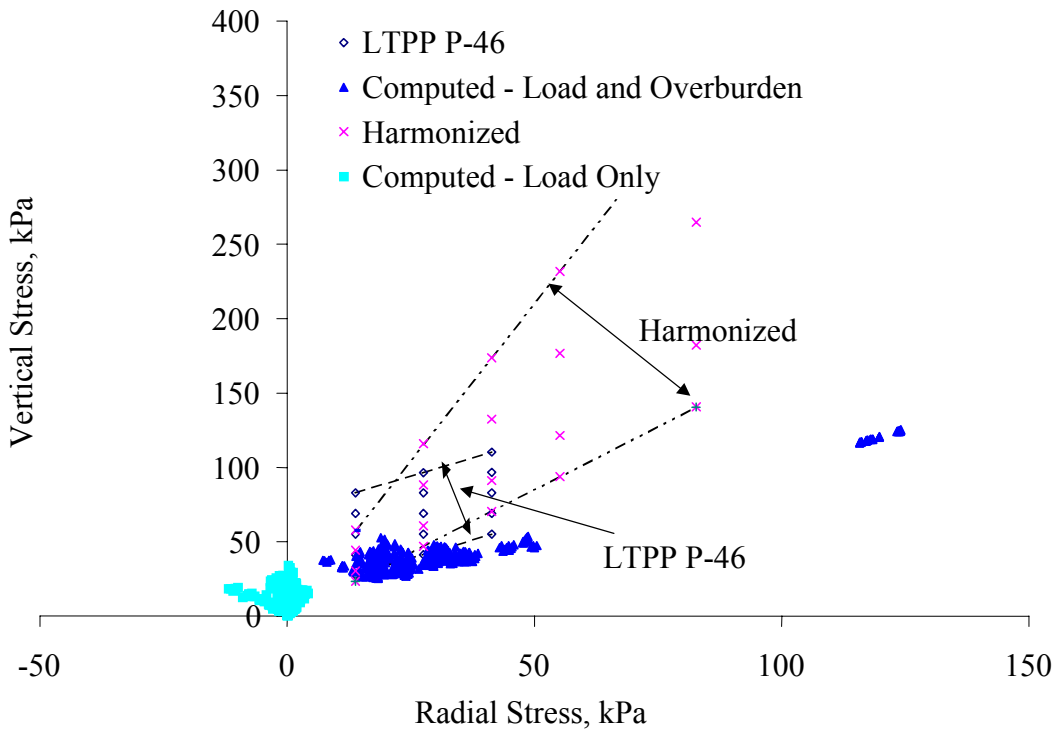

Figure 37. Comparison of radial and vertical stress components for coarse-grained subgrade layers

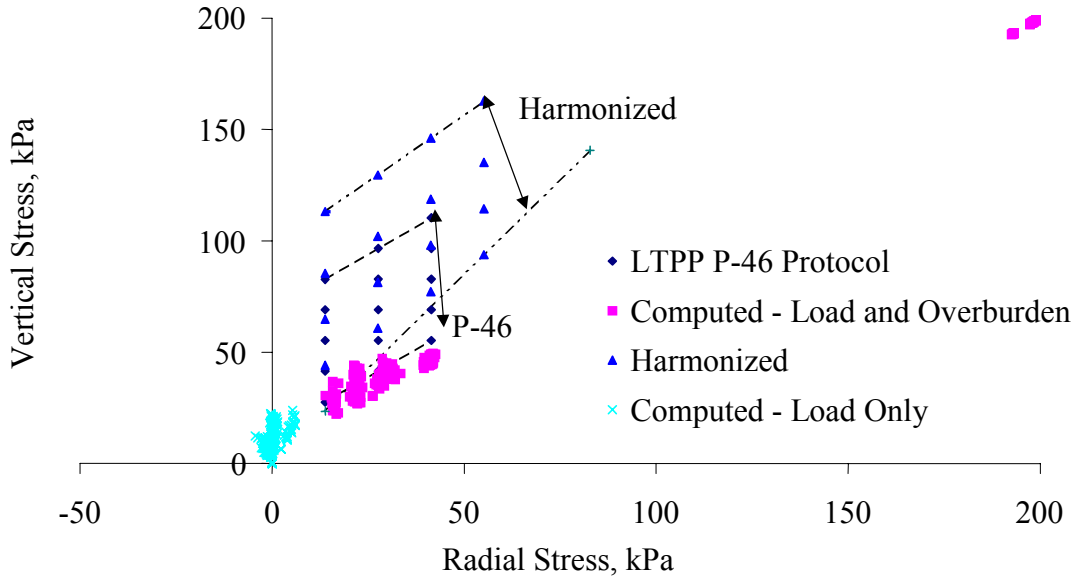

Figure 38. Comparison of radial and vertical stress components for fine-grained subgrade layers

Computed subgrade stresses illustrated in Figures 37 and 38 are more similar to those for the laboratory stresses than those for the base and subgrade layers, but many data points fall outside the envelopes defined by the laboratory test protocols. Negative computed radial stresses are again prevalent.

The corresponding bulk and octahedral shear stresses are shown in Figure 39 to Figure 41. As one would expect given the relationships observed in Figure 36 to Figure 38, the stress states computed from the backcalculated layer moduli bear little resemblance to those for either laboratory protocol. (Note that the scales used in these figures are such that the higher stress states for the harmonized protocol are not shown.) Thus, it is reasonable to conclude that the model coefficients derived for the backcalculated layer moduli differ from those obtained for laboratory resilient modulus test results because the stress states computed for the backcalculated moduli using layered-elastic theory are not directly analogous to the lab stress states. Therefore, it is impossible to derive constitutive model coefficients that are compatible with laboratory test data from the backcalculated layer moduli.

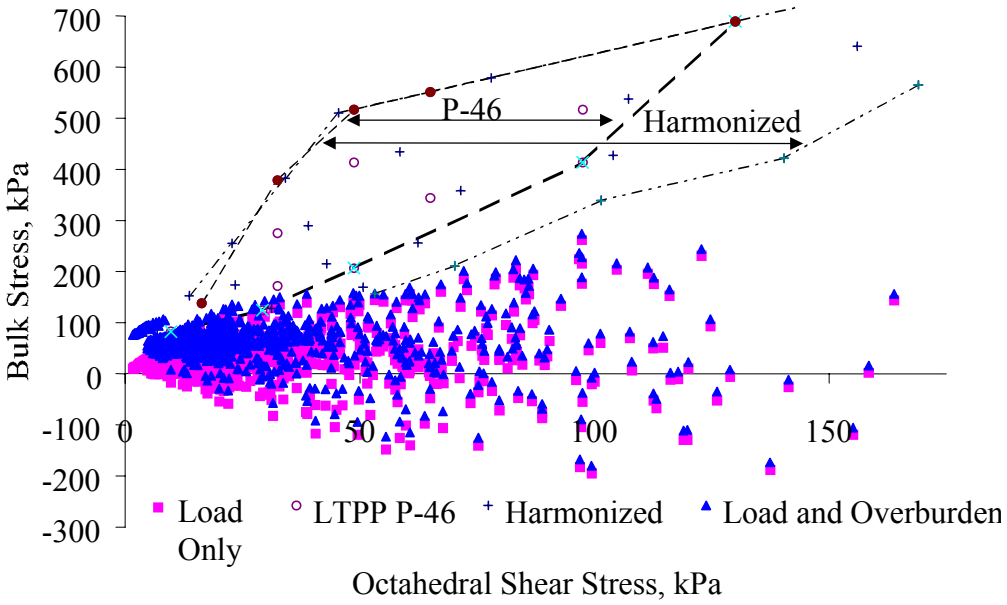

Figure 39. Comparison of bulk and octahedral shear stresses for granular base and subbase layers

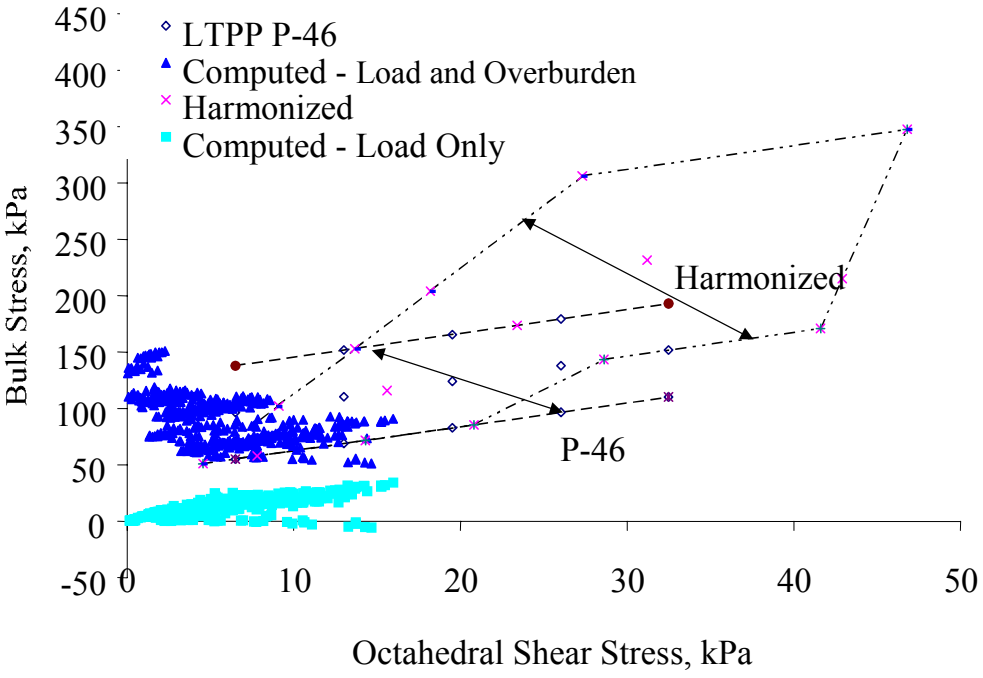

Figure 40. Comparison of bulk and octahedral shear stresses for coarse-grained subgrade layers

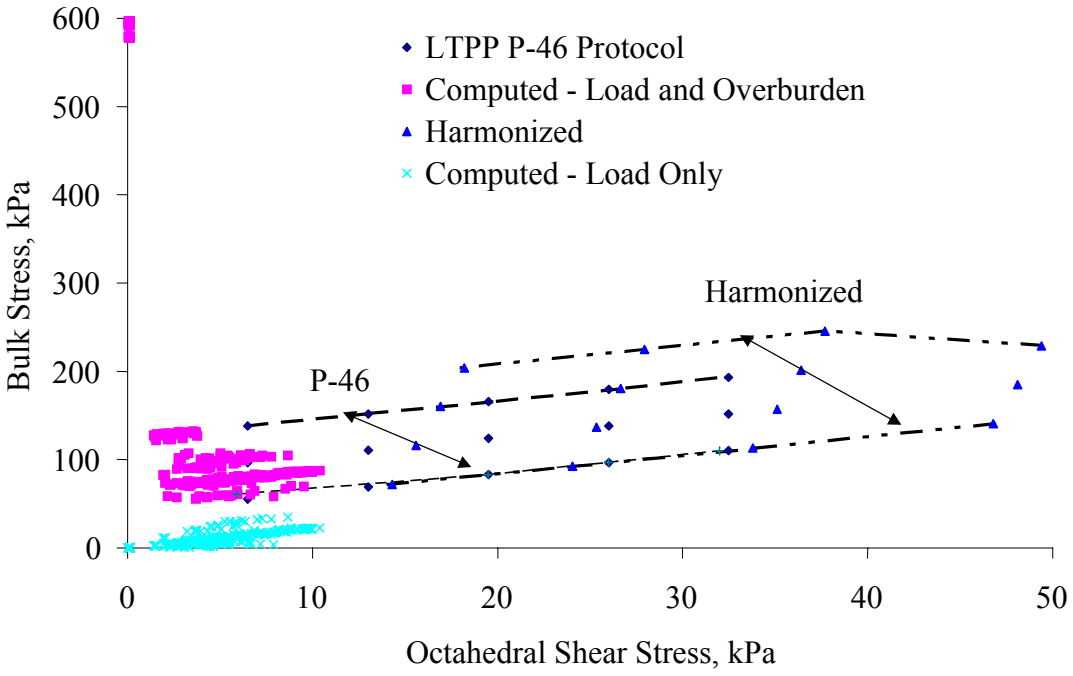

Figure 41. Comparison of bulk and octahedral shear stresses for fine-grained subgrade layers

In light of these observations, it might be argued that the solution to the observed discrepancies is to abandon the use of linear layered-elastic theory in the interpretation of pavement deflection data. However, while nonlinear backcalculation is an essential long-term goal, abandoning backcalculation based on linear layered-elastic theory is not a practical solution at this time. Given the current state of the art, it is likely that backcalculation based on linear layered-elastic theory (with or without adaptations to consider the stress sensitivity of materials in an approximate fashion) will remain the best available technology applicable in routine practice for at least the next several years. Thus, it is appropriate to pursue models to predict the observed variations in layer moduli backcalculated using linear layered-elastic theory, even though the model coefficients obtained are not directly analogous to those derived from laboratory test results for the same or similar materials.

ALTERNATIVE MODEL FORMS

Individual Pavement Layer Models

Given the differences between the computed stresses based on linear layered elastic theory and laboratory stress states discussed in the preceding section, it is appropriate to consider possible modifications of the constitutive model form to improve the predictive capability for the backcalculated layer moduli.

The primary modification considered was the substitution of a semi-log form for the bulk stress term in the model, as shown in Equation 29 (Model 2).

$$\text{Model 2}: \quad E = k_1 10^{k2\theta / P_a} (\tau / P_a + 1)^{k3} \tag{29}$$

Use of the semi-log form for the bulk stress term enables straightforward consideration of negative computed bulk stress terms. This rationale does not apply to the octahedral shear stress term, as it cannot be negative, so the log-log form was retained for the octahedral shear stress term, to maximize consistency with the original model form.

Two variations on the model form were considered: model 2A, in which k_1 was taken to be a function of the volumetric moisture content, and model 2B, in which all three regression parameters were treated as being (potentially) a function of the volumetric moisture content. These variations are presented as Equations 30 and 31, respectively.

$$\text{Model 2A: } E = c_0 10^{(c1Vw/100+k2\theta/Pa)} (\tau/P_a+1)^{k3} \tag{30}$$

$$\text{Model 2B: } E = c_0 10^{(c1Vw/100 +(c2+c2'Vw/100)\theta/Pa)} (\tau/P_a+1)^{(c3+c3'Vw/100)} \tag{31}$$

The models were fitted using multiple regression applied to the log-transformed models, as presented in Table 40. In the equations in Table 40, the $c_0' = \log c_0$. The computation of the stress parameters considered in these models differed from that for Model 1 in one respect, the value of K_0 used in the computation of the radial overburden stresses. For these models, K_0 was taken to be 1.0 for all layers.

Table 40. Log-transformed models used in regression modeling

	Transformed Equation
2A	$\log E = c_0' + c_1 V_w/100 + k_2\theta/P_a + k_3 \log(\tau/P_a+1)$
2B	$\log E = c_0' + c_1 V_w/100 + c_2\,\theta/P_a + c2'Vw/100*\theta/P_a + c_3 \log(\tau/P_a+1) +$ $c3'Vw/100*\log(\tau/P_a+1)$

Regression results obtained for individual layers using 2A and 2B are presented in Table 81 through Table 82 of Appendix E: **Multiple Regression Results for Individual Pavement Layers**. The regression coefficients obtained for all four models are summarized in Table 41.

Table 41. Summary of regression coefficients for models 2A and 2B

Parameter		2A	2B
c_0'	Mean	3.479	3.740
	Minimum	−12.06	−38.73
	Maximum	12.61	32.38
c_1	Mean	−1.527	−2.439
	Minimum	−59.78	−164.6
	Maximum	3.470	237.0
c_2/k_2	Mean	−0.408	−1.048
	Minimum	−4.558	−28.80
	Maximum	10.57	12.58
c_2'	Mean	–	1.626
	Minimum	–	−56.93
	Maximum	–	116.2
c_3/k_3	Mean	−1.883	1.401
	Minimum	−160.1	−617.3
	Maximum	56.53	924.0
c_3'	Mean	–	15.17
	Minimum	–	−5451.1
	Maximum	–	3256

The regression coefficients obtained for both equations appear to be rational in the context of linear layered-elastic backcalculated moduli and computed stresses for the majority of the pavement layers considered. (They would not be considered rational in the context of traditional laboratory resilient modulus test experience.) In this context, the traditional interpretation that negative k_2 values are associated with stress-softening behavior is not really applicable, because the relative importance of the bulk and octahedral shear stress terms is often the reverse of what is seen in the laboratory, due to the particulars of linear layered-elastic analysis. Despite the negative k_2 values, the models predict increasing modulus with increasing FWD load for the granular layers.

While the majority of the model coefficients are rational (in the context of linear layered-elastic analysis), there are several notable exceptions. For example, the c_0 values for all the models for section 831801 layer 3 for both equations are very high. The goodness of fit statistics for the section 831801 layer 3 models are very good, but the sample size is very small, so the applicability of this model is limited.

The goodness of fit statistics for Models 1, 2A, and 2B are compared on a layer-by-layer basis in Table 83 of Appendix E: **Multiple Regression Results for Individual Pavement Layers**, and summarized in Table 42. In some instances, the number of observations considered in the

regression varied between Model 1 (n_1) and the other equations (n_2), by virtue of the presence of negative bulk stresses in the data sets. This was the case for 11 of the 59 layers considered. In a few instances, the number of observations excluded due to negative bulk stresses approached the total number of observations available. In two cases, the exclusion of negative bulk stress observations made it impossible to complete the regression for Model 1, due to small sample sizes.

Table 42. Summary of goodness-of-fit statistics for Models 1, 2A and 2B

		1	2A	2B
S_e/S_y	Mean	0.58	0.55	0.52
	Minimum	0.05	0.11	0.12
	Maximum	1.01	1.00	1.02
Bias	Mean	1	0	0
	Minimum	0	0	0
	Maximum	5	5	4

In most cases, providing for the possibility that all three k-coefficients vary with moisture content yields a better fit of the data (most often reflected in a reduced standard error ratio (S_e/S_y)) than the assumption that only k_1 is a function of moisture content. In some cases (e.g., layer 4 for section 040114), the difference is negligible (zero percent change in bias, and standard error ratio changed by less than 0.01), and in others it is more substantial (e.g., layer 4 for section 251002, where the standard error ratio was reduced from 0.96 to 0.38).

The regression results were characterized as fully acceptable if the standard error ratio, S_e/S_y, computed for E_p (as opposed to $\log(E_p)$) was less than 0.5, and the absolute value of the bias was less than 2 percent. The results were characterized as unacceptable if the standard error ratio was greater than 0.85, or the absolute bias was greater than 5 percent. Results meeting neither set of criteria were characterized as marginal. Based on these criteria, all model forms considered yielded results that were at least marginally acceptable (from a standpoint of goodness of fit) for 61 percent of the pavement layers. Of 59 pavement layers considered, the regression results were unacceptable for 2, both subgrade layers, and 17 for which all model forms yielded fully acceptable results. The regression modeling was most successful for the base layers, and least successful for the semi-infinite subgrade layers. This discrepancy in the relative rate of success is consistent with the assumption that the true modulus of some of the semi-infinite subgrade layers is relatively constant with time and FWD load, such that the observed variation is primarily due to random error in the deflection testing and backcalculation process.

Model 2 is better suited to modeling the variations in pavement layer moduli backcalculated using linear layered-elastic theory. The rationale underlying this judgment is as follows:

1. More often than not (for 75 percent of the layers considered), the standard error ratio for one or both of Models 2A and 2B is less than or equal to that for Model 1. This

observation also holds if one compares only Models 1 and 2A, though the difference between models 1 and 2A is small enough that it may be attributable to the different assumed values of K_0.

2. Models 1 and 2 are essentially equal from a standpoint of bias.

3. Model 2 is applicable to negative computed bulk stresses, whereas Model 1 is not. That layered-elastic theory yields tensile stresses in some situations is theoretically problematic, from a practical standpoint. However, consideration of negative (tensile) stresses when working with pavement layer moduli backcalculated using linear layered elastic theory is necessary because they occur quite frequently. Exclusion of affected data points (where they occur) reduces the size of the data set on which to base the model and may result in a biased model.

Furthermore, for 58 percent of the pavement layers, the standard error ratio for Model 2B is somewhat better than for Model 2A; consideration of the potential for moisture to affect all three k coefficients thus is recommended. It must be recognized that this recommendation applies only to layer moduli backcalculated using linear layered-elastic theory. No assessment of the applicability of the model form to laboratory resilient modulus test data has been undertaken.

Soil Class Models

The regression models discussed in the preceding sections of this chapter were each derived from the data from a single pavement layer at a particular test section. In the interest of obtaining more broadly applicable models, the working data set of moduli, stress, and moisture parameters was subdivided by soil class and layer extent (i.e., whether the layer was finite or semi-infinite in depth). Multiple regression was used to fit the data for each subset to Model 2B, and several variations on Model 2 including material parameters, in addition to stress parameters and moisture content. The model forms considered for the coefficients k_1, k_2, and k_3 are presented in Table 44. The materials data used in the models are presented in Appendix D: **Materials Data Used In Development of E Predictive Models**. Density and plasticity index are presented in Table 70, while gradation information is provided in Table 71. The resulting models are presented in Table 43.

It is notable that the predictive capability of the soil class models (with or without material parameters) is often (but not always) better for the semi-infinite subgrade layers than it is for the soil classes most often found in the base and subbase layers—the opposite of what was observed for the individual layer models. Factors that may contribute to the observed discrepancy are as follows.

1. Differences in the extent to which the layer moduli vary. As noted in Chapter 4, variations in the backcalculated moduli for the base layers tends to be greater than those for the deeper layers.

2. Differences in the extent to which the within-section variations in backcalculated moduli are attributable to differences in stress and moisture, versus other factors, including random error in the deflection measurement and backcalculation process. The regression results for the individual pavement layers indicate that variations in stress and moisture typically explain a relatively large fraction of the observed within-section variation for the upper pavement layers, but a lesser fraction of the observed variation for the deeper layers.

3. Differences in the extent to which between-section variations in backcalculated moduli are attributable to quantifiable material characteristics as opposed to systematic errors arising from the backcalculation process. For example, as discussed in Chapter 2, the backcalculated moduli for the upper layers of the pavement are more sensitive to small errors in layer thickness than those for deeper layers. A systematic error in backcalculated moduli arising from layer thickness errors will have little or no effect on the within-section variation, but could have a very large impact on between-section variation.

4. Differences in the extent to which the data for the different layers are influenced by the limitations of linear layer-elastic theory, including the prevalence of tensile radial load stresses.

Differences in the number of sections (and therefore, the array of soils) considered in the model development may also contribute to the observed differences.

The issue of the number of soils represented in the data sets on which these models are based is an important one, as the applicability of models based on data for only a few soils is limited; application of the models to the soil class in general thus is not appropriate.

Table 43. Selected soil class models for prediction of pavement layer moduli using linear layered-elastic theory

Finite Layers	
A-1-a	$E = 10^{(4.270 + 0.004PR10/P200-0.490\rho d+0.030VwP200)} * 10^{(-0.250-1.210Vw+0.140Vw*P200)*\theta/Pa} * (\tau/P_a+1)^{(1.490+28.56Vw-3.330Vw*P200)}$
A-1-b	$E = 10^{(3.671 -0.151PR10/P200-0.163\rho d+0.092VwP200)} * 10^{(0.217-3.343Vw+0.260Vw*P200)*\theta/Pa)} * (\tau/P_a+1)^{(2.786+9.388Vw-0.717Vw*P200)}$
A-2-4	$E = 10^{3.241}(1+V_w)^{-1.193}RD^{-8.083}M^{-0.249} * 10^{-0.049(1-P200)\theta/Pa}(\tau/P_a+1)^{13.14*P200}$
A-2-6	$E = 10^{(3.003-0.102PI+0.428VwP200} * 10^{(-0.010-0.546VwP200)\theta/Pa}(\tau/P_a+1)^{(0.720+4.774VwP200)}$
A-3	$E = 10^{(5.160 + 0.090PR10/P200-0.160\rho d-1.350VwP200)} * 10^{(-2.320-21.92Vw+5.620Vw*P200)*\theta/Pa} * (\tau/P_a+1)^{(7.100 +374.0Vw-75.75Vw*P200)}$
A-4	$E = 10^{(6.825+ -1.840PR10/P200-2.012\rho d+0.009VwP200)} * 10^{(0.258+0.220Vw-0.043Vw*P200)*\theta/Pa} * (\tau/P_a+1)^{(-0.888-42.03Vw+0.863Vw*P200)}$
A-6	$E = 10^{(4.070+0.560Vw)} * 10^{(-0.990-0.040Vw)*\theta/Pa} * (\tau/P_a+1)^{(-0.700+7.260Vw)}$
Semi-Infinite Subgrade Layers	
A-1-b	$E = 10^{(35.64 -0.190PR10/P200-15.83\rho d)} * 10^{(0.820Vw -0.110VwP200)*\theta/Pa} * (\tau/P_a+1)^{(-0.980VwP200)}$
A-2-4	$E = 10^{(-26.92 - 2.580PR10/P200+16.16\rho d+0.180VwP200)} * 10^{(2.470+13.53Vw-1.180VwP200)*\theta/Pa} * (\tau/P_a+1)^{(-25.69 -101.0Vw+10.55VwP200)}$
A-3	$E = 10^{(15.09 - 38.83PR10/P200-1.438VwP200)} * 10^{(-1.185+2.251VwP200)*\theta/Pa} * (\tau/P_a+1)^{(1.263 -36.65Vw+1.868VwP200)}$
A-4	$E = 10^{(2.850 +1.510Vw)} * 10^{(1.020-2.85Vw)*\theta/Pa} * (\tau/P_a+1)^{(-9.380+25.44Vw)}$

Where: PR10/P200 = Percent retained on the No. 10 sieve/percent passing 200
P_{200} = Percent passing 200
V_w = Volumetric moisture content (decimal fraction)
ρ_d = In situ dry density
RD = Relative density ($\rho_d/\rho_{optimum}$)
D_n= Sieve opening at which n percent of soil passes, n = 10, 20, 30,…
M = Material constant (adapted from Yang[34])
PI = Plasticity index

$$M = \frac{\left(\frac{1}{2}\left(10^{(P_{200}-V_w)} + 10^{(V_w-P_{200})}\right)\right)}{DF}(1+PI) \qquad DF = \frac{D_{80}}{\left(7.14\left(\frac{D_{80}}{D_{40}} + \frac{D_{40}}{D_{20}} + \frac{D_{20}}{D_{10}}\right)\right)^{0.5}}$$

Table 44. Model forms considered for k_1, k_2, and k_3 in Model 2

Model	k_1	k_2	k_3
2C	$10^{(c0+c1PR10/P200+c1'\rho d+c1''VwP200)}$	$c_2 + c_2'V_w+c_2''V_wP_{200}$	$c_3+c_3'V_w+c_3''V_wP_{200}$
2D (coarse)	$10^{(c0+c1D60+c1'RD+c1''VwP200)}$	$c_2 + c_2'V_w+c_2''V_wP_{200}$	$c_3+c_3'V_w+c_3''V_w*P_{200}$
2D (fine)	$10^{(c0+c1PI+c1'RD+c1''VwP200)}$	$c_2 + c_2'V_w+c_2''V_wP_{200}$	$c_3+c_3'V_w+c_3''V_w*P_{200}$
2E	$10^{(c0+c1Vw+c1'P10)}$	$c_2+c_2'V_w+c2''P_{10}$	$c_3+c_3'V_w+c_3''P_{10}+c_3'''RD$
2F	$10^{c0}(1+V_w)^{c1'}RD^{c1''}M^{c1'''}$	$c_2(1-P_{200})$	c_3P_{200}
2G	$10^{c0}(1+V_w)^{c1'}RD^{c1''}M^{c1'''}$	$c_2 + c_2'V_w + c_2''(1-P_{200})$	$c_3+c_3' P_{200}+c_3''V_w$

Where: PR10/P200 = Percent retained on the No. 10 sieve/percent passing 200
P_{200} = Percent passing 200
P_{10} = Percent passing No. 10 sieve
V_w = Volumetric moisture content (decimal fraction)
ρ_d = In situ dry density (units)
RD = Relative density ($\rho_d/\rho_{optimum}$)
D_n= Sieve opening at which n percent of soil passes, n = 10, 20, 30,…
M = Material constant (adapted from Yang[34])
PI = Plasticity index

$$M = \frac{\left(\frac{1}{2}\left(10^{(P_{200}-V_w)}+10^{(V_w-P_{200})}\right)\right)}{DF}(1+PI) \qquad DF = \frac{D_{80}}{\left(7.14\left(\frac{D_{80}}{D_{40}}+\frac{D_{40}}{D_{20}}+\frac{D_{20}}{D_{10}}\right)\right)^{0.5}}$$

Development of more general models—i.e., models applicable to all coarse-grained or all fine-grained soils—was attempted, but was not successful.

SUMMARY

Regression models to predict backcalculated pavement layer modulus as a function of stress state, moisture content, and (for the soil class models) material parameters were developed. In developing these models, regression coefficients derived for layer moduli backcalculated using linear layered elastic theory were found to be inconsistent with those obtained for laboratory test results for the same constitutive model form and similar materials. In particular, the sign of the k_2 parameter for the backcalculated moduli for granular materials was consistently negative, when positive values are expected. The reasons for this discrepancy were explored, with the finding that the stress states and the relationships between the stress parameters computed for the backcalculated moduli and those typically used in laboratory testing are dissimilar. Key factors contributing to the dissimilarity include the lack of independence between the backcalculated moduli and the (computed) stress parameters used in the model development, and the potential for tensile computed stresses.

Development of empirical models to predict layer moduli derived using linear layered-elastic theory was pursued to facilitate consideration of seasonal variations pending the development of improved backcalculation procedures.

Model 2, which is restated below, is recommended for use in modeling the stress sensitivity of layer moduli backcalculated using linear layered elastic theory. It is further recommended that Model 2B be used to consider the combined effects of stress and moisture on linear elastic backcalculated pavement layer moduli.

$$\text{Model 2: } E = k_1 10^{k2(\theta/Pa)}(\tau/P_a+1)^{(c3+c3'Vw/100)} \tag{32}$$

$$\text{Model 2B: } E = c_0 10^{(c1Vw/100 +(c2+c2'Vw/100)\theta/Pa)}(\tau/P_a+1)^{(c3+c3'Vw/100)} \tag{33}$$

CHAPTER 6: APPLICATION OF RESEARCH RESULTS TO ESTIMATE SEASONAL VARIATIONS IN MODULI OF UNBOUND PAVEMENT LAYERS

INTRODUCTION

The findings and regression models presented in Chapters 4 and 5 may be applied to estimate backcalculated moduli for a given set of environmental conditions (exclusive of frost effects), and thus, the seasonal variations in the backcalculated moduli of unbound pavement layers. This chapter discusses the application of the regression models discussed in Chapter 5 to predict backcalculated pavement layer moduli for several pavement test sections to demonstrate how the findings of this research might be applied in practice.

Estimating backcalculated modulus is a straightforward computational exercise for a given state of stress (defined by the computed bulk and the octahedral shear stresses) and moisture content when applying the regression models presented in Chapter 5. Application of the models in practice, however, is less straightforward because the state of stress that should be used in the computation is not "given." Rather, the stress state is a function of the layer modulus to be predicted as well as the moduli of the other pavement layers (among other parameters).

For the purposes of the trial application discussed here, the fact that the stress state is unknown is addressed by using an iterative process in which an initial estimate of the modulus is used to estimate the applicable stress state. The estimated stress parameters are in turn used to compute a refined estimate of the modulus. By repeating this process until the moduli computed for two subsequent iterations are essentially identical, both the stress state and the associated modulus may be estimated. The basic steps in the process summarized below; a more detailed discussion of the procedure is provided in the next section.

1. Establish an initial estimate of the set of pavement layer moduli for the date and time (t) and FWD load (P) for which predictions are desired, $E_{10}(t,P)$, $E_{20}(t,P)$, …E_{n0}, where $E_{10}(t,P)$ is the estimated modulus for the surface layer, and $E_{n0}(t,P)$ is the initial modulus estimate for the deepest (semi-infinite) layer.

2. Using the estimated moduli, known layer thicknesses and densities, and estimates of Poisson's ratios, compute the bulk stress and the octahedral shear stress, considering both load-induced and overburden stresses.

3. Using the computed stress parameters from step 2 and the estimated moisture content for each unbound layer, compute a refined estimate of the modulus for each unbound layer. The second and subsequent approximations of the moduli for bound layers equal the first approximation, as these layers are assumed to be insensitive to variations in stress state (and moisture).

4. Repeat steps 2 and 3 until the change in the estimated moduli (for all layers) from one iteration to the next is deemed insignificant.

In the trial application, backcalculated moduli for an initial test date are used as the starting point for the computations. Estimated temperature-compatible moduli for the asphalt-bound layers are required, as temperature-induced variations in the modulus of asphalt-bound layers will alter the stress states in the underlying layers. The unadjusted backcalculated moduli for the remaining layers are used as the first approximation of the moduli for those layers.

Four prediction scenarios were considered:

1. Predictions based on section/layer-specific models derived from the full data set using Model 2B (i.e., those presented in Table 82 in Appendix D).

2. Two sets of predictions based on section/layer specific models derived using limited data sets

    a. Models derived from data for a single test date, using Model 2 (Equation 29).
    b. Models derived from data for two test dates, using Model 2B (Equation 31).

    The limited data set models were used to explore the feasibility of using section/layer-specific models in routine practice. Two-date models allow consideration of the effects of variation in moisture content as well as stress state, whereas the one-date models permit consideration of only stress parameters.

3. Predictions based on the soil class models presented in Table 43.

The procedures used in the trial application are described in more detail in the next section of this chapter. The results obtained are presented and discussed in the following section.

PROCEDURE FOR PREDICTION OF SEASONAL VARIATIONS IN BACKCALCULATED PAVEMENT LAYER MODULI

Required Input Data

The data elements required for the derivation of section/layer-specific prediction models are defined in Table 45. They include backcalculated pavement layer moduli for several FWD load levels, pavement cross-section information for the computation of the stress parameters, and moisture data.

The data elements required for application of the regression models to predict backcalculated pavement layer moduli are identified in Table 46 and Table 47. The data identified in Table 46 are required in all cases. These data include backcalculated pavement layer moduli and related data for an initial FWD test date and estimates of environmental conditions and temperature compatible moduli for AC-bound layers for the dates/times for which predicted moduli are desired. The data identified in Table 47 are needed only when the soil-class

models presented in Table 43 are used to predict the pavement layer moduli. The specific data required for application of the soil class models varies with the extent and classification of the pavement layer material to be considered.

Table 45. Data required for derivation of section/layer-specific models

Data Element	Variable	Units	Notes
FWD load	P	KN	For multiple sets of FWD deflection data for 4 nominal FWD load levels (27, 40, 53, and 71 kN)
Backcalculated layer moduli	E_i	MPa	For i = 1 to n, where n is the total number of layers in the pavement structure, including the subgrade
Mean volumetric moisture content for each pavement layer	V_{mi}	decimal fraction	For i = 1 to n Not required for one-date (Model 3) models
In situ (wet) layer density	ρ_i	kg/m^3	For i = 1 to n
Layer thickness	h_i	M	For i = 1 to n
Layer Poisson's ratio	μ_i	—	For i = 1 to n
Depth-to-water table	d_{gwt}	M	—

Part 1: Derivation of Section- and Layer-Specific Regression Models

The computational steps used to derive the section/layer-specific limited data set models were as follows.

1) Computation of Stress Parameters

For each of the k sets of backcalculated layer moduli and associated FWD load included in the model derivation data set (see Table 45), the vertical and radial load stresses, σ_{vlk} and $\sigma_{rlk,}$ were computed using the CHEVLAY 2 linear layered-elastic analysis program. The stresses were computed for points directly beneath the center of the loaded area, at three-quarters-depth in each unbound layer. The input data required for this computation consist of the FWD load (P_k), and the layer moduli ($E_{i,k}$), layer thicknesses, (h_i), and Poisson's ratios (μ_i) for each pavement layer.

Table 46. Data required to predict backcalculated pavement layer moduli

Data Subset	Data Element	Variable	Units	Notes
Pavement cross section	Layer thickness	h_i	m	For i = 1 to n, where n is the total number of layers in the pavement structure, including the subgrade
	Layer Poisson's ratio	μ_i	—	For i = 1 to n
Data for initial test date	FWD load	P	kN	All observations for the selected initial test date.
	Layer moduli	$E_i(0)$	MPa	For i = 1 to n
Estimated parameters for prediction date(s)	Estimated mean volumetric moisture content	$V_{mi}(t)$	—	For i = 1 to n, expressed as decimal fraction. Obtain via simulation with the EICM[19] or estimate through other means
	In situ (wet) layer density	$\rho_i(t)$	kg/m^3	For i = 1 to n
	Estimated water table depth	$d_{gwt}(t)$	m	—
	Estimated temperature-compatible modulus for asphalt-bound layers	$E_i(t)$	MPa	For all layers, i, composed of asphalt-bound materials

a) The in situ density, layer thickness, and water table depth data were used to compute the effective vertical and radial overburden stresses σ_{vok}' and σ_{rok}' at three-quarters depth in the layer of interest, as outlined in Figure 42. K_0 was assumed to be 1.0 in these computations.
b) The octahedral shear and bulk stresses, θ_k and τ_k, were computed as

$$\tau_k = 1/3\sqrt{2*((\sigma_{vlk} + \sigma_{vok}') - (\sigma_{rlk}+\sigma_{rok}'))^2} \quad (34)$$

$$\theta_k = 2*(\sigma_{rlk} + \sigma_{rok}') + (\sigma_{vlk} + \sigma_{vok}') \quad (35)$$

Table 47. Soil parameters required for application of soil class models to predict backcalculated pavement layer moduli

Layer Extent and Classification	Required Soil Parameters
All	AASHTO Soil Class
Finite A-1-a Finite A-1-b Finite A-3 Finite A-4 Semi-infinite A-1-b Semi-infinite A-2-4 Semi-infinite A-3	Dry density (kg/m^3) Gradation (percent retained on the No. 10 sieve and percent passing 200)
Finite A-2-6 layers	Dry density (kg/m^3) Laboratory optimum density (kg/m^3) D60
Finite A-2-4	Dry density (kg/m^3) Laboratory optimum density (kg/m^3) Gradation (% passing 200, D80, D60, D40, D20, D10) Plasticity Index

2) Derivation of Model Coefficients

Using the stress parameters computed in step 1, the backcalculated layer moduli, and (for the 2-date models) the in situ moisture contents as input, multiple regression was used to derive the coefficients for the models:

$$\text{Model 2 (One-date models): } E/P_a = k_1 10^{\,k2\theta/Pa}(\tau/P_a+1)^{k3} \quad (36)$$

$$\text{Model 2B (Two-date models): } E/P_a = c_0 10^{(c1Vw+(c2+c2'Vw)\theta/Pa)}(\tau/P_a+1)^{(c3+c3'Vw/100)} \quad (37)$$

For regression purposes, the log-transformed versions of the models were used:

$$\text{Model 2: } \mathrm{Log}(E/P_a) = \log k_1 + k_2\theta/P_a + k_3\log(\tau/P_a+1) \quad (38)$$

$$\text{Model 2B: } \mathrm{Log}(E/P_{a)} = \log c_0 + c_1V_w + c_2(\theta/P_a) + c_2'V_w(\theta/Pa) + c_3\log(\tau/P_a+1) + c_3'V_w\log(\tau/P_a+1) \quad (39)$$

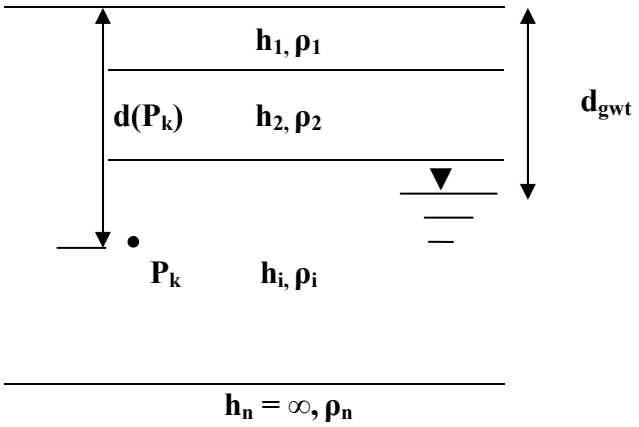

For a point P_k in layer j, the total vertical overburden stress σ_{vo} is computed as:

$$\sigma_{vo}(P_k) = \left[\sum_{i=1}^{j-1} h_i \rho_i + (d(P_k) - \sum_{i=1}^{j-1} h_i)\rho_j\right] \times g$$

For points above the water table (i.e., $d(P_k) \leq d_{gwt}$) the effective overburden stress is taken to be equal to the total overburden stress (i.e., pore pressure effects in partially saturated soils are neglected):

$$\sigma_{vo}'(P_k) = \sigma_{vo}(P_k)$$

For points below the water table (i.e., $d(P_k) > d_{gwt}$) the effective overburden stress is computed as:

$$\sigma_{vo}'(P_k) = \sigma_{vo}(P_k) - (d(P_k) - d_{gwt})\rho_w g$$

Radial overburden, σ_{ro}', is computed as:

$$\sigma_{ro}' = K_0 \sigma_{vo}'$$

Where:
ρ_i = density of layer i = $\rho_{di}+\rho_w V_{wi}$
ρ_{di} = dry density of layer i (constant)
ρ_w = density of water (constant)
V_{wi} = mean volumetric moisture content (decimal fraction) for layer i
h_i = thickness of layer i
$d(P_k)$ = depth to point P_k
d_{gwt} = depth to ground water table
g = acceleration due to gravity
$\sigma_{vo}(P_k)$ = total vertical stress due to overburden at point P_k
$\sigma_{vo}'(P_k)$ = effective vertical stress due to overburden at point P_k
K_0 = coefficient of lateral earth pressure

Figure 42. Calculation of overburden stress

Part 2: Estimation of Pavement Layer Moduli for Future Date

1) First approximation of conditions at time t:

   a) Asphalt-bound layers: $E_{i0}(t)$ = Input $E_i(t)$

   b) All other layers: Assume $E_{i0}(t)$ = Input $E_i(0)$

   c) The effective vertical and radial overburden stresses $\sigma_{vo}'(t)$ and $\sigma_{ro}'(t)$ for points beneath the center of the applied load at three-quarters depth in each unbound layer were computed using $\rho_i(t)$, h_i, $d_{gwt}(t)$, and assuming $K_0 = 1.0$ (see Figure 42).

2) Iterative computation of moduli
   For j = 1 to m, where m is the number of iterations required to achieve acceptable between-iteration agreement in moduli.

   a) Using the $E_{i(j-1)}(t)$ values, layer thicknesses (h_i) and Poisson's ratios (μ_i), and FWD load (P) as input, the CHEVLAY 2 linear layered-elastic analysis program was used to compute estimates of the vertical and radial load stresses, $\sigma_{vlj}(t)$ and $\sigma_{rlj}(t)$ for a point directly beneath the center of the loaded area, at three-quarters-depth in each unbound layer.

   b) Using the load stresses from step 2a, and the effective overburden stresses from step 1c, the estimated bulk and octahedral shear stresses at time t for each unbound layer were computed:

$$\theta_{ij}(t) = 2 * (\sigma_{rlj}(t) + \sigma_{ro}'(t)) + (\sigma j_{vlj}(t) + \sigma_{v}'(t)) \tag{40}$$

$$\tau_{ij}(t) = 1/3\sqrt{2 * ((\sigma_{vlj}(t) + \sigma_{vo}'(t)) - (\sigma_{rlj}(t) + \sigma_{r}'(t)))^2} \tag{41}$$

   c) Part 1 (limited data set models), or Table 43 was used to compute $E_{i,j}(t)$, using the stress parameters from step 2.b., the input moisture contents and (for the soil class models) material parameters (see Table 47).

   d) For bound layers, $E_{i,j}(t) = E_{i,j-1}(t)$.

   e) $E_{i,j}(t)$ was compared with $E_{i,(j-1)}(t)$. Differences of less than 5 percent for all layers were deemed small enough to proceed to step 3. (As will be discussed subsequently, substantially better agreement was achieved in most instances.)

   f) The $E_{i,j}(t)$ value for each unbound layer was compared with the applicable maximum and minimum modulus values presented in Table 48. If $E_{i,j}(t)$ were greater than the maximum value for the soil class, the maximum value was substituted for use in the

next iteration. If $E_{i,j}(t)$ were less than the minimum value, the minimum value from Table 48 was substituted. This check and substitution procedure was used to avoid computational problems arising from irrationally high or low computed modulus values that were found to occur with some data sets.

g) Continue iterating from Step 2.a.

3) The moduli were compared with the ranges presented in Table 48. If the computed moduli fell outside the applicable ranges, they were not considered further, as they were outside the inference space of the regression models.

Table 48. Modulus ranges

Soil Class	Modulus, E (MPa)	
	Minimum	Maximum
A-1-a	78	687
A-1-b	35	712
A-2-4	34	708
A-2-6	52	221
A-3	36	549
A-4	66	439

TRIAL APPLICATION

The procedure presented in the preceding section was used to estimate moduli for several test sections in this investigation. As indicated previously, sample applications considered the full data set Model 2B section/layer –specific models presented in Table 82 (Appendix E), one-date (Model 2) and two-date (Model B) section/layer-specific models, and the recommended soil class models presented in Table 43. The data sets used as initial input to the modulus prediction procedure are identified in Table 49. The test sections considered were selected on the basis of geographic distribution, and (in the case of the soil class predictions) the availability of an applicable soil class model for all layers in the pavement structure.

The model coefficients and goodness-of-fit statistics for the one- and two-date models are presented in Table 50. Two one-date models (designated by the letters A and B after the layer number) were considered for section 271018. With the exception of the two models for section 091803 layer 2, the models are unbiased; the bias for the two 091803 layer 2 models is only 1 percent. All two-date models (except that for layer 4 at section 091803) have standard error ratios (S_e/S_y) less than or equal to 0.50. Thus, they fit the data sets used in the model development quite well.

Table 49. Data sets considered in trial application of modulus prediction

Section	Time Span for Predictions		Models Considered			
			Layer/Section-Specific			Soil Class
			Single Date	2 Dates	All Dates	
040113	1/10/96	5/9/96	1/10/96	1/10/96 4/3/96	X	X
040114	2/6/96	4/2/96	—	—	X	X
091803	11/15/93	5/8/97	11/15/93	11/15/93 5/12/94	X	X
131031	8/3/95	4/25/96	—	—	X	X
161010	10/1/93	11/25/96	—	—	X	
231026	9/16/93	5/1/95	—	—	X	X
271018	9/23/93	8/8/94	A: 9/23/93 B: 5/9/94	9/23/93 5/9/94	X	—
331001	10/14/93	6/29/95	—	—	X	—
351112	4/6/94	2/4/97	—	—	X	—
481077	12/14/93	5/16/97	12/14/93	1/10/94 7/18/94	X	X
561007	1/21/94	6/19/97	—	—	X	
871622	4/26/94	6/15/95	—	—	X	X

When compared on a layer-by-layer basis, the one-date models are not as strong as the two-date models, though most are acceptable, having standard error ratios of 0.5 or less. However, the layer 4 model for section 091803 is only fair, with a standard error ratio of 0.65. The one-date model for layer 4A at section 271018 is poor, with a standard error ratio of 1.02. Section 271018 layer 4 model B is somewhat better, with a standard error ratio of 0.89, but is still only fair. In practice, the models for section 091803 layer 4, and section 271018 layer 4B should be used with caution, and section 271018 layer 4 model A should not be used at all. The trial applications were completed with these models for illustrative purposes only.

The asphalt surface moduli for the modulus estimation dates were computed by applying the Asphalt Temperature Adjustment Factor (ATAF) developed by Lukanen et al.[77] using the monitored mid-depth temperatures for the pertinent dates, and the backcalculated moduli for the initial date. The ATAF is computed as:

$$ATAF = 10^{c*(T_{ref} - T_{Meas})} \quad (42)$$

Where:

ATAF = Asphalt temperature adjustment factor.
c = Regression constant, -0.021 for mid-lane test points, -0.0195 for outer wheelpath test points.

T_{ref} = Estimated mid-depth asphalt layer temperature for the date of interest.
T_{Meas} = Mid-depth asphalt layer temperature at the time of deflection testing.

The computed temperature-compatible AC layer moduli for the prediction data sets are compared with the actual backcalculated AC layer moduli in Figure 43. Although there are several aberrant data points, overall agreement is good.

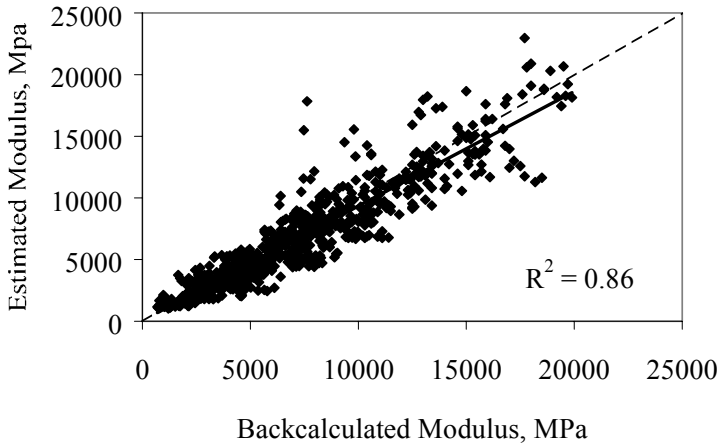

Figure 43. Backcalculated modulus versus estimated temperature compatible modulus for all sections considered in trial applications

All sets of backcalculated moduli (in the working data set) for the selected initial test dates in the time frame noted in Table 49 were used in the prediction computations. The moisture contents and depths to ground water used in the computations were also the monitored values. Thus, the trial applications do not represent a field validation of the methodology. Rather, they serve to demonstrate an approach that might be taken to applying the predictive models for backcalculated pavement layer moduli.

Table 50. Site-specific, limited data set Model 3 and 3B coefficients and goodness-of-fit statistics

Site	Layer	c_0	c_1/k_1	c_2/k_2	c_2'	c_3/k_3	c_3'	n	r^2 (log E)	% Bias	S_e/S_y
1-Date Models (Model 3)											
040113	2	–	3.087	-0.247	–	1.610	–	19	0.88	0	0.39
040113	3	–	4.931	-3.109	–	19.07	–	19	0.87	0	0.39
040113	4	–	-2.713	1.640	–	-79.86	–	19	0.80	0	0.49
091803	2	–	3.373	-0.437	–	3.168	–	34	0.87	-1	0.49
091803	3	–	7.154	-4.517	–	25.15	–	34	0.89	0	0.36
091803	4	–	-9.126	12.58	–	-60.90	–	34	0.62	0	0.65
271018	2A	–	3.259	-0.191	–	1.698	–	5	0.99	0	0.24
271018	3A	–	3.221	-0.180	–	2.857	–	5	0.94	0	0.50
271018	4A	–	7.094	-3.836	–	42.19	–	5	0.75	0	1.02
271018	2B	–	3.090	-0.122	–	1.763	–	8	0.96	0	0.25
271018	3B	–	3.974	-1.352	–	-0.334	–	8	0.92	0	0.37
271018	4B	–	6.846	-4.124	–	38.11	–	8	0.54	0	0.89
481077	2	–	3.566	-0.219	–	0.681	–	34	0.88	0	0.36
481077	3	–	5.534	-3.587	–	18.89	–	34	0.86	0	0.40
2-Date Models (Model 3B)											
040113	2	3.121	-0.317	-0.325	0.711	1.906	-2.717	28	0.89	0	0.36
040113	3	2.983	16.84	0	-26.83	0	162.9	28	0.88	0	0.37
040113	4	11.920	-164.6	0	27.28	0	-714.1	28	0.85	0	0.41
091803	2	2.677	3.160	-0.886	2.038	19.14	-72.54	73	0.88	-1	0.45
091803	3	9.053	-9.220	-6.393	9.110	25.66	-2.500	73	0.93	0	0.30
091803	4	-7.590	0.000	11.23	-0.688	-51.26	-10.80	73	0.66	0	0.61
271018	2	6.344	-23.46	-0.152	0.000	0.000	12.52	13	0.97	0	0.20
271018	3	3.556	1.358	0	-5.685	-12.33	63.67	13	0.93	0	0.34
271018	4	3.850	11.86	-4.084	0	0	151.3	13	0.83	0	0.47
481077	2	3.451	1.841	0.167	-4.331	4.259	-34.78	57	0.84	0	0.44
481077	3	-38.73	237.0	0	-13.18	0.000	62.85	57	0.94	0	0.24

The number of iterations required to achieve agreement between the moduli for two subsequent iterations varied tremendously. In some cases, fewer than 5 iterations were required to achieve absolute agreement, and in others, more than 35 iterations were required. Computations were terminated after 44 iterations, and data sets for which the difference in computed modulus between iterations 43 and 44 exceeded 5 percent were not considered in the subsequent evaluation. Fewer than 2 percent of the layer modulus estimates were rejected based on the 5-percent closure criterion. An additional 5 percent of the prediction results were

rejected because the modulus for one or more layers fell outside the inference space for the predictive models (see Table 48).

Results Obtained with Section/Layer-Specific Models Derived From the Full Data Set

The overall results obtained in the sample applications using section/layer-specific models based on the full data set are compared with the backcalculated moduli in Figure 44. The error bounds about the line of equality in these figures represent twice the within-day standard deviation for the layer type in question as reported in Table 23. The overall results for the subgrade layers are reasonably good, in the sense that the data points are clustered about the line of equality, and the backcalculated and predicted values are strongly correlated with each other, with an R^2 value of 0.87. The overall results for the subbase and base layers are not as good. The data points are more broadly dispersed about the line of equality, and the correlation between the backcalculated and predicted values is not as strong, particularly for the base layers, for which the R^2 value is only 0.47. There is a tendency toward under-prediction of the modulus for all three layers. This represents a conservative error.

The trial application results were also evaluated by means of series of paired Student's t tests on the null hypothesis that the true mean difference between the backcalculated and predicted moduli for each pavement layer is zero. Key statistics and the t-test results are presented in Table 51. In this table, n is the number of individual modulus observations considered (i.e., combination of test date/time and FWD load level) in the paired Student's t test. Entries of "A" under the column heading "t-Test Decision" indicate that the null hypothesis of zero difference between the backcalculated modulus, E, and the predicted modulus, $E_{predicted}$ is accepted at a significance level of 5 percent. Entries of R in the decision column indicate that the null hypothesis is rejected—i.e., that the difference is significantly different from zero at the 5-percent level of significance.

For the site/layer-specific complete data set predictions, the hypothesis of zero difference is accepted for all layers for 5 of the 12 test sections considered. The hypothesis of zero difference is accepted for at least 1 layer in all cases, and for 2 of 3 layers for 25 percent of the sections.

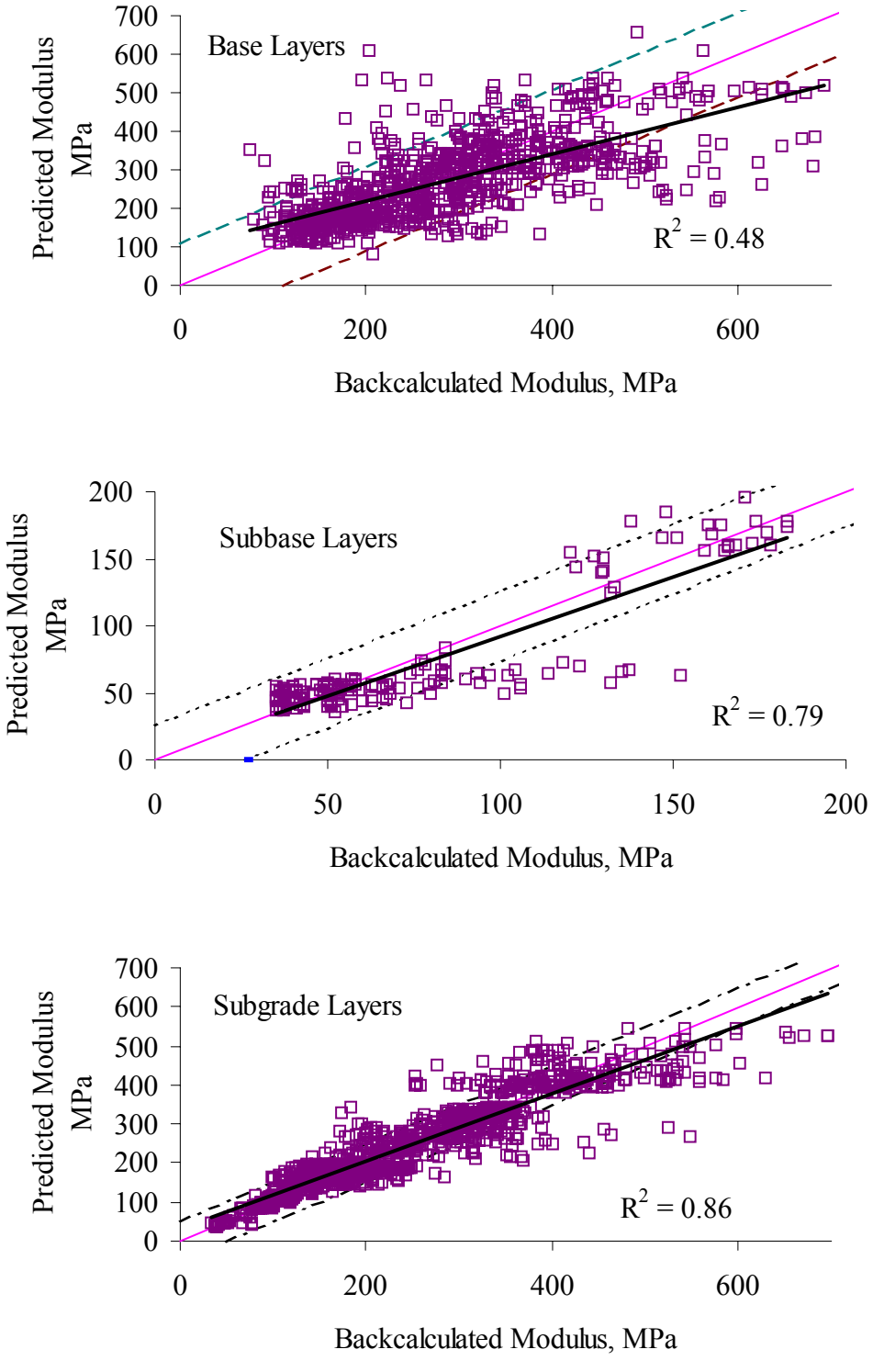

Figure 44. Backcalculated versus section/layer-specific predicted modulus for models derived using all data

The prediction results were also evaluated by examining the plots in Appendix F. Based on this examination, there are a few cases where it could be argued that although the observed differences are statistically significance, they are not large enough to be of practical significance. This occurs for the upper subgrade layer at section 040113 (see Figure 49 in Appendix F), where all of the data points are tightly clustered about the line of equality. There is also one case—the base layer for section 271018 (see Appendix F, Figure 55)—where the differences are large enough to be important from a practical standpoint, although the null hypothesis is accepted. A partial explanation for the poor base layer modulus predictions for this section may be found in Figure 45, which illustrates the relationship between the actual backcalculated AC layer moduli for this section, and the estimated values used in the predictions. Whereas the overall backcalculated versus predicted AC modulus agreement illustrated in Figure 43 is quite good, the agreement for this particular section is poor. Thus, the computed stress states (and therefore the predicted moduli) for the underlying layer(s) can be expected to differ, perhaps markedly, from those computed for the backcalculated moduli, thereby contributing to the poor prediction of base layer moduli for this section.

The column in Table 51 headed "Overall Decision" reflects the author's judgment of the acceptability of the prediction results considering both the t-test results and review of the plots in Appendix F. Entries of "U" in this column indicate that the overall prediction results for the section are deemed unacceptable, while entries of "A" indicate that the overall prediction results for the section are deemed acceptable.

Taking into consideration both the t-test results and observations drawn from the plots in Appendix F, the overall results of the section-specific model predictions are deemed acceptable for half of the sections considered. For the remaining sections, acceptable predictions were achieved for one or two of the layers, but not all three.

Collectively, these results show that the section/layer-specific regression models presented in Table 82 and the procedure presented in the preceding section of this chapter can yield acceptable results, particularly when unbiased regression models with strong predictive capability are achieved for all layers in the pavement structure. However, good results are not achieved on a consistent basis. Furthermore, these results represent a scenario that is not representative of what can be achieved in practice, by virtue of the fact that the same data were used in both the derivation of the models and their application (with the exception of the load-induced stress parameters, and the estimated AC layer moduli used in computing the load-induced stresses). The application of limited data set models derived from the data for one or two test dates provides a more realistic assessment of what can be expected in practice.

Table 51. Summary statistics and t-test results for section/layer-specific complete data set model predictions

Section	Layer	Mean E	Mean $E_{predicted}$	Mean Difference	Std. Dev. of Diff.	n	t	t-Test Decision	Overall Decision
040113	2	140	132	8.2	63.1	23	0.62	A	A
040113	3	88	91	-3.0	5.3	23	-2.70	R	
040113	4	146	146	-0.3	5.2	23	-0.28	A	
040114	2	257	261	-4.2	65.0	4	-0.13	A	A
040114	3	224	231	-7.7	12.7	4	-1.22	A	
040114	4	335	348	-13.7	14.4	4	-1.90	A	
091803	2	225	194	30.9	70.9	113	4.64	R	U
091803	3	162	164	-1.2	33.6	113	-0.37	A	
091803	4	296	293	4.8	32.7	113	1.55	A	
131031	2	473	452	21.1	109.4	42	1.25	A	A
131031	3	136	134	2.2	16.4	42	0.87	A	
131031	4	88	88	-0.3	7.2	42	-0.28	A	
161010	2	427	455	-28.3	55.4	12	-1.77	A	A
161010	3	60	55	4.4	15.8	12	0.96	A	
161010	4	218	227	-9.2	89.7	12	-0.35	A	
231026	2	248	227	20.4	56.5	59	2.77	R	U
231026	3	153	164	-11.1	24.7	59	-3.46	R	
231026	4	488	472	16.0	79.2	59	1.55	A	
271018	2	187	164	23.1	60.5	16	1.53	A	U
271018	3	184	179	4.6	17.0	16	1.09	A	
271018	4	45	45	0.1	1.1	16	0.19	A	
331001	2	191	209	-17.5	79.8	133	-2.53	R	U
331001	3	59	52	7.5	20.0	133	4.34	R	
331001	4	402	412	-10.1	66.0	133	-1.76	A	
351112	2	308	275	33.4	138.7	115	2.58	R	U
351112	3	273	252	21.2	76.1	115	2.99	R	
351112	4	328	329	-0.8	16.8	115	-0.54	A	
481077	2	361	355	5.9	83.2	260	1.15	A	U
481077	3	190	188	2.6	29.3	260	1.41	A	
561007	2	172	155	17.4	45.5	58	2.91	R	A
561007	3	111	110	1.5	9.0	58	1.30	A	
561007	4	163	163	-0.3	9.5	58	-0.26	A	
871622	2	313	294	19.7	69.9	27	1.47	A	A
871622	3	154	162	-7.6	16.3	27	-2.43	R	
871622	4	225	235	-9.7	20.8	27	-2.42	R	

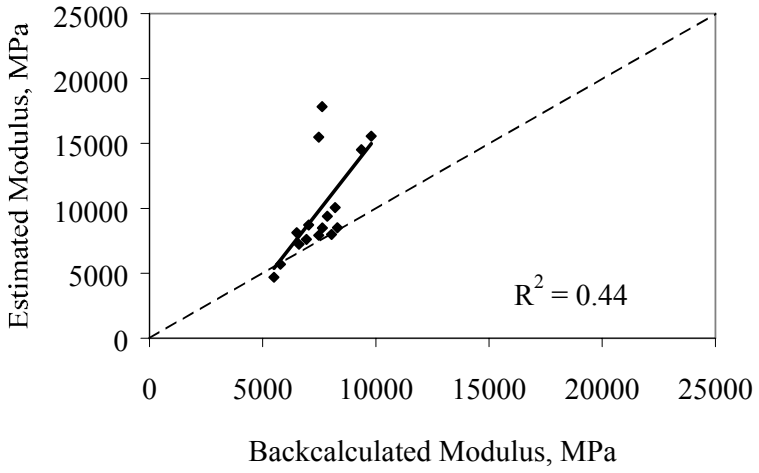

Figure 45. Backcalculated modulus versus estimated temperature compatible modulus for section 271018 (Minnesota)

Results Obtained With Section/Layer-Specific Models Derived From Limited Data Sets

Overall comparisons of the backcalculated moduli and predicted moduli derived using the one- and two-date models are provided in Figure 46 and Figure 47, respectively, while comparisons for individual pavement layers are provided in Appendix G, respectively. As before, the error bounds about the line of equality represent twice the pooled within–day standard deviation reported in Table 23 for the layer type (base or subgrade) of interest. The relationships between the backcalculated and predicted base layer moduli are weak, with R^2 values of only 0.24 and 0.32 for the single- and two-date models predictions, respectively. The relationships are much stronger for the subgrade layers, with R^2 values 0.58 and 0.69, respectively. (Note that these values are not directly comparable to those for the full data set predictions because fewer sections were considered.)

As previously, paired t-tests were used to test the null hypothesis that the mean difference between the backcalculated and predicted moduli is zero. Pertinent statistics and the t-test results are presented in Table 52 for the one-date model predictions and in Table 53 for the two-date predictions. Overall assessments of the adequacy of the predictions for each section (taking into consideration both the t-test results and the plots in Appendix G. and Appendix H) are provided in the columns headed “Overall Decision.”

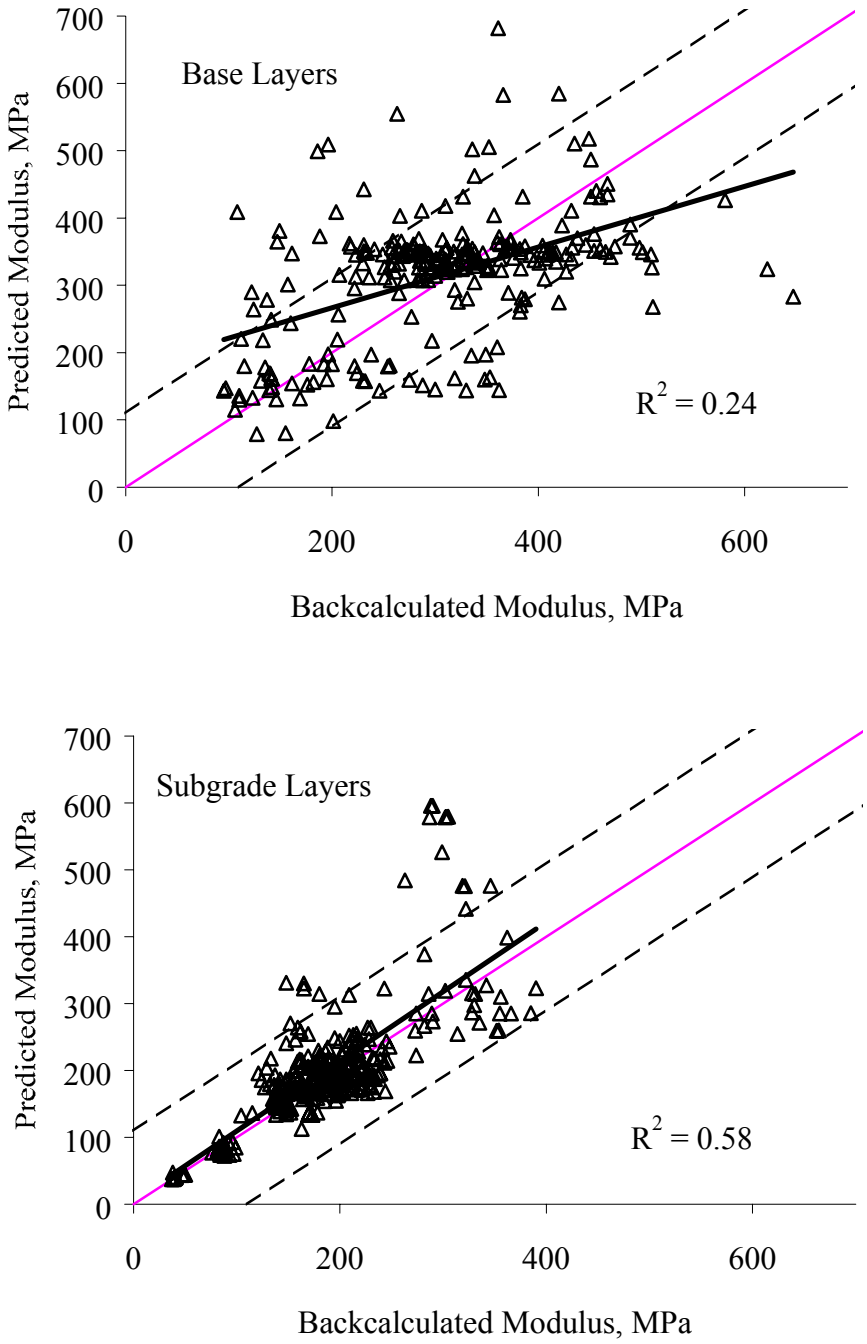

Figure 46. Backcalculated modulus versus section/layer-specific one-date predicted modulus

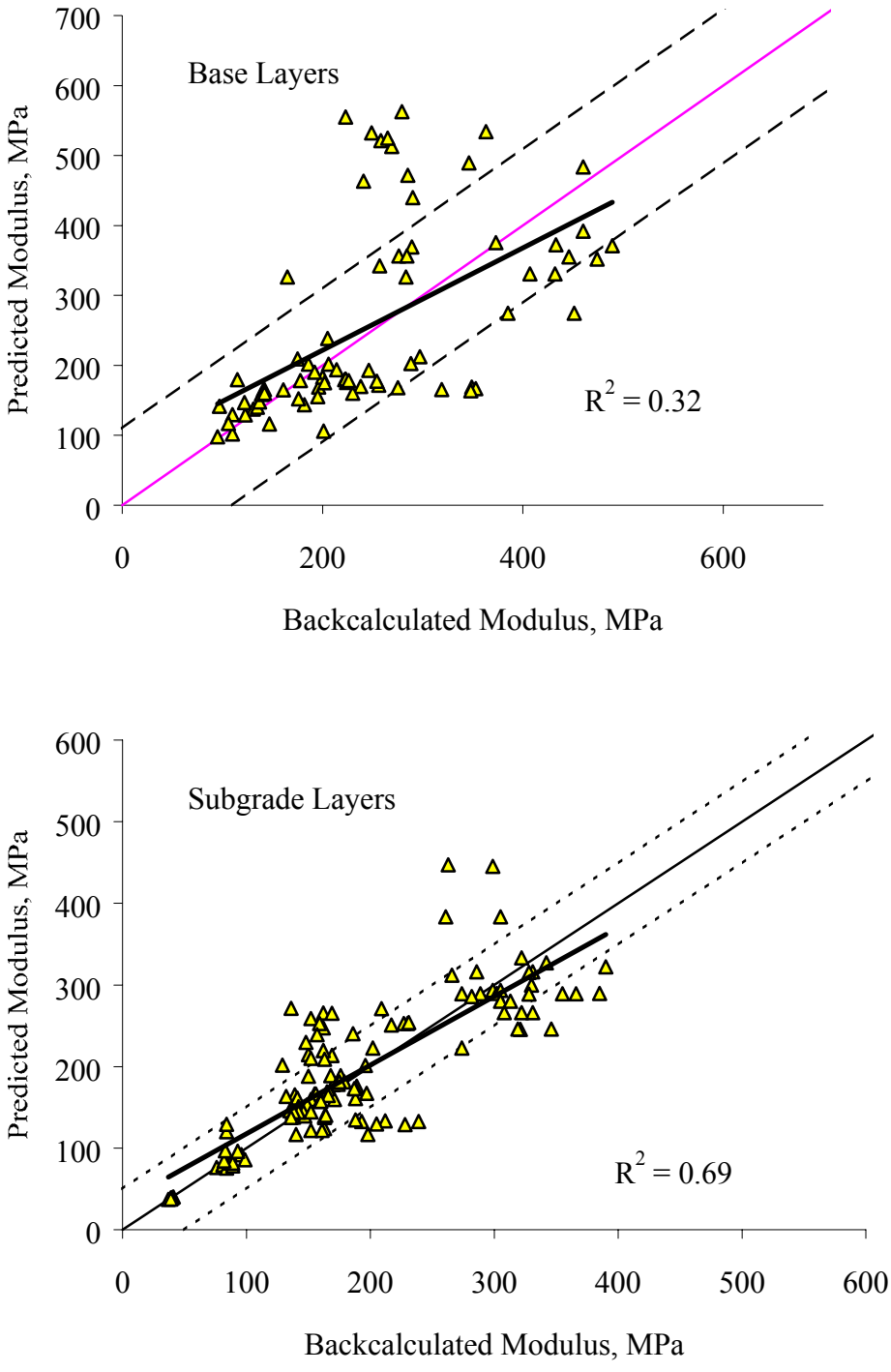

Figure 47. Backcalculated versus site/layer-specific two-date predicted modulus

For the one-date predictions, the null hypothesis was accepted for all layers for only one section, and for at least one layer at each of the remaining sections. For the two-date model predictions, the hypothesis of zero difference was accepted for all layers at two sections, no layers at one section, and one layer at a third section.

Table 52. Summary statistics and t-test results for section/layer-specific one-date model predictions

Section	Layer	Mean E	Mean $E_{predicted}$	Mean Difference	Std. Dev. of Diff.	n	t	t-Test Decision	Overall Decision
040113	2	139.6	205.60	−65.98	107.12	24	−3.02	R	U
040113	3	89.17	86.17	3.00	12.33	24	1.192	A	
040113	4	145.7	152.39	−6.68	7.64	24	−4.29	R	
091803	2	247	234	13.5	136.9	36	0.59	A	U
091803	3	173	218	−45.0	64.4	36	−4.19	R	
091803	4	319	408	−58.3	133.8	36	−2.61	R	
271018	2A	189	224	−34.9	104.3	9	−1.00	A	U
271018	3A	186	168	17.4	19.4	9	2.70	R	
271018	4A	45	43	2.0	4.7	9	1.27	A	
271018	2B	169	154	14.5	18.1	4	1.60	A	A (qualified)
271018	3B	172	176	−4.0	1.9	4	−4.28	R	
271018	4B	39	38	0.6	0.8	4	1.46	A	
481077	2	348.3	355.79	−7.50	93.16	173	−1.06	A	U
481077	3	192.2	196.03	−3.79	30.97	173	−1.61	A	

Only one set of the one-date model predictions is considered acceptable—predictions obtained for section 271018 with the "B" models. However, even that success cannot be considered complete, as the number of data sets for which successful predictions were achieved was very small.

The results obtained with the two-date models are slightly better, with acceptable results having been obtained for two of the four test sections. However, this success is again qualified by the small number of section 271018 test dates for which successful predictions were achieved. Overall, the results obtained with the limited data set models are not at all promising. However, because the scope of this trial was very limited, these findings should not be regarded as definitive.

Table 53. Summary statistics and t-test results for section/layer-specific two-date model predictions

Section	Layer	Mean E	Mean $E_{predicted}$	Mean Difference	Std. Dev. of Diff.	n	t	t-Test Decision	Overall Decision
040113	2	131.7	131.44	0.22	33.31	15	0.026	A	A
040113	3	86.2	89.85	−3.65	16.50	15	−0.86	A	
040113	4	148.9	144.78	4.08	12.99	15	1.218	A	
091803	2	230	195	35.8	79.4	30	2.47	R	U
091803	3	172	211	−39.2	51.2	30	−4.19	R	
091803	4	316	333	9.3	68.6	30	0.74	A	
271018	2	195	179	15.6	43.5	6	0.88	A	A (qualified)
271018	3	179	180	−1.1	7.1	6	−0.37	A	
271018	4	39	39	0.6	0.7	6	2.24	A	
481077	2	349.1	424.10	−75.02	159.08	25	−2.36	R	U
481077	3	175.3	157.90	17.38	40.55	25	2.143	R	

Results Obtained With Soil Class Models

The overall results obtained in the trial applications using soil class models are compared with the backcalculated moduli in Figure 48, and comparisons for individual test sections are provided in Appendix I. As before, the error limits about the line of equality represent twice the pooled within-day standard deviation for the layer type in question, as reported in Table 23. Overall, the soil class prediction results for the subgrade layers are very comparable to those obtained using the section-specific models, with an R^2 value for the backcalculated versus predicted modulus relationship of 0.86. The same cannot be said for the soil class model predictions for the subbase and subgrade layers, for which the overall backcalculated versus predicted R^2 values are 0.11 and 0.01, respectively.

Paired t-test results for the null hypothesis (the mean difference between the backcalculated and predicted moduli is zero) are presented in Table 54. The zero difference hypothesis was rejected for all layers at three sections, and accepted for all layers at no sections. The author's overall assessment of the success of the predictions for each section considering both t-test results and the plots in Appendix I are in the "Overall Decision" column.

In all, soil class model predictions were undertaken for seven sections. Considering both the distribution of the data points in the plots presented in Appendix I, and the paired t-test results for the null hypothesis, reasonable success in the prediction of subgrade modulus was achieved for four of the seven sections: 091803, 131031, 481077, and 871622. Soil class prediction of base layer modulus was less successful: acceptable overall results were not achieved for any section.

Table 54. Summary statistics and t-test results for soil class model predictions

Section	Layer	Mean E	Mean $E_{predicted}$	Mean Difference	Std. Dev. of Diff.	n	t	t-Test Decision	Overall Decision
040113	2	134	161	−26.9	69.9	15	−1.49	A	
040113	3	89	79	10.2	6.2	15	6.35	R	**U**
040113	4	148	110	38.0	11.3	15	12.98	R	
040114	2	257	125	131.2	23.5	4	11.16	R	
040114	3	224	370	−146.2	10.4	4	−28.1	R	U
040114	4	335	247	87.8	31.4	4	5.60	R	
091803	2	225	196	28.8	74.5	98	3.83	R	
091803	3	162	163	−1.1	35.7	98	−0.31	A	U
091803	4	296	297	1.1	35.7	98	0.31	A	
131031	2	482	329	152.4	154.1	47	6.78	R	
131031	3	133	128	5.0	24.6	47	1.39	A	U
131031	4	89	86	2.8	11.8	47	1.61	A	
231026	2	245	219	26.5	80.1	67	2.70	R	
231026	3	153	142	11.1	32.1	67	2.84	R	U
231026	4	478	457	21.9	78.4	67	2.28	R	
481077	2	356	177	178.4	81.3	259	35.32	R	U
481077	3	190	188	2.7	29.6	259	1.47	A	
871622	2	378	435	−57.0	78.4	53	−5.29	R	
871622	3	151	192	−40.8	27.4	53	−10.8	R	**U**
871622	4	223	234	−11.3	19.8	53	−4.16	R	

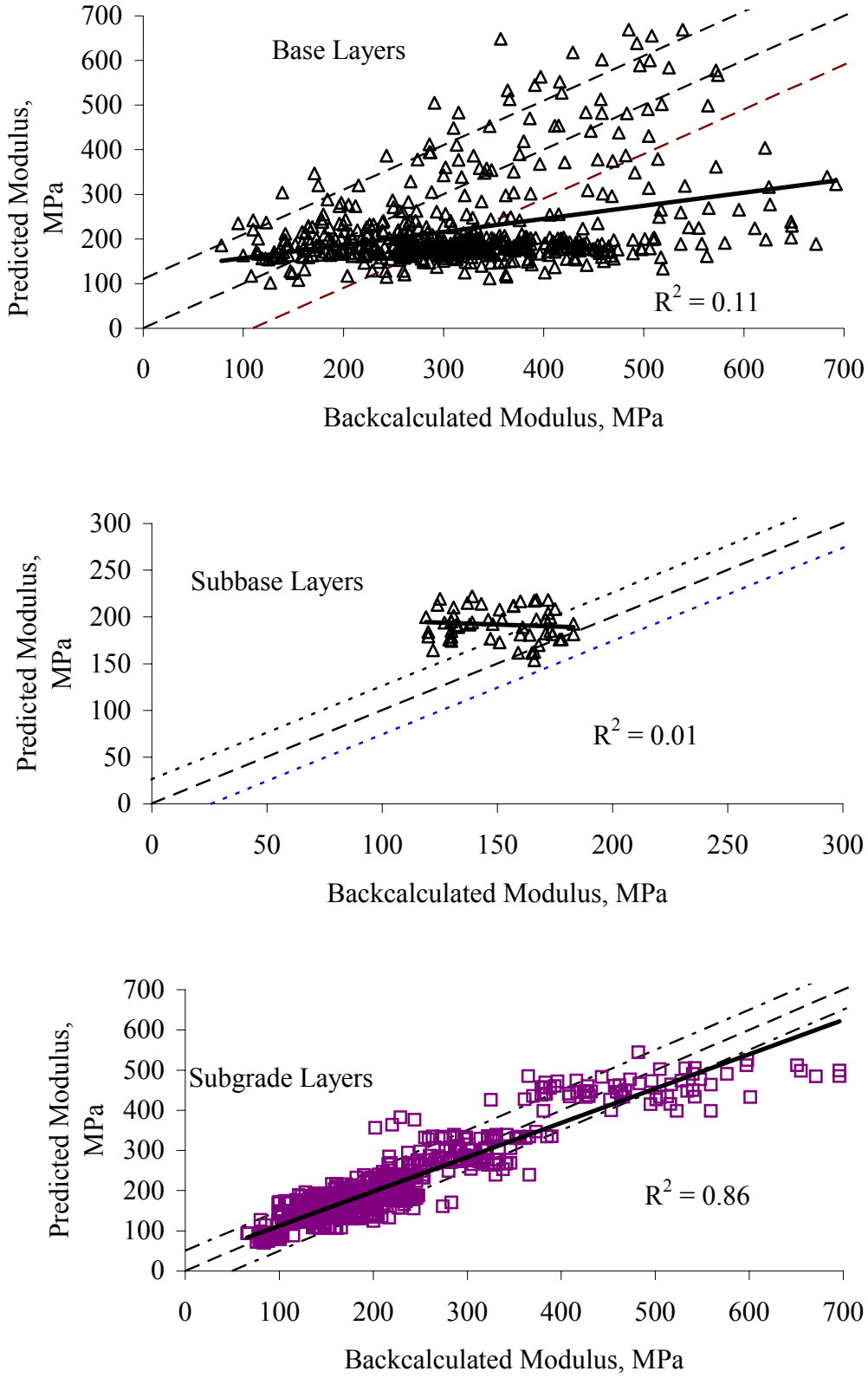

Figure 48. Backcalculated versus soil class predicted moduli—all sections

SUMMARY OBSERVATIONS

The trial applications presented in this chapter demonstrate that regression models for the prediction of backcalculated layer moduli can be used to estimate seasonal variations in the moduli of unbound pavement layers. However, deficiencies in the accuracy of the estimates (as compared to the actual backcalculated layer moduli) point to the need for further research to improve upon the results of this study. Factors known or believed to contribute to inaccurate predictions include:

- Deficiencies in the ability of many of the predictive models to explain the observed variation in backcalculated layer moduli. It may be possible to achieve some improvement in this regard by reducing the variability in backcalculated layer moduli through improvements in procedures for evaluating backcalculation results.

- Errors in the estimation of the AC layer moduli used in computing the stress states used in the predictions.

- Deficiencies of the iterative process used to estimate the stress states for the prediction dates.

Thus, potentially fruitful avenues for research include:

- Improvements in deflection testing and backcalculation technology to reduce the level of random variation in backcalculated layer moduli. In this regard, Model 2 (Equation 29) could be the basis for additional objective criteria for evaluating the plausibility of moduli backcalculated for varying overall stress conditions (encompassing FWD load level and temperature-induced variations in the stiffness of overlying layers) using linear layered-elastic theory. Such criteria are needed to aid engineers in distinguishing between backcalculation results that represent a good fit of the deflection basin, but are otherwise of limited value, and those that truly represent a reasonable characterization of the in situ properties of the pavement layers.

- Improvements in deflection testing and backcalculation technology to enable more correct consideration of the stress sensitivity of unbound materials in the backcalculation process itself. There is no doubt that inaccurate assumptions inherent in the application of linear layered-elastic theory to backcalculate and predict pavement layer moduli contribute to the deficiencies observed in the prediction results.

- Improvements in the approach to estimating the stress state to use in predictive models such as those developed in this study.

CHAPTER 7: CONCLUSIONS AND RECOMMENDATIONS

This research represents the first application of the data collected via the LTPP Seasonal Monitoring Program to the development of improved methods for estimating seasonal variations in backcalculated moduli for unbound pavement layers exclusive of frost effects. The approach taken was to build upon the foundation of the EICM by: (1) evaluating the moisture predictive capabilities of that model; (2) developing predictive equations for backcalculated pavement layer moduli; and (3) demonstrating how the resulting relationships might be applied in practice.

This investigation provided the impetus for developing EICM Version 2.6 by demonstrating the practical inadequacies of EICM Versions 2.0 and 2.1 when applied to the prediction of in situ moisture content, and then demonstrated that substantial improvement in the moisture predictive capability of the EICM had been achieved in Version 2.6. Second, the research identified fundamental discrepancies between the stress states used in laboratory resilient modulus testing and those computed using linear layered-elastic theory.

Detailed implications of these findings and other conclusions of lesser importance are presented below. The conclusions are followed by recommendations to address needs identified or reaffirmed through this study and to improve upon the results obtained.

CONCLUSIONS

The Enhanced Integrated Climatic Model

In the short term, the most important findings from this study are those related to the moisture prediction accuracy of the EICM, by virtue of their contribution to the development of the *2002 Guide for Design of New and Rehabilitated Pavement Structures* currently ongoing through NCHRP Project 1-37A. Key conclusions related to the EICM moisture prediction capabilities are as follows:

1. Application of EICM Version 2.0 with data commonly available to pavement engineers and assumed or model default values for key input parameters (e.g., the Gardener coefficients) yielded predicted moisture content profiles that were markedly different from the monitored data for two LTPP Seasonal Monitoring Program sites, one in Connecticut, the other in Minnesota. Volumetric moisture content differences of 20 percentage points or more were observed for some monitoring depths in the limited evaluation that was conducted. The EICM model revisions embodied in Version 2.1 were the direct result of this finding.

2. Application of EICM Version 2.1 with data commonly available to pavement engineers may yield poor predictions of in situ moisture contents. For the test sections and data sets considered in the evaluation of EICM Version 2.1, the R^2 values for the relationship between monitored and predicted moisture contents for base and subgrade

layers were only 0.01 and 0.30, respectively. Numerical differences between monitored and predicted volumetric moisture contents again exceeded 20 percentage points in some cases. The model revisions embodied in EICM Version 2.6 were the direct result of this finding.

3. Enhancements in EICM Version 2.6 have substantially improved the practical applicability of the model. When applied with data commonly available to pavement engineers, EICM Version 2.6 yielded predicted volumetric moisture contents that were within the estimated 95 percent confidence intervals for the monitored moisture data in most instances. The R^2 values for the relationship between monitored and predicted subgrade moisture contents for the base and subgrade layers for applications of EICM Version 2.6 were 0.71 and 0.51, respectively, a substantial improvement in predictive accuracy. Thus, application of EICM Version 2.6 with input data commonly available to pavement engineers can provide reasonable predictions of in situ moisture contents for unbound pavement layers.

4. Between-user differences in the application of the EICM may yield significant differences in the model output. In the limited evaluation of between-user differences, the observed mean difference in predicted volumetric moisture content for individual pavement layers (reported in Table 31) varied in the range of 0.1 to 11.1 percentage points, depending on the pavement section under consideration and the nature and extent of the between-user differences. The observed differences for 84 percent of the pavement layers considered were statistically significant at the 5 percent level of significance. Thus improved user guidance and other measures to ensure consistent and correct application of the EICM are needed.

Models for Prediction of Backcalculated Pavement Layer Moduli

1. Predictive models that are rational when evaluated in the context of laboratory resilient modulus test experience cannot be derived using layer moduli backcalculated using linear layered elastic theory and computed stress states. Factors that contribute to the observed inconsistencies include:

    a. The use of stress states computed for a single "representative" point for the entire layer when the location of a truly representative point is difficult to define. A single representative point is required in linear layered-elastic theory because each layer is assumed to be homogeneous, when the reality for a nonlinear unbound layer is that stresses, and thus stiffness, vary both vertically and horizontally through the layer.

    b. The fact that the computed radial stresses may increase or decrease as the applied FWD load increases, depending on the location of the point for which the stresses are computed.

c. The fact that the assumptions on which linear layered-elastic theory is based may yield negative (tensile) radial load stresses.

The net effect of these factors is that both the sign and the relative importance of the bulk and octahedral stress terms in the constitutive model $E/P_a = k_1\theta/P_a^{k2}(t/P_a+1)^{k3}$ often contradict those observed in the laboratory.

2. The preceding conclusion has several important implications for considering stress dependency in pavement modeling. First, application of laboratory-derived constitutive model coefficients in combination with stress parameters computed using linear layered-elastic theory may yield inaccurate stress-dependent modulus values by virtue of the discrepancies between the laboratory stress states and those computed using linear layered-elastic theory. Second, meaningful advances in the state of the art for backcalculation of pavement layer moduli cannot be achieved without addressing the limitations inherent in the use of linear layered-elastic theory to model structures composed of materials that are stress-dependent. Models that allow more realistic consideration of the stress-dependent nature of these materials are needed.

3. In many instances, variations in moisture content are not the most important driver of seasonal variations in backcalculated layer moduli for unbound, nonfrozen pavement layers. Evidence for this may be found in:

   a. The fact that the backcalculated layer moduli for all base layers, 82 percent of the subbase/upper subgrade (layer 3) layers, and 80 percent of the subgrade/lower subgrade (layer 4) layers were less strongly correlated with moisture than they were with one or more of the stress parameters considered.

   b. For some pavement layers (base and subgrade for section 481077 (Texas), base for section 131005 (Georgia), and base and subgrade for section 091803 (Connecticut) the observed correlation between mean layer moisture and backcalculated modulus is close to zero, indicating that there is little or no linear relationship between modulus and moisture for the unbound pavement layers represented. In contrast, relatively strong relationships between modulus and moisture are observed for other layers, such as the subgrade at section 131005 (Georgia), where the R^2 values varied in the range of 0.30 to 0.78, depending on layer (upper or lower subgrade) and FWD load level.

   c. The high degree of variability in the ratio $\Delta E/\Delta V_w$, as summarized in Table 37 (Chapter 3), suggests that other factors such as stress state and random errors in the backcalculated moduli confound the modulus-moisture relationship.

4. Given the current state of the art, the combined effects of stress and moisture on backcalculated pavement layer moduli may be modeled for practical purposes using the constitutive model form previously presented as Equation 31:

$$\text{Model 2B: } E/P_a = c_0 10^{(c1Vw/100 + (c2 + c2'Vw/100)\Theta Pa)}(t/P_a + 1)^{(c3+c3'Vw/100)} \qquad (43)$$

This conclusion applies only to moduli backcalculated using linear layered-elastic theory. Model coefficients derived using backcalculated layer moduli are not applicable to laboratory resilient modulus data. The applicability of the constitutive model form to laboratory resilient modulus test data has not been established. Soil class models based on Model 2B are presented in Table 43 (Chapter 5).

Variations in Backcalculated Moduli for Unbound Pavement Layers

Information about the extent of variation in backcalculated moduli exclusive of frost effects was presented in Table 21 through Table 26 of Chapter 3. Summary conclusions derived from this information are as follows.

1. The single point, within-day coefficient of variation for backcalculated moduli for unbound pavement layers may approach 40 percent, with values in the range of 5 to 20 percent being typical. Furthermore, the "conventional wisdom" that backcalculated moduli for deeper layers are less variable than those for the upper layers is supported by these findings. The pooled single-point within-day coefficient of variation for the base layers was 19 percent, while that for the subgrade layers was 11 percent.

2. The amplitude of seasonal variations in backcalculated layer moduli, exclusive of frost effects, ranges from less than 10 percent (typically for deeper subgrade layers) to more than 200 percent (typically for base layers). The amplitude of the variations (whether expressed on a percentage basis or absolute magnitude) is typically greatest for the base layers and least for the deepest layers.

Application of Research Results To Predict Moduli Backcalculated for Unbound Pavement Layers Using Linear Layered-Elastic Theory

In light of the low overall rate of success in predicting backcalculated layer moduli in the trial applications discussed in Chapter 6, particularly when using either limited data set or soil class models, the only well-founded conclusion that can be drawn is that further research is needed to develop: (1) procedures for backcalculation that rely on more accurate models of the pavement structure and material response; (2) better, broadly applicable predictive models; and (3) improved procedures for their application. Specific recommendations in this regard are provided in the next section.

RECOMMENDATIONS

This study has shed light on a number of issues warranting further investigation. While many are in no sense new, the findings presented earlier reinforce the need for further work. Specific recommendations are as follows.

The Enhanced Integrated Climatic Model

1. As noted in Chapter 4, the evaluation of the EICM conducted for this study was imperfect because the available data set did not include complete, section-specific values for all input parameters required by the EICM. Another limitation of the evaluation was the consideration of only one test section representing an arid climate. Further evaluation of the EICM moisture predictive capabilities is needed to: (1) more fully establish the sensitivity of the model to the input parameters; (2) confirm or refute the hypothesis that the poor results achieved for section 041024 (Arizona, see Figure 17) are attributable to incompatibility between the theory on which the EICM is based and the true mechanisms of soil moisture movement in arid climates. If possible, this work should be pursued using data sets that include all required input parameters for the test sections under consideration

2. Further enhancement to the EICM user interface is recommended to improve ease of use and reduce the potential for error arising from the need for manual manipulation of data to create input data sets. Automated entry (and interpolation) of initial temperature profiles would be particularly helpful.

3. The development of improved user documentation (relative to that available to the author when this work was initiated) is recommended. It is imperative that very specific guidance for the application of the model be provided to minimize the potential for incorrect application of the model and between-user differences. Issues that must be clearly addressed include the ramifications of using or not using input data that are recommended but not required, the selection of the initial conditions used in the moisture prediction (such as the need to avoid simulation starting dates that reflect frozen pavement conditions), and information on the required precision of the input parameters—e.g., how accurate does the depth to ground water need to be, and how does the answer vary with climatic conditions?

The State of the Art of Backcalculation of Pavement Layer Moduli

The stress-sensitive nature and lack of tensile strength in unbound pavement materials has long been recognized. The findings of this study reaffirm the importance of considering the stress sensitivity of unbound materials when analyzing pavement structures. It is therefore recommended that improved methods of backcalculation be developed that provide for more correct consideration of stress sensitivity of pavement layer materials.

Consideration of Stress Dependency in Pavement Modeling

Despite its inadequacies, it is likely that practicing pavement engineers will continue to use linear layered elastic theory in pavement analysis for some time to come. For this reason, the applicability of laboratory-derived resilient modulus nonlinear constitutive model coefficients to pavement analysis based on linear layered-elastic theory should be studied further to fully assess the magnitude and implications of the observed discrepancies between the computed stress states and those used in current laboratory test protocols (see Figure 39 through Figure 41 in Chapter 5).

LTPP Data Used in This Investigation

1. Supplementary data collection at all LTPP seasonal monitoring test sections should be undertaken to provide an expanded data set for verification of the TDR-based moisture data and to meet other data needs. (This work is in progress via NCHRP 9-23.) The collected data should be incorporated into the LTPP database.

2. A comprehensive review of all LTPP backcalculation results should be undertaken to: (1) identify those data sets for which the backcalculation conducted to date needs to be revisited, such that the data stored in and disseminated from the LTPP database are of the highest possible quality; and (2) provide the basis to advance the state of the art relative to the evaluation of backcalculation results in general. Use of Model 3 ($E/P_a = k_1 10^{k2\theta/Pa}(\tau/P_a+1)^{k3}$) as the basis for additional objective evaluation criteria should be considered.

APPENDIX A: VARIATION IN TDR MOISTURE DATA

Table 55. Pooled within-day standard deviation of volumetric moisture from individual TDR probes (percent)

	TDR Probe (Increasing Number Corresponds to Increasing Depth)									
Section	**1**	**2**	**3**	**4**	**5**	**6**	**7**	**8**	**9**	**10**
040113	0.14	0.66	0.89	0.87	1.70	1.36	1.33	3.03	1.29	1.66
040114	0.67	0.36	0.03	0.51	0.39	0.68	0.52	0.73	1.00	1.54
041024	1.52	0.83	0.24	0.42	0.44	0.28	1.11	0.79	1.20	1.11
081053	0.74	2.13	0.22	2.14	1.36	0.76	0.62	0.50	–	–
091803	0.82	0.76	1.72	1.43	0.55	0.82	0.19	0.16	0.68	0.12
131005	0.52	0.50	0.82	0.31	0.44	0.41	1.28	0.71	0.20	0.42
131031	0.95	0.19	1.06	0.72	0.27	0.51	0.83	0.32	0.33	0.23
161010	0.16	0.66	0.40	1.03	1.44	0.45	0.52	0.46	0.49	3.40
231026	0.87	0.61	0.55	0.37	0.62	0.21	0.59	0.72	0.75	0.21
241634	0.04	0.05	0.07	0.24	0.04	1.11	0.03	0.05	0.04	0.07
251002	0.48	0.73	0.93	0.80	0.39	0.69	0.76	2.08	2.22	1.86
271018	0.31	0.83	0.49	0.43	0.40	1.05	0.43	1.13	1.41	0.50
271028	0.26	0.36	0.49	0.49	0.56	0.31	0.23	1.09	1.38	1.20
276251	0.52	0.49	0.38	1.30	0.69	0.60	0.72	0.15	0.14	0.83
308129	2.41	0.68	1.20	3.26	0.46	0.65	0.57	0.80	0.61	0.59
331001	1.43	1.65	1.13	0.58	0.21	1.86	0.30	0.35	1.00	2.16
351112	0.23	0.04	0.05	0.04	0.64	0.64	0.31	0.68	0.48	–
481068	0.14	8.07	15.11	4.44	15.68	14.68	15.14	0.60	0.78	13.07
481077	0.30	0.34	0.19	0.28	0.20	0.34	0.25	0.37	0.17	0.15
491001	0.50	0.06	0.14	0.60	0.30	0.57	0.75	0.87	1.16	0.44
501002	0.87	0.74	0.77	1.11	1.10	2.33	1.90	1.76	0.58	0.30
561007	0.52	0.40	0.55	0.30	0.40	0.21	0.74	1.12	1.07	1.87
831801	0.27	0.20	0.16	0.16	0.28	0.27	0.70	1.52	1.08	0.51
871622	0.54	0.32	0.37	0.20	0.35	0.64	0.32	0.31	2.17	0.29
906405	0.26	0.34	0.62	0.74	0.30	0.34	0.24	0.29	0.50	0.18

Table 56. Number of test dates considered in computation of pooled standard deviation for individual TDR moisture probes

Section	TDR Probe (Increasing Number Corresponds to Increasing Depth)									
	1	2	3	4	5	6	7	8	9	10
040113	12	15	15	15	15	15	15	12	13	13
040114	10	10	10	10	10	10	10	8	8	8
041024	15	15	15	15	15	15	15	15	14	15
081053	10	19	3	5	8	6	15	15	–	–
091803	31	30	30	30	30	30	29	27	27	28
131005	24	24	19	23	23	23	22	24	24	24
131031	8	8	14	19	14	17	9	9	19	19
161010	28	27	28	28	29	28	28	28	29	25
231026	34	29	34	19	33	31	32	30	23	33
241634	9	9	9	9	4	9	9	9	5	9
251002	31	31	29	30	32	32	29	25	28	28
271018	25	18	26	19	18	14	23	12	26	29
271028	22	22	23	22	23	25	25	23	24	25
276251	28	30	30	30	30	30	30	30	30	30
308129	15	21	28	11	27	18	30	24	11	23
331001	25	25	25	25	25	15	23	20	14	17
351112	18	18	18	18	20	20	18	15	2	–
481068	18	6	2	1	2	2	2	1	1	2
481077	29	27	26	26	25	26	26	26	26	26
491001	16	16	16	16	12	12	12	14	17	17
501002	29	29	29	26	7	20	25	26	27	11
561007	5	5	5	5	5	5	5	5	5	5
831801	26	27	26	26	26	19	24	24	25	25
871622	21	22	22	22	21	21	22	20	19	17
906405	27	28	28	28	27	28	28	27	27	27

Table 57. Mean number of moisture observations per day considered in computation of within-day standard deviation

Section	TDR Probe (Increasing Number Corresponds to Increasing Depth)									
	1	2	3	4	5	6	7	8	9	10
040113	2.3	2.3	2.3	2.3	2.3	2.3	2.3	2.4	2.3	2.3
040114	2.3	2.3	2.3	2.3	2.3	2.3	2.3	2.3	2.3	2.3
041024	2.5	2.5	2.5	2.5	2.5	2.5	2.5	2.5	2.6	2.4
081053	2.1	2.2	2.0	2.2	2.1	2.2	2.3	2.3	–	–
091803	2.1	2.1	2.1	2.1	2.1	2.1	2.1	2.1	2.1	2.1
131005	2.7	2.7	2.6	2.7	2.7	2.7	2.7	2.6	2.7	2.7
131031	2.9	2.9	2.6	2.6	2.6	2.7	2.6	2.8	2.6	2.7
161010	2.3	2.3	2.3	2.3	2.3	2.3	2.3	2.3	2.2	2.3
231026	2.0	2.0	2.0	2.1	2.0	2.0	2.0	2.0	2.0	2.0
241634	2.0	2.0	2.0	2.0	2.0	2.0	2.0	2.0	2.0	2.0
251002	2.0	2.0	2.0	2.0	2.0	2.0	2.0	2.0	2.0	2.0
271018	2.2	2.3	2.2	2.3	2.3	2.4	2.2	2.1	2.2	2.2
271028	2.3	2.3	2.3	2.3	2.3	2.2	2.2	2.3	2.3	2.2
276251	2.2	2.2	2.2	2.2	2.2	2.2	2.2	2.2	2.2	2.2
308129	2.3	2.5	2.4	2.5	2.4	2.4	2.4	2.3	2.5	2.3
331001	2.0	2.1	2.1	2.0	2.0	2.1	2.0	2.1	2.1	2.1
351112	2.7	2.7	2.7	2.7	2.6	2.6	2.5	2.7	3.0	–
481068	2.7	2.7	2.5	3.0	2.5	2.5	2.5	3.0	3.0	2.5
481077	2.6	2.7	2.7	2.7	2.7	2.7	2.6	2.7	2.7	2.7
491001	2.4	2.4	2.4	2.4	2.4	2.4	2.4	2.3	2.4	2.4
501002	2.0	2.0	2.0	2.0	2.0	2.1	2.0	2.0	2.0	2.0
561007	2.2	2.2	2.2	2.2	2.2	2.2	2.2	2.2	2.2	2.2
831801	2.2	2.2	2.2	2.2	2.2	2.2	2.2	2.1	2.2	2.2
871622	2.0	2.0	2.0	2.0	2.0	2.0	2.0	2.0	2.0	2.0
906405	2.2	2.2	2.2	2.2	2.2	2.2	2.2	2.2	2.2	2.2

Table 58. Pooled within-day standard deviation divided by maximum Model 1 error

Section	TDR Probe (Increasing Number Corresponds to Increasing Depth)									
	1	2	3	4	5	6	7	8	9	10
040113	0.0	0.1	0.2	0.2	0.3	0.3	0.2	0.6	0.2	0.3
040114	0.1	0.1	0.0	0.1	0.1	0.1	0.1	0.1	0.2	0.3
041024	0.3	0.2	0.0	0.1	0.1	0.1	0.2	0.1	0.2	0.2
081053	0.1	0.4	0.0	0.4	0.3	0.1	0.1	0.1	–	–
091803	0.2	0.1	0.3	0.3	0.1	0.2	0.0	0.0	0.1	0.0
131005	0.1	0.1	0.2	0.1	0.1	0.1	0.2	0.1	0.0	0.1
131031	0.2	0.0	0.2	0.1	0.1	0.1	0.2	0.1	0.1	0.0
161010	0.0	0.1	0.1	0.2	0.3	0.1	0.1	0.1	0.1	0.6
231026	0.2	0.1	0.1	0.1	0.1	0.0	0.1	0.1	0.1	0.0
241634	0.0	0.0	0.0	0.0	0.0	0.2	0.0	0.0	0.0	0.0
251002	0.1	0.1	0.2	0.1	0.1	0.1	0.1	0.4	0.4	0.3
271018	0.1	0.2	0.1	0.1	0.1	0.2	0.1	0.2	0.3	0.1
271028	0.0	0.1	0.1	0.1	0.1	0.1	0.0	0.2	0.3	0.2
276251	0.1	0.1	0.1	0.2	0.1	0.1	0.1	0.0	0.0	0.2
308129	0.4	0.1	0.2	0.6	0.1	0.1	0.1	0.1	0.1	0.1
331001	0.3	0.3	0.2	0.1	0.0	0.3	0.1	0.1	0.2	0.4
351112	0.0	0.0	0.0	0.0	0.1	0.1	0.1	0.1	0.1	–
481068	0.0	1.5	2.8	0.8	2.9	2.7	2.8	0.1	0.1	2.4
481077	0.1	0.1	0.0	0.1	0.0	0.1	0.0	0.1	0.0	0.0
491001	0.1	0.0	0.0	0.1	0.1	0.1	0.1	0.2	0.2	0.1
501002	0.2	0.1	0.1	0.2	0.2	0.4	0.4	0.3	0.1	0.1
561007	0.1	0.1	0.1	0.1	0.1	0.0	0.1	0.2	0.2	0.3
831801	0.1	0.0	0.0	0.0	0.1	0.1	0.1	0.3	0.2	0.1
871622	0.1	0.1	0.1	0.0	0.1	0.1	0.1	0.1	0.4	0.1
906405	0.0	0.1	0.1	0.1	0.1	0.1	0.0	0.1	0.1	0.0

Note: Values greater than 0.5 indicate that the within-day standard deviation is greater than the estimated standard error of the prediction. Ratios greater than 0.5 are denoted in the table by gray shading.

Table 59. Data sets for which individual within-day standard deviations exceed three times the overall pooled value

Section	TDR Number	Date	Volumetric Moisture	
			Mean	Std. Deviation
040113	5	Wednesday, August 14, 1996	8.43	3.86
040113	5	Tuesday, November 17, 1998	7.01	3.73
040113	7	Wednesday, August 14, 1996	8.73	3.61
040113	8	Tuesday, November 17, 1998	6.73	5.35
040113	8	Wednesday, October 11, 1995	20.63	6.18
040113	10	Wednesday, August 14, 1996	9.26	4.10
081053	2	Thursday, February 13, 1997	7.95	5.02
081053	2	Friday, September 26, 1997	6.99	5.10
081053	4	Monday, March 14, 1994	17.43	3.58
081053	5	Thursday, June 16, 1994	21.69	4.09
091803	1	Thursday, March 10, 1994	23.30	4.67
091803	2	Thursday, March 10, 1994	24.05	3.61
091803	3	Thursday, February 17, 1994	14.15	7.00
091803	3	Thursday, March 10, 1994	25.91	6.94
091803	4	Thursday, February 17, 1994	13.85	7.42
091803	6	Thursday, March 10, 1994	20.53	4.71
131005	7	Thursday, November 30, 1995	26.57	5.08
161010	5	Monday, May 22, 1995	10.40	8.34
161010	10	Thursday, November 17, 1994	34.87	7.16
161010	10	Tuesday, December 13, 1994	35.00	6.93
161010	10	Tuesday, September 27, 1994	35.07	7.59
161010	10	Wednesday, November 2, 1994	33.00	7.64
251002	4	Wednesday, October 09, 1996	8.75	3.75
251002	8	Wednesday, February 1, 1995	31.95	10.11
251002	9	Wednesday, February 1, 1995	25.15	7.85
251002	10	Wednesday, August 24, 1994	6.40	3.96
251002	10	Wednesday, July 27, 1994	6.70	4.24
251002	10	Wednesday, October 9, 1996	5.80	4.10
251002	10	Wednesday, December 4, 1996	7.50	3.96
276251	4	Wednesday, April 9, 1997	6.70	4.24
276251	4	Wednesday, May 7, 1997	5.85	4.60
276251	4	Wednesday, April 23, 1997	6.15	4.45
276251	5	Wednesday, April 23, 1997	6.25	3.75

Table 59. Data sets for which individual within-day standard deviations exceed three times the overall pooled value, continued

Section	TDR Number	Date	Volumetric Moisture	
			Mean	Std. Deviation
276251	7	Wednesday, April 9, 1997	7.20	3.68
271028	8	Thursday, April 10, 1997	8.30	4.24
271028	9	Tuesday, June 14, 1994	6.35	4.03
271018	9	Monday, September 08, 1997	17.75	6.15
308129	1	Wednesday, October 1, 1997	10.13	6.69
308129	1	Wednesday, October 20, 1993	9.55	4.17
308129	1	Wednesday, June 18, 1997	9.12	4.98
308129	3	Wednesday, October 01, 1997	10.72	3.85
308129	3	Thursday, January 23, 1997	4.70	4.67
308129	4	Wednesday, October 01, 1997	15.02	4.84
308129	4	Wednesday, June 18, 1997	14.76	8.51
308129	8	Monday, August 11, 1997	17.25	3.89
331001	1	Monday, March 21, 1994	16.53	4.19
331001	2	Monday, March 21, 1994	17.45	4.63
331001	6	Monday, March 21, 1994	20.77	5.06
331001	10	Tuesday, January 24, 1995	36.90	7.92
481068	2	Thursday, August 21, 1997	20.95	25.53
481068	3	Thursday, August 21, 1997	21.30	26.16
481068	4	Wednesday, January 12, 1994	46.73	4.44
481068	5	Thursday, August 21, 1997	22.40	27.15
481068	6	Thursday, August 21, 1997	20.70	25.31
481068	7	Wednesday, January 12, 1994	47.57	4.43
481068	7	Thursday, August 21, 1997	20.90	25.46
481068	10	Thursday, August 21, 1997	21.70	22.63
501002	1	Wednesday, May 25, 1994	10.20	3.96
501002	4	Monday, December 20, 1993	16.49	4.32
501002	6	Wednesday, April 13, 1994	32.95	6.98
501002	7	Wednesday, April 13, 1994	31.87	6.41
501002	8	Wednesday, April 13, 1994	31.69	6.09
831801	8	Wednesday, February 15, 1995	18.40	5.94
831801	9	Wednesday, February 15, 1995	23.00	3.68
871622	9	Thursday, September 25, 1997	36.55	9.26
906405	4	Wednesday, October 6, 1993	8.26	3.75

APPENDIX B: INPUT DATA FOR THE ENHANCED INTEGRATED CLIMATIC MODEL

Table 60. Input data and sources for the EICM Versions 2.0 and 2.1 for the Connecticut (091803) and Minnesota (271018) sections

Variable	CT (091803)	MN (271018)	Remarks/Notes
Climatic region	I-A	II-A	
Weather station	User-defined	User-defined	
Year	1994	1993	
First month	6	9	
First day	30	23	
Length of analysis period (days)	360	365	
Time increment for output (hrs)	6	6	
Time increment for calculation (hrs)	0.01	0.01	
Latitude	41°23'41.5"	46°1'32.7"	LTPP database table INV_ID
Daily max/min temperatures	Site-specific data from LTPP database table SMP_ATEMP_RAIN_DAY		
Daily rainfall			
Daily windspeed	Boston	Average for region II-A	Default weather station data
Daily percent sunshine	Boston	Average for region II-A	
Daily water table depth	Range: 1.33-3.23 m	Range: 1.28-2.27 m	Site-specific data from LTPP database table SMP_WATERTAB_DEPTH_MAX
Modifier of overburden pressure	0.5	0.5	Default

Table 60. Input data and sources for the EICM Versions 2.0 and 2.1 for the Connecticut (091803) and Minnesota (271018) sections, continued

Variable	CT (091803)	MN (271018)	Remarks/Notes
Emissivity factor	0.93	0.93	Default
Surface short-wave absorptivity	0.85	0.85	Default
Maximum convection coefficient	44.7	44.7	Default
Coefficient of unsaturated permeability	1	1	Default
Time of day when max and min temperatures occur	Max: 13:29 Min: 5:43	Max: 14:09 Min: 6:25	Site averages derived from LTPP database table SMP_ATEMP_RAIN_DAY
Limits of freezing range °C	0/-1	0/-1	Default
Linear length of cracks/joints one side pavement (m)	94	648	Derived from LTPP database table MON_DIS_AC_REV
Total survey length (m)	152.4 m	152.4 m	Standard LTPP test section length
Base %fines	6	7.5	Derived from LTPP database tables TST_SS04_UG08, TST_SS01_UG01_UG02, TST_SS02_UG03, and TST_UG04_SS03. Data for sample location closest to instrumentation used where available.
Base % gravel	60	45	
Base % sand	34	47.5	
Base fines type	Silt	Silt	
One side base width (m)	4.57	5.18	Computed from data in LTPP database tables INV_GENERAL and INV_SHOULDER
Slope ratio/base tangent	1.5	1.5	Default
Internal boundary condition	Suction	Suction	Based on data in LTPP database table SMP_WATERTAB_ DEPTH_MAN

Table 60. Input data and sources for the EICM Versions 2.0 and 2.1 for the Connecticut (091803) and Minnesota (271018) sections, continued

Variable	CT (091803)	MN (271018)	Remarks/Notes
Emissivity factor	0.93	0.93	Default
Evaluation Period (years)	10	10	Default
Power of recurrence interval	0.25	0.25	Default
Constant K	0.3	0.3	Default
Power of rainfall duration	0.75	0.75	Default
Shape constant	1.65	1.65	Default
Layer 1 material	AC	AC	LTPP database table TST_L05A
Layer 2 material	A-1-a	A-1-b	LTPP database table TST_SS04_UG08 or derived from TST_SS01_UG01_UG_2 AND TST_UG04_SS03. Data for sample location closest to instrumentation used where available.91803 LAYER 3 from Klemunes[81]
Layer 3 material	A-2-4	A-3	
Asphalt surface thickness (m)	0.18	0.11	LTPP database table TST_L05A. Data for sample location closest to instrumentation
Number of elements	6	3	
Coarse aggregate content	80%	80%	
Air content	5.4	4.3	LTPP database table INV_PMA_ORIG_MIX
Gravimetric water content	2	2	
M_r vs. T	-4.1, 214643 11.8, 97252 23.4, 44203	-16.3, 153462 2.2, 78337 19.6, 63883	Backcalculation results
Thermal conductivity	8.94	8.94	Default
Heat capacity	0.22	0.22	Default

Table 60. Input data and sources for the EICM Versions 2.0 and 2.1 for the Connecticut (091803) and Minnesota (271018) sections, continued

Variable	CT (091803)	MN (271018)	Remarks/Notes
Emissivity factor	0.93	0.93	Default
Total unit weight (gm/cm^3)	2.494	2.371	Derived from LTPP database table TST_AC02
Layer thickness (m)	0.37 1.45	0.10 2.25	LTPP database table TST_L05A
Number of elements	16 58	10 60	
AASHTO classification	A-1-a A-2-4	A-1-b A-3	LTPP database table TST_SS04_UG08 or derived from TST_SS01_UG01_UG_2 AND TST_UG04_SS03. Data for sample location closest to instrumentation used where available.91803 LAYER 3 from Klemunes[81]
Porosity	0.33 0.37	0.23 0.31	Inferred from moisture and density data
Dry unit weight (gm/cm^3)	2.260 1.64	2.034 1.829	LTPP database table TST_ISD_MOIST, 91803 A-2-4 table INV_SUBGRADE
Saturated permeability (cm/hr)	6.096 6.096	6.096 1.524	Default
Dry thermal conductivity	4.47 4.023	4.47 5.066	Default
Dry heat capacity	0.17 0.17	0.17 0.2	Default
Volume compressibility	0.1 1.0	0.1 0.5	Default
Gardner's SWCC parameter AWL	0.6 0.4	0.6 0.02	Default
XWL	0.3 0.9	0.3 0.8	Default
Garner's permeability parameter AKL	1e-2 1e-4	1e-2 4e-4	Default
XKL	2.6 3.5	2.6 2.9	Default
Initial pore pressure profile	Computed from depth to water table in LTPP Database table SMP_WATERTAB_DEPTH_MAN		

Table 60. Input data and sources for the EICM Versions 2.0 and 2.1 for the Connecticut (091803) and Minnesota (271018) sections, continued

Variable	CT (091803)	MN (271018)	Remarks/Notes
Emissivity factor	0.93	0.93	Default
Initial temperature profile	Derived from LTPP database table SMP_MRCTEMP_AUTO_DAY_STAT (interpolation required)		
Initial water content profile	LTPP database table SMP_TDR_AUTO_MOISTURE; number of elements in each layer selected such that a node is close to each TDR probe depth		

Table 61. Input data and sources for EICM Version 2.1 for the Maine (231026), New Hampshire (331001), Vermont (501002), and Manitoba (831801) sections

Variable	MA (231026)	NH (331001)	VT (501002)	MB (831801)	Remarks/Notes
Integrated Model Initialization					
Climatic region	I-A	I-A	I-A	II-A or III-A	
Weather station	User-defined	User-defined	User-defined	User-defined	
Year	1994	1994	1994	1994	
First month	6	6	7	2	
First day	20	23	20	14	
Length of analysis period (days)	365	365	365	365	
Time increment for output (hrs)	6	6	6	6	
Time increment for calculation (hrs)	0.01	0.01	0.01	0.01	
Latitude	44°34’ 27.2”	43°13’ 20.1”	44°7’ 10.4”	49°46’ 9.6”	LTPP database table INV_ID
Climate/Boundary Conditions					
Daily max/min temperatures	Site specific data from LTPP database table SMP_ATEMP_RAIN_DAY				
Daily rainfall					
Daily windspeed	Boston	Boston	Boston	Fargo	Default weather station data
Daily percent sunshine	Boston	Boston	Boston	Fargo	Default weather station data
Daily water table depth (m)	(Range: 1.67 to 3.92)	(Range: 3.80 to 4.11)	(Range: 0.78 to 1.44)	(Range: 1.64 to 3.30)	Site-specific data from LTPP database table SMP_WATERTAB_DEPTH_MAX
Thermal Properties					
Time of day when max and min temperatures occur	Max: 1:55 p.m. Min: 5:12 a.m.	Max: 2:07 p.m. Min: 5:49 a.m.	Max: 1:13 p.m. Min: 6:12 a.m.	Max: 2:29 p.m. Min: 8:48 a.m.	Site averages derived from LTPP database table SMP_ATEMP_RAIN_DAY

Table 61. Input data and sources for EICM Version 2.1 for the Maine (231026), New Hampshire (331001), Vermont (501002), and Manitoba (831801) sections, continued

Variable	MA (231026)	NH (331001)	VT (501002)	MB (831801)	Remarks/Notes
Modifier of overburden pressure	0.5	0.5	0.5	0.5	Default
Emissivity factor	0.9	0.9	0.9	0.9	Default
Surface short wave absorptivity	0.85	0.85	0.85	0.85	Default
Maximum convection coefficient	44.7	44.7	44.7	44.7	Default
Coefficient of variation of unsaturated permeability	1	1	1	1	Default
Limits of freezing range (°C)	0/-1	0/-1	0/-1	0/-1	Default
Linear length of cracks/joints one side of pavement (m)	12	133	125	108	Derived from LTPP database table MON_DIS_AC_REV
Total survey length (m)	152.4	152.4	152.4	152.4	Standard LTPP test section length
Base % fines	4	4.5	3.3	10.9	Derived from LTPP database tables TST_SS04_UG08, TST_SS01_UG01_UG02, TST_SS02_UG03, and TST_UG04_SS03.
Base % gravel	73.7	62.9	89.9	52	
Base % sand	22.3	32.6	6.8	37.1	
Base fines type	Silt	Silt	Silt	Silt	

Table 61. Input data and sources for EICM Version 2.1 for the Maine (231026), New Hampshire (331001), Vermont (501002), and Manitoba (831801) sections, continued

Variable	MA (231026)	NH (331001)	VT (501002)	MB (831801)	Remarks/Notes
One side base width (m)	6.71	5.79	3.35	3.66	Computed from data in LTPP database tables INV_GENERAL and INV_SHOULDER
Slope ratio/base tangent	1.5	1.5	1.5	1.5	Default
Internal boundary condition	Suction	Suction	Suction	Suction	Based on data in LTPP database table SMP_WATERTAB_DEPTH_MAN
Evaluation period	10	10	10	10	Default
Constant K	0.3	0.3	0.3	0.3	Default
Power of recurrence interval	0.25	0.25	0.25	0.25	Default
Power of rainfall duration	0.75	0.75	0.75	0.75	Default
Shape constant	1.65	1.65	1.65	1.65	Default
Layer 1 material	AC	AC	AC	AC	LTPP database table TST_L05A
Unbound layer materials, in order from top (base) to bottom (subgrade)	A-1-a A-2-4	A-1-a A-1-b A-2-4	A-1-a A-1-a	A-1-a A-2-6 A-2-4	LTPP database table TST_SS04_UG08 or derived from TST_SS01_UG01_UG_2 and TST_UG04_SS03
Layer thickness (in order, top to bottom)	0.163 0.49 2.24	0.216 0.49 0.37 1.43	0.224 0.70 1.58	0.11 0.15 0.31 1.99	LTPP database table TST_L05A

Table 61. Input data and sources for EICM Version 2.1 for the Maine (231026), New Hampshire (331001), Vermont (501002), and Manitoba (831801) sections, continued

Variable	MA (231026)	NH (331001)	VT (501002)	MB (831801)	Remarks/Notes
Number of elements per layer (in order, top to bottom)	1 10 58	1 20 27 28	1 24 64	1 5 16 40	Selected to optimize proximity to TDR probe depths
Asphalt surface thickness (cm)	16.3	21.6	22.4	11.3	LTPP database table TST_L05A
Number of elements	1	1	1	1	
Layer porosity	0.29 0.37	0.22 0.24 0.43	0.29 0.46	0.22 0.21 0.46	Inferred from maximum observed volumetric moisture for layer (LTPP database table SMP_TDR_AUTO_MOISTURE
Dry unit weight (gm/cm^3)	2.27 1.96	2.10 2.15 1.86	2.09 1.76	2.08 1.71 2.13	Section 501002: LTPP database table TST_ISD_MOIST; sections 331001 and 831801: SMP installation reports
Saturated permeability (cm/hr)	60 15.24	0.2 0.2 0.5	0.2 0.2	0.2 0.2 0.5	Default
Dry thermal conductivity	4.47 4.023	0.3 0.3 0.27	0.3 0.3	0.3 0.3 0.27	Default
Dry heat capacity	0.17 0.17	0.17 0.17 0.17	0.17 0.17	0.17 0.17 0.17	Default
Volume capacity	0.10 0.3	0.1 0.1 0.3	0.10 0.10	0.1 0.1 0.3	Default

Table 61. Input data and sources for EICM Version 2.1 for the Maine (231026), New Hampshire (331001), Vermont (501002), and Manitoba (831801) sections, continued

Variable	MA (231026)	NH (331001)	VT (501002)	MB (831801)	Remarks/Notes
AWL (moisture)	0.6	0.6 0.6 0.4	0.6 0.6	0.6 0.6 0.4	Default
XWL	0.3	0.3 0.3 0.9	0.3 0.3	0.3 0.3 0.9	Default
AKL (permeability)	0.01	0.01 0.01 1e-4	0.01 0.01	0.01 0.01 1e-4	Default
XKL	2	2 2 3.5	2 2	2 2 3.5	Default
Initial temperature profile	Derived from LTPP database table SMP_MRCTEMP_AUTO_DAY_STAT (interpolation required)				
Initial water content profile	LTPP database table SMP_TDR_AUTO_MOISTURE; Number of elements in each layer selected such that a node is close to each TDR probe depth				
Initial temperature profile	Derived from LTPP database table SMP_MRCTEMP_AUTO_DAY_STAT (interpolation required)				
Initial water content profile	LTPP database table SMP_TDR_AUTO_MOISTURE; number of elements in each layer selected such that a node is close to each TDR probe depth				

Table 62. Input data and sources for EICM Version 2.6 for the Arizona (041024), Colorado (081053), Connecticut (091803), and Georgia (131005) sections

Variable	Arizona (041024)	Colorado (081053)	Connecticut (091803)	Georgia (131005)	Remarks /Notes
Climatic region	III-B	III-A	I-A	I-C	
Weather station	User-defined	User-defined	User-defined	User-defined	
Year	1995	1993	1994	1995	
First month	11	10	6	9	
First day	9	15	30	20	
Length of analysis period (days)	365	365	360	365	
Time increment for output (hrs)	6	6	6	6	
Time increment for calculation (hrs)	0.1	0.1	0.1	0.1	
Latitude	35°16’43”	38°41’52.3”	41°23’41.5”	32°36’53.8”	
Temperatures	Site specific data from LTPP database table SMP_ATEMP_RAIN_DAY				
Rainfall					
Windspeed	III-A	II-A	Boston	Atlanta	Default weather station data
Percent sunshine	III-A	II-A	Boston	Atlanta	Default weather station data

Table 62. Input data and sources for EICM Version 2.6 for the Arizona (041024), Colorado (081053), Connecticut (091803), and Georgia (131005) sections, continued

Variable	Arizona (041024)	Colorado (081053)	Connecticut (091803)	Georgia (131005)	Remarks/ Notes
Water table depth (m)	152.4	Range: 1.38 to 4.60	Range: 1.33 to 3.23	5.2	SMP database table SMP_WATERTAB_DEPTH_MAN
Modifier of overburden pressure	0.5	0.5	0.5	0.5	Default
Emissivity factor	0.9	0.9	0.93	0.93	Default
Surface short wave absorptivity	0.85	0.85	0.85	0.85	Default
Maximum convection coefficient (cal/cm-sec-C°)	44.7	44.7	44.7	44.7	Default
COV of unsaturated permeability	1	1	1	1	Default
Time of day when max and min temperatures occur	Max: 2:02 p.m. Min: 8:08 a.m.	Max: 2:00 p.m. Min: 8:14 a.m.	Max: 1:29 p.m. Min: 5:43 a.m.	Max: 2:59 p.m. Min: 7:40 a.m.	Section averages LTPP database table SMP_ATEMP_RAIN_DAY
Limits freezing range (°C)	0/-1	0/-1	0/-1	0/-1	Default Max: Min:

Table 62. Input data and sources for EICM Version 2.6 for the Arizona (041024), Colorado (081053), Connecticut (091803), and Georgia (131005) sections, continued

Variable	Arizona (041024)	Colorado (081053)	Connecticut (091803)	Georgia (131005)	Remarks/ Notes
Linear length of cracks/ joints (m)	53	115	94	152	Calculated from MON_DIS_AC_REV)
Total survey length (m)	152.4	152.4	152.4	152.4	Standard LTPP test section length
Base % fines	9	9	6	8.9	TST_SS04_UG08 ST_SS_UG01_UG_02)
Base % gravel	77	65	60	52	
Base % sand	14	26	34	39.1	
Base fines type	Silt	Silt	Silt	Silt	Inferred from PI
One side base width (m)	5.79	5.94	4.57	3.66	
Slope ratio/ base tangent	1.5	1.5	1.5	1.5	Default
Internal boundary condition	Flux	Flux	Flux	Flux	
Evaluation period	10	10	10	10	Default
Constant K	0.3	0.3	0.3	0.3	Default
Power of recurrence interval	0.25	0.25	0.25	0.25	Default
Power of rainfall duration	0.75	0.75	0.75	0.75	Default
Shape constant	1.65	1.65	1.65	1.65	Default
Layer 1 material	AC	AC	AC	AC	

Table 62. Input data and sources for EICM Version 2.6 for the Arizona (041024), Colorado (081053), Connecticut (091803), and Georgia (131005) sections, continued

Variable	Arizona (041024)		Colorado (081053)			Connecticut (091803)		Georgia (131005)			Remarks/ Notes
Layer 2 material	A-1-a		A-1-a			A-1-a		A-1-a			TST_SS04_UG08 or infer from TST_SS01_UG01_UG_091803 SMP installation report
Layer 3 material	A-2-6		A-1-a			A-2-4		A-4			
Layer 4 material			A-6					A-6 (Inferred from boring log)			
AC thickness (cm)	27.4		11.4			18		19.1			
Number of elements	5		4			4		4			
Coarse aggregate content	80					80%					Default except section 091803
Air content	4		4			5.4 (inventory)		4			
Gravimetric moisture	2		2			2		2			
M_r vs. T	-20,1.2e^7 15,30000 55 10000		-20,1.2e^7 15,30000 55 10000			-4.1,21463 11.8,97252 23.4,44203		-20,1.2e^7 15,30000 55 10000			Default except section 091803
Thermal conductivity of asphalt	10		10			8.94		10			Default
Heat capacity	0.22		0.22			0.22		0.22			
Total unit weight Mg/m^3	2.37		2.37			2.494		2.37			
Pavement layer	2	3	2	3	4	2	3	2	3	4	
Model layers	2	3-13	2	3-7	8-14	2	3-11	2	3-8	9-13	

Table 62. Input data and sources for EICM Version 2.6 for the Arizona (041024), Colorado (081053), Connecticut (091803), and Georgia (131005) sections, continued

Variable	Arizona (041024)		Colorado (081053)			Connecticut (091803)		Georgia (131005)			Remarks/ Notes
Class	A-1-a	A-2-6	A-1-a	A-1-a	A-6	A-1-a	A-2-4	A-1-a	A-4	A-6	131005 lower subgrade class inferred from boring log
Model layer thicknesses (cm)	22.4	1.4 28.6 1.2 30 0.6 7.65 14.5 14.5 47.7 13.1 340.8	13.7	16.4 14.8 15.6 2.9 10	15.8 18.6 11.8 50.4 9 415.2	37	7.8 22.8 7.6 22.8 7.8 22.6 38.4 22.6 445	22.4	6 24.4 5.6 25.8 3.6 .6	26 4 57.4 2.8 412.3	
Number of Elements in each model layer	12	2 10 2 10 2 4 6 6 14 4	7	8 8 6 2 4	6 6 4 14 4 41	14	2 8 4 8 4 8 12 8 44	10	2 8 4 10 2 1	10 2 10 2 61	
Porosity					.43						
Specific gravity					2.89		2.864				
PI		20			22				1		
P200		30.5			91.8				36		
D60 (mm)	14.4		7.7	13.9			0.48	8.7			

Table 62. Input data and sources for EICM Version 2.6 for the Arizona (041024), Colorado (081053), Connecticut (091803), and Georgia (131005) sections, continued

Variable	Arizona (041024)		Colorado (081053)			Connecticut (091803)		Georgia (131005)			Remarks/ Notes
Initial Water Content for each model layer (NE = Not entered)	19.93	19.9 19.93 19.95 19.9 19.93 NE 19.95 26.35 23.4 19.9 30.5	15.8	13.3 18.2 19.2 25 30.5	NE NE 46.9 47 NE NE	21.25	24.8 20.8 19.4 17.45 26.7 20.85 25.3 25.8 NE	15.8	21.6 19.7 18.9 67 19.5 16.9 3 NE	18.37 12.23 10.5 10.8 NE	
Dry unit weight (gm/cm^3)	2.28	1.96	2.17	2.161	1.64	2.260	1.64	2.23	1.83	2.25	SMP inst. rpt
Sat. permeability (cm/hr)											Not entered
Thermal K (cal/cm-sec-C°)	6	5	6	6	4	4.47	4.02	6	4	4	
Heat capacity (cal/g-C°)	.21	.20	.21	.21	.17	.17	.17	.21	.2	.17	
Volume compressi-bility	.10	.30	.10	.10	1.	.10	1.0	.1	.8	1	
Initial temperature profile	Derived from LTPP database table SMP_MRCTEMP_AUTO_DAY_STAT (interpolation required)										

Table 63. Input data and sources for EICM Version 2.6 for the Maine (231026), Minnesota (271018), and New Hampshire (331001) sections

Variable	Maine (231026)	Minnesota (271018)	New Hampshire (331001)	Remarks/ Notes
Climatic region	I-A	II-A	I-A	
Weather station	User-defined	User-defined	User-defined	
Year	1994	1993	1994	
First month	6	9	6	
First day	20	23	23	
Length of analysis period (days)	365	365	365	
Time increment for output (hrs)	6	6	6	
Time increment for calculation (hrs)	0.1	0.1	0.1	
Latitude	44°34’27.2”	46°1’32.7”	43°13’20.1”	
Temperatures	Site-specific data from LTPP database table SMP_ATEMP_RAIN_DAY			
Rainfall				
Windspeed	Boston	II-A	Boston	Default weather station data

Table 63. Input data and sources for EICM Version 2.6 for the Maine (231026), Minnesota (271018), and New Hampshire (331001) sections, continued

Variable	Maine (231026)	Minnesota (271018)	New Hampshire (331001)	Remarks/ Notes
Percent sunshine	Boston	II-A	Boston	Default weather station data
Water table depth (m)	Range: 1.67 to 3.92	Range: 1.28 to 2.27	Range: 3.80 to 4.11	SMP database table SMP_WATERTAB_DEPTH_MAN
Modifier of overburden pressure	0.5	0.5	0.5	
Emissivity factor	0.9	0.93	0.9	
Surface short wave absorptivity	0.85	0.85	0.85	
Maximum convection coefficient (cal/cm-sec-C°)	44.7	44.7	44.7	
COV of unsaturated permeability	1	1	1	
Time of day when max and min temperatures occur	Max: 1:55 p.m. Min: 5:12 a.m.	Max: 2:09 p.m. Min: 6:25 a.m.	Max: 2:07 p.m. Min: 5:49 a.m.	Site averages LTPP database table SMP_ATEMP_RAIN_DAY
Limits of freezing range (°C)	0/-1	0/-1	0/-1	
Linear length of cracks/ joints (m)	12	648	133	Calculate from MON_DIS_AC_REV

Table 63. Input data and sources for EICM Version 2.6 for the Maine (231026), Minnesota (271018), and New Hampshire (331001) sections, continued

Variable	Maine (231026)	Minnesota (271018)	New Hampshire (331001)	Remarks/ Notes
Total survey length (m)	152.4	152.4	152.4	
Base % fines	4	7.5	4.5	TST_SS04_UG08 except 821801 (TST_SS_UG01_UG_02)
Base % gravel	44.9	45	62.9	TST_SS04_UG08 except 821801 (TST_SS_UG01_UG_02)
Base % sand	22.3	47.5	32.6	
Base fines type	Silt	Silt	Silt	Inferred from PI
One side base width (m)	6.71	5.18	5.79	
Slope ratio/base tangent	1.5	1.5	1.5	
Internal Boundary condition	Flux	Flux	Flux	
Evaluation period	10	10	10	Default
Constant K	0.3	0.3	0.3	Default
Power of recurrence interval	0.25	0.25	0.25	Default
Power of rainfall duration	0.75	0.75	0.75	Default
Shape constant	1.65	1.65	1.65	Default
Layer 1 material	AC	AC	AC	

Table 63. Input data and sources for EICM Version 2.6 for the Maine (231026), Minnesota (271018), and New Hampshire (331001) sections, continued

Variable	Maine (231026)		Minnesota (271018)		New Hampshire (331001)			Remarks/ Notes
Layer 2 material	A-1-a		A-1-b		A-1-a			TST_SS04_UG08 or infer from TST_SS01_UG01_UG_2, 91803 SMP Installation Report
Layer 3 material	A-2-4		A-3		A-1-b			
Layer 4 material					A-2-4			
AC surface thickness (cm)	16.3		11		21.6			
AC layer number of elements	4		3		4			
Coarse aggregate content	80		80		80			
Air content	4		4.3		4			
Gravimetric moisture	2		2		2			
M_r vs. T	-20, $1.2e^7$ 15, 30000 55, 10000		-16.3, 153462 2.2, 78337 19.6, 63883		-23.3, $1.17e^7$ 15.6, 29648 54.4, 10342			
Thermal conductivity of asphalt	10		10		8.94			
Heat capacity	0.22		0.22		0.22			
Total unit weight Mg/m^3	2.37		2.37		2.37			
Pavement layer	2	3	2	3	2	3	4	
Model layers	2	3-10	2	3-12	2	3-5	6-11	
Class	A-1-a	A-2-4	A-1-b	A-3	A-1-a	A-1-b	A-2-4	

Table 63. Input data and sources for EICM Version 2.6 for the Maine (231026), Minnesota (271018), and New Hampshire (331001) sections, continued

Variable	Maine (231026)		Minnesota (271018)		New Hampshire (331001)			Remarks/ Notes
Model layer thicknesses (cm)	49	23.4 4.2 26.2 5.6 28 27.4 33.6 351.6	10	24 7 23 7 24 6 25 36 25 489	49	22.6 4.2 10.2	9 22 10.4 50 11 400	
Number of elements in each model layer	18	6 2 6 2 8 8 8 35	4	6 2 6 2 6 2 6 8 6 6	16	8 2 4	4 8 4 12 4 20	
Porosity		.3	0.24					
Specific gravity		2.782	2.675		2.678	2.678	2.647	
PI								
P200								
D60 (mm)	45.2	4.8	2.6	.38	12.3	1.3	0.25	
Initial water content for each model layer (NE = Not entered)	14	11.3 21.2 14.15 21.45 24.3 30.0 36.45 25.45 NE	13.3	13.4 12.9 15.05 28.7 29 29.5 27.8 30.8 30.75 NE	9.6	15.25 16.6 16.6	16.6 22.75 24.55 26.7 28.55 28.55	

Table 63. Input data and sources for EICM Version 2.6 for the Maine (231026), Minnesota (271018), and New Hampshire (331001) sections, continued

Variable	Maine (231026)		Minnesota (271018)		New Hampshire (331001)			Remarks/ Notes
Dry unit weight (gm/cm^3)	2.278	1.96	2.035	1.829	2.15	2.1	1.86	SMP inst. rpt., 231026 consistent w/ TST_ISD_ MOIST; others no additional data
Sat. permeability (cm/hr)								Not entered
Thermal K (cal/cm-sec-C°)	6	10	4.47	5.07	6	10	5	
Heat capacity (cal/g-C°)	0.21	0.21	0.17	0.2	0.21	0.21	0.20	
Volume compress-ibility	0.10	0.10	0.10	0.50	0.10	0.10	0.30	
Initial temperature profile	Derived from LTPP database table SMP_MRCTEMP_AUTO_DAY_STAT (interpolation required)							

Table 64. Input data and sources for EICM Version 2.6 for the Texas (481077), Vermont (501002), and Manitoba (831801) sections

Variable	Texas (481077)	Vermont (501002)	Manitoba (831801)	Remarks/ Notes
Climatic region	III-B	I-A	II-A	
Weather station	User-defined	User-defined	User-defined	
Year	1993	1994	1994	
First month	12	7	6	
First day	15	20	17	
Length of analysis period (days)	365	365	365	
Time increment for output (hrs)	6	6	6	
Time increment for calculation (hrs)	0.1	0.1	0.1	
Latitude	34°32’19.3”	44°7’10.4”	49°46’9.6”	
Temperatures	Site specific data from LTPP database table SMP_ATEMP_RAIN_DAY			
Rainfall				
Windspeed	San Angelo, TX	Boston	Fargo	Default weather station data
Percent sunshine	San Angelo, TX	Boston	Fargo	Default weather station data
Water table depth (m)	Range: 3.11 to 4.6	Range: 0.78 to 1.44	Range: 1.64 to 3.30	SMP database table SMP_WATERTAB_DEPTH_MAN
Modifier of overburden Pressure	0.5	0.5	0.5	
Emissivity factor	0.9	0.9	0.9	

Table 64. Input data and sources for EICM Version 2.6 for the Texas (481077), Vermont (501002), and Manitoba (831801) sections, continued

Variable	Texas (481077)	Vermont (501002)	Manitoba (831801)	Remarks/ Notes
Surface short wave absorptivity	0.85	0.85	0.85	
Maximum convection coefficient (cal/cm-sec-C°)	44.7	44.7	44.7	
COV of unsaturated permeability	1	1	1	
Time of day when max and min temperatures occur	Max: 2:00 p.m. Min: 8:06 a.m.	Max: 1:13 p.m. Min: 6:12 a.m.	Max: 2:29 p.m. Min: 8:48 a.m.	Site averages derived from LTPP database table SMP_ATEMP_RAIN_DAY
Limits of freezing range °C	0/-1	0/-1	0/-1	
Linear length of cracks/joints (m)	110	125	108	Calculated from MON_DIS_AC_REV
Total survey length (m)	152.4	152.4	152.4	
Base % fines	7	3.3	10.9	TST_SS04_UG08 except 831801 (TST_SS_UG01_UG_02)
Base % gravel	51	89.9	52	
Base % sand	42	6.8	37.1	
Base fines type	Silt	Silt	Silt	Inferred from PI
One side base width (m)	5.79	3.35	3.66	
Slope ratio/ base tangent	1.5	1.5	1.5	

Table 64. Input data and sources for EICM Version 2.6 for the Texas (481077), Vermont (501002), and Manitoba (831801) sections, continued

Variable	Texas (481077)		Vermont (501002)			Manitoba (831801)			Remarks/ Notes
Internal boundary condition	Flux		Flux			Flux			
Layer 1 material	AC		AC			AC			
Layer 2 material	A-1-a		A-1-a			A-1-a			TST_SS04_UG08 or infer from TST_SS01_UG01_UG_2
Layer 3 material	A-4		A-1-a			A-2-6			
Layer 4 material			A-7-5			A-2-4			
AC surface thickness (cm)	13.2		22.4			11.3			LTPP database table TST_L05A
Number of AC layer elements	4		4			3			
Pavement layer	2	3	2	3	4	2	3	4	
Model layers	2	3-12	2	3-4	5-12	2	3-4	5-12	
Class	A-1-a	A-4	A-1-a	A-1-a	A-7-5	A-1-a	A-2-6	A-2-4	
Model layer thicknesses (cm)	27.4	10.2 20.4 10 20.4 10.2 20.2 10.4 50.4 10.6 460	53.8	10.2 17.8	6.3 2.6 6.9 14 19 45.2 12.6 400	15	26.8 4.2	26.8 5.2 24.8 5.2 .8 38.2 21.8 355.2	

Table 64. Input data and sources for EICM Version 2.6 for the Texas (481077), Vermont (501002), and Manitoba (831801) sections, continued

Variable	Texas (481077)		Vermont (501002)			Manitoba (831801)			Remarks/ Notes
Number of elements in each model layer	12	4 8 4 8 4 8 4 14 4 46	18	4 6	2 2 4 6 6 14 6 10	8	8 2	8 2 8 2 6 10 6 35	
Porosity	.18	0.36						0.4	
Specific gravity	2.6	2.685			2.815			2.831	
PI					13				
P200					94.6				
D60 (mm)	9	0.04	25.6	7.7		4.35	6	0.22	
Initial Water Content for each model layer (NE = Not entered)	10.53	22.4 26.83 26.13 28.23 21.5 21.03 19.53 19.23 3 20.3	11	20.25 20.25	33.45 33.45 38 41.7 41.15 45.3 45.3 45.3	18.55	14.3 18.7	19.4 28.2 36.1 31.45 31.35 32.35 28.5 NE	
Dry unit weight (gm/cm^3)	2.139	1.72	2.027	1.759	1.5	2.084	2.131	1.709	SMP inst. rpt.
Sat. permeability (cm/hr)									Not entered
Thermal K (cal/cm-sec-C°)	6	4	4.47	4.47	3	4.47	4.47	4.02	
Heat capacity (cal/g-C°)	0.21	0.2	.17	0.17	0.2	.17	.17	0.17	
Volume compressibility	0.1	0.8	0.1	0.1	1	0.1	0.1	0.1	

Table 64. Input data and sources for EICM Version 2.6 for the Texas (481077), Vermont (501002), and Manitoba (831801) sections, continued

Variable	Texas (481077)	Vermont (501002)	Manitoba (831801)	Remarks/ Notes
Initial temperature profile	Derived from LTPP database table SMP_MRCTEMP_AUTO_DAY_STAT (interpolation required)			

Table 65. Daily rainfall, temperature, and water table depth input for sections 091803 and 131005 (Connecticut and Georgia)

Connecticut (091803)					Georgia (131005)				
Date	Rain (cm)	Max. Temp. °C	Min. Temp. °C	Water Table Depth (m)	Date	Rain (cm)	Max. Temp. °C	Min. Temp. °C	Water Table Depth (m)
6/30/94	0.0	23.2	19	2.54	9/20/95	0.04	38.1	17.1	5.2
7/1/94	0.0	26.2	17	2.57	9/21/95	0	31.2	18.3	5.2
7/2/94	0.0	26.3	18.1	2.6	9/22/95	0	32.3	19.1	5.2
7/3/94	0.0	26.7	17	2.64	9/23/95	0.06	20.2	13.7	5.2
7/4/94	0.0	25.4	15.6	2.67	9/24/95	0.47	14.4	11.1	5.2
7/5/94	0.0	24.5	13.3	2.71	9/25/95	0.05	21.9	14.2	5.2
7/6/94	0.0	29.6	21.7	2.74	9/26/95	0.89	26.9	19.4	5.2
7/7/94	0.0	31.4	20.4	2.78	9/27/95	0	28.9	18	5.2
7/8/94	0.2	29.6	20.3	2.81	9/28/95	0	27.5	16.5	5.2
7/9/94	0.0	29.3	20.3	2.85	9/29/95	0	27.3	15.1	5.2
7/10/94	0.0	28.8	21.9	2.88	9/30/95	0	27.8	16.7	5.2
7/11/94	0.0	26.6	15.9	2.91	10/1/95	0	25.3	18.1	5.2
7/12/94	0.0	27.2	14	2.95	10/2/95	0	30.2	18.8	5.2
7/13/94	0.0	30.8	19	2.98	10/3/95	0.46	28.4	21.4	5.2
7/14/94	0.0	28.2	19.2	3.02	10/4/95	1.14	29.2	21.7	5.2
7/15/94	1.2	20.3	17.9	3.05	10/5/95	0.09	26.6	19	5.2
7/16/94	0.0	27.6	17.2	3.09	10/6/95	0	29.1	17.2	5.2
7/17/94	0.0	26.7	18.1	3.12	10/7/95	0	27.4	14.9	5.2
7/18/94	0.2	23.6	17.4	3.16	10/8/95	0	28.4	9.9	5.2
7/19/94	0.0	26.7	17.2	3.19	10/9/95	0	27.5	14	5.2
7/20/94	0.0	28.7	21.6	3.22	10/10/95	0	26.2	17.3	5.2
7/21/94	0.0	29.6	21.6	3.26	10/11/95	0.17	25.2	19.2	5.2
7/22/94	0.0	27.9	24	3.29	10/12/95	0.05	25.4	17.3	5.2
7/23/94	0.3	27	21.5	3.33	10/13/95	0.1	26.9	20.4	5.2
7/24/94	0.0	26.9	22	3.36	10/14/95	3.15	24.6	14.7	5.2
7/25/94	0.0	28.8	20.1	3.4	10/15/95	0	21.5	9.8	5.2
7/26/94	0.0	27.9	21.4	3.43	10/16/95	0	24.4	9.4	5.2
7/27/94	0.0	27.7	21.5	3.47	10/17/95	0	23.7	8.9	5.2
7/28/94	0.4	26.6	21.3	3.5	10/18/95	0	24.7	11.5	5.2
7/29/94	0.0	27	21	3.49	10/19/95	0	26.8	13.8	5.2
7/30/94	0.0	27.5	21.1	3.47	10/20/95	0	27.3	11.4	5.2

Table 65. Daily rainfall, temperature, and water table depth input for sections 091803 and 131005 (Connecticut and Georgia), continued

Connecticut (091803)					Georgia (131005)				
Date	Rain (cm)	Max. Temp. °C	Min. Temp. °C	Water Table Depth (m)	Date	Rain (cm)	Max. Temp. °C	Min. Temp. °C	Water Table Depth (m)
7/31/94	0.0	27.9	21.2	3.46	10/21/95	0	20.5	4.9	5.2
8/1/94	0.0	27.4	19.5	3.45	10/22/95	0	23.5	3.2	5.2
8/2/94	0.0	29.2	21.6	3.44	10/23/95	0	25.6	7	5.2
8/3/94	0.1	28.3	20.8	3.42	10/24/95	0	27.9	14	5.2
8/4/94	0.0	29	20.1	3.41	10/25/95	0	25.2	12.9	5.2
8/5/94	1.2	27.2	14	3.4	10/26/95	0	25.3	6.4	5.2
8/6/94	1.2	22.3	11.3	3.39	10/27/95	3.92	27.5	13	5.2
8/7/94	0.0	23.3	10.3	3.38	10/28/95	0.58	21.9	9.3	5.2
8/8/94	0.0	24.2	10.8	3.36	10/29/95	0	18.8	5	5.2
8/9/94	0.0	25.6	13.1	3.35	10/30/95	0	18.7	6.4	5.2
8/10/94	0.0	25	15.4	3.34	10/31/95	0.37	14.8	11.4	5.2
8/11/94	0.0	21.9	13.2	3.33	11/1/95	0.36	21	13.8	5.2
8/12/94	0.8	22.8	17.2	3.31	11/2/95	0	26.3	20.2	5.2
8/13/94	0.4	27.3	19.8	3.3	11/3/95	0.49	20.1	9.3	5.2
8/14/94	0.0	28	18.9	3.29	11/4/95	0	15.7	2.7	5.2
8/15/94	0.0	20.9	12	3.28	11/5/95	0	8.5	1.6	5.2
8/16/94	0.0	22.9	10.7	3.26	11/6/95	0.08	16	1.9	5.2
8/17/94	0.0	23.5	15.6	3.25	11/7/95	2.38	23.1	11.8	5.2
8/18/94	0.0	25.2	20.2	3.24	11/8/95	0	14.4	5.6	5.2
8/19/94	0.0	20.7	18.6	3.23	11/9/95	0	14.6	-0.5	5.2
8/20/94	0.0	24	17.5	3.21	11/10/95	0	20.8	2.4	5.2
8/21/94	0.0	24.8	19.2	3.2	11/11/95	1.58	21.6	2.6	5.2
8/22/94	0.0	20.5	14.5	3.19	11/12/95	0	14.2	-1.3	5.2
8/23/94	0.0	21.5	12	3.18	11/13/95	0	14.7	0	5.2
8/24/94	0.0	22.7	10.6	3.16	11/14/95	0.01	13	2.6	5.2
8/25/94	0.0	22.4	11.7	3.15	11/15/95	0	10.7	-1.8	5.2
8/26/94	0.0	25	17	3.15	11/16/95	0	13.9	1.2	5.2
8/27/94	0.0	27.7	18.2	3.14	11/17/95	0	16	0.4	5.2
8/28/94	0.0	26.5	17.4	3.14	11/18/95	0	19	4.3	5.2
8/29/94	0.8	23.9	12	3.13	11/19/95	0	21.9	5	5.2
8/30/94	0.0	22.3	11	3.13	11/20/95	0	18.4	6.6	5.2
8/31/94	0.0	21.6	12.1	3.13	11/21/95	0	18.4	7	5.2
9/1/94	0.0	25.1	14.6	3.12	11/22/95	0	16.5	1.3	5.2

Table 65. Daily rainfall, temperature, and water table depth input for sections 091803 and 131005 (Connecticut and Georgia), continued

Connecticut (091803)					Georgia (131005)				
Date	Rain (cm)	Max. Temp. °C	Min. Temp. °C	Water Table Depth (m)	Date	Rain (cm)	Max. Temp. °C	Min. Temp. °C	Water Table Depth (m)
9/2/94	0.0	20.5	10.5	3.12	11/23/95	0	18.5	-0.8	5.2
9/3/94	0.0	19.6	8.4	3.11	11/24/95	0.16	13.3	8.3	5.2
9/4/94	0.0	17	9.4	3.11	11/25/95	0	15.4	3	5.2
9/5/94	0.0	16.9	12	3.11	11/26/95	0	19.7	0.3	5.2
9/6/94	0.0	21.7	12.6	3.1	11/27/95	0	21.7	5.1	5.2
9/7/94	0.0	22.8	9.1	3.1	11/28/95	0	24.9	15.9	5.2
9/8/94	0.0	23.4	10.1	3.09	11/29/95	0	18.5	5.1	5.2
9/9/94	0.6	24.6	13.6	3.09	11/30/95	0	16	1.3	5.2
9/10/94	0.0	19.6	10.5	3.09	12/1/95	0	18.7	0.2	5.2
9/11/94	0.0	19.2	7.7	3.08	12/2/95	0	22.4	1.2	5.2
9/12/94	0.0	22.3	10.6	3.08	12/3/95	0	21.5	1.8	5.2
9/13/94	0.0	26.3	13.4	3.07	12/4/95	0.03	21.8	7.6	5.2
9/14/94	1.2	24	16	3.07	12/5/95	0.01	21.4	12.3	5.2
9/15/94	0.0	22	12.5	3.07	12/6/95	2.18	15.6	11.5	5.2
9/16/94	0.0	19.8	10.7	3.06	12/7/95	0.04	19	4.8	5.2
9/17/94	0.1	25.5	19.9	3.06	12/8/95	0	9	2.1	5.2
9/18/94	2.0	20.2	11.7	3.05	12/9/95	0.71	8.7	0.8	5.2
9/19/94	0.0	20.9	7.1	3.05	12/10/95	0	4.2	-7	5.2
9/20/94	0.0	20.4	7.1	3.05	12/11/95	0	10	-4.9	5.2
9/21/94	0.0	23.6	11.5	3.04	12/12/95	0	15.6	-4.2	5.2
9/22/94	0.6	17.9	14.7	3.04	12/13/95	0	16.3	8.7	5.2
9/23/94	5.5	19.7	15.6	3.03	12/14/95	0	21.9	4.4	5.2
9/24/94	0.4	20.1	14.4	3.03	12/15/95	0	20.8	8.7	5.2
9/25/94	0.0	20.2	13.9	3.03	12/16/95	0.01	23.6	15.4	5.2
9/26/94	0.0	18.3	16.1	3.02	12/17/95	0	15.8	12.9	5.2
9/27/94	1.1	17.6	15.4	3.02	12/18/95	1.59	13.9	11.1	5.2
9/28/94	0.0	21.5	14.6	3.01	12/19/95	3.72	20.4	7.6	5.2
9/29/94	0.0	17.7	11.1	3.01	12/20/95	0	8.7	0.5	5.2
9/30/94	0.0	16.7	9.4	3.03	12/21/95	0	9.1	-2.6	5.2
10/1/94	0.5	12.5	6.5	3.05	12/22/95	0	3	-3.4	5.2
10/2/94	0.0	15.8	7.4	3.06	12/23/95	0	7.1	-3.2	5.2
10/3/94	0.0	14.9	1.1	3.08	12/24/95	0	4.8	-4.3	5.2
10/4/94	0.0	14.2	4.2	3.1	12/25/95	0	9.2	-5.2	5.2

Table 65. Daily rainfall, temperature, and water table depth input for sections 091803 and 131005 (Connecticut and Georgia), continued

Connecticut (091803)					Georgia (131005)				
Date	Rain (cm)	Max. Temp. °C	Min. Temp. °C	Water Table Depth (m)	Date	Rain (cm)	Max. Temp. °C	Min. Temp. °C	Water Table Depth (m)
10/5/94	0.0	12.4	4	3.12	12/26/95	0	8.9	-2.8	5.2
10/6/94	0.0	14.8	2.8	3.13	12/27/95	0	11	-1.2	5.2
10/7/94	0.0	17.9	3.3	3.15	12/28/95	0	8	-4	5.2
10/8/94	0.0	18.8	8.9	3.17	12/29/95	0	11.2	-4.4	5.2
10/9/94	0.0	21.5	11.1	3.18	12/30/95	0.08	15.9	-0.1	5.2
10/10/94	0.0	15.1	5.9	3.2	12/31/95	0.83	13.6	8.7	5.2
10/11/94	0.0	13.1	0.6	3.22	1/1/96	0.74	18.1	12.3	5.2
10/12/94	0.0	14.6	-0.4	3.24	1/2/96	0.01	22.9	13.8	5.2
10/13/94	0.0	16.4	1.8	3.25	1/3/96	0	13.8	1.4	5.2
10/14/94	0.0	19.9	6	3.27	1/4/96	0	8.8	-2.7	5.2
10/15/94	0.0	15	2.4	3.29	1/5/96	0	12.6	-2.1	5.2
10/16/94	0.0	17.6	1.2	3.31	1/6/96	0.71	14.5	4.4	5.2
10/17/94	0.0	17	2	3.33	1/7/96	1.34	10.3	-4.8	5.2
10/18/94	0.2	15.8	2.7	3.34	1/8/96	0	4.1	-5.5	5.2
10/19/94	0.1	17.1	11.5	3.36	1/9/96	0	10.6	-6.6	5.2
10/20/94	0.1	18.1	13.7	3.38	1/10/96	0	13.9	0.3	5.2
10/21/94	0.0	19	11.3	3.39	1/11/96	0.27	11.5	-2.4	5.2
10/22/94	0.0	20.1	11	3.41	1/12/96	0	8.8	1.7	5.2
10/23/94	1.0	16.4	6.7	3.43	1/13/96	0	15.9	-2.1	5.2
10/24/94	0.0	19	7.8	3.45	1/14/96	0	20.8	-0.4	5.2
10/25/94	0.0	17.5	7.5	3.46	1/15/96	0	20.5	3	5.2
10/26/94	0.0	13.5	5	3.48	1/16/96	0	18.2	5.2	5.2
10/27/94	0.0	14.4	3.6	3.5	1/17/96	0	17.2	8.9	5.2
10/28/94	0.1	14.2	0.8	3.46	1/18/96	0.35	22.8	12	5.2
10/29/94	0.0	16	6.5	3.42	1/19/96	0.03	14.3	-5.3	5.2
10/30/94	0.0	19.5	7.9	3.38	1/20/96	0	8.9	-7.4	5.2
10/31/94	0.0	19.4	8.8	3.34	1/21/96	0	9.9	-2	5.2
11/1/94	0.9	17.6	15	3.3	1/22/96	0	13.2	-3	5.2
11/2/94	0.1	13.4	7.5	3.27	1/23/96	0	17.6	0.5	5.2
11/3/94	0.0	18.3	1.7	3.23	1/24/96	1.86	17.6	2.5	5.2
11/4/94	0.0	20	10.7	3.19	1/25/96	0	11.9	-2.6	5.2
11/5/94	0.0	19.7	11.2	3.15	1/26/96	0.91	20.2	2.7	5.2
11/6/94	0.3	19	9.1	3.11	1/27/96	4.52	17.5	1.3	5.2

Table 65. Daily rainfall, temperature, and water table depth input for sections 091803 and 131005 (Connecticut and Georgia), continued

Connecticut (091803)					Georgia (131005)				
Date	Rain (cm)	Max. Temp. °C	Min. Temp. °C	Water Table Depth (m)	Date	Rain (cm)	Max. Temp. °C	Min. Temp. °C	Water Table Depth (m)
11/7/94	0.0	15.2	5.1	3.07	1/28/96	0	10.6	-3.4	5.2
11/8/94	0.0	15.9	2.8	3.03	1/29/96	0	14.7	4.3	5.2
11/9/94	0.1	18.5	10.6	2.99	1/30/96	0.03	16.2	6.6	5.2
11/10/94	1.5	11	2.9	2.95	1/31/96	0.94	17.9	1.7	5.2
11/11/94	0.0	8.3	-1	2.91	2/1/96	0.04	10	0.7	5.2
11/12/94	0.0	9.2	-1.9	2.87	2/2/96	3.11	11.2	3.5	5.2
11/13/94	0.0	14.2	2.7	2.84	2/3/96	0.01	3.7	-4.7	5.2
11/14/94	0.0	13.4	-0.5	2.8	2/4/96	0	-1.8	-9.8	5.2
11/15/94	0.0	17.9	9.7	2.76	2/5/96	0	2.3	-12	5.2
11/16/94	0.0	9.3	5.1	2.72	2/6/96	0	11.6	-6.4	5.2
11/17/94	0.0	14.2	2.6	2.68	2/7/96	0	14	-2.7	5.2
11/18/94	5.6	16.7	7.4	2.64	2/8/96	0	20.3	2.9	5.2
11/19/94	1.5	15	6.3	2.6	2/9/96	0	22.6	8.4	5.2
11/20/94	0.0	10.3	-0.1	2.56	2/10/96	0	22	3.3	5.2
11/21/94	1.2	15.4	-1.1	2.52	2/11/96	0	20.9	8	5.2
11/22/94	0.2	15.4	2.6	2.48	2/12/96	0	10.3	1.1	5.2
11/23/94	0.0	6.5	-4.4	2.44	2/13/96	0	13.4	-2.7	5.2
11/24/94	0.0	1.4	-5.8	2.4	2/14/96	0	22.1	5.6	5.2
11/25/94	0.0	10.6	0.6	2.37	2/15/96	0.02	19.4	6.8	5.2
11/26/94	0.0	6.5	-2.8	2.33	2/16/96	0	6.9	-1.1	5.2
11/27/94	0.7	2.8	-6.5	2.29	2/17/96	0	10	-5.8	5.2
11/28/94	4.0	15.6	2.2	2.25	2/18/96	0	17	-1.8	5.2
11/29/94	0.0	11.7	6.6	2.21	2/19/96	0.46	17.9	5.8	5.2
11/30/94	0.0	9.9	1.5	2.17	2/20/96	0.86	19.9	10	5.2
12/1/94	0.0	7.2	-3.4	2.15	2/21/96	0.01	21.6	6.2	5.2
12/2/94	0.0	10.7	-3	2.13	2/22/96	0	22.1	8.5	5.2
12/3/94	0.0	14.2	0.1	2.12	2/23/96	0	25.2	14.2	5.2
12/4/94	0.0	14.9	2.1	2.1	2/24/96	0	23.7	11.8	5.2
12/5/94	2.8	15	6.1	2.08	2/25/96	0	24.7	5.2	5.2
12/6/94	0.0	15.5	6	2.06	2/26/96	0	25.3	7.8	5.2
12/7/94	0.3	11.5	1.2	2.04	2/27/96	0	22.5	13.7	5.2
12/8/94	0.0	1.3	-5	2.03	2/28/96	2.3	19.6	11.8	5.2
12/9/94	0.1	7.3	-5.3	2.01	2/29/96	0	12.7	5.6	5.2

Table 65. Daily rainfall, temperature, and water table depth input for sections 091803 and 131005 (Connecticut and Georgia), continued

Connecticut (091803)					Georgia (131005)				
Date	Rain (cm)	Max. Temp. °C	Min. Temp. °C	Water Table Depth (m)	Date	Rain (cm)	Max. Temp. °C	Min. Temp. °C	Water Table Depth (m)
12/10/94	1.8	7.3	2.5	1.99	3/1/96	0	11.7	3.8	5.2
12/11/94	0.5	10.8	-1.5	1.97	3/2/96	0	15.7	3.8	5.2
12/12/94	0.0	-1.5	-7.8	1.95	3/3/96	0	18.6	2.8	5.2
12/13/94	0.0	2.8	-7.9	1.94	3/4/96	0	20.8	0.8	5.2
12/14/94	0.0	0.8	-1.7	1.92	3/5/96	0	23.1	8.6	5.2
12/15/94	0.0	3.6	-1.5	1.9	3/6/96	5.14	18.9	14.8	5.2
12/16/94	0.0	1.7	-0.8	1.88	3/7/96	2.23	21.1	0.7	5.2
12/17/94	0.6	6.2	-0.4	1.86	3/8/96	0	2.5	-4.9	5.2
12/18/94	0.5	6.4	-0.7	1.85	3/9/96	0	6.7	-7.8	5.2
12/19/94	0.0	4.9	-1.8	1.83	3/10/96	0	8.1	-3.3	5.2
12/20/94	0.0	5.7	-6.4	1.81	3/11/96	0	14.2	0.1	5.2
12/21/94	0.0	10.2	-2.2	1.79	3/12/96	0	16.2	-1.3	5.2
12/22/94	0.0	12.3	-1.6	1.77	3/13/96	0	20.7	-0.4	5.2
12/23/94	2.1	9.7	-0.6	1.75	3/14/96	0	23	6.2	5.2
12/24/94	4.5	9.1	6	1.74	3/15/96	0	25	11.7	5.2
12/25/94	0.0	14.4	4.7	1.72	3/16/96	0.63	23.5	15.6	5.2
12/26/94	0.0	9.5	-2.3	1.7	3/17/96	3.54	18.4	13.3	5.2
12/27/94	0.0	7.9	-4.1	1.68	3/18/96	0.04	18	13	5.2
12/28/94	0.0	9.9	0	1.66	3/19/96	0.55	17.3	4.5	5.2
12/29/94	0.0	5.8	-8.1	1.65	3/20/96	0	7.3	1.5	5.2
12/30/94	0.0	-0.9	-10.8	1.63	3/21/96	0	13.1	1.6	5.2
12/31/94	0.1	2.9	-7.2	1.61	3/22/96	0	17.3	-1.5	5.2
1/1/95	1.5	11.6	1.5	1.59	3/23/96	0	20.1	-1	5.2
1/2/95	0.3	8.4	-3	1.57	3/24/96	0	22.7	5.5	5.2
1/3/95	0.0	0.4	-6	1.56	3/25/96	1.71	17.9	10.7	5.2
1/4/95	0.0	1.6	-7.4	1.54	3/26/96	0	23.9	9.7	5.2
1/5/95	0.0	-3.3	-10.7	1.52	3/27/96	1.82	13.2	9.3	5.2
1/6/95	0.2	5.5	-6	1.52	3/28/96	0.09	12	8.4	5.2
1/7/95	2.1	12.5	0.7	1.52	3/29/96	0	21.6	7.9	5.2
1/8/95	0.0	2.3	-5.8	1.51	3/30/96	0.38	15.8	11	5.2
1/9/95	0.0	1.7	-7.1	1.51	3/31/96	0.78	17.6	10.7	5.2
1/10/95	0.0	-0.2	-9.6	1.51	4/1/96	0.22	14	6.4	5.2
1/11/95	0.0	-2.8	-6.7	1.51	4/2/96	0	21.6	3.7	5.2

Table 65. Daily rainfall, temperature, and water table depth input for sections 091803 and 131005 (Connecticut and Georgia), continued

Connecticut (091803)					Georgia (131005)				
Date	Rain (cm)	Max. Temp. °C	Min. Temp. °C	Water Table Depth (m)	Date	Rain (cm)	Max. Temp. °C	Min. Temp. °C	Water Table Depth (m)
1/12/95	1.2	8.8	-2.9	1.5	4/3/96	0	23	4.8	5.2
1/13/95	0.0	13.8	4.1	1.5	4/4/96	0	23.2	8.7	5.2
1/14/95	0.0	17.3	5.7	1.5	4/5/96	0	24.1	12.2	5.2
1/15/95	0.6	16.6	12.6	1.5	4/6/96	0.48	12.5	6.4	5.2
1/16/95	0.2	15.6	10.1	1.5	4/7/96	0	17.7	1.7	5.2
1/17/95	0.0	14	7.5	1.49	4/8/96	0	20.7	2.4	5.2
1/18/95	0.0	7.6	2.7	1.49	4/9/96	0	16.6	6.6	5.2
1/19/95	0.0	4.8	2.1	1.49	4/10/96	0	17.9	3.3	5.2
1/20/95	2.0	9	4.2	1.49	4/11/96	0	23.3	0.6	5.2
1/21/95	0.1	6.6	2.9	1.49	4/12/96	0	24.5	5.1	5.2
1/22/95	0.0	3.1	0.5	1.48	4/13/96	0	24.3	12.8	5.2
1/23/95	0.4	1.9	-2	1.48	4/14/96	0	29.1	16	5.2
1/24/95	0.1	1.9	-1.6	1.48	4/15/96	0.51	22.2	11.9	5.2
1/25/95	0.0	3.4	-2.6	1.48	4/16/96	0	21	6.9	5.2
1/26/95	0.0	2.5	-4.9	1.475	4/17/96	0	25.7	6.5	5.2
1/27/95	0.0	1.9	-5.6	1.49	4/18/96	0	25.2	7.9	5.2
1/28/95	0.0	-2	-11.2	1.51	4/19/96	0.06	26	15.1	5.2
1/29/95	0.0	2.2	-10.5	1.52	4/20/96	0.81	29.5	15.3	5.2
1/30/95	0.0	4.9	-8.4	1.54	4/21/96	0	28.8	13.5	5.2
1/31/95	0.0	3.9	-5.5	1.55	4/22/96	0	28.2	15.7	5.2
2/1/95	0.0	8	1	1.57	4/23/96	0	—	—	5.2
2/2/95	0.0	5.4	-6.1	1.59	4/24/96	0	28.5	19	5.2
2/3/95	0.0	-0.6	-11.3	1.6	4/25/96	0	26.6	15.6	5.2
2/4/95	1.9	5.1	-6.4	1.62	4/26/96	0	27.1	14.9	5.2
2/5/95	0.0	-2.1	-14.8	1.63	4/27/96	0	28.6	15.3	5.2
2/6/95	0.0	-9.6	-16.3	1.65	4/28/96	0	27.5	19.3	5.2
2/7/95	0.0	-4.2	-19.1	1.66	4/29/96	0	30.1	17	5.2
2/8/95	0.0	-3.2	-14.3	1.68	4/30/96	0	31.1	18	5.2
2/9/95	0.0	-1.8	-12.1	1.7	5/1/96	0	32.5	15.7	5.2
2/10/95	0.2	3.3	-6.6	1.71	5/2/96	0	32.9	18.5	5.2
2/11/95	0.0	7.3	0.4	1.73	5/3/96	0	26.9	19.6	5.2
2/12/95	0.0	1.8	-11.6	1.74	5/4/96	0	29.9	20.7	5.2
2/13/95	0.0	-4	-14	1.76	5/5/96	0	28.2	17.1	5.2

Table 65. Daily rainfall, temperature, and water table depth input for sections 091803 and 131005 (Connecticut and Georgia), continued

Connecticut (091803)					Georgia (131005)				
Date	Rain (cm)	Max. Temp. °C	Min. Temp. °C	Water Table Depth (m)	Date	Rain (cm)	Max. Temp. °C	Min. Temp. °C	Water Table Depth (m)
2/14/95	0.0	-0.2	-9	1.77	5/6/96	0	30.6	17.6	5.2
2/15/95	2.1	9.1	-12.9	1.79	5/7/96	0	32.5	18.1	5.2
2/16/95	0.8	9.7	1.8	1.81	5/8/96	0	33.6	20.3	5.2
2/17/95	0.0	7.1	-3.3	1.82	5/9/96	0	30.7	21.1	5.2
2/18/95	0.0	9	-4.4	1.84	5/10/96	0	32.9	20	5.2
2/19/95	0.0	10.2	-5.7	1.85	5/11/96	0	32.4	17.6	5.2
2/20/95	0.0	10.4	-1.5	1.87	5/12/96	0	31.7	19.8	5.2
2/21/95	0.0	4.1	1.1	1.88	5/13/96	0	33.1	19.6	5.2
2/22/95	0.0	2.9	-3.6	1.9	5/14/96	0	32.9	21.1	5.2
2/23/95	0.4	7.2	-3.6	1.92	5/15/96	0	32.7	21.7	5.2
2/24/95	0.6	6.6	-2.6	1.93	5/16/96	0	34.1	21.6	5.2
2/25/95	0.0	1.5	-6.6	1.95	5/17/96	0	36.3	21.2	5.2
2/26/95	0.0	0.2	-7.8	1.96	5/18/96	0	36.9	22.7	5.2
2/27/95	0.0	-0.2	-6.1	1.98	5/19/96	0	37.3	22.3	5.2
2/28/95	3.7	8.9	-1.7	1.99	5/20/96	0	35.8	22.7	5.2
3/1/95	0.0	1.8	-2.1	2.01	5/21/96	0	34.7	23	5.2
3/2/95	0.0	3.5	-3.5	2.025	5/22/96	0	31.8	22.2	5.2
3/3/95	0.0	1.3	-5.1	1.97	5/23/96	0	32.8	17.5	5.2
3/4/95	0.0	4.2	-5.3	1.92	5/24/96	0	33	17.8	5.2
3/5/95	0.0	5.4	-3.9	1.86	5/25/96	0	34.4	19.1	5.2
3/6/95	0.0	7.4	0.3	1.81	5/26/96	0	37.3	24.1	5.2
3/7/95	0.0	10.4	-0.5	1.76	5/27/96	0	37.9	25.5	5.2
3/8/95	0.1	13.7	7.7	1.7	5/28/96	0	35.7	24.2	5.2
3/9/95	2.3	13.6	-7.1	1.65	5/29/96	0	34.7	17.9	5.2
3/10/95	0.0	2.4	-8.8	1.6	5/30/96	0	29.6	21.4	5.2
3/11/95	0.0	2.6	-5.6	1.54	5/31/96	0	29.9	21.5	5.2
3/12/95	0.0	4.5	-0.3	1.49	6/1/96	0	33.1	22.3	5.2
3/13/95	0.0	13.8	1.2	1.44	6/2/96	0	30.8	23.3	5.2
3/14/95	0.0	11.1	1.8	1.38	6/3/96	0.03	33.9	23.8	5.2
3/15/95	0.0	11.9	4	1.33	6/4/96	0.11	34.4	21.2	5.2
3/16/95	0.2	9	3	1.35	6/5/96	0	32.3	23.6	5.2
3/17/95	0.6	11.9	4.4	1.36	6/6/96	0	32.3	20.6	5.2
3/18/95	0.1	10.8	4.2	1.38	6/7/96	1.04	33.8	21.1	5.2

Table 65. Daily rainfall, temperature, and water table depth input for sections 091803 and 131005 (Connecticut and Georgia), continued

Connecticut (091803)					Georgia (131005)				
Date	Rain (cm)	Max. Temp. °C	Min. Temp. °C	Water Table Depth (m)	Date	Rain (cm)	Max. Temp. °C	Min. Temp. °C	Water Table Depth (m)
3/19/95	0.0	10.3	-0.4	1.4	6/8/96	0.82	32.7	21.2	5.2
3/20/95	0.0	8.9	-0.8	1.42	6/9/96	0.05	30.8	22.5	5.2
3/21/95	2.3	12.7	2.7	1.43	6/10/96	0	31.5	21.1	5.2
3/22/95	0.3	9.3	2.5	1.45	6/11/96	0	33	21.6	5.2
3/23/95	0.0	10	0.4	1.47	6/12/96	0	34.1	21.2	5.2
3/24/95	0.0	5.3	-2.1	1.48	6/13/96	0	35.3	23	5.2
3/25/95	0.0	8.9	-1.9	1.5	6/14/96	0.32	35.9	22.8	5.2
3/26/95	0.0	13.5	-1.6	1.52	6/15/96	0.14	34.7	23.2	5.2
3/27/95	0.0	10.3	-1.4	1.54	6/16/96	0	35.2	23.5	5.2
3/28/95	0.0	8.9	-2.5	1.55	6/17/96	0	34.9	23	5.2
3/29/95	0.0	13.1	-2.4	1.57	6/18/96	0	34	22.5	5.2
3/30/95	0.1	9.3	-1	1.58	6/19/96	0	29.9	22.1	5.2
3/31/95	0.1	11.1	3	1.58	6/20/96	0.22	28.5	21.5	5.2
4/1/95	0.0	9.7	-0.3	1.59	6/21/96	0.04	32	21.9	5.2
4/2/95	0.0	8.7	-2	1.6	6/22/96	0	31.1	22.7	5.2
4/3/95	0.0	9.1	-2.5	1.61	6/23/96	0	32.3	21	5.2
4/4/95	0.1	14.4	-2.5	1.61	6/24/96	0	33.3	19.8	5.2
4/5/95	0.0	0.4	-7	1.62	6/25/96	0	33	22.3	5.2
4/6/95	0.0	5.8	-6.2	1.63	6/26/96	0	30.1	22.1	5.2
4/7/95	0.1	13.8	-0.2	1.63	6/27/96	0	31.4	22.7	5.2
4/8/95	1.2	4.4	-2.7	1.64	6/28/96	0	30.7	22.6	5.2
4/9/95	1.2	16	4.2	1.65	6/29/96	0	32.5	22.3	5.2
4/10/95	0.4	11.7	-0.3	1.66	6/30/96	0	33.3	22.2	5.2
4/11/95	0.0	12.9	-1.6	1.66	7/1/96	0	32.5	21.7	5.2
4/12/95	0.5	12.2	0.6	1.67	7/2/96	0	33.4	21.1	5.2
4/13/95	1.7	16.1	8.3	1.67	7/3/96	0	29.2	22.6	5.2
4/14/95	0.0	13.1	5.6	1.67	7/4/96	0	31.4	21.5	5.2
4/15/95	0.0	12.2	4	1.66	7/5/96	1.11	32.1	20.9	5.2
4/16/95	0.0	12.4	2.7	1.66	7/6/96	0.07	30.6	22.5	5.2
4/17/95	0.0	10	-1.9	1.66	7/7/96	0	30.3	23.2	5.2
4/18/95	0.0	14.2	1.9	1.66	7/8/96	0.8	30.2	20.9	5.2
4/19/95	2.3	14.1	6.1	1.65	7/9/96	0	28.6	19.4	5.2
4/20/95	0.0	20.1	9.9	1.65	7/10/96	0	31.4	19.3	5.2

Table 65. Daily rainfall, temperature, and water table depth input for sections 091803 and 131005 (Connecticut and Georgia), continued

Connecticut (091803)					Georgia (131005)				
Date	Rain (cm)	Max. Temp. °C	Min. Temp. °C	Water Table Depth (m)	Date	Rain (cm)	Max. Temp. °C	Min. Temp. °C	Water Table Depth (m)
4/21/95	0.7	13.6	7.1	1.65	7/11/96	0	32.7	18.9	5.2
4/22/95	0.0	20.3	7.9	1.65	7/12/96	0	34	19.7	5.2
4/23/95	0.0	15.2	4.3	1.65	7/13/96	0.11	33.4	20.7	5.2
4/24/95	0.0	12.4	2.5	1.64	7/14/96	0.67	32.9	20.9	5.2
4/25/95	0.0	16.5	0.8	1.64	7/15/96	0.23	32.7	21.3	5.2
4/26/95	0.0	18.1	4.7	1.64	7/16/96	0.01	32.7	20.8	5.2
4/27/95	0.0	19.1	3	1.64	7/17/96	0	33.1	18.1	5.2
4/28/95	0.4	18.5	9.2	1.64	7/18/96	0	33.5	20	5.2
4/29/95	0.0	14.3	7.6	1.64	7/19/96	0	33.8	21.7	5.2
4/30/95	1.0	13.3	5.6	1.64	7/20/96	0.13	31	21.3	5.2
5/1/95	1.9	13.9	2.5	1.65	7/21/96	0	30.2	19.9	5.2
5/2/95	0.0	12.4	1.6	1.65	7/22/96	0.08	30.7	20.4	5.2
5/3/95	0.0	18.2	5.3	1.65	7/23/96	0	29.7	21	5.2
5/4/95	0.0	20.6	5.2	1.65	7/24/96	0	31.8	20.9	5.2
5/5/95	0.1	14.8	10.2	1.65	7/25/96	4.55	28.7	22.1	5.2
5/6/95	0.0	18.6	7.2	1.65	7/26/96	0.07	26.3	20.8	5.2
5/7/95	0.0	17.2	0.5	1.65	7/27/96	0	25.3	21.1	5.2
5/8/95	0.0	19.4	5.1	1.65	7/28/96	0.18	27.8	20.6	5.2
5/9/95	0.0	19	3.1	1.66	7/29/96	0.01	29.5	22.2	5.2
5/10/95	0.8	10.9	8.4	1.66	7/30/96	0	31.8	20.2	5.2
5/11/95	2.8	11.5	7.9	1.66	7/31/96	0.09	31.2	21.6	5.2
5/12/95	0.2	17.1	8.3	1.66	8/1/96	0.97	32.7	20.6	5.2
5/13/95	0.0	16	8.2	1.66	8/2/96	0.01	32.8	21.2	5.2
5/14/95	0.0	20	6.8	1.66	8/3/96	0	33.1	20.5	5.2
5/15/95	0.8	10.8	7.9	1.66	8/4/96	0	34.7	20	5.2
5/16/95	0.0	19	5.9	1.66	8/5/96	0.01	29.3	21.6	5.2
5/17/95	1.4	15.3	8.7	1.67	8/6/96	0	31.2	20.5	5.2
5/18/95	0.0	22.4	13.8	1.67	8/7/96	0.77	31.2	18.6	5.2
5/19/95	0.9	14.7	8.2	1.67	8/8/96	0	28.1	18.1	5.2
5/20/95	0.0	22.4	6.9	1.67	8/9/96	0	27.6	13.3	5.2
5/21/95	0.0	22	8.1	1.67	8/10/96	0	30.8	13.5	5.2
5/22/95	0.0	22.7	9.8	1.67	8/11/96	1.34	28	22.3	5.2
5/23/95	0.0	21.5	7	1.67	8/12/96	0.02	31.8	22.1	5.2

Table 65. Daily rainfall, temperature, and water table depth input for sections 091803 and 131005 (Connecticut and Georgia), continued

Connecticut (091803)					Georgia (131005)				
Date	Rain (cm)	Max. Temp. °C	Min. Temp. °C	Water Table Depth (m)	Date	Rain (cm)	Max. Temp. °C	Min. Temp. °C	Water Table Depth (m)
5/24/95	0.0	23.1	9.9	1.67	8/13/96	0	27.5	16	5.2
5/25/95	0.2	18.6	12.8	1.675	8/14/96	0	38.1	17.1	5.2
5/26/95	0.5	16.9	10.7	1.69	8/15/96	0	31.2	18.3	5.2
5/27/95	0.0	18.6	7.6	1.7	8/16/96	0	32.3	19.1	5.2
5/28/95	0.0	17.7	5	1.71	8/17/96	0	20.2	13.7	5.2
5/29/95	1.8	17.9	11.8	1.72	8/18/96	0	14.4	11.1	5.2
5/30/95	0.9	22.7	12	1.74	8/19/96	0	21.9	14.2	5.2
5/31/95	0.0	29	10.5	1.75	8/20/96	0	26.9	19.4	5.2
6/1/95	0.0	28.2	12.9	1.76	8/21/96	0	28.9	18	5.2
6/2/95	0.0	24.6	12.7	1.77	8/22/96	0	27.5	16.5	5.2
6/3/95	0.5	23.7	16.4	1.79	8/23/96	0	27.3	15.1	5.2
6/4/95	0.1	25.2	14.5	1.8	8/24/96	0.79	27.8	16.7	5.2
6/5/95	0.0	23.2	9.5	1.81	8/25/96	0.11	25.3	18.1	5.2
6/6/95	0.1	24.9	12.7	1.82	8/26/96	2.2	30.2	18.8	5.2
6/7/95	2.0	22.1	17.8	1.84	8/27/96	0.3	28.4	21.4	5.2
6/8/95	0.1	29.6	16.9	1.85	8/28/96	0.01	29.2	21.7	5.2
6/9/95	0.0	23.2	12	1.86	8/29/96	0	26.6	19	5.2
6/10/95	0.0	20.8	10.7	1.87	8/30/96	0.05	29.1	17.2	5.2
6/11/95	0.1	18.3	13.1	1.88	8/31/96	0.06	27.4	14.9	5.2
6/12/95	1.9	20.3	14.2	1.9	9/1/96	0.17	28.4	9.9	5.2
6/13/95	0.6	16.3	13.1	1.91	9/2/96	0.12	27.5	14	5.2
6/14/95	0.3	18.8	13.8	1.92	9/3/96	0	26.2	17.3	5.2
6/15/95	0.0	21.7	11.7	1.93	9/4/96	0	25.2	19.2	5.2
6/16/95	0.0	24.5	10.6	1.95	9/5/96	0	25.4	17.3	5.2
6/17/95	0.0	27.3	12.7	1.96	9/6/96	0	26.9	20.4	5.2
6/18/95	0.0	28.8	14.7	1.97	9/7/96	0	24.6	14.7	5.2
6/19/95	0.0	30.4	17.2	1.98	9/8/96	0	21.5	9.8	5.2
6/20/95	0.1	34	17	2	9/9/96	1.13	24.4	9.4	5.2
6/21/95	0.0	24.8	14.2	2.01	9/10/96	0.2	23.7	8.9	5.2
6/22/95	0.0	24.8	14.2	2.02	9/11/96	1.27	24.7	11.5	5.2
6/23/95	0.0	24.8	14.2	2.02	9/12/96	0.97	26.8	13.8	5.2
6/24/95	0.0	24.8	14.2	2.02	9/13/96	0	27.3	11.4	5.2
6/25/95	0.0	24.8	14.2	2.02	9/14/96	0	20.5	4.9	5.2

Table 65. Daily rainfall, temperature, and water table depth input for sections 091803 and 131005 (Connecticut and Georgia), continued

Connecticut (091803)					Georgia (131005)				
Date	**Rain (cm)**	**Max. Temp. °C**	**Min. Temp. °C**	**Water Table Depth (m)**	**Date**	**Rain (cm)**	**Max. Temp. °C**	**Min. Temp. °C**	**Water Table Depth (m)**
6/26/95	0.0	24.8	14.2	2.02	9/15/96	0	23.5	3.2	5.2
6/27/95	0.0	24.8	14.2	2.02	9/16/96	0.3	25.6	7	5.2
6/28/95	0.0	24.8	14.2	2.02	9/17/96	0.03	27.9	14	5.2
6/29/95	0.0	24.8	14.2	2.02	9/18/96	0	25.2	12.9	5.2

Table 66. Daily rainfall, temperature, and water table depth input for sections 231026 and 271018 (Maine and Minnesota)

Maine (231026)					Minnesota (271018)				
Date	Rain (cm)	Max. Temp. °C	Min. Temp. °C	Water Table Depth (m)	Date	Rain (cm)	Max. Temp. °C	Min. Temp. °C	Water Table Depth (m)
6/20/94	0	26.6	10	1.74	9/24/93	0.0	18.6	-0.6	1.81
6/21/94	0.35	18	13.3	1.75	9/25/93	0.0	20.6	0.9	1.82
6/22/94	0.18	23.6	11.9	1.75	9/26/93	0.0	11.8	5.6	1.82
6/23/94	0	24.4	11.3	1.76	9/27/93	0.3	11.1	-1.5	1.83
6/24/94	0	24.4	11.9	1.77	9/28/93	0.0	8.6	1.1	1.84
6/25/94	1.45	17.6	10.2	1.78	9/29/93	0.0	10.6	-1.2	1.85
6/26/94	0.2	27.6	15.6	1.78	9/30/93	0.0	19.6	2.1	1.85
6/27/94	0.8	28.1	14.5	1.79	10/1/93	0.0	9.9	-1.4	1.86
6/28/94	0.5	23.8	15.3	1.8	10/2/93	0.0	9.7	-6.9	1.87
6/29/94	0.03	26.3	13.8	1.8	10/3/93	0.0	22.3	7.4	1.88
6/30/94	0.2	26.3	18	1.81	10/4/93	0.0	12.3	0.6	1.89
7/1/94	0.45	25.8	15.2	1.82	10/5/93	0.0	17.1	-2.9	1.89
7/2/94	0.64	29	11.9	1.83	10/6/93	0.0	26.8	4.2	1.90
7/3/94	0.01	24.5	11.2	1.83	10/7/93	0.0	16.7	2.3	1.91
7/4/94	0	26.8	9.3	1.84	10/8/93	0.0	6.9	0.1	1.92
7/5/94	0	26	10.6	1.85	10/9/93	0.0	6.1	-6.1	1.92
7/6/94	0.02	28.7	17.8	1.85	10/10/93	0.0	14.2	-3.8	1.93
7/7/94	0.74	26.8	17.1	1.86	10/11/93	0.0	15.1	0.9	1.94
7/8/94	0.05	27.7	18.2	1.87	10/12/93	0.0	7.8	-3.4	1.95
7/9/94	1.01	18.6	17	1.88	10/13/93	0.0	10.8	1.1	1.96
7/10/94	0.08	27.2	17.2	1.88	10/14/93	0.0	13.3	-1.4	1.96
7/11/94	0	26.3	11.6	1.89	10/15/93	0.3	11.7	0.7	1.97
7/12/94	0	27	9.2	1.9	10/16/93	0.0	12.1	2.1	1.98
7/13/94	0	28.8	12.9	1.9	10/17/93	0.0	9.5	-1.3	1.99
7/14/94	0	24.3	11.4	1.91	10/18/93	0.2	10.1	2.5	1.99
7/15/94	0.24	23.9	10.6	1.92	10/19/93	0.0	13.6	4.8	2.00
7/16/94	0	26.4	12.3	1.93	10/20/93	0.7	8.2	-0.4	2.01
7/17/94	0	26.8	12.6	1.93	10/21/93	0.0	7.5	-3.1	2.02
7/18/94	0.02	22.2	13.6	1.94	10/22/93	0.0	16.5	-5.7	2.01
7/19/94	0.11	27.9	17.7	1.97	10/23/93	0.0	23.7	-1.5	2.00

Table 66. Daily rainfall, temperature, and water table depth input for sections 231026 and 271018 (Maine and Minnesota), continued

Maine (231026)					Minnesota (271018)				
Date	Rain (cm)	Max. Temp. °C	Min. Temp. °C	Water Table Depth (m)	Date	Rain (cm)	Max. Temp. °C	Min. Temp. °C	Water Table Depth (m)
7/20/94	0	30.1	14.8	1.99	10/24/93	0.0	19.7	0.4	1.99
7/21/94	0	32.3	16.5	2.02	10/25/93	0.0	15.1	7.2	1.99
7/22/94	0.76	30	19.4	2.04	10/26/93	0.0	5.7	2.1	1.98
7/23/94	0.02	28.5	20.5	2.07	10/27/93	0.0	7.3	-0.4	1.97
7/24/94	0	28.7	17	2.09	10/28/93	0.0	8.6	-3.8	1.96
7/25/94	0.06	26.1	18.4	2.12	10/29/93	0.0	-1.2	-3.3	1.95
7/26/94	0.94	28.3	18.6	2.14	10/30/93	0.0	-2.5	-5.6	1.94
7/27/94	0.03	26.5	16.1	2.17	10/31/93	0.0	1.6	-11.5	1.94
7/28/94	0.92	18.2	16	2.19	11/1/93	0.0	6.8	-3.2	1.93
7/29/94	0	27.2	15.5	2.22	11/2/93	0.0	8	-1.5	1.92
7/30/94	0.06	26.4	14.4	2.24	11/3/93	0.0	9.7	-4.6	1.91
7/31/94	0	27.4	16	2.27	11/4/93	0.6	4.2	-3.1	1.90
8/1/94	0	28.1	12.6	2.3	11/5/93	0.0	-3.5	-8.6	1.90
8/2/94	2.16	27.9	15.2	2.32	11/6/93	0.5	-4.8	-13.5	1.89
8/3/94	0.01	26.2	17.8	2.35	11/7/93	0.2	-0.6	-12.1	1.88
8/4/94	0	28.8	15.1	2.37	11/8/93	0.1	-3.3	-12.9	1.87
8/5/94	0.82	23.4	11.6	2.4	11/9/93	0.1	1.5	-6.6	1.86
8/6/94	0	21.7	6	2.42	11/10/93	0.0	-1	-14.1	1.85
8/7/94	0	24.7	6.7	2.45	11/11/93	0.0	1	-8.9	1.85
8/8/94	0	25.7	8.6	2.47	11/12/93	1.2	0.5	-11.6	1.84
8/9/94	0	27.1	9	2.5	11/13/93	0.3	1.4	-1.4	1.83
8/10/94	0.2	22.3	8.9	2.52	11/14/93	0.0	0.2	-5.4	1.82
8/11/94	0	22.6	6.6	2.55	11/15/93	0.0	3.4	-8.4	1.81
8/12/94	0	24.8	9.2	2.57	11/16/93	0.0	3.7	-1.1	1.81
8/13/94	0	22.5	11.9	2.6	11/17/93	0.0	3.7	-6.1	1.80
8/14/94	0.11	24.5	17.2	2.62	11/18/93	0.0	3.9	-2.8	1.79
8/15/94	0.01	18.5	8.2	2.65	11/19/93	0.0	0.9	-7.4	1.76
8/16/94	0	21.8	9.1	2.65	11/20/93	0.0	4.5	-7	1.76
8/17/94	0	25.8	7.7	2.66	11/21/93	0.0	6.7	-2.1	1.76
8/18/94	1.5	19.3	14.9	2.66	11/22/93	0.0	-3.2	-7.2	1.77
8/19/94	0.01	23.9	15.4	2.66	11/23/93	0.0	-4	-6.4	1.77
8/20/94	0	26.4	13.2	2.67	11/24/93	0.0	-2.3	-7.6	1.77
8/21/94	2.03	25	15.6	2.67	11/25/93	0.0	-2.5	-5.4	1.78

Table 66. Daily rainfall, temperature, and water table depth input for sections 231026 and 271018 (Maine and Minnesota), continued

Maine (231026)					Minnesota (271018)				
Date	Rain (cm)	Max. Temp. °C	Min. Temp. °C	Water Table Depth (m)	Date	Rain (cm)	Max. Temp. °C	Min. Temp. °C	Water Table Depth (m)
8/22/94	0.01	18.2	9	2.68	11/26/93	0.0	-5	-15.7	1.78
8/23/94	0	22.1	6.3	2.68	11/27/93	0.0	-9.4	-18.7	1.78
8/24/94	0	23.1	6.6	2.68	11/28/93	0.0	-7.7	-13.7	1.79
8/25/94	0	24.9	5.4	2.69	11/29/93	0.0	-5.3	-15.3	1.79
8/26/94	0	27.6	13.2	2.69	11/30/93	0.1	-1.2	-14	1.79
8/27/94	0.01	26.5	12.8	2.69	12/1/93	0.0	0.1	-4	1.80
8/28/94	0	24.8	10.1	2.7	12/2/93	0.1	-0.2	-5.6	1.80
8/29/94	0	22.2	8.3	2.7	12/3/93	0.0	-5	-9.9	1.80
8/30/94	0	18.9	7.2	2.71	12/4/93	0.0	-2.1	-6.9	1.80
8/31/94	0.07	15.3	6.9	2.71	12/5/93	0.0	-0.2	-2.8	1.81
9/1/94	0.12	16.9	5.5	2.71	12/6/93	0.0	-3.3	-15.3	1.81
9/2/94	0	17.4	5	2.72	12/7/93	0.0	-4.5	-15	1.82
9/3/94	0	16.5	3.8	2.72	12/8/93	0.0	-3.3	-14.2	1.81
9/4/94	0	17.8	4.8	2.72	12/9/93	0.2	1	-10.1	1.82
9/5/94	1.7	13.6	7.8	2.73	12/10/93	0.0	-0.4	-19.3	1.83
9/6/94	0	16.1	10.9	2.73	12/11/93	0.0	-5.7	-22.3	1.83
9/7/94	0	20	6.4	2.74	12/12/93	0.5	4.2	-5.5	1.84
9/8/94	0.1	20.1	9	2.74	12/13/93	0.0	2	-3.3	1.85
9/9/94	0.94	20.6	6.2	2.74	12/14/93	0.1	1.1	-3.3	1.85
9/10/94	0.16	14.6	5.1	2.75	12/15/93	0.0	3.7	-0.7	1.86
9/11/94	0.16	17.7	9.4	2.75	12/16/93	0.0	1	-2.1	1.87
9/12/94	0	20.5	8.6	2.75	12/17/93	0.4	0.2	-1.6	1.87
9/13/94	0.62	21.2	12.7	2.76	12/18/93	0.3	-0.6	-2.6	1.88
9/14/94	0.3	23.7	8.9	2.76	12/19/93	0.0	-2.2	-6.5	1.89
9/15/94	0	23.1	4.5	2.77	12/20/93	0.0	-4.9	-17.3	1.89
9/16/94	0.17	18.5	5	2.77	12/21/93	0.0	-8.7	-15.3	1.90
9/17/94	0	26.4	13.7	2.77	12/22/93	0.0	-10.2	-19.6	1.91
9/18/94	0	16.3	3.4	2.78	12/23/93	0.0	-13	-21	1.91
9/19/94	0	16	1.5	2.78	12/24/93	0.0	-14.6	-23.4	1.92
9/20/94	0	24.9	2.5	2.78	12/25/93	0.0	-15.2	-24.7	1.93
9/21/94	0	25.2	7.8	2.77	12/26/93	0.0	-21.4	-27.9	1.93
9/22/94	0	18.8	7.4	2.77	12/27/93	0.0	-20	-29.3	1.94
9/23/94	3.45	13.5	7.2	2.76	12/28/93	0.0	-8.2	-32	1.94

Table 66. Daily rainfall, temperature, and water table depth input for sections 231026 and 271018 (Maine and Minnesota), continued

Maine (231026)					Minnesota (271018)				
Date	Rain (cm)	Max. Temp. °C	Min. Temp. °C	Water Table Depth (m)	Date	Rain (cm)	Max. Temp. °C	Min. Temp. °C	Water Table Depth (m)
9/24/94	4.2	14.8	13.4	2.76	12/29/93	0.0	-10.9	-26.5	1.95
9/25/94	0.07	15.8	12.9	2.75	12/30/93	0.0	-3.8	-26.6	1.96
9/26/94	0	18.7	12.5	2.75	12/31/93	0.0	-2.8	-9.6	1.96
9/27/94	0.15	15.7	13	2.74	1/1/94	0.0	-3.5	-15.3	1.97
9/28/94	0.56	20.1	12.7	2.74	1/2/94	0.0	-14.5	-24.8	1.98
9/29/94	0.2	17.9	8.7	2.73	1/3/94	0.0	-12.4	-27.5	1.98
9/30/94	0	10.7	6.8	2.73	1/4/94	0.0	-12.3	-22.4	1.99
10/1/94	0	14.8	4.2	2.72	1/5/94	0.0	-15.5	-25.5	2.00
10/2/94	0	11.7	0.3	2.72	1/6/94	0.0	-11.6	-22	2.00
10/3/94	0	10.7	3.3	2.72	1/7/94	0.0	-15.6	-25.1	2.01
10/4/94	0	13.3	6.4	2.71	1/8/94	0.0	-12.3	-27.5	2.02
10/5/94	0	10.8	1.3	2.71	1/9/94	0.0	-10.5	-29.1	2.02
10/6/94	0	12.3	-0.7	2.7	1/10/94	0.0	-5.1	-20.7	2.03
10/7/94	0	21.2	-1	2.7	1/11/94	0.0	-15.5	-28	2.05
10/8/94	0	23.9	2.9	2.69	1/12/94	0.0	-13.2	-21	2.04
10/9/94	0.14	22.8	3.4	2.69	1/13/94	0.0	-20	-30.4	2.05
10/10/94	0.24	12.3	3.3	2.68	1/14/94	0.0	-25.3	-33.8	2.06
10/11/94	0	11	-3	2.68	1/15/94	0.0	-26.5	-36.7	2.07
10/12/94	0	14.7	-4.3	2.67	1/16/94	0.0	-21.5	-27.5	2.07
10/13/94	0	21.1	-2.8	2.67	1/17/94	0.0	-24.7	-34.3	2.08
10/14/94	0	17.2	-2.3	2.66	1/18/94	0.0	-28.6	-37.5	2.09
10/15/94	0	15.3	-5.9	2.66	1/19/94	0.0	-21.2	-39.6	2.10
10/16/94	0	17.9	-3.6	2.65	1/20/94	0.0	-14.9	-34.2	2.10
10/17/94	0	16.5	-1.7	2.65	1/21/94	0.3	-4.8	-16.3	2.11
10/18/94	0.05	17	-1.8	2.63	1/22/94	0.0	-5.4	-15.4	2.12
10/19/94	0.01	18.4	4.7	2.62	1/23/94	0.3	-1.1	-16.2	2.13
10/20/94	0.98	12.1	6.8	2.6	1/24/94	0.0	-8.1	-13.7	2.14
10/21/94	0.69	13.1	10.5	2.59	1/25/94	0.0	-9.1	-11.7	2.14
10/22/94	0.21	14.8	10.6	2.57	1/26/94	0.0	-9.6	-13.3	2.15
10/23/94	0	16.7	9.9	2.56	1/27/94	0.0	-8.2	-12.3	2.16
10/24/94	0	18.5	1.6	2.54	1/28/94	0.0	-5.8	-10.4	2.17
10/25/94	0	14.7	-0.5	2.52	1/29/94	0.0	-11.1	-21.9	2.18
10/26/94	0	12.9	-1.5	2.51	1/30/94	0.0	-15.7	-33.3	2.18

Table 66. Daily rainfall, temperature, and water table depth input for sections 231026 and 271018 (Maine and Minnesota), continued

Maine (231026)					Minnesota (271018)				
Date	Rain (cm)	Max. Temp. °C	Min. Temp. °C	Water Table Depth (m)	Date	Rain (cm)	Max. Temp. °C	Min. Temp. °C	Water Table Depth (m)
10/27/94	0	10.5	-1.8	2.49	1/31/94	0.0	-15	-30.7	2.19
10/28/94	0	14.1	-2.2	2.48	2/1/94	0.0	-12.8	-29.4	2.20
10/29/94	0	14.4	-2	2.46	2/2/94	0.0	-12.5	-23.8	2.21
10/30/94	0	18.2	0.3	2.45	2/3/94	0.0	-14.8	-24	2.21
10/31/94	0.08	15	0.7	2.43	2/4/94	0.0	-14	-24.6	2.22
11/1/94	1.3	9.6	7	2.41	2/5/94	0.0	-12.2	-17.4	2.23
11/2/94	4.49	10.8	5.8	2.4	2/6/94	0.0	-15.2	-29.1	2.24
11/3/94	0	13.8	-0.9	2.38	2/7/94	0.0	-24.6	-31	2.25
11/4/94	0.14	10.7	2	2.37	2/8/94	0.0	-20	-26.6	2.27
11/5/94	0	20.7	5.9	2.35	2/9/94	0.0	-18	-31.5	2.28
11/6/94	0.75	11.8	4.5	2.34	2/10/94	0.0	-12.3	-22.6	2.27
11/7/94	0.01	9.2	4.1	2.32	2/11/94	0.0	-8.6	-28	2.26
11/8/94	0	13	0.4	2.3	2/12/94	0.2	-4.6	-18.5	2.25
11/9/94	0	12.8	0.9	2.29	2/13/94	0.0	-7.6	-23.1	2.24
11/10/94	0	5.3	-1.1	2.27	2/14/94	0.3	4.3	-16.1	2.23
11/11/94	0	4.7	-1.7	2.26	2/15/94	0.1	-3	-12	2.22
11/12/94	0	8.1	-2.4	2.24	2/16/94	0.0	3.6	-9.7	2.21
11/13/94	0	12	-4.7	2.23	2/17/94	0.0	3.8	-9.9	2.20
11/14/94	0	11.1	-4	2.21	2/18/94	0.0	7.2	-1.1	2.20
11/15/94	0	16.6	3	2.2	2/19/94	0.0	4.6	-10.8	2.19
11/16/94	0	9.5	-4.8	2.2	2/20/94	0.0	-6	-15.4	2.18
11/17/94	0	11.8	-7	2.19	2/21/94	0.0	-11.9	-18	2.17
11/18/94	0.18	7.5	-7.5	2.18	2/22/94	0.0	-9.2	-18.7	2.16
11/19/94	0.01	11.6	1.8	2.18	2/23/94	0.0	-9.5	-13	2.15
11/20/94	0	7	-6.4	2.17	2/24/94	0.0	-7.3	-19	2.14
11/21/94	0.9	7.3	-8.1	2.17	2/25/94	0.0	-9.2	-19.1	2.13
11/22/94	0.5	11	0.1	2.16	2/26/94	0.2	-7.5	-22.2	2.12
11/23/94	0.03	-0.6	-9.7	2.15	2/27/94	0.0	-6.9	-17.7	2.11
11/24/94	0	-2.8	-8.5	2.15	2/28/94	0.0	-1.6	-13.3	2.10
11/25/94	0	3.2	-7.3	2.14	3/1/94	0.0	-0.3	-14.8	2.09
11/26/94	0	2.9	-10	2.13	3/2/94	0.0	1.4	-3.7	2.08
11/27/94	0	-0.9	-14.1	2.13	3/3/94	0.0	10.2	-9	2.07
11/28/94	0.07	-0.2	-7.5	2.12	3/4/94	0.0	9.9	-2	2.07

Table 66. Daily rainfall, temperature, and water table depth input for sections 231026 and 271018 (Maine and Minnesota), continued

Maine (231026)					Minnesota (271018)				
Date	Rain (cm)	Max. Temp. °C	Min. Temp. °C	Water Table Depth (m)	Date	Rain (cm)	Max. Temp. °C	Min. Temp. °C	Water Table Depth (m)
11/29/94	1.66	7.9	-2.9	2.11	3/5/94	0.0	9.5	-3.7	2.06
11/30/94	0	4.9	-6	2.11	3/6/94	0.0	2.8	-3.8	2.05
12/1/94	0	1.9	-9.5	2.1	3/7/94	0.0	-2.3	-9.4	2.04
12/2/94	0	7.6	-9.4	2.09	3/8/94	0.0	-7	-15	2.01
12/3/94	0.05	10.7	-6.1	2.09	3/9/94	0.0	-3.1	-17.8	2.04
12/4/94	0.05	14.4	-2.6	2.08	3/10/94	0.0	-3.2	-12.6	2.01
12/5/94	2.25	3.4	-2.9	2.07	3/11/94	0.0	2.2	-13.2	1.98
12/6/94	0.02	9	1.5	2.07	3/12/94	0.0	4.9	-6.5	1.94
12/7/94	0.03	5.5	-6.5	2.06	3/13/94	0.0	6.1	-3.2	1.91
12/8/94	0	-1.3	-7.9	2.06	3/14/94	0.0	8.3	1.5	1.88
12/9/94	0	2.7	-10.9	2.05	3/15/94	0.0	2.3	-5	1.84
12/10/94	0.03	2	-3.1	2.04	3/16/94	0.0	1.2	-10	1.81
12/11/94	0.49	2.6	-8.8	2.04	3/17/94	0.0	3.9	-4	1.77
12/12/94	0	-8	-18.6	2.03	3/18/94	0.4	3.2	-5.1	1.74
12/13/94	0	-9.7	-22.8	2.03	3/19/94	0.2	6.2	-3.6	1.71
12/14/94	0	-5.3	-13.4	2.03	3/20/94	1.4	2.9	-1.7	1.67
12/15/94	0.01	-0.3	-14.4	2.03	3/21/94	0.0	11.6	-3.2	1.64
12/16/94	0	-3.3	-16.9	2.03	3/22/94	0.0	11.2	-1.4	1.54
12/17/94	0	-2.7	-8.3	2.02	3/23/94	0.0	-0.7	-6.1	1.53
12/18/94	0.35	1.5	-2.6	2.02	3/24/94	0.5	1.9	-6.9	1.54
12/19/94	0.1	0.6	-13.4	2.02	3/25/94	0.0	3.8	-11.6	1.55
12/20/94	0	-1.8	-12.1	2.02	3/26/94	0.3	2.6	-3	1.57
12/21/94	0.91	9.3	-8.8	2.02	3/27/94	0.1	2.3	-3.1	1.58
12/22/94	0	14.5	-6.2	2.02	3/28/94	0.0	2.4	-4.1	1.60
12/23/94	0	6.8	-7.5	2.02	3/29/94	0.0	0.6	-5.6	1.61
12/24/94	1.76	5.3	1.6	2.02	3/30/94	0.0	5.5	-7.9	1.62
12/25/94	0	10.1	-3.8	2.02	3/31/94	0.0	12	-4	1.64
12/26/94	0	1.6	-9.6	2.01	4/1/94	0.0	16.4	-3.5	1.65
12/27/94	0	1.1	-11.3	2.01	4/2/94	0.0	2.3	-3.4	1.66
12/28/94	0	0.3	-4.6	2.01	4/3/94	0.0	7.3	-6.2	1.68
12/29/94	0	2.8	-15.9	2.01	4/4/94	0.1	3.4	-4.8	1.72
12/30/94	0	-7.5	-16.9	2.01	4/5/94	0.0	1.3	-9.3	1.74
12/31/94	0	0.5	-13.3	2.01	4/6/94	0.0	6.6	-8	1.72

Table 66. Daily rainfall, temperature, and water table depth input for sections 231026 and 271018 (Maine and Minnesota), continued

Maine (231026)					Minnesota (271018)				
Date	Rain (cm)	Max. Temp. °C	Min. Temp. °C	Water Table Depth (m)	Date	Rain (cm)	Max. Temp. °C	Min. Temp. °C	Water Table Depth (m)
1/1/95	0	-1.9	-3.8	2.01	4/7/94	0.0	9	-1.5	1.70
1/2/95	0	-0.6	-4.7	2.01	4/8/94	0.4	10	1.5	1.68
1/3/95	0.01	-2.1	-10	2.01	4/9/94	0.0	6.5	0	1.66
1/4/95	0	-3.6	-18	2	4/10/94	0.0	13.7	-2.7	1.64
1/5/95	0	-7.1	-19.6	2	4/11/94	0.0	15.6	-2.6	1.62
1/6/95	0	-1.9	-22.2	2	4/12/94	0.0	15.7	-0.9	1.59
1/7/95	0.02	0.3	-5.3	2	4/13/94	0.0	19.2	-1.6	1.57
1/8/95	0.01	-3.7	-15.6	2	4/14/94	0.0	19	4.7	1.55
1/9/95	0.01	-2.8	-18.5	2	4/15/94	4.2	9.9	4.3	1.53
1/10/95	0	-10.6	-25.1	2	4/16/94	0.0	14.4	1.1	1.51
1/11/95	0	-17.6	-28.3	2	4/17/94	0.0	18.4	0.5	1.49
1/12/95	0	-6.7	-17.6	2	4/18/94	0.0	25.1	6	1.47
1/13/95	0.7	3.1	-6.8	1.99	4/19/94	0.0	12.1	1.8	1.45
1/14/95	1.07	2.5	-0.1	1.99	4/20/94	0.0	9	-2.1	1.43
1/15/95	0.89	13.4	0.4	1.99	4/21/94	0.0	15.3	-2.6	1.41
1/16/95	1.21	12.8	4.4	1.99	4/22/94	0.0	18.2	-2.1	1.38
1/17/95	0.22	6.7	0.1	1.99	4/23/94	0.0	22	9.9	1.36
1/18/95	0	0.6	-1.8	1.99	4/24/94	0.1	19.2	10.8	1.34
1/19/95	0	0.1	-1.9	1.99	6/14/94	0.1	33.3	21.1	1.28
1/20/95	2.49	0.9	-1.2	1.98	6/15/94	1.4	20.4	15.2	1.28
1/21/95	1.21	0.9	-0.4	1.98	6/16/94	0.7	15.6	13.8	1.28
1/22/95	0	-0.6	-3.1	1.98	6/17/94	2.1	21.3	13.6	1.28
1/23/95	0.42	0.2	-9.2	1.97	6/18/94	0.0	25.2	15.8	1.29
1/24/95	0.06	-1.2	-11.8	1.97	6/19/94	3.2	29	15	1.29
1/25/95	0.15	-0.8	-12.4	1.97	6/20/94	1.7	26.9	16.9	1.30
1/26/95	0	-5.4	-14.8	1.97	6/21/94	0.0	26.8	12.7	1.30
1/27/95	0	-9.6	-15.4	1.96	6/22/94	0.0	25	16	1.31
1/28/95	0	-6.4	-15.2	1.96	6/23/94	0.7	26.3	16.2	1.31
1/29/95	0	-1.6	-17.5	1.96	6/24/94	0.0	26.9	13.7	1.31
1/30/95	0	-0.1	-15.7	1.96	6/25/94	0.4	26.9	13.7	1.32
1/31/95	0	0.7	-10.5	1.95	6/26/94	0.0	25.6	12.7	1.32
2/1/95	0.2	4.4	-3.2	1.95	6/27/94	0.1	24.7	16	1.33
2/2/95	0	0.3	-13.7	1.95	6/28/94	0.1	22.4	14.3	1.34

Table 66. Daily rainfall, temperature, and water table depth input for sections 231026 and 271018 (Maine and Minnesota), continued

Maine (231026)					Minnesota (271018)				
Date	Rain (cm)	Max. Temp. °C	Min. Temp. °C	Water Table Depth (m)	Date	Rain (cm)	Max. Temp. °C	Min. Temp. °C	Water Table Depth (m)
2/3/95	0	-3.4	-18.6	1.95	6/29/94	0.0	21.8	14	1.32
2/4/95	0	-7.6	-15.7	1.94	6/30/94	0.0	25.5	11	1.34
2/5/95	0	-7.9	-21.1	1.94	7/1/94	0.0	18.3	9.6	1.36
2/6/95	0	-19.9	-24.3	1.94	7/2/94	0.0	21.8	6	1.38
2/7/95	0	-13.1	-26	1.94	7/3/94	0.0	22.6	13.4	1.39
2/8/95	0	-8.2	-27.8	1.93	7/4/94	0.5	25.3	17.5	1.41
2/9/95	0	-4	-14.9	1.93	7/5/94	0.9	28.1	18.8	1.43
2/10/95	0.07	-2.2	-16.7	1.93	7/6/94	0.0	27.6	17.1	1.45
2/11/95	0.17	1.8	-9.5	1.93	7/7/94	3.8	24.8	18.3	1.46
2/12/95	0	-8.2	-17.9	1.92	7/8/94	0.1	18.7	16.5	1.48
2/13/95	0	-5.8	-17.4	1.92	7/9/94	0.0	22.2	13.1	1.50
2/14/95	0	-5	-21.9	1.92	7/10/94	0.0	23.7	10.6	1.52
2/15/95	0	-1.9	-22.1	1.92	7/11/94	0.0	28.1	15.5	1.53
2/16/95	0.65	3.4	-4	1.92	7/12/94	0.0	26.1	13.6	1.55
2/17/95	0	1	-12.4	1.93	7/13/94	0.1	18.6	14	1.57
2/18/95	0	6.4	-14.5	1.93	7/14/94	0.0	23.4	14	1.59
2/19/95	0	8.5	-7.5	1.93	7/15/94	0.0	26.6	10.9	1.61
2/20/95	0	2.2	-8.2	1.93	7/16/94	0.0	26.5	14.5	1.62
2/21/95	0	-0.7	-6.1	1.94	7/17/94	0.0	24.7	12	1.64
2/22/95	0	0.5	-12.9	1.94	7/18/94	1.6	25	9.9	1.66
2/23/95	0	4.2	-8.7	1.94	7/19/94	3.0	26.6	15.8	1.68
2/24/95	0.86	1.3	-7.3	1.94	7/20/94	0.1	26	14.3	1.69
2/25/95	0	-8.2	-16.1	1.95	7/21/94	1.4	22.8	16.6	1.71
2/26/95	0	-9.2	-24.1	1.95	7/22/94	0.0	25.4	15.1	1.73
2/27/95	0	-12.4	-26.1	1.95	7/23/94	0.0	24.4	15	1.75
2/28/95	0	-2.7	-12.1	1.96	7/24/94	0.0	24.9	13.2	1.77
3/1/95	0	-2.9	-12	1.96	7/25/94	0.0	19.6	10.5	1.78
3/2/95	0.42	-1.2	-16.9	1.96	7/26/94	0.1	22.6	13.8	1.80
3/3/95	0.17	-2	-20.8	1.96	7/27/94	0.0	23.5	9.9	1.82
3/4/95	0.45	3.5	-22.4	1.97	7/28/94	0.0	25.3	12.9	1.84
3/5/95	0.13	4	-16.8	1.97	7/29/94	0.0	25.3	12.1	1.85
3/6/95	0.03	-0.5	-1.9	1.97	7/30/94	0.1	26.2	14.2	1.87
3/7/95	0	-0.3	-3.3	1.96	7/31/94	0.0	25.9	17.4	1.89

Table 66. Daily rainfall, temperature, and water table depth input for sections 231026 and 271018 (Maine and Minnesota), continued

Maine (231026)					Minnesota (271018)				
Date	Rain (cm)	Max. Temp. °C	Min. Temp. °C	Water Table Depth (m)	Date	Rain (cm)	Max. Temp. °C	Min. Temp. °C	Water Table Depth (m)
3/8/95	3.18	9	-0.2	1.95	8/1/94	0.0	28	17	1.91
3/9/95	1.16	1.3	-9.5	1.94	8/2/94	0.0	26.4	14.3	1.96
3/10/95	0	-3.8	-11.5	1.93	8/3/94	1.6	29	17.7	1.98
3/11/95	0	-1.2	-16.6	1.92	8/4/94	0.0	19.3	9.6	1.96
3/12/95	0	-0.5	-6.9	1.91	8/5/94	0.0	22	6.7	1.94
3/13/95	0.09	5.6	-1	1.9	8/6/94	0.0	23.1	10.6	1.92
3/14/95	0	3.4	0.3	1.88	8/7/94	1.1	25.2	15.8	1.90
3/15/95	0.01	6.7	0.4	1.87	8/8/94	0.0	15.7	9.2	1.88
3/16/95	0.1	3.8	0.6	1.86	8/9/94	0.0	15.6	9.6	1.86
3/17/95	0.54	2.3	-0.1	1.85	8/10/94	0.2	18.7	12.1	1.84
3/18/95	0.12	9	-0.1	1.84	8/11/94	0.0	23.7	11.1	1.83
3/19/95	0	8.1	-5	1.83	8/12/94	0.0	20.6	16.1	1.81
3/20/95	0	8.9	-6.8	1.82	8/13/94	0.6	18.3	8	1.79
3/21/95	0.81	9.4	-2.3	1.82	8/14/94	0.0	20.3	6.8	1.77
3/22/95	0	8.8	-2.2	1.82	8/15/94	0.0	23.5	7.1	1.75
3/23/95	0.04	5.8	-1.8	1.82	8/16/94	0.0	25.7	10.6	1.73
3/24/95	0.06	3.8	-2.3	1.82	8/17/94	0.0	25.8	13	1.71
3/25/95	0	3.2	-4.1	1.82	8/18/94	0.1	21.8	14.5	1.69
3/26/95	0	7.1	-1.5	1.82	8/19/94	0.8	21.6	15.5	1.67
3/27/95	0	8	-2.4	1.83	8/20/94	0.0	23	12	1.65
3/28/95	0	11.1	-4.3	1.83	8/21/94	0.0	24.4	8.7	1.63
3/29/95	0	12.9	-4.9	1.83	8/22/94	0.0	24.8	10	1.61
3/30/95	0.1	7.6	-3.7	1.83	8/23/94	0.7	25.3	16.7	1.59
3/31/95	0.62	6	0.3	1.83	8/24/94	0.0	30.3	15.3	1.57
4/1/95	0	4.6	-5.3	1.83	8/25/94	0.9	28.5	13.5	1.55
4/2/95	0	6.8	-8.9	1.83	8/26/94	0.0	25	13.9	1.54
4/3/95	0	8.3	-8.6	1.83	8/27/94	0.0	28.5	15.1	1.52
4/4/95	0.96	2.5	-7.7	1.83	8/28/94	0.0	20.8	8.3	1.50
4/5/95	0	-8.8	-13.8	1.83	8/29/94	0.0	23	6.9	1.48
4/6/95	0	3.6	-10.3	1.83	8/30/94	0.1	14.2	11.3	1.42
4/7/95	0	6.6	-4.3	1.83	8/31/94	0.0	17.9	7.6	1.40
4/8/95	0	9.3	-7.7	1.84	9/1/94	0.0	17	4.5	1.42
4/9/95	0	7.2	-1.5	1.84	9/2/94	0.5	12.3	2.5	1.44

Table 66. Daily rainfall, temperature, and water table depth input for sections 231026 and 271018 (Maine and Minnesota), continued

Maine (231026)					Minnesota (271018)				
Date	Rain (cm)	Max. Temp. °C	Min. Temp. °C	Water Table Depth (m)	Date	Rain (cm)	Max. Temp. °C	Min. Temp. °C	Water Table Depth (m)
4/10/95	0	9.4	-4	1.84	9/3/94	0.2	16.7	9.6	1.45
4/11/95	0	11.9	-6.3	1.84	9/4/94	0.6	16.4	13.9	1.47
4/12/95	0.24	5.7	-2.3	1.84	9/5/94	0.1	19.6	10.4	1.48
4/13/95	0.81	16.1	1.9	1.84	9/6/94	0.0	22	9	1.50
4/14/95	0	8.4	0.4	1.84	9/7/94	0.0	25.9	6.4	1.51
4/15/95	0	5.6	0.3	1.84	9/8/94	0.0	26.6	7.8	1.53
4/16/95	0.01	5.5	-1.8	1.84	9/9/94	0.0	27.8	11.4	1.54
4/17/95	0	10.4	-2.6	1.85	9/10/94	0.0	26.8	14.8	1.56
4/18/95	0	16.6	-3.5	1.85	9/11/94	0.0	26.7	17.7	1.57
4/19/95	0.35	6.9	-1.4	1.85	9/12/94	0.7	21.6	17	1.59
4/20/95	0.01	13.4	-1.8	1.85	9/13/94	0.1	24.9	18.3	1.60
4/21/95	0.8	15.2	-2.7	1.85	9/14/94	1.1	22.8	18.1	1.62
4/22/95	0.01	12.7	5.1	1.85	9/15/94	0.0	25.5	15	1.63
4/23/95	0	8.7	1.7	1.85	9/16/94	0.0	19.3	9.9	1.65
4/24/95	0	12.7	-4.3	1.85	9/17/94	0.0	25	7.4	1.66
4/25/95	0	14.5	-4.1	1.85	9/18/94	0.0	25.9	9.7	1.68
4/26/95	0.04	13.4	-0.3	1.85	9/19/94	0.0	26.1	9.3	1.69
4/27/95	0	14.5	0	1.86	9/20/94	1.6	24.9	11.7	1.71
4/28/95	0.32	10	3	1.86	9/21/94	0.1	20.7	10.5	1.72
4/29/95	0.06	7.7	2.4	1.86	9/22/94	0.7	13.5	9.4	1.74
4/30/95	0.07	10.2	-0.9	1.86	9/23/94	0.0	18.5	9.8	1.75
5/1/95	0.01	16.5	-1.7	1.86	9/24/94	0.0	20.3	9.8	1.77
5/2/95	0	18.3	-0.8	1.86	9/25/94	0.0	14	8	1.78
5/3/95	0	17.9	-0.2	1.86	9/26/94	0.0	9.5	1.4	1.80
5/4/95	0	20.4	-1.2	1.86	9/27/94	0.0	16	0	1.84
5/5/95	0	19.7	0.5	1.86	9/28/94	0.0	15.3	4.3	1.86
5/6/95	0	11.3	1.1	1.86	9/29/94	0.0	20.6	1.3	1.84
5/7/95	0	8.5	-1.3	1.86	9/30/94	0.4	13.7	7.3	1.82
5/8/95	0	15.4	1.6	1.86	10/1/94	0.0	14.5	4.2	1.80
5/9/95	0	21.6	-1.6	1.86	10/2/94	1.2	11.2	3.5	1.79
5/10/95	0	16.6	0.2	1.86	10/3/94	2.0	8.2	5.6	1.77
5/11/95	0.14	12.9	5.9	1.86	10/4/94	0.0	12	6.3	1.75
5/12/95	3.36	10.8	5.9	1.86	10/5/94	0.0	13.5	6.2	1.73

Table 66. Daily rainfall, temperature, and water table depth input for sections 231026 and 271018 (Maine and Minnesota), continued

Maine (231026)					Minnesota (271018)				
Date	Rain (cm)	Max. Temp. °C	Min. Temp. °C	Water Table Depth (m)	Date	Rain (cm)	Max. Temp. °C	Min. Temp. °C	Water Table Depth (m)
5/13/95	1.02	18.7	6.7	1.86	10/6/94	0.3	19	11.6	1.71
5/14/95	0	19.5	4.3	1.86	10/7/94	0.3	14.5	8.7	1.69
5/15/95	2.23	9.1	6.6	1.86	10/8/94	0.2	12	4.5	1.68
5/16/95	0.26	17.5	6.6	1.86	10/9/94	0.0	11.1	-0.3	1.66
5/17/95	1.3	9.1	5.5	1.86	–	–	–	–	–
5/18/95	0.01	18.4	5.6	1.86	–	–	–	–	–
5/19/95	0	18.5	5.9	1.86	–	–	–	–	–
5/20/95	0	19.6	4.3	1.86	–	–	–	–	–
5/21/95	0.98	22.4	1.7	1.86	–	–	–	–	–
5/22/95	0.32	19.5	5.3	1.86	–	–	–	–	–
5/23/95	0	22.8	3.7	1.86	–	–	–	–	–
5/24/95	0	23.1	10.1	1.86	–	–	–	–	–
5/25/95	0	22.9	9.7	1.86	–	–	–	–	–
5/26/95	0	16.4	8.2	1.86	–	–	–	–	–
5/27/95	0.45	16.1	4.8	1.86	–	–	–	–	–
5/28/95	0.17	20.4	1.9	1.86	–	–	–	–	–
5/29/95	0.55	13.6	8.1	1.86	–	–	–	–	–
5/30/95	0.01	20	10.2	1.86	–	–	–	–	–
5/31/95	0	28.2	9	1.86	–	–	–	–	–
6/1/95	0	30.6	10.4	1.86	–	–	–	–	–
6/2/95	0	29.2	13.3	1.86	–	–	–	–	–
6/3/95	1.79	23.1	15.7	1.86	–	–	–	–	–
6/4/95	0.04	23.3	9.9	1.86	–	–	–	–	–
6/5/95	0.1	25	7.8	1.86	–	–	–	–	–
6/6/95	0.16	24.9	9.7	1.86	–	–	–	–	–
6/7/95	0.25	19.2	8.8	1.86	–	–	–	–	–
6/8/95	0	19.5	7.8	1.86	–	–	–	–	–
6/9/95	0	21.8	4.2	1.86	–	–	–	–	–
6/10/95	0	23.4	5.2	1.86	–	–	–	–	–
6/11/95	0.41	15	11.6	1.86	–	–	–	–	–
6/12/95	0.68	17.3	11.9	1.86	–	–	–	–	–
6/13/95	0	22.1	9.4	1.86	–	–	–	–	–
6/14/95	0.95	22.1	7.1	1.86	–	–	–	–	–

Table 66. Daily rainfall, temperature, and water table depth input for sections 231026 and 271018 (Maine and Minnesota), continued

Maine (231026)					Minnesota (271018)				
Date	Rain (cm)	Max. Temp. °C	Min. Temp. °C	Water Table Depth (m)	Date	Rain (cm)	Max. Temp. °C	Min. Temp. °C	Water Table Depth (m)
6/15/95	0.3	16.3	9.2	1.86	–	–	–	–	–
6/16/95	0	26.4	8.9	1.86	–	–	–	–	–
6/17/95	0.04	21.6	8	1.86	–	–	–	–	–
6/18/95	0	30.5	13.5	1.86	–	–	–	–	–
6/19/95	0	36	17.5	1.86	–	–	–	–	–

Table 67. Initial temperature profile data by section used as input to the EICM

041024 (AZ)		081053 (CO)		091803 (CT)		131005 (GA)		231026 (ME)	
Depth (m)	**Temp. (°C)**	**Depth (m)**	**Temp. (°C)**	**Depth (m)**	**Temp. (°C)**	**Depth (m)**	**Temp. (°C)**	**Depth (m)**	**Temp. (°C)**
0.01	23.5	0.01	15.6	0.03	28.7	0.03	31.7	0.03	32.8
0.13	22.4	0.06	15.9	0.09	26.2	0.08	31.2	0.07	30.9
0.25	22.5	0.11	16.4	0.15	25.5	0.14	30.8	0.12	30.5
0.34	22.6	0.17	16.8	0.24	25.0	0.26	30.5	0.21	30.0
0.42	22.7	0.25	17.2	0.32	24.8	0.34	30.3	0.29	29.5
0.50	22.8	0.32	17.5	0.39	24.7	0.42	30.2	0.36	29.2
0.57	23.0	0.40	17.9	0.47	24.3	0.49	30.1	0.44	28.0
0.64	23.0	0.47	18.2	0.54	24.0	0.57	30.0	0.51	27.1
0.80	23.3	0.63	18.6	0.70	23.4	0.72	29.9	0.66	25.6
0.95	23.6	0.78	19.0	0.85	22.9	0.87	29.4	0.82	24.1
1.10	23.9	0.93	19.3	1.00	22.4	1.03	29.3	0.97	22.6
1.25	24.6	1.08	19.6	1.15	21.5	1.18	29.1	1.12	21.0
1.41	25.5	1.24	19.9	1.31	20.8	1.33	28.9	1.28	19.7
1.56	26.3	1.39	20.2	1.46	20.0	1.48	28.7	1.43	18.3
1.71	27.1	1.54	20.4	1.61	18.9	1.64	28.4	1.58	17.2
1.87	27.9	1.69	20.5	1.76	18.2	1.79	28.4	1.73	16.3
2.02	28.6	1.84	20.5	1.92	17.5	1.94	28.2	1.88	15.4
2.17	28.9	1.97	20.4	2.07	16.9	2.09	27.9	2.04	14.6

Table 67. Initial temperature profile data by section used as input to the EICM, continued

271018 (MN)		331001 (NH)		481077 (TX)		501002 (VT)		831801 (MB)	
Depth (m)	Temp. (°C)	Depth (m)	Temp. (°C)	Depth (m)	Temp. (°C)	Depth (m)	Temp. (°C)	Depth (m)	Temp. (°C)
0.03	17.2	0.025	30.3	0.03	6.0	0.03	33.5	0.03	26.3
0.06	17.0	0.1	28.9	0.07	6.9	0.10	30.3	0.05	25.5
0.09	16.9	0.175	28.1	0.11	7.9	0.17	29.3	0.08	24.3
0.38	16.7	0.266	27.0	0.18	8.9	0.25	28.4	0.36	21.3
0.45	16.7	0.342	26.5	0.26	9.4	0.33	27.8	0.43	19.9
0.53	16.6	0.418	26.3	0.33	10.2	0.40	27.9	0.51	18.6
0.60	16.7	0.496	25.5	0.41	10.9	0.48	26.9	0.58	17.7
0.68	16.6	0.57	24.8	0.49	11.5	0.56	26.1	0.66	18.6
0.83	16.7	0.723	23.9	0.64	12.4	0.71	25.4	0.81	15.7
0.99	16.9	0.874	22.7	0.79	13.1	0.86	24.7	0.97	14.1
1.14	17.1	1.028	21.7	0.94	13.8	1.01	24.2	1.12	12.9
1.29	17.3	1.178	20.8	1.10	14.3	1.16	23.3	1.27	11.5
1.45	17.4	1.332	19.7	1.25	15.0	1.32	22.5	1.43	10.3
1.60	17.6	1.482	18.7	1.40	15.7	1.47	21.6	1.58	9.0
1.75	17.7	1.634	18.0	1.55	16.1	1.62	20.7	1.73	7.9
1.90	17.7	1.787	17.3	1.70	16.5	1.78	19.8	1.88	6.8
2.05	17.8	1.941	16.6	1.86	17.0	1.93	18.7	2.03	6.1
2.20	17.8	2.09	15.9	2.01	17.3	2.08	17.6	2.18	5.5

Table 68. Initial moisture profile data by section used in running EICM Version 2.1

041024 (AZ)		081053 (CO)		091803 (CT)		131005 (GA)		231026 (ME)	
Depth (m)	V_w (%)	Depth (m)	V_w (%)	Depth (m)	V_w (%)	Depth (m)	V_w (%)	Depth (m)	V_w (%)
0.35	21.3	0.18	16.5	0.34	20.0	0.30	15.8	0.30	11.3
0.51	21.0	0.33	14.8	0.44	22.5	0.45	21.6	0.46	10.4
0.66	20.1	0.49	18.5	0.59	24.8	0.60	19.7	0.61	12.1
0.80	19.6	0.64	19.8	0.74	20.8	0.75	19.0	0.77	21.2
0.96	20.2	0.80	30.5	0.89	19.4	0.90	19.5	0.91	14.2
1.11	20.0	1.25	45.6	1.05	17.5	1.05	16.9	1.06	21.5
1.27	21.1	—	—	1.20	26.7	1.21	18.4	1.22	24.3
1.41	25.5	—	—	1.35	20.9	1.36	12.2	1.66	36.5
1.72	22.4	—	—	1.66	25.3	1.66	10.5	1.97	25.5
2.03	18.9	—	—	1.96	25.8	1.96	10.8	—	—
271018 (ME)		**331001 (NH)**		**481077 (TX)**		**501002 (VT)**		**831801 (MB)**	
Depth (m)	**V_w (%)**	**Depth (m)**	**V_w (%)**	**Depth (m)**	**V_w (%)**	**Depth (m)**	**V_w (%)**	**Depth (m)**	**V_w (%)**
0.18	13.3	0.36	9.6	0.31	10.5	0.37	10.0	0.20	18.6
0.33	13.4	0.52	9.3	0.46	17.3	0.52	12.0	0.34	14.3
0.49	12.9	0.68	10.1	0.61	21.8	0.66	10.7	0.50	18.7
0.64	15.1	0.82	15.3	0.76	21.0	0.81	20.3	0.65	19.4
0.79	28.7	0.95	16.6	0.91	23.2	1.12	33.5	0.81	28.2
0.94	29.0	1.12	16.6	1.07	16.4	1.27	41.7	0.96	36.1
1.09	29.5	1.28	22.8	1.22	15.9	1.44	41.2	1.11	31.5
1.25	27.8	1.44	24.6	1.37	14.4	1.76	45.3	1.25	31.4
1.55	30.8	1.74	26.7	1.68	14.1	2.05	45.3	1.56	32.4
1.86	30.8	2.05	28.6	1.98	15.2	—	—	1.86	28.5

APPENDIX C: BETWEEN-USER DIFFERENCES IN APPLICATION OF EICM VERSION 2.6

Table 69. Between-user differences in the application of EICM Version 2.6

Section	Input Parameter	Author's Application	NCHRP 1-37A Application[19]
041024	Climatic region (windspeed and percent sunshine)	III-B	III-A
	Depth to water table	152.4 m	90 m
	Number of elements in AC layer	5	6
	Number of elements in base layer	12	5
	Base specific gravity	Not entered	2.65
	Base dry unit weight (gm/cm^3)	2.28	2.23
	Base PI	Not entered	0
	Base p200	Not entered	9.3
	Number of subgrade sublayers	11	10
	Subgrade specific gravity	Not entered	2.7
081053	Climatic region (windspeed and percent sunshine data)	III-A	II-A
	Length of analysis period (days)	571	365
	Number of elements in AC surface	4	3
	Number of elements in base layer	7	3
	Specific gravity	Not entered	2.65
	Base plasticity index	0	Not entered
	Base percent passing 200	Not entered	8.9
	Equilibrium moisture content	15.8	16
	Number of subbase sublayers	5	4
	Subbase specific gravity	Not entered	2.65
	Subbase PI	Not entered	0
	Subbase p200	Not entered	9.4

Table 69. Between-user differences in the application of EICM Version 2.6, continued

Section	Input Parameter	Author's Application	NCHRP 1-37A Application[19]
091803	Number of base layer elements	14	8
	Base layer specific gravity	Not entered	2.65
	Base P200	Not entered	5.8%
	Equilibrium volumetric water content	21.25	22
	Dry thermal K	4.47	6
	Heat capacity	0.17	0.21
	Subgrade dry density	1.64	2.06
	Subgrade PI	Not entered	0
	Subgrade P200	Not entered	12.6
	Subgrade porosity	Not entered	0.34 sublayer 3, 0.28 sublayers 4-6
131005	Simulation start date and analysis period	9/20/95 365 days	8/8/95 435 days
	Base percent fines	8.9	9
	Base percent gravel	52	59
	Base percent sand	39.1	32
	Number of elements in base layer	10	5
	Base specific gravity	Not entered	2.65
	base pi	Not entered	0
	Base percent passing 200	Not entered	8.9
	Equilibrium water content (due to different initial date)	15.77	16.2
	Number of upper subgrade sublayers	6	4
	Number of lower subgrade sublayers	6	5
	Upper subgrade specific gravity	Not entered	2.68
	Lower subgrade specific gravity	Not entered	2.73
	Lower subgrade PI	Not entered	20
	Lower subgrade p200	Not entered	50
	Lower subgrade dry density	1.5	2.0
	Upper subgrade equilibrium water content (due to different initial date)	21.6, 19.7, 18.97, 19.5, 16.93, not entered	19.55, 16, 14.85, 15.6

Table 69. Between-user differences in the application of EICM Version 2.6, continued

Section	Input Parameter	Author's Application	NCHRP 1-37A Application[19]
	Lower subgrade equilibrium water content (due to different initial date)	18.37, 12.23, 10.5, 10.8, not entered	13.5, 16.4, 10.45, 9.55, 9.3, not entered
231026	Emissivity factor	0.9	0.93
	AC thickness (cm)	16.3	16
	Number of elements in base layer	18	10
	Base specific gravity	Not entered	2.65
	Number of subgrade sublayers	8	7
	Subgrade PI	Not entered	0
	Subgrade P200	Not entered	12.6
	Subgrade porosity	Not entered	0.3
271018	Base percent gravel	45	43
	Base percent sand	47.5	49.5
	AC thickness (cm)	11	11.2
	Number of elements in base layer	4	3
	Base porosity	0.24	Not entered
	Equilibrium volumetric water content	13.3	13.4
	Subgrade P200	Not entered	5.2
	Subgrade specific gravity	Not entered	2.65
331001	Emissivity factor	0.9	0.93
	Base percent gravel	62.9	63
	Base percent sand	32.5	32.6
	Number of elements in AC layer	4	5
	Number of elements in base layer	16	10
	Base specific gravity	2.678	2.65
	Equilibrium volumetric water content	9.6	9.7
	Number of subbase sublayers	3	2
	Subbase PI	Not entered	0
	Subgrade PI	Not entered	0
481077	Simulation start date and analysis period	12/15/93, 365 days	4/10/94, 439 days
	Base percent gravel	51	58
	Base percent sand	42	35

Table 69. Between-user differences in the application of EICM Version 2.6, continued

Section	Input Parameter	Author's Application	NCHRP 1-37A Application[19]
	Number of elements for AC layer	4	3
	Number of elements for base layer	12	6
	Base porosity	0.18	Not entered
	Base PI	Not entered	0
	Base p200	Not entered	7
	Base equilibrium water content	10.58	14.9
	Subgrade PI	Not entered	0
	Subgrade P200	Not entered	73.6
	Equilibrium subgrade moisture content	22.4, 26.83, 26.13, 28.23, 21.5, 21.03, 19.53, 19.23, 20.3, not entered	26.7, 30.9, 29.7, 25.7, 22.1, 24.5, 22.4, 20.2, 20.4, not entered
501002	Emissivity factor	0.9	0.93
	Base percent fines	3.3	3.5
	Base percent gravel	89.9	90
	Base percent sand	6.8	6.5
	AC thickness (cm)	22.4	21.1
	Number of elements in AC layer	4	5
	Number of elements in base layer	18	11
	Base specific gravity	Not entered	2.65
	Base percent passing 200	Not entered	3.4
	Base equilibrium volumetric water content	9.6	11
	Number of upper subgrade sublayers	1	2
	Upper subgrade specific gravity	Not entered	2.65
	Number of lower subgrade sublayers	8	6
	Upper subgrade PI	Not entered	0
	Upper subgrade p200	Not entered	6.9
831801	Emissivity factor	0.9	0.93
	Base percent fines	10.9	11
	Base percent sand	37.1	37
	AC thickness (cm)	5.6	11.5

Table 69. Between-user differences in the application of EICM Version 2.6, continued

Section	Input Parameter	Author's Application	NCHRP 1-37A Application[19]
	Base specific gravity	Not entered	2.65
	Percent passing 200	Not entered	10.9
	Base D60	25.6	Not entered
	Subbase specific gravity	Not entered	2.7
	Subbase dry density	2.131	2.17
	Subbase PI	Not entered	11
	Subbase p200	Not entered	10.5
	Subbase D60	6	Not entered
	Subgrade PI	Not entered	0
	Subgrade p200	Not entered	28.8
	Subgrade porosity	0.4	Not entered

APPENDIX D: MATERIALS DATA USED IN DEVELOPMENT OF E PREDICTIVE MODELS

Table 70. Material density, relative density, and PI used in soil class models

Section	Layer	Class	Thickness (m)	Layer Type*	Dry Density (kg/m^3)	Relative Density	PI
040113	2	**A-1-a**	0.19	GB	2164	0.96	0
040113	3	A-1-b	0.91	SS	2097	1.04	0
040113	4	A-1-b	6.40	SS	1930	0.96	0
040114	2	A-1-a	0.31	GB	2108	0.93	0
040114	3	A-2-4	0.91	SS	1800	0.84	7
040114	4	A-2-4	6.22	SS	1800	0.84	7
041024	2	A-1-a	0.16	GB	2278	0.95	0
041024	3	A-2-6	0.91	SS	1956	1.03	20
041024	4	A-2-6	–	SS	1960	1.03	20
081053	2	A-1-a	0.11	GB	2166	0.99	0
081053	3	A-1-a	0.60	GS	2161	1.01	0
081053	4	A-6	0.91	SS	1640	1.02	22
081053	5	A-6	–	SS	1630	1.02	22
091803	2	A-1-a	0.31	GB	2260	1.04	0
091803	3	A-1-a	0.91	SS	1997	0.88	0
091803	4	A-4	–	SS	2265	1.27	4
131005	2	A-1-a	0.23	GB	2230	1.02	0
131005	3	A-4	0.91	SS	1829	0.89	1
131005	4	A-4	–	SS	1690	0.82	1
131031	2	A-1-b	0.22	GB	2168	1.00	0
131031	3	A-4	0.91	SS	1500	0.81	9
131031	4	A-4	13.80	SS	1500	0.81	9
161010	2	A-1-a	0.14	GB	2047	0.90	0
161010	3	A-2-4	0.91	SS	1878	1.03	0

Table 70. Material density, relative density, and PI used in soil class models, continued

Section	Layer	Class	Thickness (m)	Layer Type*	Dry Density (kg/m^3)	Relative Density	PI
161010	4	**A-2-4**	–	SS	1877	1.03	0
231026	2	A-1-a	0.45	GB	2278	1.04	0
231026	3	A-1-b	0.91	SS	1961	0.92	0
231026	4	A-1-b	–	SS	1960	0.92	0
241634	3	A-4	0.33	GS	2006	0.98	0
241634	4	A-4	–	SS	1680	1.03	0
251002	2	A-1-a	0.10	GB	1940	0.81	0
251002	3	A-1-b	0.21	GS	2030	0.98	0
251002	4	A-3	–	SS	1790	1.07	0
271018	2	A-1-b	0.13	GB	2035	0.92	0
271018	3	A-3	0.91	SS	1829	0.98	0
271018	4	A-3	1.16	SS	1828	0.98	0
271028	3	A-1-b	0.91	SS	2017	1.09	0
271028	4	A-1-b	–	SS	2017	1.09	0
276251	2	A-1-b	0.26	GB	2076	0.96	0
276251	3	A-3	0.91	SS	1895	1.00	0
276251	4	A-3	1.39	SS	1858	0.98	0
308129	2	A-1-a	0.58	GB	2209	1.00	0
308129	3	A-6	1.67	SS	1816	0.97	16
308129	4	A-6	–	SS	–	–	16
331001	2	A-1-a	0.49	GB	2150	0.99	0
331001	3	A-1-b	0.37	GS	2100	1.02	0
331001	4	A-2-4	–	SS	1860	1.00	0
351112	2	A-2-4	0.15	GB	1722	0.90	7
351112	3	A-3	0.91	SS	1646	0.97	0
351112	4	A-3	–	SS	1646	0.97	0
481077	2	A-1-a	0.26	GB	2139	0.96	0
481077	3	A-4	0.91	SS	1720	0.94	0
481122	2	A-1-b	0.40	GB	2154	0.97	1
481122	3	A-2-4	0.21	GS	1821	0.94	0
481122	4	A-2-6	–	SS	1851	0.98	12
491001	2	A-1-b	0.15	GB	2094	0.98	0
491001	3	A-2-4	0.91	SS	1812	0.99	0

Table 70. Material density, relative density, and PI used in soil class models, continued

Section	Layer	Class	Thickness (m)	Layer Type*	Dry Density (kg/m^3)	Relative Density	PI
161010	4	**A-2-4**	–	SS	1877	1.03	0
231026	2	A-1-a	0.45	GB	2278	1.04	0
231026	3	A-1-b	0.91	SS	1961	0.92	0
231026	4	A-1-b	–	SS	1960	0.92	0
241634	3	A-4	0.33	GS	2006	0.98	0
491001	4	A-2-4	–	SS	1810	0.99	0
501002	2	A-1-a	0.66	GB	2027	0.88	0
501002	3	A-1-a	0.91	SS	1759	0.80	0
501002	4	A-1-a	–	SS	1761	0.80	0
561007	2	A-1-a	0.16	GB	2046	0.91	0
561007	3	A-2-4	0.91	SS	1917	0.99	0
561007	4	A-2-4	–	SS	1916	0.99	0
831801	2	A-1-a	0.14	GB	2084	0.95	5
831801	3	A-2-6	0.34	GS	1936	0.89	11
831801	4	A-2-4	–	SS	1829	1.08	0
871622	2	A-1-b	0.17	GB	2007	0.90	0
871622	3	A-1-b	0.67	GS	1951	1.02	0
871622	4	A-4	–	SS	1809	1.02	0
906405	2	A-1-a	0.23	GB	2151	0.95	0
906405	3	A-1-b	0.91	SS	2039	1.16	0
906405	4	A-1-b	–	SS	2039	1.16	0

*GB = granular base; GS = granular subbase; SS = subgrade soil

Table 71. Material gradation used in soil class models

Section and Layer		Percent Passing											
		3”	2”	1.5”	1”	¾”	½”	⅜”	No. 4	No. 10	No. 40	No. 80	No. 200
040113	2	100	100	100	100	94	81	75	61	49	27	18	11
040113	3	100	100	98	96	93	89	86	77	58	22	11	9
040113	4	100	100	98	96	93	89	86	77	58	22	11	9
040114	2	100	100	100	100	94	81	75	61	49	27	18	11
040114	3	100	96	94	85	82	77	74	64	51	31	24	18
040114	4	100	96	94	85	82	77	74	64	51	31	24	18
041024	2	100	100	100	88	71	53	46	32	23	17	14	9
041024	3	100	100	97	92	89	85	83	79	73	59	47	31
041024	4	100	100	97	92	89	85	83	79	73	59	47	31
081053	2	100	100	100	100	98	78	66	47	35	22	14	9
081053	3	100	77	77	72	65	57	52	42	33	21	14	9
081053	4	100	100	100	100	100	100	100	97	97	96	94	92
081053	5	100	100	100	100	100	100	100	97	97	96	94	92
091803	2	92	89	85	76	71	63	58	49	40	22	11	6
091803	3	91	89	83	75	69	62	57	49	43	28	18	11
091803	4	100	100	100	98	97	94	90	89	86	74	64	54
131005	2	100	100	100	94	83	68	61	48	41	30	18	9
131005	3	100	100	100	100	100	100	100	100	100	95	79	36
131005	4	100	100	100	100	100	100	100	100	100	95	79	36
131031	2	100	100	100	99	97	95	94	93	78	48	29	11
131031	3	100	100	99	97	94	91	90	88	84	69	56	43
131031	4	100	100	99	97	94	91	90	88	84	69	56	43
161010	2	100	100	100	100	100	87	68	46	34	25	16	8
161010	3	100	100	100	100	100	100	99	97	88	66	38	13
161010	4	100	100	100	100	100	100	99	97	88	66	38	13
231026	2	71	61	59	50	45	41	38	32	26	13	7	4
231026	3	94	89	85	78	74	69	66	60	54	36	23	11
231026	4	94	89	85	78	74	69	66	60	54	36	23	11

Table 71. Material gradation used in soil class models, continued

Section and Layer		Percent Passing											
		3”	2”	1.5”	1”	¾”	½”	⅜”	No. 4	No. 10	No. 40	No. 80	No. 200
241634	3	100	100	100	100	100	100	100	100	99	99	99	99
241634	4	100	100	100	100	100	100	100	100	100	99	99	99
251002	2	100	100	97	79	69	62	57	46	24	13	9	7
251002	3	91	86	83	80	77	72	69	61	52	28	15	10
251002	4	100	100	100	100	100	100	99	99	98	72	19	7
271018	2	100	100	100	100	95	85	80	68	57	29	13	8
271018	3	100	100	100	100	100	99	98	97	95	72	12	5
271018	4	100	100	100	100	100	99	98	97	95	72	12	5
271028	3	100	100	100	99	98	97	96	92	86	43	12	6
271028	4	100	100	100	99	98	97	96	92	86	43	12	6
276251	2	100	100	100	100	98	93	91	85	75	38	16	9
276251	3	100	100	100	100	100	100	99	99	97	72	18	8
276251	4	100	100	100	100	100	100	99	99	97	72	18	8
308129	2	100	100	100	100	95	76	66	43	29	21	12	8
308129	3	100	100	100	99	97	93	90	84	79	76	72	60
308129	4	100	100	100	99	97	93	90	84	79	76	72	60
331001	2	100	100	100	77	68	59	52	44	37	16	8	5
331001	3	100	100	97	93	89	85	81	75	68	37	17	8
331001	4	100	100	100	99	99	98	97	95	93	74	40	15
351112	2	100	100	100	98	95	89	83	67	59	49	36	15
351112	3	100	100	100	100	100	100	100	99	99	96	70	4
351112	4	100	100	100	100	100	100	100	99	99	96	70	4
481077	2	100	100	100	91	82	69	61	49	42	25	12	7
481077	3	100	100	100	100	99	99	98	97	97	94	90	74
481122	2	100	99	99	94	88	77	69	53	43	31	27	23
481122	3	100	99	99	99	98	97	97	96	96	64	34	19
481122	4	100	100	100	100	100	100	99	99	98	72	46	32
491001	2	100	100	100	100	99	86	74	63	56	49	32	13
491001	3	100	100	100	100	100	100	99	97	96	91	50	14
491001	4	100	100	100	100	100	100	99	97	96	91	50	14
501002	2	100	93	83	56	45	31	24	15	10	5	4	3
501002	3	94	92	88	80	76	70	62	48	38	17	10	7
501002	4	94	92	88	80	76	70	62	48	38	17	10	7
561007	2	100	100	100	100	98	81	70	51	40	28	18	10

Table 71. Material gradation used in soil class models, continued

Section and Layer		Percent Passing											
		3”	2”	1.5”	1”	¾”	½”	⅜”	No. 4	No. 10	No. 40	No. 80	No. 200
561007	3	100	100	100	100	100	98	96	88	84	78	52	24
561007	4	100	100	100	100	100	98	96	88	84	78	52	24
831801	2	100	100	100	100	100	85	78	62	48	23	12	11
831801	3	100	100	100	91	85	74	69	57	47	17	12	11
831801	4	100	100	100	100	100	100	100	100	99	93	49	29
871622	2	100	100	100	100	96	83	75	63	53	31	19	13
871622	3	80	80	79	76	74	72	70	67	63	47	23	12
871622	4	100	100	100	100	100	100	100	100	100	99	84	52
906405	2	100	100	100	99	99	90	88	65	48	28	12	9
906405	3	100	100	100	100	100	100	99	99	98	40	7	5
906405	4	100	100	100	100	100	100	99	99	98	40	7	5

Table 72. Source tables for materials data used in predictive models for backcalculated pavement layer moduli

Variable	Source Data Table	Comments
Moisture content	SMP_TDR_AUTO_MOISTURE	Within-day mean of all observations for layer
Moisture content; optimum moisture content	SMP_TDR_AUTO_MOISTURE + TST_SS05_UG05	
Distance to water table	SMP_WATERTAB_DEPTH_MAN	Relative to mid-layer depth for finite layers; relative to depths used for stress computations for semi-infinite layers
Density	TST_ISD_MOIST	Values for instrumented end of section where available; those for opposite end of section as backup. Gradation and density for section 091803 subgrade layers from reference [82]

APPENDIX E: MULTIPLE REGRESSION RESULTS FOR INDIVIDUAL PAVEMENT LAYERS

Table 73. Multiple regression results for Model 1

Section	Layer & Class	Log k_0	c_1	k_2	k_3	r2 (log E)	n	% Bias	S_e/S_y (ref. E)
040113	**2 A-1-a**	2.904	-0.002	-0.256	**1.369**	0.81	63	0	0.59
040113	3 A-1-b	2.085	0.009	-1.552	8.287	0.89	110	0	0.33
040113	4 A-1-b	6.214	0.008	21.799	-104.9	0.67	110	0	0.57
040114	2 A-1-a	3.197	-0.012	-0.629	3.312	0.79	13	5	0.88
040114	3 A-2-4	2.614	0.001	-1.548	8.334	0.55	13	0	0.77
040114	4 A-2-4	2.999	-0.037	84.985	-283.7	0.78	13	0	0.52
041024	2 A-1-a	3.190	-0.006	-0.346	0.310	0.78	16	-1	0.49
041024	3 A-2-6	1.006	-0.002	-4.861	29.47	0.94	18	0	0.26
041024	4 A-2-6	4.996	0.006	4.459	-24.25	0.83	17	0	0.46
081053	2 A-1-a	3.235	0.000	-0.092	0.812	0.83	21	0	0.47
081053	3 A-1-a	2.604	0.004	-0.679	4.983	0.82	43	0	0.45
091803	2 A-1-a	3.502	-0.024	-0.522	2.593	0.78	288	-1	0.69
131005	2 A-1-a	3.077	-0.007	-0.496	2.130	0.71	76	-1	0.58
131005	3 A-4	2.837	-0.026	-1.757	12.832	0.74	76	0	0.53
131005	4 A-4	3.385	-0.007	-1.424	0.405	0.59	76	0	0.65
131031	2 A-1-b	3.890	-0.009	-0.140	-2.983	0.54	30	-1	0.77
131031	3 A-4	4.155	-0.029	0.087	-11.24	0.47	107	-1	0.73
131031	4 A-4	-2.011	-0.003	54.244	-164.6	0.19	107	0	0.91
161010	3 A-2-4	0.785	0.000	-3.940	29.79	0.60	31	-1	0.66
161010	4 A-2-4	9.309	0.008	16.768	-70.52	0.78	31	-1	0.61
231026	2 A-1-a	3.169	-0.013	-0.545	2.267	0.73	191	-1	0.54
231026	3 A-1-b	0.353	0.003	-7.910	35.23	0.88	191	0	0.36
241634	3 A-4	3.255	-0.035	-1.015	6.935	0.85	109	-1	0.38
241634	4 A-4	4.418	-0.031	0.247	-1.975	0.33	109	0	0.84
251002	2 A-1-a	2.959	-0.015	-0.071	2.419	0.92	14	-1	0.35
251002	3 A-1-b	2.394	-0.006	-1.578	7.833	0.85	15	0	0.38
251002	4 A-3	3.314	-0.007	-0.084	1.241	0.27	15	0	0.97
271018	2 A-1-b	2.845	0.009	-0.329	1.838	0.87	33	-1	0.42
271018	3 A-3	3.208	-0.017	-0.763	0.489	0.37	33	0	0.83
271028	3 A-1-b	1.690	0.001	-3.406	13.78	0.80	80	0	0.45
271028	4 A-1-b	2.629	0.000	-1.665	5.658	0.02	80	0	1.01
276251	2 A-1-b	3.189	-0.005	-0.419	2.213	0.68	13	0	0.66

Table 73. Multiple regression results for Model 1, continued

Section	Layer & Class	Log k_0	c_1	k_2	k_3	r2 (log E)	n	% Bias	S_e/S_y (ref. E)
276251	**3 A-3**	2.602	0.002	-1.296	**5.432**	0.92	13	0	0.32
308129	2 A-1-a	2.733	0.003	-0.599	2.370	0.77	201	0	0.48
308129	3 A-6	1.184	0.010	-8.615	18.32	0.76	178	0	0.49
331001	2 A-1-a	2.881	0.004	-0.383	2.796	0.81	216	-1	0.48
331001	3 A-1-b	-0.626	-0.001	-6.563	57.14	0.82	216	-1	0.63
331001	4 A-2-4	4.573	-0.003	1.933	-11.56	0.26	216	-1	0.86
351112	2 A-2-4	3.152	0.004	-0.152	1.979	0.59	285	-5	0.85
351112	3 A-3	1.520	-0.008	-3.948	16.46	0.87	321	-1	0.37
351112	4 A-3	4.007	0.001	0.937	-6.440	0.30	276	0	0.84
481077	2 A-1-a	3.189	0.010	-0.150	1.178	0.68	467	-1	0.61
481077	3 A-4	2.858	-0.001	-0.810	4.574	0.10	533	-1	0.97
491001	2 A-1-b	3.140	-0.013	-0.173	0.705	0.89	7	0	0.50
491001	3 A-2-4	0.753	0.006	-4.013	21.93	0.88	11	0	0.45
491001	4 A-2-4	4.423	0.017	3.206	-15.86	0.78	10	0	0.59
501002	2 A-1-a	3.043	0.000	-0.824	2.132	0.71	356	-1	0.55
561007	2 A-1-a	3.119	-0.003	-0.455	0.743	0.80	104	0	0.54
561007	3 A-2-4	2.052	-0.007	-2.582	9.198	0.38	107	0	0.80
831801	3 A-2-6	5.890	-0.211	-0.881	4.494	0.99	5	0	0.19
831801	4 A-2-4	4.723	-0.015	1.544	-10.01	1.00	5	0	0.05
871622	2 A-1-b	3.230	-0.002	-0.130	1.247	0.85	143	0	0.41
871622	3 A-1-b	1.961	0.000	-2.400	11.56	0.55	198	0	0.69
871622	4 A-4	3.969	-0.004	0.964	-5.956	0.15	198	0	0.93
906405	2 A-1-a	3.447	-0.024	-0.466	1.430	0.85	18	0	0.42
906405	3 A-1-b	1.917	0.004	-3.075	10.31	0.89	18	0	0.38
906405	4 A-1-b	5.693	0.006	6.671	-22.88	0.54	18	0	0.75

Table 74. Multiple regression results for set 1 (both load and overburden with K_0 values of 0.7 and 0.5 for base and subbase/subgrade layers, respectively)

Section	Layer	k_1	k_2	k_3	r^2	S_e/S_y	n
040113	2	759.70	-0.23	1.39	0.80	0.46	41
040113	3	232.31	-1.31	6.37	0.87	0.36	88
040114	2	1108.25	-0.61	2.87	0.71	0.61	11
040114	3	1110.13	-0.46	4.79	0.57	0.73	11
041024	2	1261.30	-0.41	-0.26	0.72	0.55	28
041024	3	320.81	-1.99	6.42	0.35	0.83	36
081053	2	1690.59	-0.09	0.83	0.85	0.41	24
081053	3	449.61	-0.78	5.19	0.75	0.53	19
091803	2	914.91	-0.55	2.72	0.75	0.50	238
131005	2	874.96	-0.47	2.19	0.67	0.59	66
131005	3	354.51	-0.86	10.91	0.48	0.73	66
131031	2	5338.20	-0.11	-2.61	0.49	0.74	30
131031	3	1316.86	-0.40	-4.22	0.18	0.91	115
161010	2	2114.72	-0.17	1.87	0.34	0.89	13
161010	3	40.47	-3.31	13.63	0.79	0.47	59
231026	2	1139.25	-0.51	2.09	0.64	0.60	166
231026	3	122.96	-3.56	14.72	0.37	0.80	166
251002	2	962.85	-0.16	1.30	0.73	0.53	32
251002	3	267.11	-0.41	6.05	0.73	0.53	188
271018	2	1020.12	-0.24	1.58	0.83	0.42	34
271028	3	503.71	-1.28	6.33	0.51	0.71	80
276251	2	1614.02	-0.18	1.84	0.59	0.67	23
308129	2	615.37	-0.55	2.23	0.78	0.47	146
308129	3	314.10	-5.42	4.91	0.44	0.75	104
331001	2	857.87	-0.40	2.68	0.75	0.50	226
331001	3	31.96	-2.31	25.04	0.40	0.78	226
351112	2	1533.68	-0.15	2.00	0.61	0.63	292
351112	3	72.82	-3.40	13.49	0.72	0.53	316
481077	2	1907.43	-0.17	1.21	0.67	0.58	454
481077	3	1096.66	-0.48	2.50	0.05	0.98	517
491001	2	885.58	-0.25	0.66	0.77	0.51	19
491001	3	191.43	-1.18	5.87	0.30	0.88	23
501002	2	1115.68	-0.81	2.21	0.71	0.54	325
561007	2	1319.13	-0.50	0.61	0.77	0.49	118

Table 74. Multiple regression results for set 1 (both load and overburden with K0 values of 0.7 and 0.5 for base and subbase/subgrade layers, respectively), continued

Section	Layer	k_1	k_2	k_3	r^2	S_e/S_y	N
561007	3	154.57	-2.07	7.36	0.54	0.68	121
831801	3	135.33	-1.08	9.40	0.31	0.88	21
871622	2	1592.09	-0.13	1.25	0.82	0.42	131
871622	3	381.00	-1.23	6.14	0.42	0.77	182
906405	2	1274.81	-0.45	1.30	0.64	0.64	19
906405	3	381.34	-1.81	5.29	0.77	0.51	19

Table 75. Multiple regression results for set 2 (overburden only in computation of octahedral shear stress, K_0 values of 0.7 and 0.5 for base and subbase/subgrade layers, respectively)

Section	Layer	k_1	k_2	k_3	r^2	S_e/S_y	n
040113	2	761.58	-0.23	1.41	0.80	0.46	41
040113	3	398.55	-1.04	4.47	0.83	0.41	88
040114	2	940.31	-0.79	3.52	0.85	0.43	11
040114	3	1695.79	-0.22	2.98	0.34	0.91	11
041024	2	1275.96	-0.42	-0.39	0.72	0.55	28
041024	3	416.90	-2.04	7.62	0.38	0.81	36
081053	2	1693.11	-0.09	0.84	0.85	0.40	24
081053	3	681.92	-0.64	3.82	0.68	0.60	19
091803	2	939.87	-0.55	2.75	0.75	0.50	238
131005	2	904.72	-0.46	2.16	0.68	0.58	66
131005	3	673.56	-0.72	9.50	0.43	0.77	66
131031	2	4807.23	-0.11	-2.25	0.42	0.79	30
131031	3	1032.31	-0.58	-6.87	0.30	0.85	115
161010	2	1731.02	-0.20	2.76	0.40	0.85	13
161010	3	77.72	-3.19	14.35	0.73	0.53	59
231026	2	1167.66	-0.51	2.10	0.63	0.61	166
231026	3	275.01	-3.85	14.90	0.52	0.70	166
251002	2	1126.50	-0.85	0.20	0.62	0.64	25
251002	3	295.14	-0.46	6.21	0.74	0.51	188
271018	2	1032.97	-0.24	1.56	0.83	0.43	34
271028	3	381.89	-2.00	7.83	0.57	0.67	80

Table 75. Multiple regression results for set 2 (overburden only in computation of octahedral shear stress, K0 values of 0.7 and 0.5 for base and subbase/subgrade layers, respectively), continued

Section	Layer	k_1	k_2	k_3	r^2	S_e/S_y	n
276251	2	1647.40	-0.18	1.85	0.61	0.65	23
308129	2	646.00	-0.52	2.19	0.75	0.50	146
308129	3	377.80	-4.87	18.51	0.47	0.74	104
331001	2	892.74	-0.41	2.62	0.76	0.49	226
331001	3	134.05	-1.73	23.75	0.38	0.79	226
351112	2	1555.58	-0.15	1.99	0.61	0.63	292
351112	3	127.28	-3.39	12.94	0.76	0.49	316
481077	2	1935.18	-0.17	1.20	0.66	0.58	454
481077	3	1408.19	-0.32	1.63	0.03	0.99	517
491001	2	890.86	-0.25	0.63	0.77	0.51	19
491001	3	296.42	-0.81	6.86	0.49	0.75	23
501002	2	1169.05	-0.82	2.14	0.70	0.55	325
561007	2	1317.74	-0.50	0.62	0.77	0.48	118
561007	3	355.03	-1.58	4.13	0.42	0.77	121
831801	3	168.04	-1.08	9.40	0.31	0.88	21
871622	2	1608.17	-0.13	1.24	0.82	0.43	131
871622	3	396.81	-1.41	6.85	0.25	0.87	182
906405	2	1264.00	-0.45	1.32	0.65	0.63	19
906405	3	516.81	-1.69	5.08	0.80	0.48	19

Table 76. Multiple regression results for set 3 (both load and overburden with K_0 values of 1.0 for all layers)

Section	Layer	k_1	k_2	k_3	r^2	S_e/S_y	n
040113	2	755.02	-0.28	1.43	0.83	0.42	41
040113	3	569.77	-1.02	3.66	0.85	0.40	88
040114	2	949.52	-0.88	3.65	0.85	0.43	11
040114	3	1801.15	-0.31	2.97	0.34	0.91	11
041024	2	1569.42	-0.12	0.57	0.31	0.86	29
041024	3	724.80	-2.91	7.71	0.41	0.79	36
081053	2	1698.31	-0.10	0.83	0.87	0.38	25
081053	3	734.30	-0.84	3.99	0.70	0.58	19
091803	2	985.97	-0.58	2.75	0.74	0.51	239

Table 76. Multiple regression results for set 3 (both load and overburden with K0 values of 1.0 for all layers), continued

Section	Layer	k_1	k_2	k_3	r^2	S_e/S_y	n
131005	2	902.91	-0.53	2.21	0.68	0.57	66
131005	3	819.89	-1.01	9.27	0.43	0.76	66
131031	2	4566.10	-0.17	-2.11	0.48	0.75	33
131031	3	1361.67	-0.45	-7.45	0.26	0.87	115
161010	2	4021.59	-0.01	0.16	0.00	1.07	17
161010	3	162.73	-4.62	14.87	0.72	0.54	59
231026	2	1197.10	-0.59	2.11	0.64	0.61	166
231026	3	984.64	-6.02	14.19	0.53	0.69	166
251002	2	922.50	-0.23	1.33	0.82	0.44	32
251002	3	297.87	-0.61	6.52	0.74	0.51	188
271018	2	1035.21	-0.26	1.58	0.83	0.42	34
271028	3	576.52	-2.69	7.79	0.58	0.65	80
276251	2	1626.15	-0.21	1.90	0.63	0.64	23
308129	2	667.58	-0.58	2.20	0.75	0.50	146
308129	3	2872.10	-4.90	7.21	0.28	0.86	104
331001	2	882.36	-0.52	2.67	0.77	0.48	226
331001	3	206.03	-2.31	23.33	0.38	0.79	226
351112	2	1521.36	-0.23	2.01	0.64	0.60	294
351112	3	235.52	-4.49	12.74	0.75	0.50	316
481077	2	1962.00	-0.18	1.18	0.66	0.59	459
481077	3	1682.95	-0.16	0.90	0.01	1.00	517
491001	2	1012.21	-0.19	0.68	0.57	0.69	20
491001	3	354.65	-1.07	6.58	0.56	0.70	23
501002	2	1248.78	-0.96	2.15	0.71	0.54	325
561007	2	1500.09	-0.31	0.29	0.57	0.66	119
561007	3	504.41	-2.02	3.91	0.42	0.77	121
831801	3	191.00	-1.23	9.36	0.30	0.88	21
871622	2	1684.76	-0.06	1.30	0.78	0.48	136
871622	3	575.42	-1.59	6.12	0.20	0.90	182
906405	2	1276.23	-0.45	1.32	0.64	0.63	19
906405	3	775.60	-2.23	5.06	0.77	0.51	19

Table 77. Multiple regression results for set 4 (both load and overburden with K_0 values of 2.0 and 1.0 for base and subbase/subgrade layers, respectively)

		Set 4: Load & Overburden, k0 = 2.0, 1.0					
Section	**Layer**	**k_1**	**k_2**	**k_3**	**r^2**	**S_e/S_y**	**n**
040113	2	794.49	-0.38	1.43	0.86	0.38	41
040113	3	569.77	-1.02	3.66	0.85	0.40	88
040114	2	1410.32	-0.95	3.05	0.75	0.56	11
040114	3	1801.15	-0.31	2.97	0.34	0.91	11
041024	2	1427.35	-0.60	-0.27	0.72	0.55	31
041024	3	724.80	-2.91	7.71	0.41	0.79	36
081053	2	1687.40	-0.10	0.91	0.85	0.41	28
081053	3	734.30	-0.84	3.99	0.70	0.58	19
091803	2	1328.95	-0.71	2.38	0.69	0.56	240
131005	2	1049.00	-0.75	2.20	0.68	0.58	66
131005	3	819.89	-1.01	9.27	0.43	0.76	66
131031	2	4406.89	-0.18	-1.47	0.34	0.83	50
131031	3	1361.67	-0.45	-7.45	0.26	0.87	115
161010	2	3858.45	-0.01	0.54	0.02	1.03	27
161010	3	162.73	-4.62	14.87	0.72	0.54	59
231026	2	1558.81	-0.84	2.02	0.64	0.60	166
231026	3	984.64	-6.02	14.19	0.53	0.69	166
251002	2	1129.93	-0.25	0.93	0.76	0.50	38
251002	3	297.87	-0.61	6.52	0.74	0.51	188
271018	2	1091.74	-0.32	1.62	0.86	0.39	34
271028	3	576.52	-2.69	7.79	0.58	0.65	80
276251	2	1809.70	-0.30	1.83	0.60	0.66	23
308129	2	862.64	-0.86	2.11	0.76	0.50	146
308129	3	2872.10	-4.90	7.21	0.28	0.86	104
331001	2	1161.50	-0.83	2.76	0.76	0.49	226
331001	3	206.03	-2.31	23.33	0.38	0.79	226
351112	2	1660.70	-0.23	1.97	0.64	0.60	300
351112	3	235.52	-4.49	12.74	0.75	0.50	316
481077	2	2077.54	-0.25	1.16	0.68	0.57	463
481077	3	1682.95	-0.16	0.90	0.01	1.00	517
491001	2	893.57	-0.40	0.64	0.76	0.52	21
491001	3	354.65	-1.07	6.58	0.56	0.70	23
501002	2	2012.55	-1.47	2.21	0.66	0.58	325

Table 77. Multiple regression results for set 4 (both load and overburden with K values of 2.0 and 1.0 for base and subbase/subgrade layers, respectively), continued

Section	Layer	k_1	k_2	k_3	r^2	S_e/S_y	n
561007	2	1525.87	-0.24	0.25	0.51	0.71	121
561007	3	504.41	-2.02	3.91	0.42	0.77	121
831801	3	191.00	-1.23	9.36	0.30	0.88	21
871622	2	1748.98	-0.12	1.22	0.81	0.43	145
871622	3	575.42	-1.59	6.12	0.20	0.90	182
906405	2	1389.72	-0.50	1.31	0.70	0.58	19
906405	3	775.60	-2.23	5.06	0.77	0.51	19

Table 78. Multiple regression results for set 5 (octahedral shear stress based on computed for load stresses only, K_0 values of 2.0 and 1.0 for base and subbase/subgrade layers, respectively)

Section	Layer	k_1	k_2	k_3	r^2	S_e/S_y	n
040113	2	763.22	-0.38	1.47	0.87	0.37	41
040113	3	569.77	-1.02	3.66	0.85	0.40	88
040114	2	93.77	-0.99	1.13	0.76	0.55	11
040114	3	1801.15	-0.31	2.97	0.34	0.91	11
041024	2	1462.56	-0.62	-0.41	0.72	0.54	31
041024	3	724.80	-2.91	7.71	0.41	0.79	36
081053	2	1656.90	-0.09	0.93	0.85	0.40	28
081053	3	734.30	-0.84	3.99	0.70	0.58	19
091803	2	1189.00	-0.71	2.50	0.69	0.56	240
131005	2	973.39	-0.74	2.26	0.68	0.57	66
131005	3	819.89	-1.01	9.27	0.43	0.76	66
131031	2	4795.73	-0.18	-1.61	0.34	0.83	50
131031	3	1361.67	-0.45	-7.45	0.26	0.87	115
161010	2	3716.49	-0.01	0.66	0.02	1.03	27
161010	3	162.73	-4.62	14.87	0.72	0.54	59
231026	2	1393.96	-0.84	2.12	0.64	0.61	166
231026	3	984.64	-6.02	14.19	0.53	0.69	166
251002	2	1096.84	-0.25	0.96	0.77	0.50	38
251002	3	297.87	-0.61	6.52	0.74	0.51	188
271018	2	1057.94	-0.32	1.62	0.85	0.40	34
271028	3	576.52	-2.69	7.79	0.58	0.65	80
276251	2	1648.88	-0.32	1.97	0.64	0.63	23
308129	2	780.08	-0.81	2.16	0.74	0.51	146
308129	3	2872.10	-4.90	7.21	0.28	0.86	104
331001	2	999.51	-0.85	2.74	0.78	0.47	226
331001	3	206.03	-2.31	23.33	0.38	0.79	226
351112	2	1579.95	-0.22	2.01	0.64	0.60	300
351112	3	235.52	-4.49	12.74	0.75	0.50	316
481077	2	2001.72	-0.25	1.18	0.68	0.57	463
481077	3	1682.95	-0.16	0.90	0.01	1.00	517
491001	2	880.53	-0.40	0.64	0.76	0.52	21
491001	3	354.65	-1.07	6.58	0.56	0.70	23
501002	2	1767.21	-1.54	2.15	0.70	0.55	325

Table 78. Multiple regression results for set 5 (octahedral shear stress based on computed for load stresses only, K0 values of 2.0 and 1.0 for base and subbase/subgrade layers, respectively), continued

Section	Layer	k_1	k_2	k_3	r^2	S_e/S_y	n
561007	2	1524.13	-0.24	0.24	0.50	0.71	121
561007	3	504.41	-2.02	3.91	0.42	0.77	121
831801	3	191.00	-1.23	9.36	0.30	0.88	21
871622	2	1694.34	-0.12	1.24	0.82	0.43	145
871622	3	575.42	-1.59	6.12	0.20	0.90	182
906405	2	1329.92	-0.49	1.34	0.67	0.61	19
906405	3	775.60	-2.23	5.06	0.77	0.51	19

Table 79. Multiple regression results for set 6 (bulk and octahedral shear stress computed based on load only)

Section	Layer	k_1	k_2	k_3	r^2	S_e/S_y	n
040113	2	738.37	-0.21	1.29	0.82	0.43	139
040113	3	246.91	-0.48	7.44	0.53	0.69	141
040114	2	947.43	-0.47	3.12	0.72	0.57	15
040114	3	1917.47	-0.01	2.51	0.35	0.87	15
041024	2	961.57	-0.23	1.08	0.61	0.64	43
041024	3	411.49	-0.44	7.62	0.33	0.83	66
081053	2	1686.24	-0.10	0.81	0.69	0.58	38
081053	3	456.58	-0.44	5.27	0.76	0.49	118
091803	2	976.20	-0.23	2.67	0.68	0.57	323
131005	2	1062.33	-0.18	1.76	0.57	0.66	76
131005	3	738.28	-0.15	7.83	0.38	0.80	78
131031	2	4579.75	0.01	-1.35	0.72	0.68	6
131031	3	405.53	-0.32	2.81	0.79	0.46	138
161010	2	1506.32	-0.20	2.35	0.66	1.01	4
161010	3	316.30	-0.13	15.49	0.28	0.87	46
231026	2	1076.09	-0.27	2.17	0.62	0.62	187
231026	3	226.75	-0.74	13.95	0.44	0.75	192
251002	2	784.17	-0.14	1.72	0.82	0.44	33
251002	3	307.00	-0.22	5.59	0.74	0.51	270

Table 79. Multiple regression results for set 6 (bulk and octahedral shear stress computed based on load only), continued

Section	Layer	k_1	k_2	k_3	r^2	S_e/S_y	n
271018	2	919.76	-0.30	1.77	0.82	0.42	80
271028	3	483.81	-0.50	8.16	0.60	0.64	80
276251	2	1256.96	-0.18	2.58	0.76	0.52	23
308129	2	584.03	-0.30	2.28	0.73	0.52	217
308129	3	223.89	-0.31	26.09	0.48	0.72	217
331001	2	951.20	-0.08	3.17	0.64	0.60	201
331001	3	150.27	-0.44	21.03	0.35	0.81	245
351112	2	1436.31	-0.19	2.03	0.64	0.60	303
351112	3	164.89	-1.04	13.58	0.77	0.48	337
481077	2	1887.45	-0.14	1.16	0.65	0.59	505
481077	3	526.13	-0.44	7.11	0.22	0.88	573
491001	2	964.72	-0.06	0.69	0.38	0.81	40
491001	3	185.72	-0.39	9.33	0.30	0.84	105
501002	2	1319.73	-0.19	2.34	0.63	0.61	387
561007	2	1202.55	-0.44	0.67	0.73	0.52	147
561007	3	472.42	-0.42	2.76	0.33	0.82	151
831801	3	146.47	-0.73	9.19	0.31	0.87	21
871622	2	1547.85	-0.09	1.31	0.81	0.44	141
871622	3	410.74	-0.52	6.56	0.22	0.89	211
906405	2	1234.98	-0.40	1.26	0.61	0.66	21
906405	3	533.69	-0.47	4.90	0.74	0.54	21

Table 80. Multiple regression results for set 7 (bulk stress computed based on load stresses only, octahedral shear stress computed based on both load and overburden with K_0 values of 0.7 and 0.5 for base and subbase/subgrade layers, respectively)

Section	Layer	k_1	k_2	k_3	r^2	S_e/S_y	n
040113	2	667.16	-0.27	1.56	0.90	0.33	40
040113	3	115.20	-0.59	10.13	0.41	0.78	88
040114	2	1050.50	-0.38	2.80	0.71	0.61	11
040114	3	1075.57	-0.12	4.91	0.57	0.73	11
041024	2	902.12	-0.25	1.44	0.66	0.62	21
041024	3	295.52	-0.48	6.70	0.37	0.82	36
081053	2	1595.86	-0.07	0.92	0.81	0.46	18
081053	3	401.69	-0.39	5.37	0.79	0.49	19
091803	2	961.16	-0.21	2.78	0.67	0.58	227
131005	2	1031.14	-0.18	1.79	0.57	0.67	64
131005	3	419.06	-0.17	9.41	0.46	0.75	66
131031	3	381.02	-0.31	2.67	0.81	0.44	115
161010	2	1777.41	-0.19	1.63	0.51	1.21	4
161010	3	165.62	-0.25	11.27	0.22	0.90	44
231026	2	1054.38	-0.27	2.16	0.63	0.62	163
231026	3	90.93	-0.75	14.57	0.35	0.81	166
251002	2	753.61	-0.10	1.95	0.87	0.38	25
251002	3	279.62	-0.21	5.52	0.72	0.53	188
271018	2	923.62	-0.21	1.74	0.82	0.44	33
271028	3	557.45	-0.33	6.69	0.53	0.69	80
276251	2	1252.19	-0.17	2.51	0.70	0.58	21
308129	2	588.59	-0.29	2.18	0.76	0.49	146
308129	3	178.74	-0.36	6.12	0.52	0.70	104
331001	2	833.02	-0.12	3.22	0.78	0.48	188
331001	3	31.25	-0.71	23.69	0.38	0.79	226
351112	2	1423.09	-0.18	2.06	0.63	0.61	282
351112	3	110.33	-0.99	13.22	0.70	0.55	316
481077	2	1791.16	-0.14	1.25	0.68	0.56	430
481077	3	418.46	-0.42	6.70	0.22	0.89	517

Table 80. Multiple regression results for set 7 (bulk stress computed based on load stresses only, octahedral shear stress computed based on both load and overburden with K_0 values of 0.7 and 0.5 for base and subbase/subgrade layers, respectively), continued

Section	Layer	k_1	k_2	k_3	r^2	S_e/S_y	n
491001	2	886.82	-0.10	1.16	0.61	0.69	12
491001	3	189.31	-0.35	6.55	0.29	0.88	23
501002	2	1250.56	-0.19	2.40	0.64	0.60	314
561007	2	1282.97	-0.43	0.56	0.74	0.52	118
561007	3	200.90	-0.63	5.94	0.48	0.73	121
831801	3	118.54	-0.73	9.19	0.31	0.87	21
871622	2	1561.41	-0.09	1.29	0.80	0.45	121
871622	3	376.59	-0.49	6.01	0.41	0.77	182
906405	2	1198.44	-0.42	1.32	0.64	0.63	19
906405	3	438.83	-0.47	4.76	0.66	0.62	19

Table 81. Regression results for individual layers using Model 2A

Section	Layer	Class	c_0'	c_1	k_2	k_3	n	r^2 (log E)	% Bias (E)	S_e/S_y (E)
040113	2	**A-1-a**	**3.035**	-0.093	-0.193	**1.728**	63	0.89	0	0.34
040113	3	A-1-b	3.162	0.827	-0.594	5.584	110	0.83	0	0.41
040113	4	A-1-b	3.698	0.870	-0.154	-51.92	110	0.67	0	0.58
040114	2	A-1-a	3.742	-1.621	-0.446	3.418	13	0.79	0	0.53
040114	3	A-2-4	4.180	0.395	-1.315	8.976	13	0.57	0	0.76
040114	4	A-2-4	-12.06	-6.356	4.812	-160.1	13	0.82	0	0.48
041024	2	A-1-a	3.527	-0.377	-0.479	0.286	17	0.82	-1	0.45
041024	3	A-2-6	5.307	0.503	-3.126	27.90	18	0.95	0	0.24
041024	4	A-2-6	0.599	1.321	2.855	-22.60	17	0.82	0	0.46
081053	2	A-1-a	3.406	-0.107	-0.152	0.673	35	0.91	0	0.33
081053	3	A-1-a	3.116	0.500	-0.377	4.327	43	0.76	0	0.52
091803	2	A-1-a	3.890	-2.182	-0.487	2.923	288	0.84	-1	0.45
131005	2	A-1-a	3.507	-0.791	-0.486	2.417	76	0.70	-1	0.57
131005	3	A-4	4.516	-1.940	-1.388	15.09	76	0.76	0	0.51
131005	4	A-4	4.619	-0.612	-1.047	0.973	76	0.59	0	0.64
131031	2	A-1-b	4.087	-0.872	-0.485	-2.568	77	0.66	-1	0.66
131031	3	A-4	4.024	-2.882	-0.206	-10.63	107	0.53	-1	0.68
131031	4	A-4	1.815	-0.442	0.211	-84.90	107	0.19	0	0.91
161010	2	A-1-a	3.588	1.062	-0.450	-2.325	31	0.81	-1	0.48
161010	3	A-2-4	4.736	0.478	-3.011	28.28	31	0.60	-1	0.66
161010	4	A-2-4	-5.557	0.615	10.57	-59.34	31	0.76	-1	0.61
231026	2	A-1-a	3.564	-1.184	-0.407	2.332	191	0.72	-1	0.55
231026	3	A-1-b	6.980	0.880	-4.558	32.11	191	0.88	0	0.36
241634	3	A-4	3.884	-3.069	-0.709	7.570	109	0.87	-1	0.36
241634	4	A-4	4.245	-3.433	0.393	-2.684	109	0.35	0	0.83
251002	2	A-1-a	3.157	-1.569	-0.152	2.080	15	0.99	0	0.14
251002	3	A-1-b	3.219	-0.466	-0.727	8.243	15	0.87	0	0.37
251002	4	A-3	3.361	-0.684	0.031	0.669	15	0.27	0	0.96
271018	2	A-1-b	3.360	-1.483	-0.185	2.037	33	0.92	0	0.31
271018	3	A-3	4.149	-1.709	-1.066	0.272	33	0.38	0	0.83
271028	3	A-1-b	4.991	0.420	-2.931	13.49	80	0.81	0	0.44
271028	4	A-1-b	4.295	-0.029	-1.390	5.667	80	0.04	0	1.00
276251	2	A-1-b	3.069	3.470	-0.249	1.424	13	0.57	0	0.76
276251	3	A-3	4.017	0.277	-1.250	5.144	13	0.92	0	0.32

Table 81. Regression results for individual layers using Model 2A, continued

Section	Layer	Class	c_0'	c_1	k_2	k_3	n	r^2 (log E)	% Bias (E)	S_e/S_y (E)
308129	2	**A-1-a**	3.155	0.305	-0.410	2.347	201	0.78	0	0.47
308129	3	A-6	7.503	1.782	-4.156	15.89	178	0.75	0	0.50
331001	2	A-1-a	3.267	0.494	-0.471	3.013	216	0.84	0	0.38
331001	3	A-1-b	5.618	0.109	-4.429	56.53	216	0.85	-1	0.61
331001	4	A-2-4	2.754	-0.295	1.330	-10.32	216	0.25	-1	0.86
351112	2	A-2-4	3.301	0.414	-0.138	1.932	300	0.62	-5	0.81
351112	3	A-3	5.252	-2.099	-3.216	15.31	321	0.85	-1	0.40
351112	4	A-3	3.011	0.099	0.809	-6.150	276	0.30	0	0.84
481077	2	A-1-a	3.350	0.998	-0.196	1.224	486	0.75	-1	0.52
481077	3	A-4	3.322	0.138	-0.157	1.515	533	0.03	-1	1.00
491001	2	A-1-b	3.161	0.879	-0.317	0.178	11	0.78	-1	0.64
491001	3	A-2-4	4.542	0.994	-3.218	22.36	11	0.86	0	0.49
491001	4	A-2-4	1.124	2.297	2.573	-15.59	10	0.80	0	0.57
501002	2	A-1-a	3.709	-0.009	-0.671	2.148	356	0.71	-1	0.55
561007	2	A-1-a	3.381	-0.961	-0.160	0.824	107	0.87	0	0.37
561007	3	A-2-4	4.288	-0.604	-1.928	9.214	107	0.38	0	0.80
831801	2	A-1-a	5.274	-10.58	0.139	2.065	5	0.99	0	0.27
831801	3	A-2-6	12.61	-59.78	0.274	-3.569	5	0.99	0	0.13
831801	4	A-2-4	4.083	-2.405	-0.253	0.292	5	1.00	0	0.11
871622	2	A-1-b	3.367	-0.290	-0.121	1.149	198	0.91	0	0.32
871622	3	A-1-b	4.110	0.274	-1.924	11.69	198	0.55	0	0.69
871622	4	A-4	2.948	-0.420	0.888	-5.957	198	0.16	0	0.92
906405	2	A-1-a	3.586	-2.412	-0.126	1.330	18	0.83	0	0.44
906405	3	A-1-b	4.494	0.868	-2.137	9.654	18	0.89	0	0.38
906405	4	A-1-b	0.848	0.367	3.120	-14.72	18	0.47	0	0.80

Table 82. Regression results for individual layers using Model 2B

Section	Layer	c_0'	c_1	c_2	c_2'	c_3	c_3'	n	r^2 (log E)	% Bias (E)	S_e/S_y (E)
040113	2	3.227	-1.360	-0.358	**1.067**	**1.396**	**1.907**	63	0.91	0	0.25
040113	3	2.890	4.277	0.293	-9.462	-5.314	106.5	110	0.87	0	0.33
040113	4	3.619	1.184	-0.143	0	-26.25	-216.2	110	0.67	0	0.48
040114	2	3.742	-1.621	-0.446	0	3.418	0	13	0.79	0	0.53
040114	3	4.567	-1.212	-1.420	0	-8.939	95.32	13	0.59	0	0.78
040114	4	-31.18	0	10.81	-4.942	-617.3	2259	13	0.85	0	0.48
041024	2	3.566	-0.340	-0.073	-2.324	-3.455	17.83	17	0.84	-1	0.46
041024	3	3.602	9.519	-1.327	-9.565	28.45	0	18	0.96	0	0.24
041024	4	3.269	-10.43	0	12.54	-14.54	-33.37	17	0.83	0	0.47
081053	2	2.877	3.140	-0.094	-0.327	2.534	-11.42	35	0.92	0	0.31
081053	3	2.377	4.706	1.196	-8.858	-2.791	39.80	43	0.81	0	0.47
081053	4	24.20	-42.19	-25.57	52.95	-12.47	48.68	46	0.76	0	0.56
091803	2	4.104	-3.141	0.495	-4.369	-7.524	46.69	288	0.85	-1	0.40
091803	3	28.21	-101.3	-28.80	116.2	158.0	-620.8	288	0.44	-1	0.76
091803	4	3.916	-1.934	-0.234	1.455	-3.159	-10.64	293	0.27	-1	0.86
131005	2	3.109	1.268	-0.670	0.721	8.117	-28.25	76	0.75	-1	0.45
131005	3	4.784	-2.763	0.000	-6.867	-42.80	271.3	76	0.82	0	0.40
131005	4	5.046	-3.968	-1.470	3.498	0	-0.477	76	0.60	0	0.58
131031	2	4.005	-0.402	-0.542	0.335	-2.007	-3.075	77	0.66	-1	0.65
131031	3	4.293	-4.227	-0.693	2.425	-5.834	-24.00	107	0.54	-1	0.68
131031	4	2.673	-5.108	0	1.144	924.0	-5451	107	0.19	0	0.92
161010	2	3.645	0.654	-0.879	**3.573**	-4.075	14.09	31	0.82	0	0.47
161010	3	4.870	6.843	0	-27.43	-226.4	1531	31	0.80	-1	0.50
161010	4	3.118	-29.80	0	37.05	0	-208.7	31	0.76	-1	0.61
231026	2	3.455	-0.331	0.149	-4.622	-0.704	26.04	191	0.74	-1	0.51
231026	3	5.448	8.607	-2.881	-8.455	24.23	40.05	191	0.88	0	0.35
231026	4	1.289	3.366	2.533	-3.678	-11.52	0	173	0.32	-1	0.81
241634	3	3.985	-3.291	0.758	-6.616	-22.41	127.6	109	0.90	-1	0.32
241634	4	4.276	-3.545	0	1.346	1.606	-14.59	109	0.35	0	0.83
251002	2	3.279	-2.621	-0.296	1.203	1.829	2.318	15	0.99	0	0.11
251002	3	4.022	-6.274	-0.799	0	0	67.14	15	0.92	0	0.26
251002	4	4.758	-18.39	0.811	0	-30.72	286.5	15	0.89	0	0.38
271018	2	3.506	-2.542	0.006	-1.417	0.613	10.46	33	0.92	0	0.28
271018	3	9.343	-30.04	-8.715	42.09	-22.97	123.1	33	0.42	0	0.74
271018	4	7.363	-21.09	-3.423	15.84	-13.82	0	33	0.96	0	0.23

Table 82. Regression results for individual layers using Model 2B, continued

Section	Layer	c_0'	c_1	c_2	c_2'	c_3	c_3'	n	r^2 (log E)	% Bias (E)	S_e/S_y (E)
271028	3	5.447	-5.033	-3.606	8.090	14.31	-10.31	80	0.81	0	0.44
271028	4	3.245	7.275	0	-9.242	2.589	-0.430	80	0.04	0	1.02
276251	2	2.519	7.920	0	-2.087	4.670	-25.84	13	0.57	0	0.80
276251	3	3.179	10.79	-0.542	-8.201	15.59	-147.0	13	0.98	0	0.23
276251	4	32.38	0	-20.90	-2.563	0	3256	13	0.84	0	0.43
308129	2	3.116	0.778	-0.413	0.052	2.761	-5.050	201	0.78	0	0.47
308129	3	4.954	9.881	-2.178	-6.309	20.38	-9.492	178	0.78	0	0.48
331001	2	2.756	5.604	0.200	-6.785	7.538	-45.06	216	0.85	0	0.36
331001	3	5.929	-1.873	-4.862	2.760	60.54	-25.53	216	0.86	-1	0.61
331001	4	-0.115	11.76	5.483	-17.44	-44.73	143.0	216	0.28	-1	0.85
351112	2	3.710	-4.822	-0.337	2.487	-0.477	30.71	300	0.64	-4	0.79
351112	3	5.644	-9.892	-4.095	17.82	19.94	-94.35	321	0.86	-1	0.40
351112	4	3.549	-2.041	0	3.211	-3.802	-9.076	276	0.30	0	0.84
481077	2	3.234	2.196	-0.308	1.015	2.396	-11.56	486	0.76	-1	0.47
481077	3	4.508	-6.076	-1.867	8.936	5.899	-21.99	533	0.04	-1	0.90
491001	2	4.396	-8.898	-0.189	-1.094	-9.670	78.05	11	0.81	-1	0.49
491001	3	2.765	9.749	0	-15.86	-10.47	161.5	11	0.85	0	0.37
491001	4	-1.574	26.19	5.685	-26.43	0	-209.3	10	0.93	0	0.25
501002	2	3.674	0.288	-0.549	-0.991	1.272	6.927	356	0.71	-1	0.55
501002	3	3.040	7.342	-0.080	-7.142	18.34	-21.21	356	0.47	-4	0.73
501002	4	10.28	-17.79	-6.473	16.60	24.18	-54.89	141	0.50	-1	0.70
561007	2	2.977	1.636	-0.349	1.218	3.501	-17.15	107	0.87	0	0.37
561007	3	3.012	6.577	0	-10.85	2.634	36.99	107	0.39	0	0.80
561007	4	3.814	0	-0.505	-1.930	-9.932	77.36	104	0.41	0	0.77
831801	2	5.516	-11.69	0	0.612	0	9.609	5	0.99	0	0.27
831801	3	12.68	-60.23	0	1.702	0	-22.12	5	0.99	0	0.13
831801	4	3.992	-1.638	0	-2.127	0	7.923	5	1.00	0	0.12
871622	2	3.396	-0.538	-0.148	0.222	1.030	1.012	198	0.91	0	0.32
871622	3	1.376	28.37	3.648	-56.93	-23.23	354.2	198	0.63	0	0.63
871622	4	3.610	-3.656	0	4.246	-7.427	10.06	198	0.17	0	0.92
906405	2	2.133	7.347	-1.474	8.739	17.89	-108.8	18	0.90	0	0.37
906405	3	3.002	11.45	0	-15.23	3.277	46.57	18	0.89	0	0.39
906405	4	3.392	-12.51	0	15.81	-6.878	-40.01	18	0.46	0	0.84

Table 83. Goodness-of-fit statistics for Models 1 and 2

Section	Layer	n_1	n_2	S_e/S_y			% Bias		
				1	2A	2B	1	2A	2B
040113	2	63	63	0.59	0.34	0.25	0	0	0
040113	3	110	110	0.33	0.41	0.33	0	0	0
040113	4	110	110	0.57	0.58	0.48	0	0	0
040114	2	13	13	0.88	0.53	0.53	5	0	0
040114	3	13	13	0.77	0.76	0.78	0	0	0
040114	4	13	13	0.52	0.48	0.48	0	0	0
041024	2	16	17	0.49	0.45	0.46	-1	-1	-1
041024	3	18	18	0.26	0.24	0.24	0	0	0
041024	4	17	17	0.46	0.46	0.47	0	0	0
081053	2	21	35	0.47	0.33	0.31	0	0	0
081053	3	43	43	0.45	0.52	0.47	0	0	0
091803	2	288	288	0.69	0.45	0.40	-1	-1	-1
131005	2	76	76	0.58	0.57	0.45	-1	-1	-1
131005	3	76	76	0.53	0.51	0.40	0	0	0
131005	4	76	76	0.65	0.64	0.58	0	0	0
131031	2	30	77	0.77	0.66	0.65	-1	-1	-1
131031	3	107	107	0.73	0.68	0.68	-1	-1	-1
131031	4	107	107	0.91	0.91	0.92	0	0	0
161010	2	2	31	—	0.48	0.47	—	-1	0
161010	3	31	31	0.66	0.66	0.50	-1	-1	-1
161010	4	31	31	0.61	0.61	0.61	-1	-1	-1
231026	2	191	191	0.54	0.55	0.51	-1	-1	-1
231026	3	191	191	0.36	0.36	0.35	0	0	0
241634	3	109	109	0.38	0.36	0.32	-1	-1	-1
241634	4	109	109	0.84	0.83	0.83	0	0	0
251002	2	14	15	0.35	0.14	0.11	-1	0	0
251002	3	15	15	0.38	0.37	0.26	0	0	0
251002	4	15	15	0.97	0.96	0.38	0	0	0
271018	2	33	33	0.42	0.31	0.28	-1	0	0
271018	3	33	33	0.83	0.83	0.74	0	0	0
271028	3	80	80	0.45	0.44	0.44	0	0	0
271028	4	80	80	1.01	1.00	1.02	0	0	0
276251	2	13	13	0.66	0.76	0.80	0	0	0
276251	3	13	13	0.32	0.32	0.23	0	0	0
308129	2	201	201	0.48	0.47	0.47	0	0	0

Table 83. Goodness-of-fit statistics for Models 1 and 2, continued

Section	Layer	n_1	n_2	S_e/S_y			% Bias		
				1	2A	2B	1	2A	2B
308129	3	178	178	0.49	0.50	0.48	0	0	0
331001	2	216	216	0.48	0.38	0.36	-1	0	0
331001	3	216	216	0.63	0.61	0.61	-1	-1	-1
331001	4	216	216	0.86	0.86	0.85	-1	-1	-1
351112	2	285	300	0.85	0.81	0.79	-5	-5	-4
351112	3	321	321	0.37	0.40	0.40	-1	-1	-1
351112	4	276	276	0.84	0.84	0.84	0	0	0
481077	2	467	486	0.61	0.52	0.47	-1	-1	-1
481077	3	533	533	0.97	1.00	0.90	-1	-1	-1
491001	2	7	11	0.50	0.64	0.49	0	-1	-1
491001	3	11	11	0.45	0.49	0.37	0	0	0
491001	4	10	10	0.59	0.57	0.25	0	0	0
501002	2	356	356	0.55	0.55	0.55	-1	-1	-1
561007	2	104	107	0.54	0.37	0.37	0	0	0
561007	3	107	107	0.80	0.80	0.80	0	0	0
831801	2	1	5	—	0.27	0.27	—	0	0
831801	3	5	5	0.19	0.13	0.13	0	0	0
831801	4	5	5	0.05	0.11	0.12	0	0	0
871622	2	143	198	0.41	0.32	0.32	0	0	0
871622	3	198	198	0.69	0.69	0.63	0	0	0
871622	4	198	198	0.93	0.92	0.92	0	0	0
906405	2	18	18	0.42	0.44	0.37	0	0	0
906405	3	18	18	0.38	0.38	0.39	0	0	0
906405	4	18	18	0.75	0.80	0.84	0	0	0

APPENDIX F: TRIAL APPLICATION RESULTS BASED ON SECTION/LAYER-SPECIFIC MODELS DERIVED FROM ALL AVAILABLE DATA

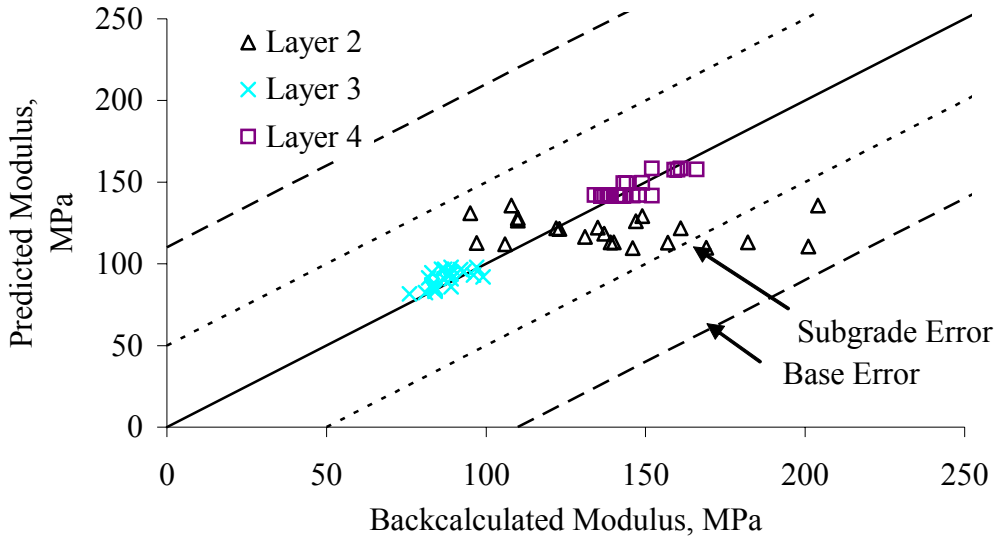

Figure 49. Section 040113 (Arizona) E versus E predicted for section-specific models based on data for all available test dates

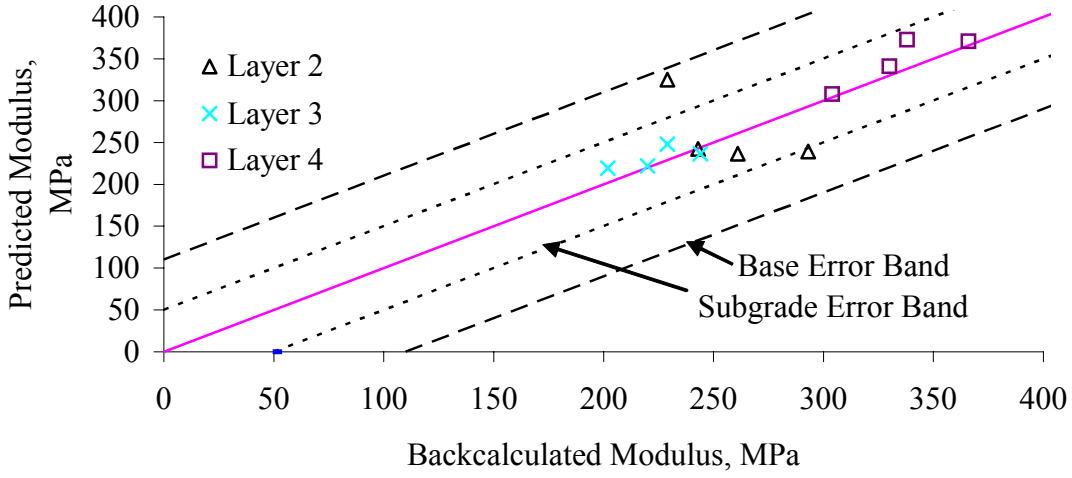

Figure 50. Section 040114 (Arizona) E versus $E_{predicted}$ for section-specific models based on data for all available test dates

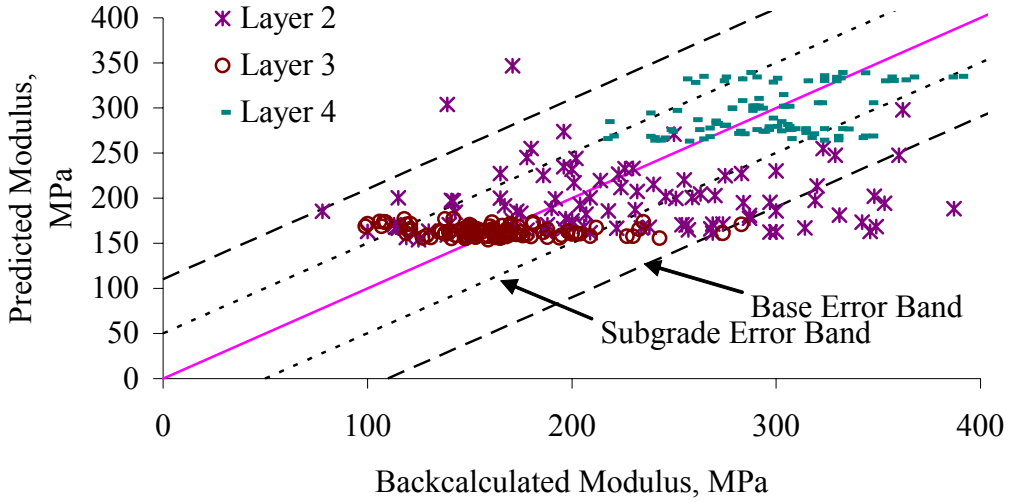

Figure 51. Section 091803 (Connecticut) E versus E $_{predicted}$ for section-specific models based on data for all available test dates

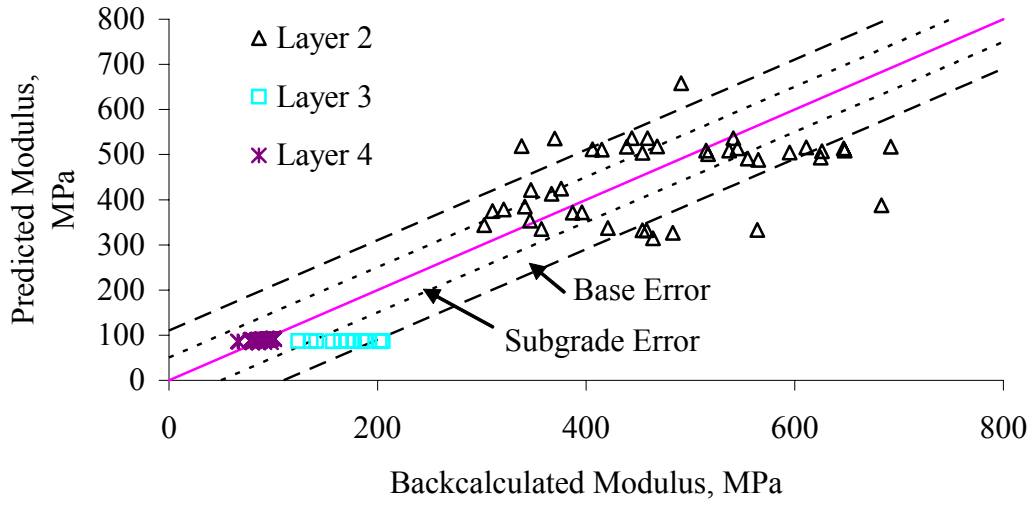

Figure 52. Section 131031 (Georgia) E versus E $_{predicted}$ for section-specific models based on data for all available test dates

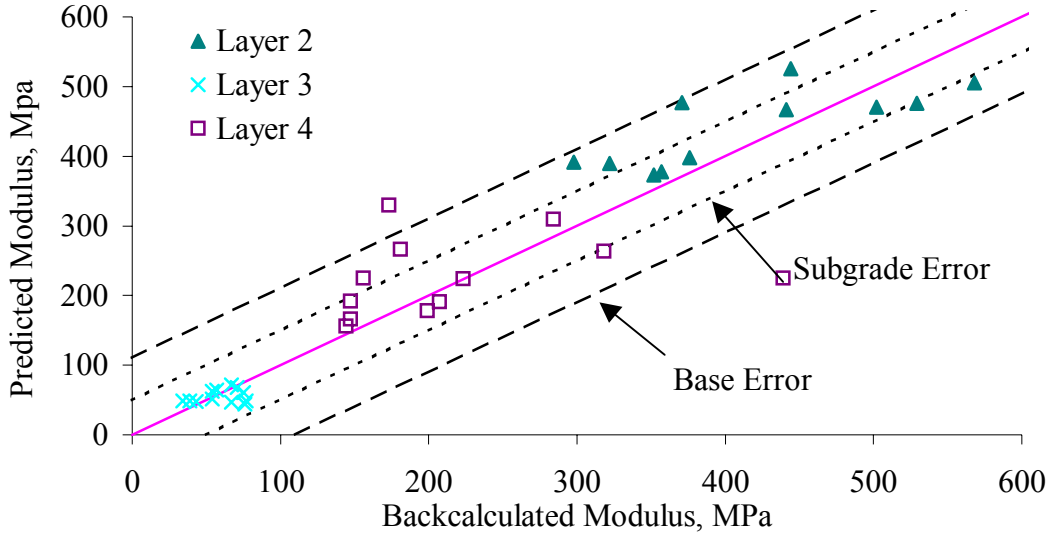

Figure 53. Section 161010 (Idaho) E versus $E_{predicted}$ for section-specific models based on data for all available test dates

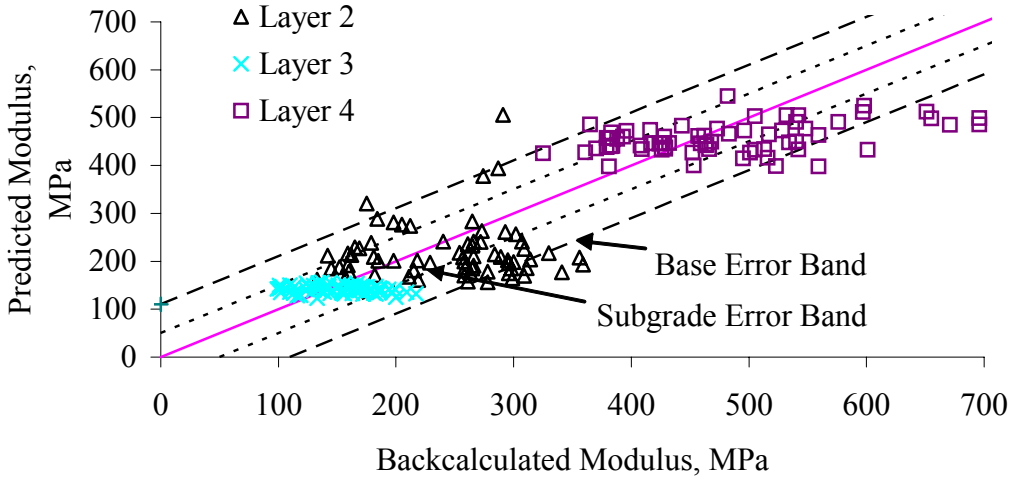

Figure 54. Section 231026 (Maine) E versus $E_{predicted}$ for section-specific models based on data for all available test dates

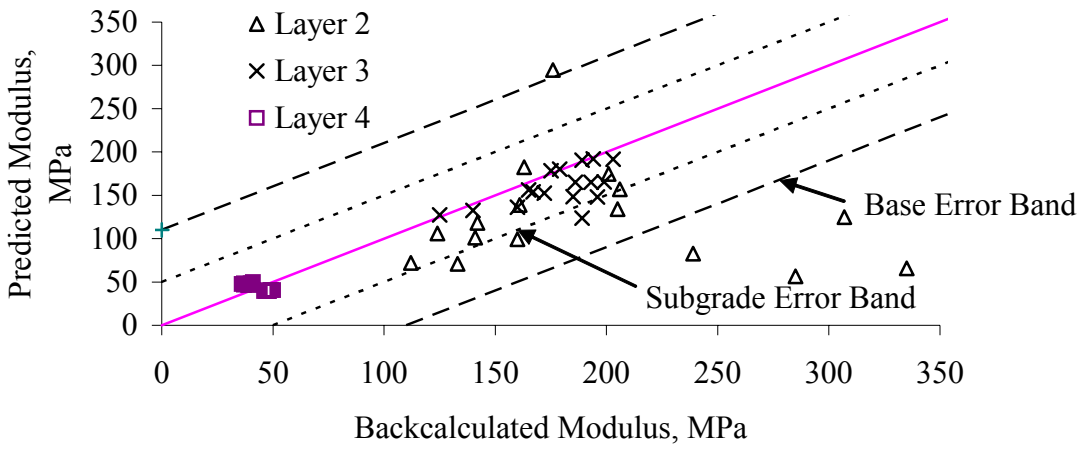

Figure 55. Section 271018 (Minnesota) E versus $E_{predicted}$ for section-specific models based on data for all available test dates

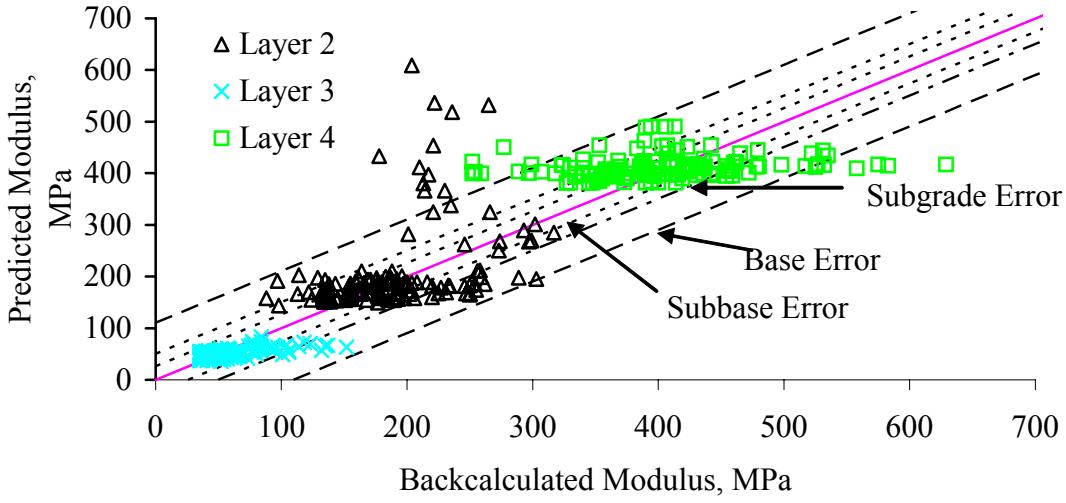

Figure 56. Section 331001 (New Hampshire) E versus $E_{predicted}$ for section-specific models based on data for all available test dates

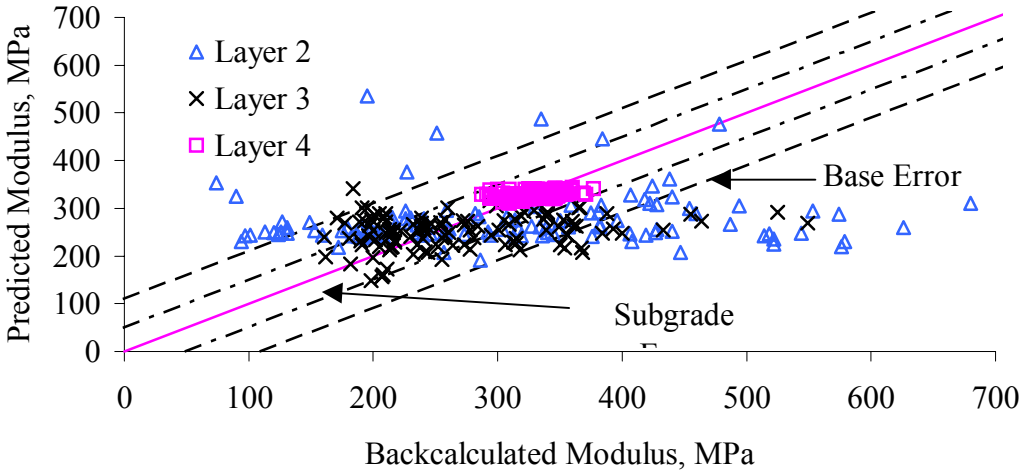

Figure 57. Section 351112 (New Mexico) E versus E $_{predicted}$ for section-specific models based on data for all available test dates

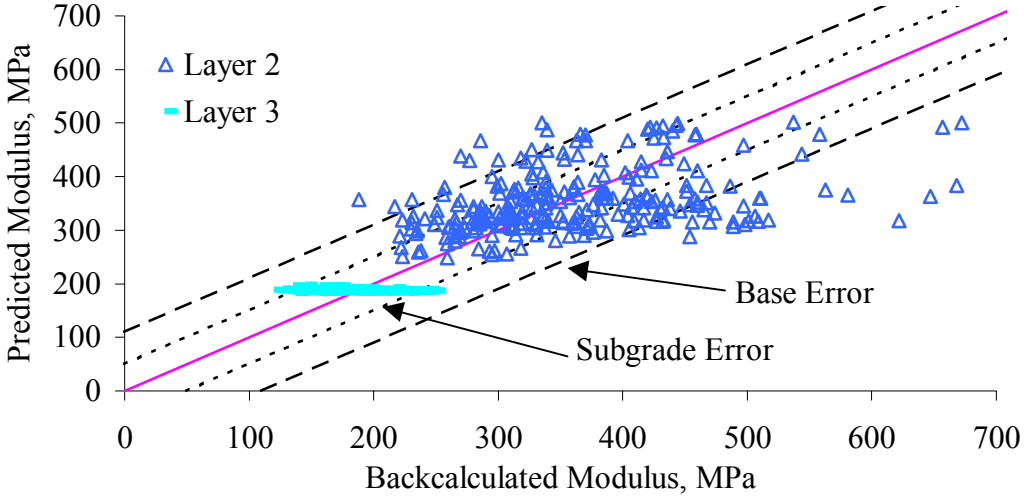

Figure 58. Section 481077 (Texas) E versus $E_{predicted}$ for section-specific models based on data for all available test dates

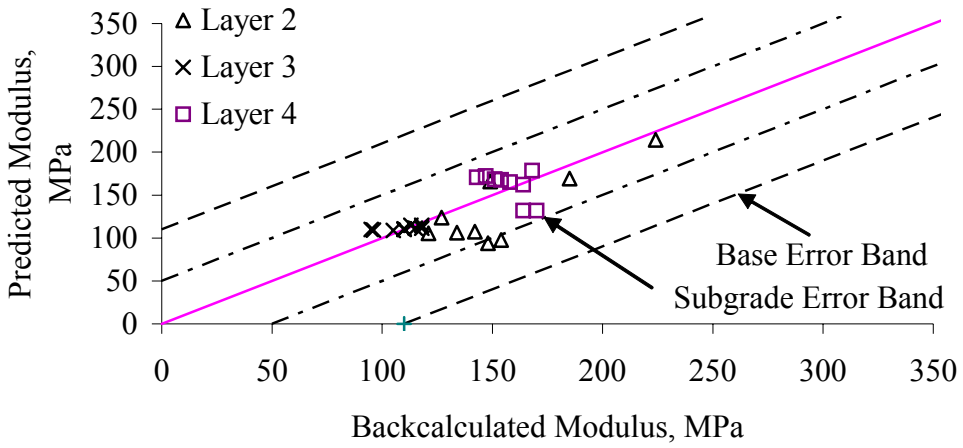

Figure 59. Section 561007 (Wyoming) E versus $E_{predicted}$ for site-specific models based on data for all available test dates

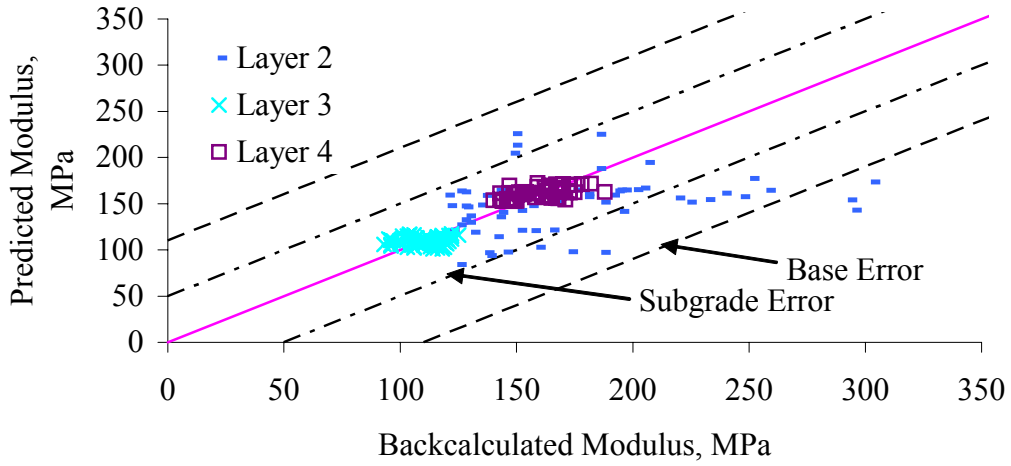

Figure 60. Section 871622 (Ontario) E versus $E_{predicted}$ for section-specific models based on data for all available test dates

APPENDIX G: TRIAL APPLICATION RESULTS OBTAINED WITH ONE-DATE SECTION/LAYER-SPECIFIC MODELS

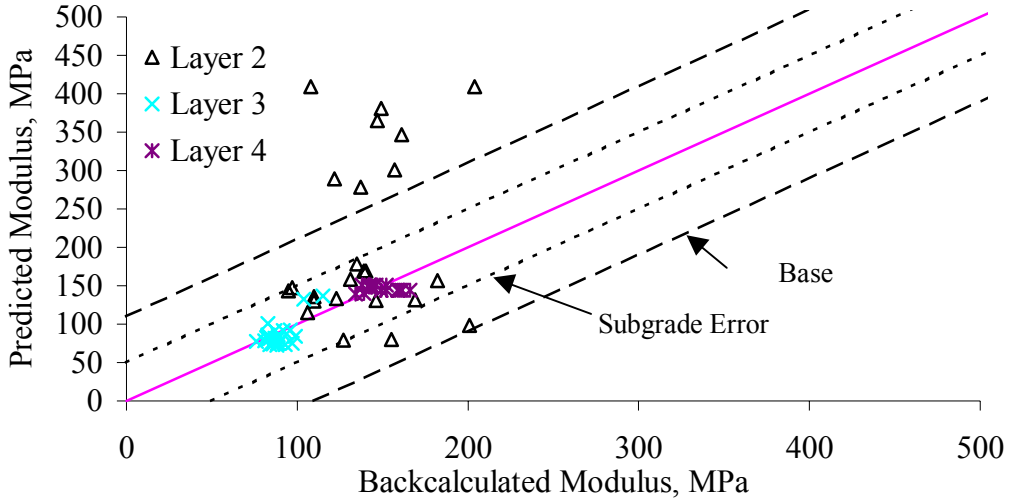

Figure 61. Section 040113 (Arizona) E versus E $_{predicted}$ for section-specific models based on data for a single test date

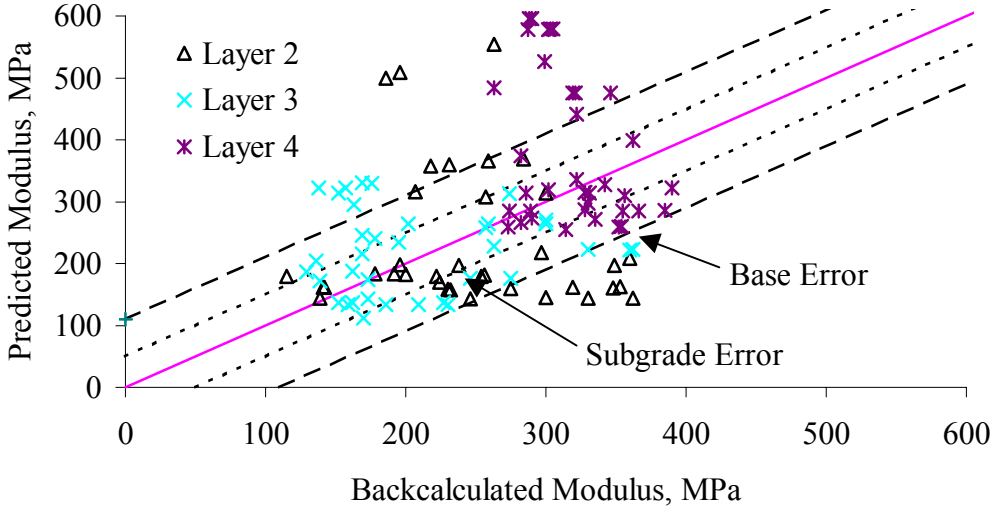

Figure 62. Section 091803 (Connecticut) E versus E $_{predicted}$ for section-specific models based on data for a single test date

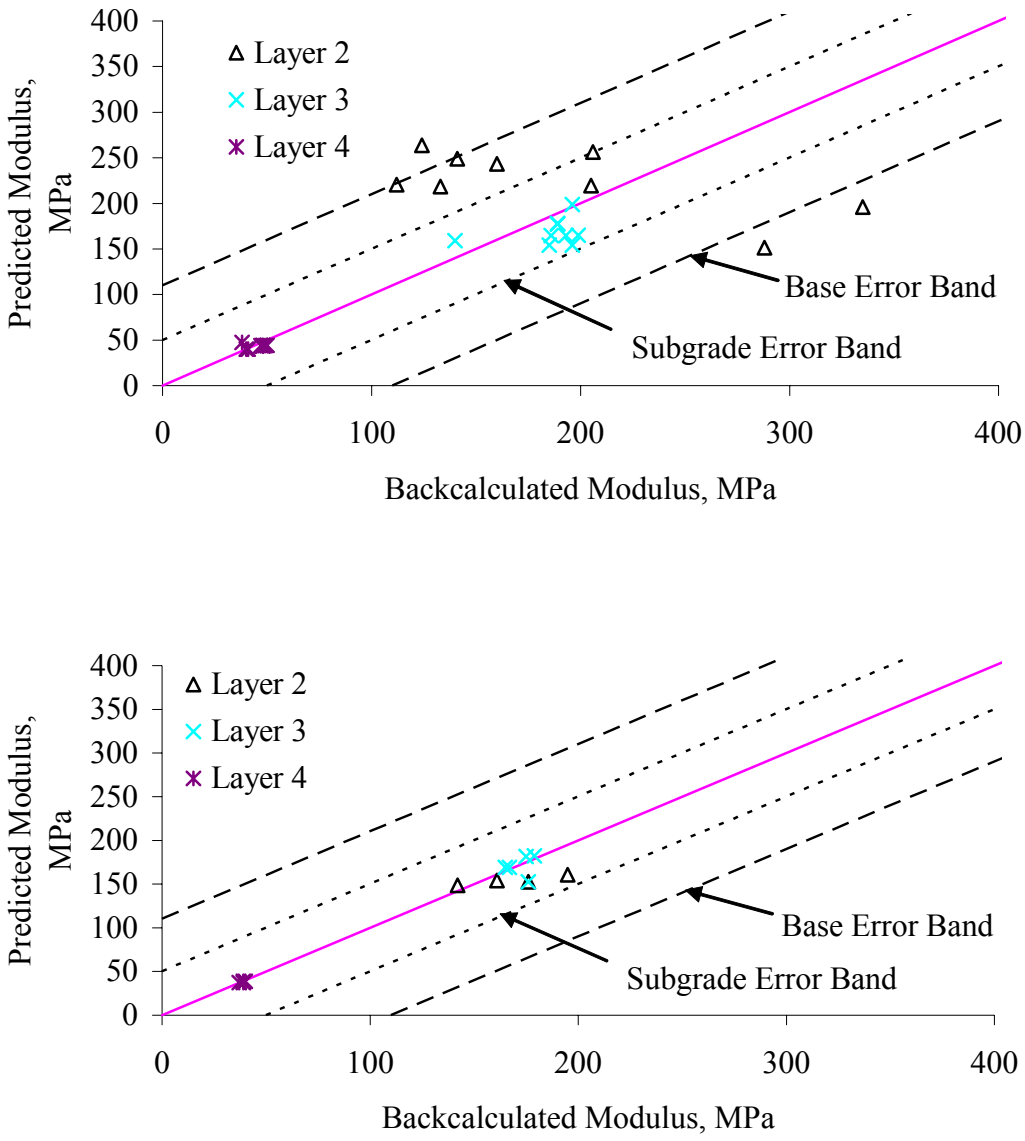

Figure 63. Section 271018 (Minnesota) E versus E predicted for section-specific models based on data for a single test date (A (top) and B (bottom))

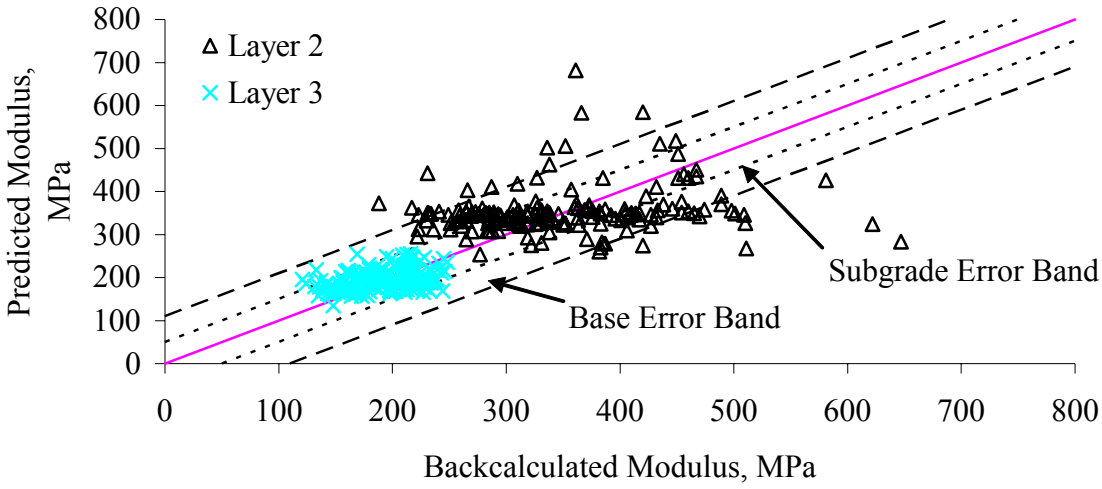

Figure 64. Section 481077 (Texas) E versus E $_{predicted}$ for section-specific models based on data for a single test date

APPENDIX H: TRIAL APPLICATION RESULTS OBTAINED WITH TWO-DATE SECTION/LAYER-SPECIFIC MODELS

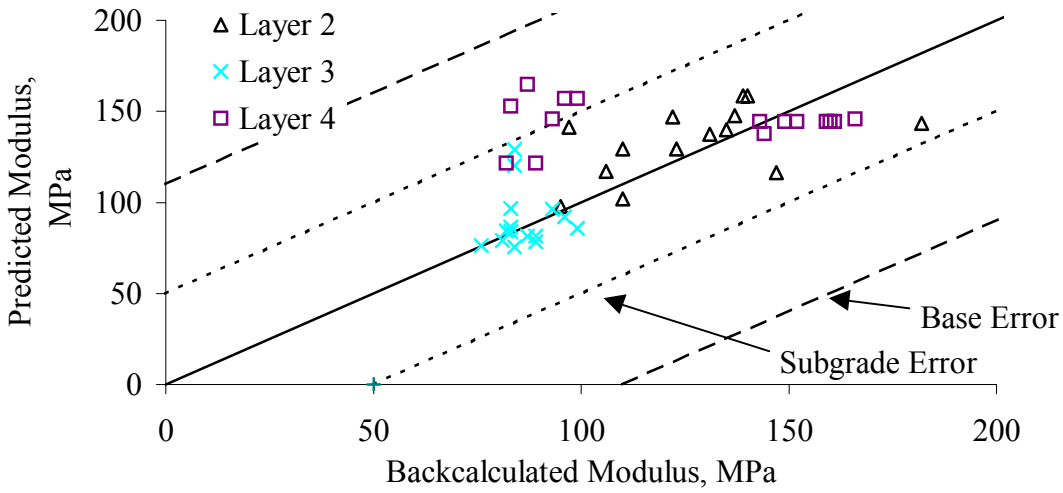

Figure 65. Section 040113 (Arizona) E versus E $_{predicted}$ for section-specific models based on data for two test dates

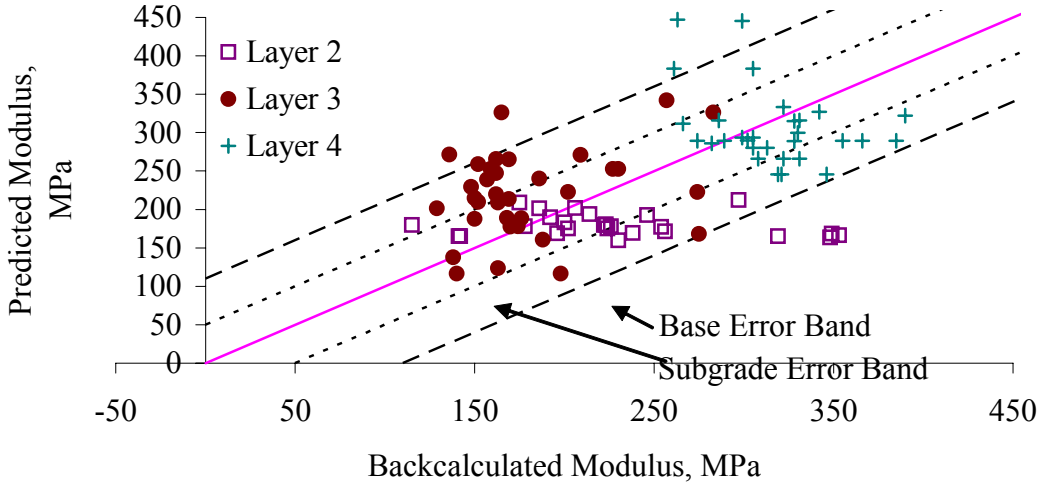

Figure 66. Section 091803 (Connecticut) E versus E $_{predicted}$ for section-specific models based on data for two test dates

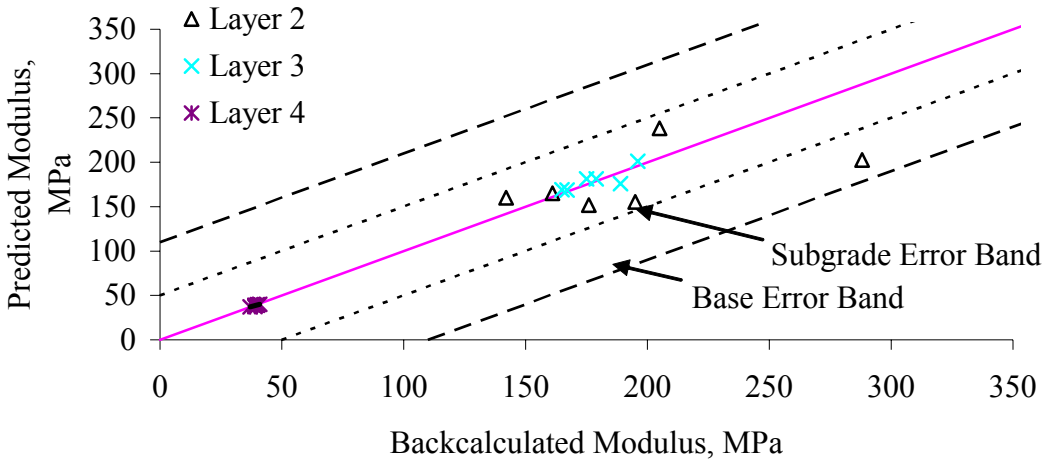

Figure 67. Section 271018 (Minnesota) E versus $E_{predicted}$ for section-specific models based on data for two test dates

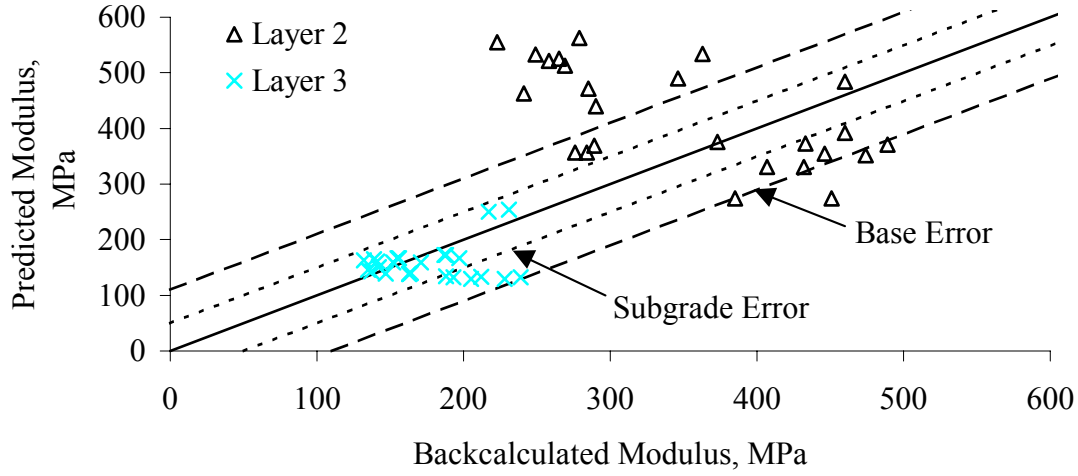

Figure 68. Section 481077 (Texas) E versus $E_{predicted}$ for section-specific models based on data for two test dates

APPENDIX I: TRIAL APPLICATION RESULTS OBTAINED WITH SOIL CLASS MODELS

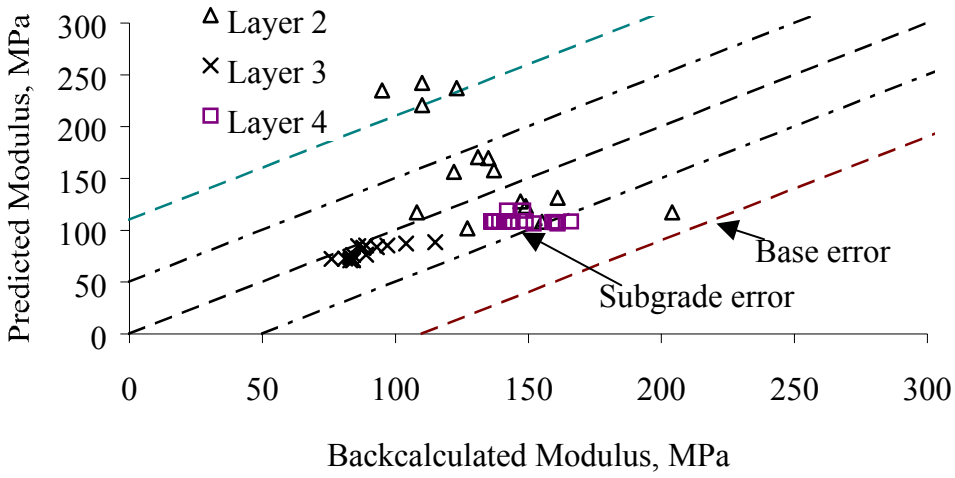

Figure 69. Section 040113 (Arizona) E versus E predicted for soil class models

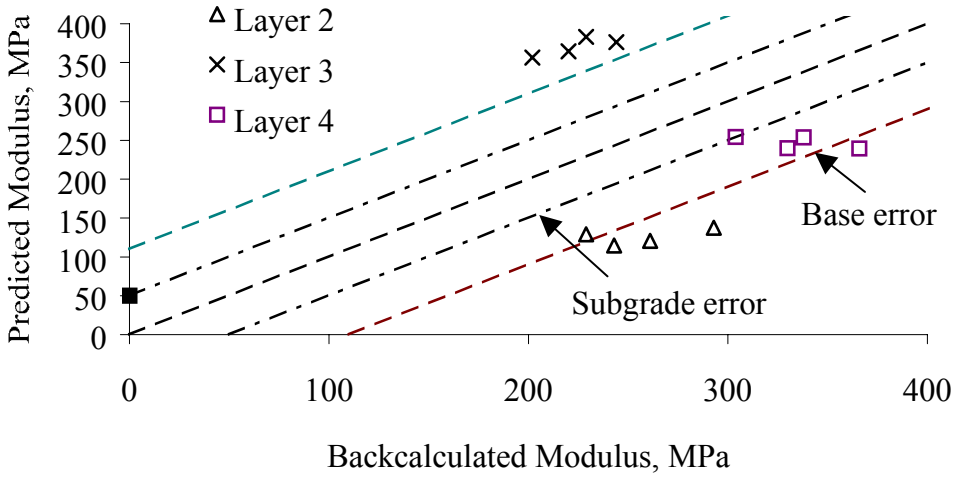

Figure 70. Section 040114 (Arizona) E versus E predicted for soil class models

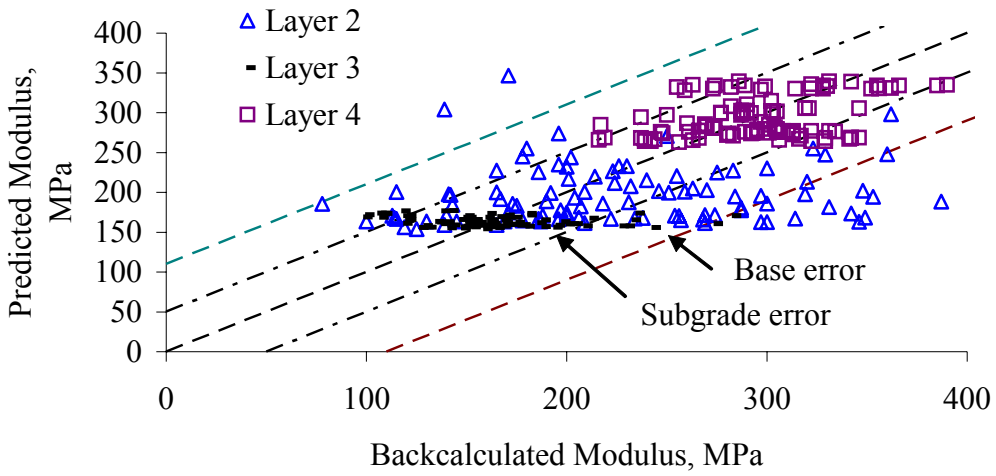

Figure 71. Section 091803 (Connecticut) E versus $E_{predicted}$ for soil class models

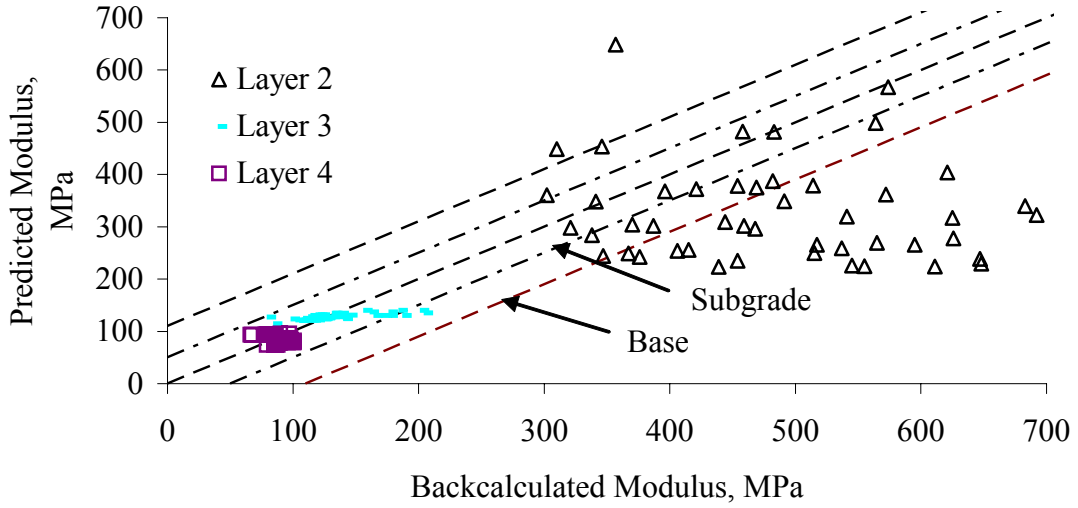

Figure 72. Section 131031 (Georgia) E versus $E_{predicted}$ for soil class models

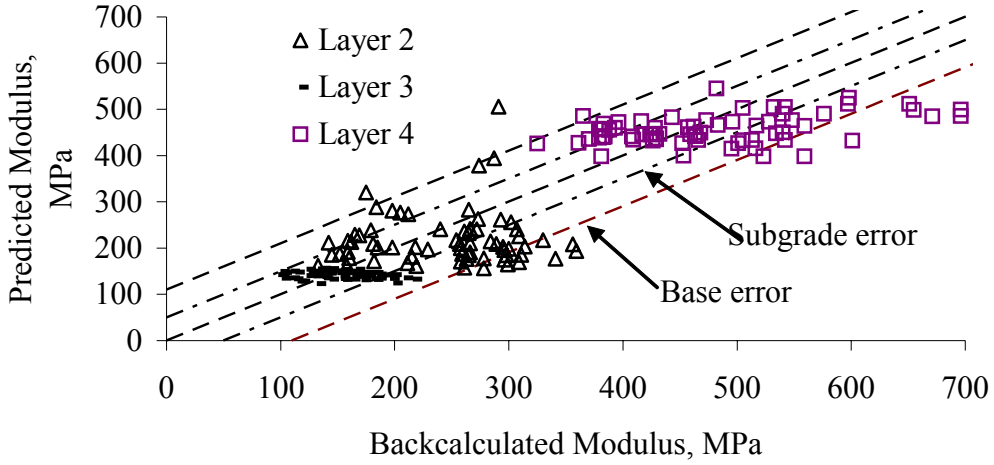

Figure 73. Section 231026 (Maine) E versus E $_{predicted}$ for soil class models

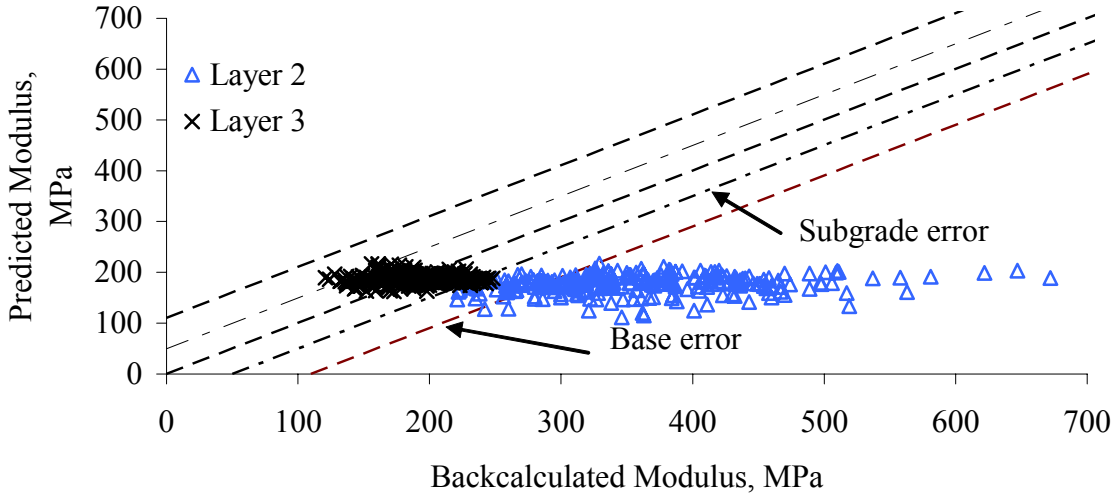

Figure 74. Section 481077 (Texas) E versus E $_{predicted}$ for soil class models

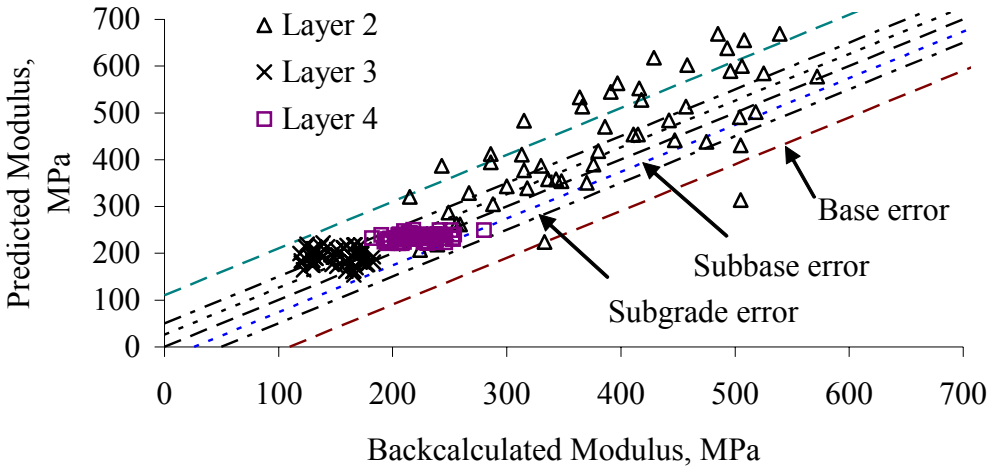

Figure 75. Section 871622 (Ontario) E versus $E_{predicted}$ for soil class models

REFERENCES

1 Rada, G.R., Elkins, G.E., Henderson, B., Van Sambeek, R.J., and Lopez, Jr., A., *LTPP Seasonal Monitoring Program: Instrumentation Installation and Data Collection Guidelines*. FHWA-RD-94-110, U.S. Department of Transportation, Federal Highway Administration, McLean, VA, 1994.

2 Lee, S.W., Mahoney, J.P., and Jackson, N.C., "Verification of Backcalculation of Pavement Moduli," in Transportation Research Record 1196, *Pavement Evaluation and Rehabilitation,* Transportation Research Board, National Research Council, Washington, DC, 1988.

3 Daleiden, J.F., Killingsworth, B.M., Simpson, A.L., and Zamora, R.A., "Analysis of Procedures for Establishing In Situ Subgrade Moduli" in Transportation Research Record 1462, *Compaction of Difficult Soils and Resilient Modulus Testing,* Transportation Research Board, National Research Council, Washington, DC, 1994.

4 American Association of State Highway and Transportation Officials, *AASHTO Guide for Design of Pavement Structures,* American Association of State Highway and Transportation Officials, Washington, DC, 1993.

5 Von Quintus, H. and Killingsworth, B., *Analyses Relating to Pavement Material Characterizations and Their Effects on Pavement Performance,* FHWA-RD-97-085, U.S. Department of Transportation, Federal Highway Administration, McLean, VA, 1998.

6 Yoder, E.J., and Witczak, M.W., Principles of Pavement Design. John Wiley and Sons, Inc., New York, New York, 1975.

7 American Association of State Highway and Transportation Officials*, AASHTO Guide for Design of Pavement Structures*, American Association of State Highway and Transportation Officials, Washington, DC, 1986.

8 Finn, F., Saraf, C. Kulkarni, R., Nair, K., Smith, W., and Abdullah, A., "The Use of Distress Prediction Subsystems for the Design of Pavement Structures," *Proceedings of the Fourth International Conference, Structural Design of Asphalt Pavements*, The University of Michigan, Ann Arbor, MI, 1977.

9 *Research and Development of The Asphalt Institute's Thickness Design Manual (MS-1) Ninth Edition*, Research Report No. 82-2, The Asphalt Institute, College Park, MD, August, 1982.

10 Barker, W.R., Brabston, W.N., and Chou, Y.T., "A General System for the Structural Design of Flexible Pavements," Proceedings of the Fourth International Conference, Structural Design of Asphalt Pavements, The University of Michigan, Ann Arbor, MI, 1977.

11 Richter, C.A. and Irwin, L.H., *Application of Deflection Testing to Pavement Overlay Design: A Case Study* in Transportation Research Record 1196, *Pavement Evaluation and Rehabilitation,* Transportation Research Board, National Research Council, Washington, DC, 1988.

12 The Asphalt Institute, *Research and Development of The Asphalt Institute's Thickness Design Manual (MS-1) Ninth Edition*, The Asphalt Institute, Research Report No. 82-2, College Park, MD, 1982.

13 Departments of the Army and the Air Force, *Flexible Pavement Design for Airfields (Elastic Layered Method)*, Army TM 5-825-2-1, Air Force AFM 88-6, Chap. 2, Section A, Departments of the Army and the Air Force Technical Manual, November 1989.

14 Mahoney, J.P., Lee, S.W., Jackson, N.C., and Newcomb, D.E., *Mechanistic-based Overlay Design Procedure for Washington State Flexible Pavements,* Final Report, Prepared for Washington State Transportation Commission, Washington State Transportation Center, University of Washington, Seattle, WA, January 1989.

15 Pierce, L.M., Jackson, N.C., and Mahoney, J.P., "Development and Implementation of a Mechanistic, Empirically Based Overlay Design Procedure for Flexible Pavements," in Transportation Research Record No. 1388, *Rigid and Flexible Pavement Design and Rehabilitation,* Transportation Research Board, National Research Council, National Academy Press, Washington, DC, 1993.

16 Witczak, M.W., Andrei, D., and Houston, W.N., *Development of the 2002 Guide for the Design of New and Rehabilitated Pavement Structures, Inter Team Technical Report (Seasonal 1), Resilient Modulus as Function of Soil Moisture – Summary of Predictive Models,* College of Engineering and Applied Sciences, Department of Civil and Environmental Engineering, Arizona State University, June 2000.

17 Witczak, M.W., Houston, W.N., and Andrei, D., *Development of the 2002 Guide for the Design of New and Rehabilitated Pavement Structures, Inter Team Technical Report (Seasonal 2), Resilient Modulus as Function of Soil Moisture – A Study of Expected Changes in Resilient Modulus of the Unbound Layers with Changes in Moisture for 10 LTPP Sites*, College of Engineering and Applied Sciences, Department of Civil and Environmental Engineering, Arizona State University, June 2000.

18 Witczak, M.W., Houston, W.N., and Andrei, D., *Development of the 2002 Guide for the Design of New and Rehabilitated Pavement Structures, Inter Team Technical Report (Seasonal 3), Selection of Resilient Moduli for Frozen/Thawed Unbound Materials,* College of Engineering and Applied Sciences, Department of Civil and Environmental Engineering, Arizona State University, June 2000.

19 Witczak, M.W., Houston, W.N., Zapata, C., Richter, C., Larson, G., and Walsh, K., *Development of the 2002 Guide for the Design of New and Rehabilitated Pavement Structures, Inter Team Technical Report (Seasonal 4), Improvement of the Integrated Climatic Model for Moisture Content Predictions*, College of Engineering and Applied Sciences, Department of Civil and Environmental Engineering, Arizona State University, June 2000.

20 Brown, S.F., and Pappin, J.W., *Analysis of Pavements with Granular Bases*, in Transportation Research Record 810, *Layered Pavement Systems,* Transportation Research Board, National Research Council, National Academy of Sciences, Washington, DC, 1981.

21 Monismith, C.L., Seed, H.B., Mitry, F.G., and Chan, C.K., "Prediction of Pavement Deflections From Laboratory Tests," in *Proceedings, 2nd International Conference on the Structural Design of Asphalt Pavements*, Ann Arbor, MI, Aug. 1967.

22 Hicks, R.G., and Monismith, C.L., *Factors Influencing the Resilient Response of Granular Materials*, in Highway Research Record 345, Highway Research Board, National Academy of Sciences, Washington, DC, 1971.

23 Monismith, C.L., Hicks, R.G., and Salam, Y.M., *Basic Properties of Pavement Components*, Report No. FHWA-RD-72-19, Federal Highway Administration, Washington, DC, 1971.

24 Thompson, M.R., and Robnett, Q.L., *Resilient Properties of Subgrade Soils,* Transportation Engineering Series No. 14. Illinois Cooperative Highway and Transportation Series No. 160, University of Illinois, June 1976.

25 Edris, Earl V. Jr., and Lytton, Robert L., *Dynamic Properties of Subgrade Soils Including Environmental Effects*, Texas Transportation Institute Report No. TTI-2-18-74-164-3, Texas A&M University, College Station, TX, May 1976.

26 Rada, G., and Witczak, M.W., *Comprehensive Evaluation of Laboratory Resilient Moduli Results for Granular Material*, in Transportation Research Record 810, *Layered Pavement Systems,* Transportation Research Board, National Research Council, National Academy of Sciences, Washington, DC, 1981.

27 Cole, D.M., Irwin, L.H., and Johnson, T.C., *Effect of Freezing and Thawing on Resilient Modulus of a Granular Soil Exhibiting Nonlinear Behavior* in Transportation Research Record 809, *Frost Action and Risk Assessment in Soil Mechanics,* Transportation Research Board, National Research Council, Washington, DC, 1981.

28 Ishibashi, I., Irwin, L.H., and Lee, Wai-Shing, *Resilient Behavior of Base and Subgrade Materials*, Geotechnical Engineering Report 84-4 and Cornell Local Roads Program Report 84-2, School of Civil and Environmental Engineering and Department of Agricultural Engineering, Cornell University, Ithaca, NY, August 1984.

29 Cole, D., Bentley, D., Durell, G., and Johnson, T., *Resilient Modulus of Freeze-Thaw Affected Granular Soils for Pavement Design and Evaluation, Part 1. Laboratory tests on soils from Winchendon, Massachusetts Test Sections,* CRREL Report 86-4, U.S. Army Corps of Engineers, Cold Regions Research and Engineering Laboratory, July 1986.

30 Johnson, T.C., Bentley, D.L, and Cole, D.M., *Resilient Modulus of Freeze-Thaw Affected Granular Soils for Pavement Design and Evaluation, Part 2. Field Validation of Tests at Winchendon, Massachusetts Test Sections,* CRREL Report 86-12, U.S. Army Corps of Engineers, Cold Regions Research and Engineering Laboratory, October 1986.

31 Cole, D.M., Bentley, D.L., Durell, G.D., and Johnson, T.C., *Resilient Modulus of Freeze-Thaw Affected Granular Soils for Pavement Design and Evaluation, Part 3. Laboratory Tests on Soils from Albany County Airport,* CRREL Report 87-2, U.S. Army Corps of Engineers, Cold Regions Research and Engineering Laboratory, February 1987.

32 Johnson, T.C., Crowe, A., Erickson, M. and Cole, D.M., *Resilient Modulus of Freeze-Thaw Affected Granular Soils for Pavement Design and Evaluation, Part 4. Field validation tests at Albany County Airport,* CRREL Report 86-13, U.S. Army Corps of Engineers, Cold Regions Research and Engineering Laboratory, October 1986.

33 Fredlund, D.G. and Rahardjo, H., "Soil Mechanics Principles for Highway Engineering in Arid Regions," in Transportation Research Record 1137, *Soil Mechanics Considerations in Arid and Semiarid Areas*, Transportation Research Board, National Research Council, Washington, DC, 1987.

34 Yang, Wei-shih, *Mechanistic Analysis of Nondestructive Pavement Deflection Data,* Ph.D. Thesis, Cornell University, Ithaca, NY, January 1988.

35 Thompson, M.R., and Smith, K.L., "Repeated Triaxial Characterization of Granular Bases," in Transportation Research Record 1278, *Dynamic Testing of Aggregates and Soils and Lateral Stress Measurements*, Transportation Research Board, National Research Council, National Academy Press, Washington, DC, 1990.

36 Pezo, R.F., Claros, G., Hudson, W.R., and Stokoe, K. H., *Development of a Reliable Resilient Modulus Test for Subgrade and Non-Granular Subbase Materials for Use in Routine Pavement Design*, Research Report 1177-4F, CTR 2/3/10-8-88/0-1177-4F, Center for Transportation Research, The University of Texas at Austin, January 1992.

37 Santha, B.L., "Resilient Modulus of Subgrade Soils: Comparison of Two Constitutive Equations," in Transportation Research Record 1462, *Compaction of Difficult Soils and Resilient Modulus Testing*, Transportation Research Board, National Academy Press, Washington, DC, 1994.

38 Kolisoja, P., "Large Scale Dynamic Triaxial Tests with Coarse Grained Aggregates" in *Proceedings, The 4th International Conference on the Bearing Capacity of Roads and Airfields*, University of Minnesota, 1994.

39 Jin, M., Lee, S., Wayne, K., and Kovacs, W.D., "Seasonal Variation of Resilient Modulus of Subgrade Soils," in *Journal of Transportation Engineering,* Volume 120, No. 4, American Society of Civil Engineers, July/August 1994.

40 Li, D., and Selig, E.T., "Resilient Modulus for Fine-Grained Subgrade Soils," in *Journal of Geotechnical Engineering*, Volume 120, No. 6, American Society of Civil Engineers, June 1994.

41 Titus-Glover, L., and Fernando, E.B., *Evaluation of Pavement Subgrade Material Properties and Test Procedures*, Report No. FHWA/TX-96/1335-2, Texas Transportation Institute, Texas A&M University, College Station, TX, November 1995.

42 Chou, Yu T., *Engineering Behavior of Pavement Materials: State of the Art*, Report No. FAA-RD-77-37, WES TR S-77-9, U.S. Army Waterways Experiment Station, Vicksburg, MI, 1977.

43 Uzan, J., "Characterization of Granular Material," in Transportation Research Record 1022, Transportation Research Board, National Academy of Sciences, Washington, DC, 1988.

44 Witczak, M.W., and Uzan, J., *The Universal Airport Pavement Design System, Report I of IV: Granular Material Characterization,* University of Maryland, College of Engineering, College Park, MD, September 1988.

45 Andrei, D., *Development of a Harmonized Test Protocol for the Resilient Modulus of Unbound Materials Used in Pavement Design,* Master's Thesis, University of Maryland, College Park, MD, 1999.

46 Noureldin, S.A., "Influence of Stress Levels and Seasonal Variations in In Situ Pavement Layer Properties," in Transportation Research Record 1448, *Strength and Deformation Characteristics of Pavement Sections*, Transportation Research Board, National Research Council, National Academy Press, Washington, DC, 1994.

47 Ksaibati, K., Armaghani, J., and Fisher, J., "Effect of Moisture on Modulus Values of Base and Subgrade Materials," in Transportation Research Record 1716, *Pavement Assessment and Testing,* Transportation Research Board, National Research Council, National Academy Press, Washington, DC, 2000.

48 Thompson, M.R., and Smith, K.L., "Repeated Triaxial Characterization of Granular Bases," in Transportation Research Record 1278, *Dynamic Testing of Aggregates and Soils and Lateral Stress Measurements*, Transportation Research Board, National Research Council, National Academy Press, Washington, DC, 1990.

49 Chen, D-H., Aman, M.M., and Laguros, J.G., "Resilient Moduli of Aggregate Materials: Variability Due to Testing Procedure and Aggregate Type," in Transportation Research Record 1462, *Compaction of Difficult Soils and Resilient Modulus Testing*, Transportation Research Board, National Research Council, National Academy Press, Washington, DC, 1994.

50 Janoo, V.C., and Berg, R.L., **"**Thaw Weakening of Pavement Structures in Seasonal Frost Areas," in Transportation Research Record 1286, *Design and Evaluation of Rigid and Flexible Pavements 1990,* Transportation Research Board, National Research Council, Washington, DC, 1990.

51 Allen, W., Berg, R., and Bigl, S., "Prediction of Damage to Flexible Pavements in Seasonal Frost Areas," in Transportation Research Record 1286, *Design and Evaluation of Rigid and Flexible Pavements 1990,* Transportation Research Board, National Research Council, Washington, DC, 1990.

52 Allen, W., Berg, R., and Bigl, S., "Prediction of Damage to Flexible Pavements in Seasonal Frost Areas," in Transportation Research Record 1286, *Design and Evaluation of Rigid and Flexible Pavements 1990,* Transportation Research Board, National Research Council, Washington, DC, 1990.

53 Rada, G.R., Richter, C.A., and Jordahl, P., "SHRP's Layer Moduli Backcalculation Procedure," in *Nondestructive Testing of Pavements and Backcalculation of Moduli, ASTM STP 1198,* American Society for Testing and Materials, Philadelphia, PA, 1994.

54 Killingsworth, B. and Von Quintus, H., *Backcalculation of Layer Moduli of LTPP General Pavement Study (GPS) Sites*, Report No. FHWA-RD-95-C-00029, Federal Highway Administration, Washington, DC, September 1997.

55 Irwin, L.H., "Report of the Discussion Group on Practical Limitations and What Can be Done to Overcome Them," in Transportation Research Record 1377, *Nondestructive Deflection Testing and Backcalculation for Pavements, Proceedings of a Symposium,* Transportation Research Board, National Research Council, National Academy of Sciences, Washington, DC, 1995.

56 Irwin, L.H., Yang, W.S., and Stubstad, R.N., "Deflection Reading Accuracy and Layer Thickness Accuracy in Backcalculation of Pavement Layer Moduli," in *Nondestructive Testing of Pavements and Backcalculation of Moduli*, ASTM STP 1026, A.J. Bush III and G. Y. Baladi, Eds. American Society for Testing and Materials, Philadelphia, 1989, pp. 229-244.

57 Von Quintus, H.L., Bush, A.J., III, and Baladi, G.Y., *Nondestructive Testing of Pavements and Backcalculation of Moduli, Second Volume*, ASTM STP 1198, American Society for Testing and Materials, Philadelphia, PA, 1994

58 Bush, A.J., III, and Baladi, G.Y., *Nondestructive Testing of Pavements and Backcalculation of Moduli,* ASTM STP 1026, American Society for Testing and Materials, Philadelphia, PA, 1989.

59 Ullidtz, Per and Coetzee, N.F., "Analytical Procedures in Nondestructive Testing Pavement Evaluation" in Transportation Research Record 1482, *Pavement Design and Analysis,* Transportation Research Board, National Research Council, National Academy of Sciences, Washington, DC, 1995.

60 Von Quintus, H.L. and Simpson, A.L., *Backcalculation of Layer Parameters for LTPP Test Sections, Volume II: Layered Elastic Analysis for Flexible and Rigid Pavements,* FHWA-RD-01-113, Federal Highway Administration, Washington, DC, 2002.

61 Scrivner, F.H., Peohl, R., Moore, W.M., and Phillips, M.B., *Detecting Seasonal Changes in Load-Carrying Capabilities of Flexible Pavements*, National Cooperative Highway Research Program Report 76, Highway Research Board, National Research Council, National Academy of Sciences, Washington, DC, 1969.

62 Newcomb, D.E., Lee, S.W., Mahoney, J.P., and Jackson, N.C., "The Use of Falling Weight Deflectometer Data in Monitoring Flexible Pavement Systems," in *Nondestructive Testing of Pavements and Backcalculation of Moduli,* ASTM STP 1026, A. J. Bush III and G.Y. Baladi, Eds., American Society for Testing and Materials, Philadelphia, PA, 1989, pp. 470-486.

63 Uhlmeyer, J.S., Mahoney, J.P., Hanek, G., Wang, G., Copstead, R.L., and Janssen, D.J., *Estimation of Seasonal Effects for Pavement Design and Performance—Volume 1,* Report No. FHWA-FLP-95-006, Federal Highway Administration, Washington, DC, August 1996.

64 Sebaaly, P.E., Schoener, P., Siddharthan, R., and Epps, J., "Implementation of Nevada's Overlay Design Procedure," in *Proceedings, 4th International Conference on the Bearing Capacity of Roads and Airfields,* University of Minnesota, 1994.

65 Lindly, J.K., and White, T.D., "Using NDT to Calculate the 1986 AASHTO Guide Subgrade Effective Resilient Modulus," in *Nondestructive Testing of Pavements and Backcalculation of Moduli,* ASTM STP 1026, A.J. Bush III and G.Y. Baladi, Eds., American Society for Testing and Materials, Philadelphia, PA, 1989, pp. 683-691.

66 Larson, G., and Dempsey, B.J., *Enhanced Integrated Climatic Model, Version 2.0, Final Report,* Contract DTFA MN/DOT 72114, Department of Civil Engineering, University of Illinois at Urbana-Champaign, Urbana, IL, 1997.

67 Lytton, R.L., Pufahl, D.E., Michalak, C.H., Liang, H.S., and Dempsey, B.J., *An Integrated Model of the Climatic Effects on Pavements,* Report No. FHWA-RD-90-033, U.S. Department of Transportation, Federal Highway Administration, McLean, VA, 1993.

68 Dempsey, B.J., Herlach, W.A. and Patel, A.J., *The Climatic-Materials-Structural Pavement Analysis Program,* Final Report, FHWA/RD-84-115, Volume 3, Federal Highway Administration, Washington, DC, 1985.

69 Liu, S.J. and Lytton, R.L., *Environmental Effects on Pavement Drainage,* Volume IV, Report No. FHWA-DTFH61-87-C-00057, Federal Highway Administration, Washington, DC, 1985.

70 Guymon, G.L., Berg, R.L., and Johnston, T.C., *Mathematical Model of Frost Heave and Thaw Settlement in Pavements,* Report: U.S. Army Cold Regions Research and Engineering Laboratory, 1986.

71 Solaimanian, M. and Bolzan, P., *Analysis of the Integrated Model of Climatic Effects on Pavements*, Report No. SHRP-A-637, Strategic Highway Research Program, National Research Council, Washington, DC, 1993.

72 DataPave 2.0, U.S. Department of Transportation, Federal Highway Administration, McLean, VA, September 1999.

73 Von Quintus, H.L., and Simpson, A.L., *Documentation of the Backcalculation of Layer Parameters for LTPP Test Sections*, Draft Final Report, Federal Highway Administration, McLean, VA, 2000.

74 Rada, G. R., Richter, C.A., and Jordahl, P., "SHRP's Layer Moduli Backcalculation Procedure" in *Nondestructive Testing of Pavements and Backcalculation of Moduli, Second Volume,* ASTM STP 1198, American Society for Testing and Materials, Philadelphia, PA, December 1994.

75 Rada, G.R., Elkins, G.E., Henderson, B., Van Sambeek, R.J., and Lopez, Jr., A. *LTPP Seasonal Monitoring Program: Instrumentation Installation and Data Collection Guidelines*, Publication No. FHWA-RD-94-110, U.S. Department of Transportation, Federal Highway Administration, McLean, VA, 1994.

76 Jiang, Y. J. and Tayabji, S.D., *Analysis of Time Domain Reflectometry Data From LTPP Seasonal Monitoring Program Test Sections*, Final Report, Publication No. FHWA-RD-99-115, U.S. Department of Transportation, Federal Highway Administration, McLean, VA, 1999.

77 Lukanan, Erland O., Stubstad, Richard N., and Briggs, Robert, Temperature Predictions and Temperature Adjustment Factors for Asphalt Pavements, Publication No, FHWA-RD-98-085, U.S. Department of Transportation, Federal Highway Administration, McLean, VA, 2000.

78 Lytton, R.L., Pufahl, D.E., Michalak, C.H., Liang, H.S., and Dempsey, B.J., *An Integrated Model of the Climatic Effects on Pavements,* Report No. FHWA-RD-90-033, Federal Highway Administration, McLean, VA, November 1993.

79 Larson, Gregg, and Dempsey, Barry J., *Enhanced Integrated Climatic Model, Version 2.0, Final Report*, Contract DTFA MN/DOT 72114, Department of Civil Engineering, University of Illinois at Urbana-Champaign, Urbana, IL, 1997.

80 Alavi, S., Merport, T., Wilson, T., Groeger, J., and Lopez, A., *LTPP Materials Characterization Program: Resilient Modulus of Unbound Materials (LTPP Protocol P46) Laboratory Startup and Quality Control Procedure*, Report No. FHWA-RD-96-176, Federal Highway Administration, McLean, VA, 1997.

81 Klemunes, J.A., *Determining Soil Volumetric Moisture Content Using Time Domain Reflectometry,* Master of Science Thesis, University of Maryland Department of Civil Engineering, 1995.

82 Henderson, B., *LTPP Seasonal Monitoring Program, Supplemental Data Collection Prior to Site Rehabilitation, Section 091803, Groton, Connecticut*, Report No. FHWA-TS-00-09-01, Federal Highway Administration, McLean, VA, December 2000.